

# NOTE TO USERS

This reproduction is the best copy available.

**UMI**<sup>®</sup>



©Copyright 2005  
Karen Bobbitt Gran





Fluvial recovery following basin-wide sediment loading at  
Mount Pinatubo, Philippines

Karen Bobbitt Gran

A dissertation  
submitted in partial fulfillment of the  
requirements for the degree of

Doctor of Philosophy

University of Washington

2005

Program Authorized to Offer Degree:  
Department of Earth and Space Sciences

UMI Number: 3198790

Copyright 2005 by  
Gran, Karen Bobbitt

All rights reserved.

### INFORMATION TO USERS

The quality of this reproduction is dependent upon the quality of the copy submitted. Broken or indistinct print, colored or poor quality illustrations and photographs, print bleed-through, substandard margins, and improper alignment can adversely affect reproduction.

In the unlikely event that the author did not send a complete manuscript and there are missing pages, these will be noted. Also, if unauthorized copyright material had to be removed, a note will indicate the deletion.

**UMI**<sup>®</sup>

---

UMI Microform 3198790

Copyright 2006 by ProQuest Information and Learning Company.

All rights reserved. This microform edition is protected against  
unauthorized copying under Title 17, United States Code.

ProQuest Information and Learning Company  
300 North Zeeb Road  
P.O. Box 1346  
Ann Arbor, MI 48106-1346

University of Washington  
Graduate School

This is to certify that I have examined this copy of a doctoral dissertation by

Karen Bobbitt Gran

and have found that it is complete and satisfactory in all respects,  
and that any and all revisions required by the final  
examining committee have been made.


Chair of the Supervisory Committee:

  
\_\_\_\_\_  
David Montgomery

Reading Committee:

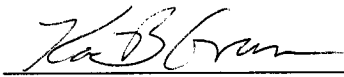
  
\_\_\_\_\_  
David Montgomery

  
\_\_\_\_\_  
Jeffrey Parsons

  
\_\_\_\_\_  
Derek Booth

Date: Dec. 14, 2005

In presenting this thesis in partial fulfillment of the requirements for the doctoral degree at the University of Washington, I agree that the Library shall make its copies freely available for inspection. I further agree that extensive copying of the dissertation is allowable only for scholarly purposes, consistent with "fair use" as prescribed in the U.S. Copyright Law. Requests for copying or reproduction of this dissertation may be referred to Proquest Information and Learning, 300 North Zeeb Road, Ann Arbor, MI 48106-1346, 1-800-521-0600, to whom the author has granted "the right to reproduce and sell (a) copies of the manuscript in microform and/or (b) printed copies of the manuscript made from microform."

Signature 

Date 12-14-05

University of Washington

**Abstract**

Fluvial recovery following basin-wide sediment loading at  
Mount Pinatubo, Philippines

Karen Bobbitt Gran

Chair of the Supervisory Committee:  
Professor David R. Montgomery  
Department of Earth and Space Sciences

The June 1991 eruption of Mount Pinatubo, Philippines, was the second largest of the 20<sup>th</sup> century, emplacing 5-6 km<sup>3</sup> of pyroclastic-flow material and creating record high sediment yields on rivers draining the volcano. This thesis explores landscape response to and recovery from sediment loading in the 1991 eruption from the drainage basin scale to mobility of individual clasts on the bed. Basin-scale erosion patterns were studied on the Pasig-Potrero and Sacobia Rivers for one decade following the eruption using digital elevation models, multispectral imagery, geomorphic terrain maps, and field observations. In the latter half of the decade, channel recovery was examined more closely through a multi-year field campaign on five east side basins measuring flow and channel parameters, grain size distributions, roughness, sediment mobility, and sediment transport. The details of bed coarsening and sediment transport under conditions similar to those at Mount Pinatubo were explored through physical experiments modeling future conditions as sand is depleted.

Sediment yields on the Pasig-Potrero and Sacobia Rivers declined exponentially for the first decade following the eruption. Decay coefficients were inversely correlated with initial sediment loading. Erosion of pyroclastic flow deposits from valley incision, widening, and extension dominated sediment yields as early as 1991. Ten years later, sediment yields remained 20 times higher than pre-eruption levels. In the most disturbed basins, mainstem channels were braided and highly mobile. Coarse clasts moved independently over a smooth bed of sand and fine gravel. As sediment yields

declined, selective transport preferentially removed sand and pumice, starting in the upper basin, causing downstream fining and gradients in pumice content. As sand content on the bed declined, coarse clasts interacted, leading to cluster formation and decreasing clast mobility. As sand content declines, bed reorganization into coarse and fine patches enables transport rates to remain high over a wide range of sand contents. In the near future, sediment yields on the Pasig-Potrero and Sacobia Rivers should remain elevated rather than declining to pre-eruption levels, sending an additional 14 million m<sup>3</sup> of sediment downstream in the second decade after the eruption.

## TABLE OF CONTENTS

	Page
List of Figures .....	iii
List of Tables .....	v
Chapter 1: Introduction.....	1
Background on Mount Pinatubo.....	3
Overview of thesis.....	6
Notes to chapter.....	10
Chapter 2: Basin-scale erosion at Mount Pinatubo, Philippines, and implications for long-term sediment yield following volcanic eruptions .....	14
Summary.....	14
Introduction .....	15
Background.....	17
Methods .....	20
Results .....	26
Discussion.....	33
Conclusions .....	40
Notes to chapter.....	60
Chapter 3: Spatial and temporal patterns in fluvial recovery following volcanic eruptions: Channel response to basin-wide sediment loading at Mount Pinatubo, Philippines.....	64
Summary.....	64
Introduction .....	65
Theoretical context.....	69
Study area.....	70
Methods.....	72
Results .....	75
Discussion.....	82
Conclusions .....	90
Notes to chapter.....	112
Chapter 4: Channel bed evolution and sediment transport under declining sand inputs.....	119
Summary.....	119
Introduction .....	119
Background.....	121
Methodology.....	123
Results and analyses.....	127
Discussion.....	138
Conclusions .....	143
Notes to chapter.....	162
Chapter 5: Conclusions.....	168
Directions for future research.....	170
Bibliography .....	172
Appendix A: Variable list.....	185

Appendix B: Sediment transport, Pasig-Potrero River, 2001.....	187
Appendix C: Grain size distributions of bedload samples, Pasig-Potrero River, 2001 .....	189
Appendix D: Flume experiment sediment transport data.....	190



## LIST OF FIGURES

Figure Number	Page
1.1: Regional tectonic map .....	8
1.2: Map of Mount Pinatubo .....	9
2.1: Map of Pasig-Potrero and Sacobia River basins .....	44
2.2: Geomorphic terrain map for 2001 .....	45
2.3: Stream capture events on Pasig-Potrero/Sacobia/Abacan Rivers .....	46
2.4: Sediment volume change map for 1993 .....	47
2.5: Sediment yield from Pasig-Potrero/Sacobia Rivers and Toutle River .....	48
2.6: Deposit remaining on Pasig-Potrero/Sacobia Rivers and Toutle River .....	49
2.7: Sediment yield decay coefficients .....	50
2.8: Pyroclastic-flow deposit depth distributions .....	51
2.9: Change in storage for upper, middle, and lower basins, 1991-1993 .....	52
2.10: NDVI for 1993 and 2001, Pasig-Potrero/Sacobia Rivers.....	53
2.11: Cumulative sediment volume changes in the Pasig-Potrero/Sacobia basins ..	54
2.12: Valley erosion processes in 1992 and 1993 .....	55
2.13: Valley width 1991 – 2001 .....	56
2.14: Conversion of pyroclastic flow deposits into valley terrain.....	57
2.15: Valley wall interaction model results.....	58
2.16: Secondary explosions at Mount Pinatubo, 1991 – 2001 .....	59
3.1: Sediment yield following eruptions, compared to non-volcanic channels.....	96
3.2: Sediment yield at Mount Pinatubo and on Pasig-Potrero/Sacobia Rivers .....	97
3.3: Map of east flank of Mount Pinatubo.....	98
3.4: Photos of typical channel features.....	99
3.5: Cross-sections from Porac and Gumain Rivers.....	100
3.6: Cross-sectional surveys and repeat photography from Hanging Sabo site ...	101
3.7: Longitudinal profiles from Pasig-Potrero River.....	102
3.8: Channel bed surface grain size distributions, Pasig-Potrero River .....	103
3.9: Grain mobility results from Pasig-Potrero River .....	104
3.10: Dry season photos showing channel incision.....	105
3.11: Channel bed surface grain size distributions, Sacobia River .....	106
3.12: Manning’s n roughness .....	107
3.13: Longitudinal profiles from Sacobia River.....	108
3.14: Primary sediment sources.....	109
3.15: Bed armor development .....	110
3.16: Conceptual model of channel recovery following volcanic eruptions .....	111
4.1: Map of Pasig-Potrero River .....	148
4.2: Sand content on channel bed surface, Pasig-Potrero River.....	149
4.3: Bed structure development on Pasig-Potrero River .....	150
4.4: Sediment transport rating curves, Pasig-Potrero River .....	151
4.5: Bedload transport versus basal shear stress, Pasig-Potrero River .....	152
4.6: Surface grain size distributions for flume experiments.....	153
4.7: Bed surface photographs, flume experiments .....	154

4.8: Friction angle distributions, flume experiments.....	155
4.9: Mean friction angles, flume experiments .....	156
4.10: Friction angle histograms, 40% sand run .....	157
4.11: Dimensionless bedload transport, Pasig-Potrero River and experiments.....	158
4.12: Fractional bedload transport rates, flume experiments .....	159
4.13: Critical shear stress, flume experiments.....	160
4.14: Dimensionless bedload transport on world rivers .....	161

## LIST OF TABLES

Table Number	Page
2.1: Annual sediment yield from Pasig-Potrero and Sacobia River basins .....	42
2.2: Volume change by process, 1991 – 1993 .....	43
3.1: Basin characteristics .....	92
3.2: Data summary, field surveys .....	93
3.3: Summary of basin results, 1997-98, and 2000-02.....	94
3.4: Summary of basin observations .....	95
4.1: Flow conditions for flume runs .....	145
4.2: Surface and bedload grain size distributions for flume runs .....	146
4.3: Friction angle and critical shear stress ratios, flume experiments.....	147

## ACKNOWLEDGEMENTS

This research was funded through a grant from the U. S. National Science Foundation (EAR-0106681), with additional research support from the Department of Earth & Space Sciences, the Department of Geological Sciences, and the Geological Society of America. Support for my education came from a graduate fellowship from the U. S. Environmental Protection Agency's Science to Achieve Results (STAR) program. I would like to thank all of the funding agencies and departments for their assistance with this research.

This research would not have been possible without support from a number of individuals and groups. In the field, I received logistical support from the Philippine Institute of Volcanology and Seismology (PHIVOLCS). Special thanks go to the staff of the Pinatubo Volcano Observatory (PVO) and Arturo Daag and Norman Tuñgol in the main office. I would like to thank Boy Tanglao and the Aeta of Haduan Baranguay for assistance with field work. I also received field help from a number of fellow students including Cami Apfelbeck, Tim Cook, Heidi Guetschow, Cristina Hoff, Betsy Meek, Drew Stolar, and the students of Geology 411.

Flume experiments were carried out at an experimental facility at Humboldt State University. I want to thank the staff and students at both HSU and the U. S. Forest Service's Redwood Sciences Laboratory for logistical support and help with experimental runs and data collection. In particular, I want to thank Tom Lisle and Diane Sutherland at the Redwood Sciences Laboratory for useful discussions and logistical support. Thomas Dunklin helped with photography of the flume bed.

Most of all, I would like to thank my advisor, Dave Montgomery, for discussions and support on many levels throughout the past five years, both in Seattle and in the field. Thanks for your help and understanding. Thanks also to Chris Newhall, for his immeasurable assistance with all topics related to Mount Pinatubo. Many thanks to my committee and readers, Jeff Parsons and Derek Booth.

For support in all endeavors of life, I want to thank my husband, Rik. Hugs as well to our little boy, Alex, for opening up my eyes to the greater things in life, and for helping this thesis take a little bit longer than it would have otherwise.

## CHAPTER 1

### Introduction

The June 1991 eruption of Mount Pinatubo, Philippines, was the second-most voluminous pyroclastic eruption of the twentieth century, with an estimated 5 - 6 km<sup>3</sup> of pyroclastic-flow material deposited on the flanks of the volcano (Scott et al., 1996b) and 3.8 – 4.8 km<sup>3</sup> of tephra-fall (Paladio-Melosantos et al., 1996). Rivers were buried up to 200 meters deep by loose, sand-rich pyroclastic-flow deposits. The abundance of loose pyroclastic-flow and tephra material coupled with tropical rainstorms led to the generation of massive lahars on rivers draining the flanks of the volcano. These lahars led to great destruction of property and economic hardship (Mercado et al., 1996), and they continued for many years on the most disturbed basins (Arboleda and Martinez, 1996; Janda et al., 1996; Martinez et al., 1996; Rodolfo et al., 1996; Tuñgol, 2002; Torres et al., 2004). This thesis examines landscape response to and recovery from this 1991 eruption on the east flank of Mount Pinatubo.

Following the eruption, sediment yields increased by several orders of magnitude (Umbal, 1997; Tuñgol, 2002). Most of the sediment was removed initially through lahars, but erosion occurred through a number of different processes including channel incision, valley-wall collapse, network extension, mobilization of sediment from secondary explosions, rilling, gullyng, and surface erosion from rainsplash and sheetwash. Chapter two presents an overview of erosion in the wake of the eruption, how patterns of erosion changed through time, and how the magnitude of initial sediment loading and the dominant erosional processes affect long term sediment yields.

After the cessation of major lahars, normal fluvial processes once again controlled the transport and removal of sediment. How channels adjusted as sediment inputs to the channel network declined through time is covered in chapter three. I focus on five basins on the east flank of the volcano that had variable amounts of sediment loading in the eruption, and monitored them through repeat field surveys. Observations from the field campaign showed that channel bed coarsening and organization led to

decreasing sediment mobility and transport rates. The details of channel bed response to lower sand inputs as sandy pyroclastic-flow deposits continue to be removed or stabilized are investigated in chapter four. This chapter combines field surveys on the Pasig-Potrero River with flume experiments designed to study channel bed development and sediment transport under conditions of declining sand.

By combining these studies at multiple scales, I provide an in-depth view into channel recovery following the eruption of Mount Pinatubo which should be applicable to other explosive volcanic eruptions with voluminous, unwelded tephra and pyroclastic-flow deposits. It was the abundant loose material, coupled with heavy tropical rainfall at Mount Pinatubo that led to sediment yields two to three orders of magnitude higher than pre-eruption yields. Other Plinian eruptions should experience similar patterns of recovery, but perhaps over different time scales depending on the volume of eruptive material and the local climate.

Sediment loading from a sand-rich source occurs in non-volcanic environments as well. Basin-scale disturbances from widespread landsliding are common in tectonically active watersheds, sending large volumes of sediment into channels (Dietrich and Dunne, 1978; Swanson et al., 1982; Pearce and Watson, 1986). Dam removal can leave behind large deposits of previously trapped sediment, affecting local and downstream reaches (Doyle et al., 2002a, b; Pizzuto, 2002). Land use changes including forest clearing, agricultural practices, and mining can release excess sediment to channels, often in significant volumes forcing changes in channel bed morphology and sediment transport (Gilbert, 1917; Knighton, 1989; Madej and Ozaki, 1996). Recovery from such disturbances is similar to recovery from sediment loading at Mount Pinatubo, although the spatial scale and recovery time period may vary greatly.

Recovery in the context of this study is not meant to imply a return to exact pre-eruption conditions, but the rather the reestablishment of dynamic equilibrium in the fluvial system. Once a channel has recovered, it should be able to support an aquatic ecosystem of pre-eruption complexity, although it may take additional decades for a complex aquatic ecosystem to reoccupy the channel.

## **Background on Mount Pinatubo**

### ***Geologic setting and eruptive history***

Mount Pinatubo is located on the island of Luzon, Philippines, at 15°8'N, 120°21'E. It is part of the Luzon Arc, a north-south trending volcanic arc formed due to eastward subduction of the South China Sea Plate along the Manila Trench (Figure 1.1). Prior to the June 1991 eruption, the summit of Mount Pinatubo rose to 1,745 m above sea level, making it one of the highest peaks in west central Luzon.

Eruptive activity at Mount Pinatubo began in the Pleistocene, and can be divided into two main phases: the Ancestral Phase beginning ~1 Ma and continuing to >35 ka, and the Modern Phase beginning >35 ka and continuing to the present (Newhall et al., 1996). Ancestral Pinatubo was an andesite and dacite stratovolcano with no evidence for large explosive eruptions. Much of the highlands surrounding the current peak of Mount Pinatubo are relics of the Ancestral Pinatubo. Mount Donald Macdonald and Mount Tayawan lie on the ancestral caldera rim. Several other peaks in the area including Mount Negron, Mount Cuadrado, Mataba dome, Bituin plug, and the Tapungho plug, represent volcanic domes and plugs from other vents contemporaneous to ancestral Pinatubo (Newhall et al., 1996) (Figure 1.2).

The Modern Pinatubo eruption phase began >35 ka, and has been separated into six major eruptive periods by Newhall et al. (1996). Based on comparisons of deposits from each eruptive phase, the pattern is one of decreasing eruption size and recurrence interval. The 1991 eruption was smaller than the maximum eruption recorded in deposits from each of the six previous eruption periods. However, the eruptive material has remained similar through time, with eruptions of relatively cool, crystal-rich dacitic magma in the form of pumiceous pyroclastic flows with minor volumes of lithic-rich pyroclastic flows and pumiceous tephra-fall (Newhall et al., 1996).

Despite being smaller than previous eruptions in the modern Pinatubo phase, the June 1991 eruption had devastating effects of the landscape and the local populace. The eruption produced 5 - 6 km<sup>3</sup> of pyroclastic-flow material (Scott et al., 1996b) and an additional 3.8 - 4.8 km<sup>3</sup> in tephra airfall deposits (Paladio-Melosantos et al., 1996). The

pyroclastic-flow deposits filled valleys draining the flanks of the volcano with as much as 200 m of loose, easily erodible material (Scott et al., 1996b).

The climatic eruption of June 15, 1991, coincided with the arrival of Tropical Storm Yunya, generating lahars that day in all major rivers draining the flanks of the volcano (Pierson et al., 1992; Major et al., 1996; Rodolfo et al., 1996). These volcanic debris flows and hyperconcentrated flows continued for many years in the basins hardest hit by the eruption. Lahars have had devastating effects on downstream communities, leading to destruction of infrastructure and loss of life. In the first year alone, lahars affected 364 villages, home to 2.1 million people (Mercado et al., 1996). Upstream of alluvial fan heads, lahars have triggered massive stream captures, rearranged watershed boundaries, and caused changes in base level of 10 m or more in a single event (Tuñgol, 2002).

### ***Study area and climate***

The climate at Mount Pinatubo is strongly seasonal, with a rainy season from May through October, and dry weather over the winter months. During the rainy season, the area experiences monsoonal rains as well as tropical storms and typhoons. On average, five typhoons pass over central Luzon each year (Tuñgol, 2002; Daag, 2003). Monsoonal rains come from the southwest, and orographic effects are substantial, leading to about twice as much precipitation on the western slopes than on the eastern side (JICA, 1996). The rain gage at Clark Air Base at the eastern edge of Pinatubo records an average of 1,950 mm of rainfall each year, 60% of which falls in the summer months of June, July, and August (Scott et al., 1996a).

My study area lies on the east flank of the volcano, where drainage basins were variably affected, with 1% to 33% of each basin covered with pyroclastic-flow deposits. All references to percent fill for each basin refer specifically to the valley-filling primary pyroclastic-flow deposits. I focus on five rivers which are, in order from the most impacted to the least, the Sacobia, Pasig-Potrero, O'Donnell, Gumain, and Porac Rivers (Figure 1.2).



In addition to the direct effects of the eruption, the Pasig-Potrero and Sacobia Rivers have a unique history that involves a massive stream capture in October 1993. At the time of the eruption, the Sacobia River basin extended up into the area that is now occupied by the 1991 crater. The Pasig-Potrero River initiated several kilometers downstream. In October 1993, the Pasig-Potrero River captured the upper half of the Sacobia basin, essentially doubling the basin area of the Pasig-Potrero while halving that of the Sacobia (Punongbayan et al., 1994). Since this capture occurred after three rainy seasons, a substantial amount of sediment had already left the upper Sacobia River basin (Daag, 1994), and the Pasig-Potrero inherited transport capacity (increased discharge) without a commensurate increase in sediment load from the upper watershed. Because the two rivers shared the upper basin at different points in time following the eruption, I sometimes refer to the Pasig-Potrero/Sacobia basin as a single unit, which includes the basin area for both rivers.

One decade after the eruption, the Pasig-Potrero River and others with intense sediment loading were still highly active. During the rainy season they were shallow and braided, with braids ranging in size from a few centimeters in width to tens of meters, all of which were actively transporting sediment. Transport occurred as a moving carpet of sand and fine gravel over a smooth bed, with coarse clasts rolling or sliding independently over the predominantly sand bed. Any clast that became stationary in an active channel was quickly scoured around, sank into the bed, and was buried, thus maintaining a smooth bed. Flow was often super-critical, and transient antidunes were present. During high flows, the water level could rise high enough to completely fill the valley, and channel-spanning roll waves pulsed downstream. These conditions were changing as sand was removed from the fluvial system and coarse clast interactions increased. Understanding how these sediment-rich channels transport high sediment loads, and how transport rates are changing as sediment yields decline on a decadal time scale is important in assessing long term hazards from downstream sedimentation and flooding.

### Overview of thesis

This thesis is organized into three main chapters. Each is written as a stand alone paper, and two of the three chapters have been submitted for publication or already published. Chapter two, entitled “Basin-scale erosion at Mount Pinatubo, Philippines, and implications for long-term sediment yield following volcanic eruptions” offers an overview of landscape disturbance and response in the Pasig-Potrero and Sacobia River basins for the first decade following the eruption. This chapter tracks changes in sediment sources through time as the pyroclastic-flow deposits were eroded and/or stabilized and relate these changes to records of long-term sediment yield. Analyses of sequential digital elevation models (DEMs) coupled with air photo and satellite image-based terrain maps show annual erosion patterns in the first three rainy seasons, with partial coverage continuing through 2001. Connections between the size and nature of the eruptive disturbance and patterns of long-term sediment yield are examined by comparing sediment yield records from the Pasig-Potrero and Sacobia Rivers with the Toutle River basin at Mount St. Helens. This chapter helps set the scene for the subsequent, more in-depth chapters on fluvial response and recovery.

Chapter three, entitled “Spatial and temporal patterns in fluvial recovery following volcanic eruptions: Channel response to basin-wide sediment loading at Mount Pinatubo, Philippines” focuses on fluvial recovery in the latter half of the decade, from 1996 – 2003. This is the time after major lahars ceased in most basins, and normal streamflow dominated the transport of sediment out of the upper basins and onto alluvial fans. The results come predominately from a field campaign covering five different basins on the east flank of Mount Pinatubo. I used field surveys to address the question of how channels respond as sediment yields decline following the emplacement of voluminous, loose, sandy, pyroclastic-flow deposits. The results are summarized in a conceptual model for channel recovery following basin-wide sediment loading. This chapter was published in *GSA Bulletin* (Gran and Montgomery, 2005).

The final chapter, entitled “Channel Bed Evolution and Sediment Transport under Declining Sand Inputs” investigates how declines in sand, specifically, affect bed

structure and sediment transport. The pyroclastic-flow deposits contained 70-85% sand (Scott et al., 1996b), and as these deposits are removed or stabilized, the overall sand content in the bed is declining. I focus on sediment transport surveys from the Pasig-Potrero River and compare them to a series of flume experiments run under conditions of declining sand. The flume experiments were based on conditions on the Pasig-Potrero River and were designed to model future conditions as sand continues to leave the system. As sand was removed, distinct gravel and sand patches formed, enabling high transport rates to continue in sandy transport zones even as the bed coarsened. This chapter was submitted for publication to *Water Resources Research* in June 2005.

Through the entire thesis, I investigate the theme of recovery from large-scale landscape disturbance. Although I focus on a specific type of disturbance (volcanic sediment loading) from a specific eruption, the results are generalizable both to other eruptions and to other forms of large-scale sediment loading from sources like landsliding or large dam removal. In both cases, large volumes of loose material are suddenly added to a river system, and the channel rapidly adjusts to excess sediment in the channel network. The recovery period following that initial sediment loading event is the focus of this thesis, from the scale of basin-wide erosion patterns to the organization and development of surface armor on the channel bed.

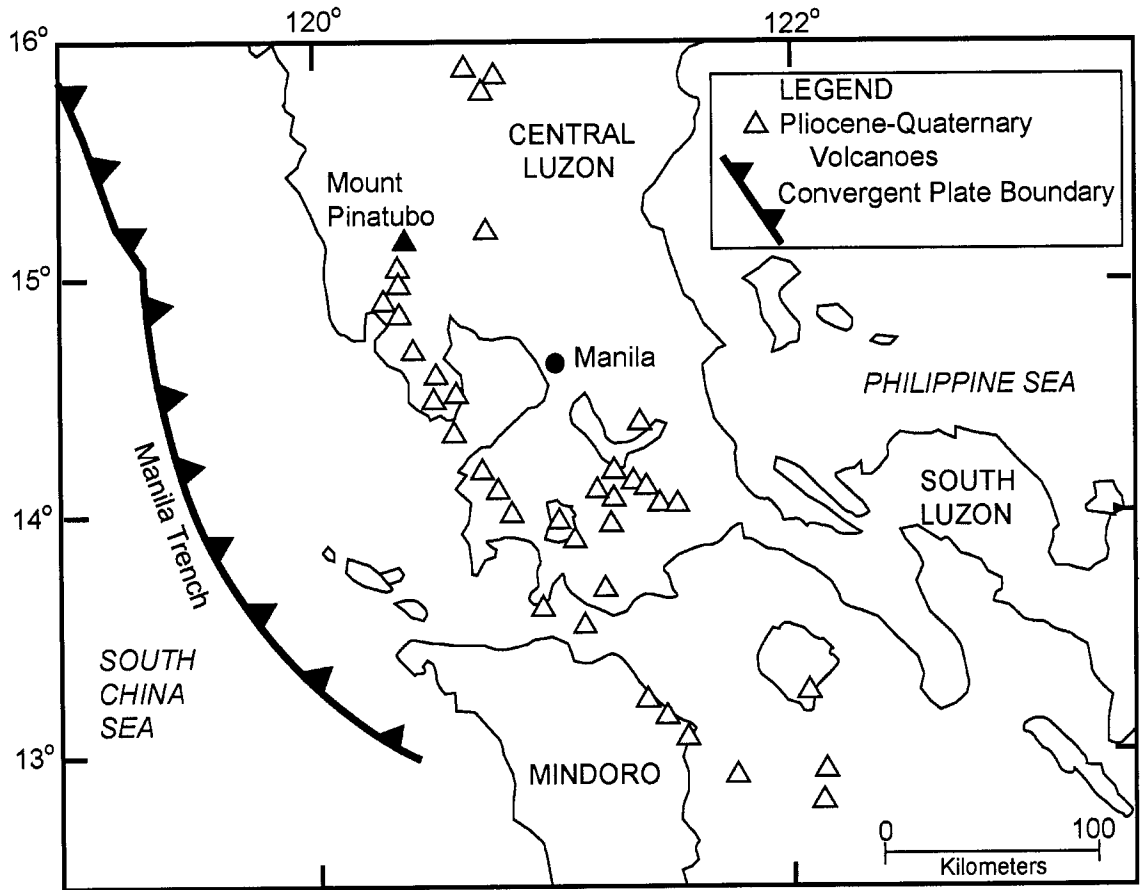


Figure 1.1: Regional map showing the location of Mount Pinatubo in central Luzon, Philippines, formed from eastward subduction of the South China Sea plate along the Manila trench. Map is from Newhall et al. (1996).

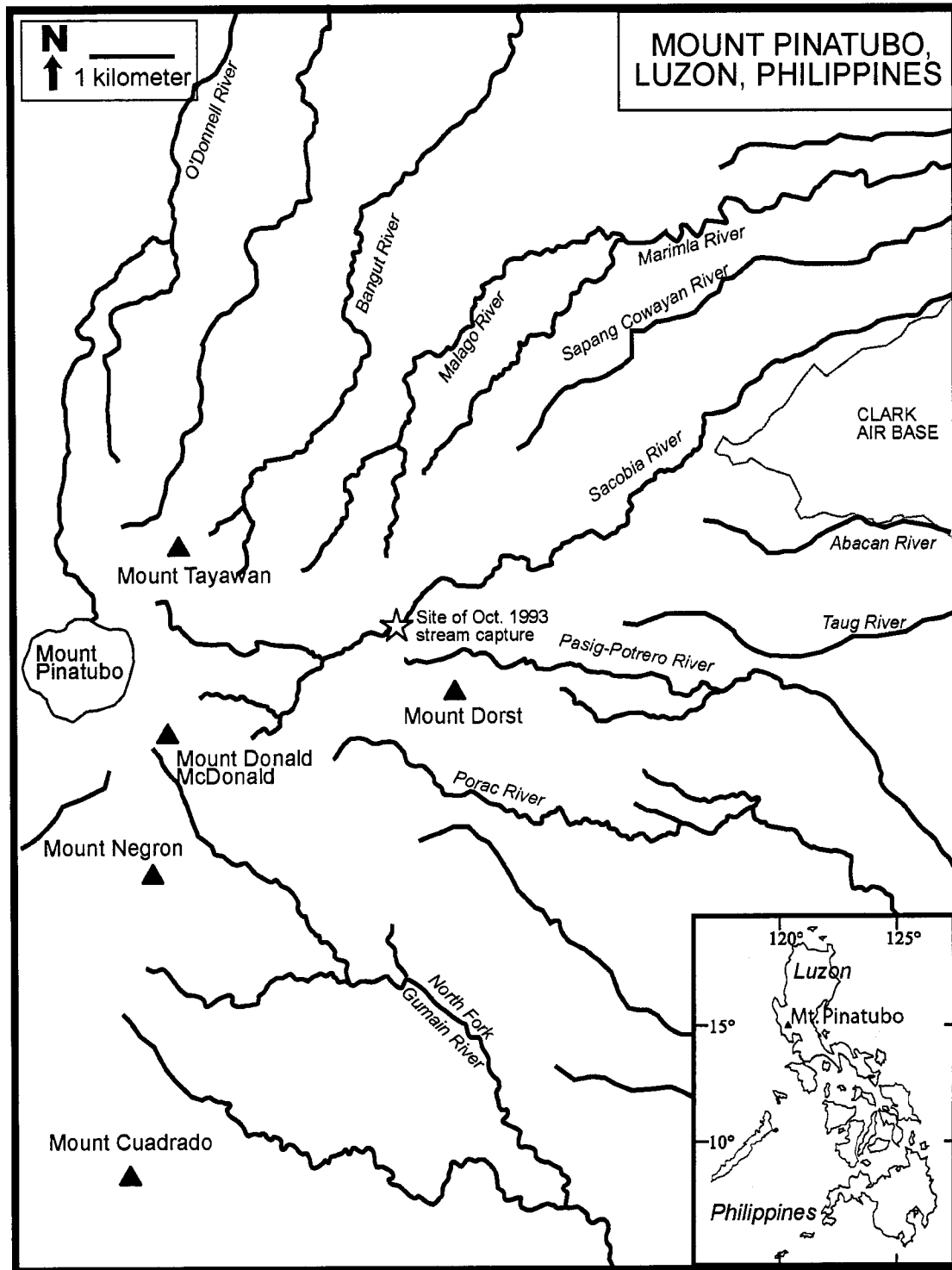


Figure 1.2: Map showing major rivers and peaks on the east flank of Mount Pinatubo.

### Notes to chapter

- Arboleda, R. A., and Martinez, M. M. L., 1996, 1992 lahars in the Pasig-Potrero River system, *in* Newhall, C. G., and Punongbayan, R. S., eds., Fire and mud: eruptions and lahars of Mount Pinatubo, Philippines: Quezon City, Philippine Institute of Volcanology and Seismology, and Seattle, University of Washington Press, p. 1045-1052.
- Daag, A. S., 1994, Geomorphic developments and erosion of the Mount Pinatubo 1991 pyroclastic flows in the Sacobia watershed, Philippines: A study using remote sensing and Geographic Information Systems (GIS) [M.S. thesis]: Enschede, Netherlands, International Institute for Geoinformation Science and Earth Observation (ITC), 106 p.
- , 2003, Modelling the erosion of pyroclastic flow deposits and the occurrences of lahars at Mt. Pinatubo, Philippines [Ph.D. thesis]: Enschede, Netherlands, International Institute for Geoinformation Science and Earth Observation (ITC), 232 p.
- Dietrich, W. E., and Dunne, T., 1978, Sediment budget for a small catchment in mountainous terrain: *Zeitschrift für Geomorphologie N. F. Suppl. Bd.*, v. 29, p. 191-206.
- Doyle, M. W., Stanley, E. H., and Harbor, J. M., 2002a, Channel adjustments following two dam removals in Wisconsin: *Water Resources Research*, v. 39, no. 1, p. ESG 2-1 - 2-15.
- , 2002b, Geomorphic analogies for assessing probably channel response to dam removal: *Journal of the American Water Resources Association*, v. 38, no. 6, p. 1567-1579.
- Gilbert, G. K., 1917, Hydraulic mining debris in the Sierra Nevada: U.S. Geological Survey Professional Paper, v. 105, 154 p.
- Gran, K. B., and Montgomery, D. R., 2005, Spatial and temporal patterns in fluvial recovery following volcanic eruptions: Channel response to basin-wide sediment loading at Mount Pinatubo, Philippines: *Geological Society of America Bulletin*, v. 117, no. 1/2, p. 195-211.
- Janda, R. J., Daag, A. S., de los Reyes, P. J., and Newhall, C., 1996, Assessment and response to lahar hazard around Mount Pinatubo, 1991 to 1993, *in* Newhall, C., G., and Punongbayan, R. S., eds., Fire and mud: eruptions and lahars of Mount

- Pinatubo, Philippines: Quezon City, Philippine Institute of Volcanology and Seismology, and Seattle, University of Washington Press, p. 107-139.
- JICA, 1996, The study on flood and mudflow control for Sacobia-Bamban/Abacan River draining from Mt. Pinatubo: Japan International Cooperation Agency (JICA) and Department of Public Works and Highways, Philippines, 45 p.
- Knighton, A. D., 1989, River adjustment to changes in sediment load: The effects of tin mining on the Ringarooma River, Tasmania, 1875-1984: *Earth Surface Processes and Landforms*, v. 14, p. 333-359.
- Madej, M. A., and Ozaki, V., 1996, Channel response to sediment wave propagation and movement, Redwood Creek, California, USA: *Earth Surface Processes and Landforms*, v. 21, p. 911-927.
- Major, J. J., Janda, R. J., and Daag, A. S., 1996, Watershed disturbance and lahars on the east side of Mount Pinatubo during the mid-June 1991 eruptions, *in* Newhall, C. G., and Punongbayan, R. S., eds., *Fire and mud: eruptions and lahars of Mount Pinatubo, Philippines: Quezon City, Philippine Institute of Volcanology and Seismology, and Seattle, University of Washington Press*, p. 895-919.
- Martinez, M. M. L., Arboleda, R. A., Delos Reyes, P. J., Gabinete, E., and Dolan, M. T., 1996, Observations of 1992 lahars along the Sacobia-Bamban River system, *in* Newhall, C. G., and Punongbayan Raymundo, S., eds., *Fire and mud: eruptions and lahars of Mount Pinatubo, Philippines: Quezon City, Philippine Institute of Volcanology and Seismology, and Seattle, University of Washington Press*, p. 1033-1043.
- Mercado, R. A., Lacsamana, J. B. T., and Pineda, G. L., 1996, Socioeconomic impacts of the Mount Pinatubo eruption, *in* Newhall, C. G., and Punongbayan, R. S., eds., *Fire and Mud: Eruptions and Lahars of Mount Pinatubo, Philippines: Quezon City, Philippine Institute of Volcanology and Seismology, and Seattle, University of Washington Press*, p. 1063-1069.
- Newhall, C. G., Daag, A. S., Delfin, F. G., Jr., Hoblitt, R. P., McGeehin, J., Pallister, J. S., Regalado, M. T. M., Rubin, M., Tubianosa, B. S., Tamayo, R. A., Jr., and Umbal, J. V., 1996, Eruptive history of Mount Pinatubo, *in* Newhall, C. G., and Punongbayan Raymundo, S., eds., *Fire and mud: eruptions and lahars of Mount Pinatubo, Philippines: Quezon City, Philippine Institute of Volcanology and Seismology, and Seattle, University of Washington Press*, p. 165-195.
- Paladio-Melosantos, M. L. O., Solidum, R. O., Scott, W. E., Quiambao, R. B., Umbal, J. V., Rodolfo, K. S., Tubianosa, B. S., de los Reyes, P. J., Alonso, R. A., and Ruelo, H. B., 1996, Tephra falls of the 1991 eruptions of Mount Pinatubo, *in*

- Newhall, C. G., and Punongbayan, R. S., eds., *Fire and Mud: Eruptions and lahars of Mount Pinatubo, Philippines*: Quezon City, Philippine Institute of Volcanology and Seismology, and Seattle, University of Washington Press, p. 513-535.
- Pearce, A. J., and Watson, A. J., 1986, Effects of earthquake-induced landslides on sediment budget and transport over a 50-year period: *Geology*, v. 14, p. 52-55.
- Pierson, T. C., Janda, R. J., Umbal, J. V., and Daag, A. S., 1992, Immediate and long-term hazards from lahars and excess sedimentation in rivers draining Mt. Pinatubo, Philippines: U. S. Geological Survey Water Resources Investigation, 92-4039, 35 p.
- Pizzuto, J. E., 2002, Effects of dam removal on river form and process: *BioScience*, v. 52, no. 8, p. 683-691.
- Punongbayan, R. S., Tuñgol, N. M., Arboleda, R. A., Delos Reyes, P. J., Isada, M., Martinez, M. M. L., Melosantos, M. L. P., Puertollano, J. R., Regalado, M. T. M., Solidum, R. U., Jr., Tubianosa, B. S., Umbal, J. V., Alonso, R. A., and Remotigue, C. T., 1994, Impacts of the 1993 lahars, and long-term lahar hazards and risks around Pinatubo Volcano, PHIVOLCS, Pinatubo Lahar Studies 1993: Final Report of the UNESCO-funded lahar studies program: PHIVOLCS Press, p. 1-40.
- Rodolfo, K. S., Umbal, J. V., Alonso, R. A., Remotigue, C. T., Paladio-Melosantos, M. L. O., Salvador, J. H. G., Evangelista, D., and Miller, Y., 1996, Two years of lahars on the western flank of Mount Pinatubo: Initiation, flow processes, deposits, and attendant geomorphic and hydraulic changes, *in* Newhall, C. G., and Punongbayan, R. S., eds., *Fire and Mud: Eruptions and lahars of Mount Pinatubo, Philippines*: Quezon City, Philippine Institute of Volcanology and Seismology, and Seattle, University of Washington Press, pp. 989-1013.
- Scott, K. M., Janda, R. J., de la Cruz, E. G., Gabinete, E., Eto, I., Isada, M., Sexton, M., and Hadley, K., 1996a, Channel and sedimentation responses to large volumes of 1991 volcanic deposits on the east flank of Mount Pinatubo, *in* Newhall, C. G., and Punongbayan, R. S., eds., *Fire and mud: eruptions and lahars of Mount Pinatubo, Philippines*: Quezon City, Philippine Institute of Volcanology and Seismology, and Seattle, University of Washington Press, p. 971-988.
- Scott, W. E., Hoblitt, R. P., Torres, R. C., Self, S., Martinez, M. M. L., and Nillos, T., 1996b, Pyroclastic flows of the June 15, 1991, climactic eruption of Mount Pinatubo, *in* Newhall, C. G., and Punongbayan, R. S., eds., *Fire and mud: eruptions and lahars of Mount Pinatubo, Philippines*: Quezon City, Philippine



Institute of Volcanology and Seismology, and Seattle, University of Washington Press, p. 545-570.

- Swanson, F. J., Fredrickson, R. L., and McCorison, F. M., 1982, Material transfer in a western Oregon forested watershed, *in* Edmonds, R. L., ed., *Analysis of Coniferous Forest Ecosystems in the Western United States*: Stroudsburg, PA, Hutchinson Ross, p. 233-266.
- Torres, R. C., Mougini-Mark, P. J., Garbeil, H., Kallianpur, K., Self, S., and Quiambao, R. B., 2004, Monitoring the evolution of the Pasig-Potrero alluvial fan, Pinatubo volcano, using a decade of remote sensing data: *Journal of Volcanology and Geothermal Research*, v. 138, no. 3-4, p. 371-392.
- Tuñgol, N. M., 2002, Lahar initiation and sediment yield in the Pasig-Potrero River basin, Mount Pinatubo, Philippines [Ph.D. thesis]: University of Canterbury, New Zealand, 172 p.
- Umbal, J. V., 1997, Five years of lahars at Pinatubo volcano: Declining but still potentially lethal hazards: *Journal of the Geological Society of the Philippines*, v. 52, no. 1, p. 1-19.

## CHAPTER 2

### **Basin-scale erosion at Mount Pinatubo, Philippines, and implications for long-term sediment yield following volcanic eruptions**

#### **Summary**

Basin-scale erosion patterns are examined for the Pasig-Potrero and Sacobia Rivers in the decade following the 1991 eruption of Mount Pinatubo, Philippines, using digital elevation models, geomorphic terrain maps, and field observations. Erosion was measured annually from 1991 - 1993 from five different processes including valley-bottom incision, valley-wall retreat, network extension, secondary explosions, and bulk erosion on pyroclastic-flow deposit surfaces from rainsplash, sheetwash, rilling, and gullyng. Sediment released from valley incision, widening, and extension dominated the sediment budget as early as the 1991 rainy season, with valley-wall retreat continuing as an important erosional process through at least 2000. Secondary explosions were a significant mechanism for mobilizing sediment for at least four to five years after the eruption, further enhancing valley widening. Bulk erosion on the pyroclastic-flow surface accounted for one-third of all erosion in 1991, declining in importance through time, particularly in the upper third of the Pasig-Potrero/Sacobia basin.

An exponential decay function effectively models sediment yield on the Pasig-Potrero and Sacobia Rivers throughout the entire first decade following the eruption of Mount Pinatubo. The decay constant is low, and sediment yields in 2001 were still twenty times higher than pre-eruption levels. A comparison with the Toutle River at Mount St. Helens shows a more complex pattern for long-term sediment yields; after decaying exponentially for five to six years, sediment yields leveled off at a value 10 to 100 times higher than background levels (Major et al. 2000). If the Pasig-Potrero and Sacobia Rivers follow a similar pattern, and sediment yields level off one order of magnitude higher than pre-eruption levels, it will send an additional 14 million m<sup>3</sup> of sediment downstream from 2001-2011. The lower exponential decay constant and

longer time to transition to an elevated tail on the Pasig-Potrero and Sacobia Rivers are correlated with greater initial sediment loading.

### Introduction

Dramatically elevated post-eruptive sediment yields are a primary volcanic hazard, due to a combination of increased source material and changes in the hydrologic system that lead to elevated flood peaks. Sediment yield,  $Q_s$ , following several eruptions has been modeled using a simple exponential decay model of the form:

$$Q_s = \beta e^{-\varepsilon t} \quad (2.1)$$

with the decay constant,  $\varepsilon$ , varying depending on local conditions (Hirao and Yoshida, 1989; Pierson et al., 1992; Punongbayan et al., 1994; Umbal, 1997; Simon, 1999). Here,  $t$  is time in years, and  $\beta$  is a parameter related to total volume of material eroded. It is unclear how the decay constant should vary based on eruption volume or type, if exponential decay is the most appropriate model for post-eruptive sediment yield in all cases, or if the decay coefficient varies through time. Long-term patterns of post-eruptive sediment yield are not well understood since most sediment yield studies examine only the first few years after an eruption, even though sediment yields may remain elevated for decades (Major et al., 2000; Major, 2004).

The geomorphic effects of the 1980 eruption of Mount St. Helens remain the most thoroughly studied record of long-term landscape impact following a voluminous pyroclastic eruption. Records of sediment yield extending out two decades after the eruption have been analyzed and published (Major et al., 2000; Major, 2004). The 1991 eruption of Mount Pinatubo offers a good opportunity to test generalities and trends generated from long-term erosion and sediment yield data at Mount St. Helens.

The June 15, 1991, climactic eruption of Mount Pinatubo was the second largest eruption of the 20<sup>th</sup> century, producing 5-6 km<sup>3</sup> of pyroclastic-flow deposits and 3.4 – 4.4 km<sup>3</sup> of ash and tephra-fall deposits (Paladio-Melosantos et al., 1996; Scott et al.,

1996b). Mount Pinatubo lies in a tropical climate, subject to strong typhoons and heavy monsoonal rains. The abundance of loose, easily erodible sediment and heavy rainfall led to record sediment yields on rivers draining the flanks of the volcano. Sediment yield for the entire volcano decayed exponentially for the first four years after the eruption (Umbal, 1997).

Erosional processes at Mount Pinatubo ranged from non-channelized rainsplash and sheetwash to rill and gully development to channel network extension, incision, and widening. Channel and valley widening occurred through a mix of gravity-driven mass wasting processes and secondary explosions. “Secondary explosions” is a term used by the Philippine Institute of Volcanology and Seismology (PHIVOLCS) to include both secondary hydroeruptions, resulting from groundwater and surface water interactions with hot deposits, and secondary pyroclastic flows generated from massive collapse and remobilization of the primary ignimbrite (Torres et al., 1996; Tuñgol, 2002). In basins with thick pyroclastic-flow deposits, hillslope tephra erosion played only a minor role, and erosion of the valley-filling pyroclastic-flow material dominated sediment yields (Tuñgol, 2002). The balance between smaller-scale erosional processes on the pyroclastic-flow surface and processes associated with valley growth and development evolved through time.

To address the underlying changes in erosion following the Pinatubo eruption, this study focuses on which sediment sources and erosional processes dominated at different points in time in the Pasig-Potrero and Sacobia basins on the east side of the volcano (Figure 2.1). Erosional processes examined include valley incision, valley-wall retreat, and network extension. I also measure bulk erosion on the surface of the pyroclastic-flow deposit from multiple processes and erosion directly attributable to secondary explosions. I focus on the first few years after the eruption with annual resolution, dropping to 3- to 4-year resolution for the remainder of the decade. Finally, compiled records of total sediment yield for the entire decade are compared with similar records from the Toutle River at Mount St. Helens (Major et al., 2000; Major, 2004) to better understand decadal-scale patterns of sediment yield following volcanic eruptions,

and how differences in erosional environment and initial sediment loading affect long-term sediment yields.

### **Background**

During the eruption, the main impact to the Pasig-Potrero and Sacobia River watersheds was the emplacement of pumiceous pyroclastic-flow deposits, filling valleys with an estimated  $1.1 - 1.3 \times 10^9 \text{ m}^3$  of sediment (Daag and van Westen, 1996; Scott et al., 1996b). Airfall tephra played a minor role, blanketing hillslopes an average of 0.5 m deep, with an estimated volume of  $2.4 \times 10^7 \text{ m}^3$  (Tuñgol, 2002). Whereas hillslope tephra was insignificant in terms of eruptive volume, tephra-fall deposits did compose the first lahars that developed during the eruption, before the emplacement of pyroclastic-flow deposits (Pierson et al., 1992). In addition, tephra may have reduced infiltration capacity, as seen at other volcanoes (Segerstrom, 1950; Waldron, 1967; Herkelrath and Leavesley, 1981; Kadomura et al., 1983; Mizuyama and Kobashi, 1996), thereby increasing peak floods and response times.

Because hillslope tephra was a minor component of total sediment yield (Tuñgol, 2002), this study focused on erosion within the pyroclastic-flow deposits only. Erosion within the pyroclastic-flow deposits was subdivided into two main categories: erosion on the pyroclastic-flow surface including rainsplash, sheetwash, and rill and gully erosion; and erosion in valleys from valley incision, valley-wall collapse and widening, network extension, and secondary explosions. Erosion due to secondary explosions was categorized as valley erosion since most of the secondary explosions were triggered by valley-wall collapse and contributed to valley widening.

The valley network developed rapidly following the eruption, achieving a drainage density equal to the pre-eruption drainage density by the end of the first rainy season (Daag, 1994). After this initial drainage development phase, network extension continued up into pyroclastic-flow and pre-eruption deposits. Valley incision and widening occurred throughout the next few years, with most adjustments occurring during lahars. Lahars both eroded and deposited, so valley incision was actually the net effect of erosion vs. deposition. Valley widening was generally a one-way process;

however, valley width reductions did occur due to valley incision and/or deposition of new lahar terraces. In addition, locations of active valleys sometimes shifted, incising new channels in pyroclastic-flow deposits. Thus, “valley widening” encompassed the net effect of valley width adjustments for a given time period. Even small changes in valley width were important. Pyroclastic-flow deposits at Pinatubo had a high apparent cohesion (13 – 18.5 kPa) and could maintain steep cliffs to heights reaching 40 m at slopes  $> 60^\circ$  (JICA, 1996; Tuñgol, 2002). A small increase in valley width thus added a substantial amount of sediment to the fluvial system.

Secondary explosions were responsible for some of the valley widening. These include both secondary hydroeruptions, resulting from groundwater or surface water interactions with hot deposits, and secondary pyroclastic flows, which result mainly from gravitational bank collapse (Moyer and Swanson, 1987; Torres et al., 1996; Tuñgol, 2002). From 1991 to 1994, secondary explosions occurred almost every day during the rainy season, some with ash clouds that reached over 10 km in height (Tuñgol, 2002). Most originated from gravitational bank collapse along river valleys, aiding valley widening. Secondary explosions were not only responsible for directly mobilizing significant volumes of sediment into rivers for transport out of the system but also were responsible for several large-scale stream captures, realigning watershed boundaries and indirectly increasing sediment yields (Punongbayan et al., 1994; Tuñgol, 2002). Using maps of large secondary explosion craters or landslide scars, I was able to determine a lower bound on the importance of secondary explosions on erosion in the Pasig-Potrero/ Sacobia River basin.

On the pyroclastic-flow surface, rainsplash, sheetwash, rilling, and gullying all contributed sediment to the channel network. These processes were not treated separately here, due to the resolution of the study (20-m-grid DEMs). For 1991, it was possible to estimate sediment contribution due to channelized flow on the pyroclastic-flow surface (rilling and gullying) vs. non-channelized erosional processes (rainsplash and sheetwash) from volume estimates of the newly developed rill and gully network. In later years, all erosion on the pyroclastic-flow surface was measured together.

These erosional processes operate on different spatial and temporal scales. As sources were depleted or stabilized, other erosional processes came to dominate sediment yield. The spatial scale of this study made it impossible to measure finer-scale processes like rainsplash and sheetwash directly, so these processes were measured in bulk along with other erosion on the pyroclastic-flow deposit surface. Measurements could only be made once a year, masking the complex patterns of erosion and deposition occurring within valleys. However, the spatial and temporal scales should be adequate to determine the balance of valley erosion vs. erosion on the pyroclastic-flow surface and how that balance shifted on an annual scale for the first three rainy seasons following the eruption. Where possible, erosion from different environments was monitored for the entire decade, providing a better understanding of the source of elevated sediment yields in the latter half of the decade.

Total sediment yields were compiled or calculated through 2001 to examine how sediment yields changed over a decadal time scale. This long-term sediment yield record was compared with that from the Toutle River at Mount St. Helens, the closest analog to rivers at Mount Pinatubo. The Toutle River received  $2.83 \times 10^9 \text{ m}^3$  of sediment in the 1980 eruption, most from a massive debris avalanche ( $2.50 \times 10^9 \text{ m}^3$ ) (Janda et al., 1984; Simon, 1999). This is twice as much material as was emplaced in the Pasig-Potrero and Sacobia River basins, but the Toutle River basin is much larger ( $1300 \text{ km}^2$  vs.  $64 \text{ km}^2$ ). Most of the disturbance was in the North Fork Toutle River basin which received the debris avalanche and all pyroclastic-flow deposits.

Many of the same erosional processes at Mount Pinatubo were important in the Toutle River basin but not all were important to the same degree, primarily because the volume and depth of hot pyroclastic-flow deposits at Mount Pinatubo were much greater than at Mount St. Helens. The differences between type and volume of eruptive deposits and the magnitude and importance of erosional processes led to patterns of long-term sediment yield on the Pasig-Potrero/Sacobia basin and the Toutle River basin that initially look quite different. However, these differences may be related to decay time scales. Taking these decay time scales into account, predictions of future sediment

yields on the Pasig-Potrero and Sacobia River basins were made based on trends from the Toutle River at Mount St. Helens.

### **Methods**

Previous studies of sediment yield at Mount Pinatubo have approached the problem from both erosional and depositional viewpoints. Initially, most of the sediment was transported through lahars, so mapping lahar deposits was a viable technique for measuring sediment yield. Umbal (1997) compiled field measurements from PHIVOLCS through 1995 based on lahar deposit surveys. Tuñgol (2002) extended these measurements through 1997 on the Pasig-Potrero River based on deposit mapping and acoustic flow monitoring of lahars. JICA (1996), Daag (1994; 2003) and Daag and van Westen (1996) took the upstream approach and measured erosion volume by subtracting successive DEMs from before the eruption through 1994 -1996. This study followed the upstream approach, with erosion volume measured by subtracting successive DEMs in the Sacobia and Pasig-Potrero watersheds. Erosion volumes were coupled with geomorphic terrain maps to determine source areas and thereby infer the processes responsible for erosion.

Sediment budgets were derived from a series of digital elevation models (DEMs), multispectral satellite imagery, and published geomorphic terrain maps (Daag and van Westen, 1996). The data resolution and quality varies between years, and efforts were made to maintain consistency between years while utilizing the best possible resource available for that year. Field observations and surveys starting in 1996 along both the Pasig-Potrero River and the Sacobia River were used to help constrain sediment yields in the latter half of the decade.

### **Data sources**

#### ***Digital elevation models and multispectral imagery***

Pre-eruption DEMs were produced by the Japan International Cooperation Agency (JICA) in 1980. Immediately following the eruption, the pyroclastic-flow surface was mapped by Daag and van Westen (1996) at 20-meter resolution based on a



series of oblique air photos. Combined, these two DEMs give a measure of the volume of pyroclastic-flow deposits in the Pasig-Potrero and Sacobia River basins. These two DEMs are referred to as PreErupt and PostErupt.

Two sets of DEMs were available in the years after the eruption. JICA produced DEMs from 1:15000 scale air photos, digitized at 20-meter resolution. The second set of DEMs were derived by Daag and van Westen (1996) from the same air photos to estimate erosional volumes from the pyroclastic-flow fan. Thus, valley locations, widths, and depths were measured and plotted carefully, but smaller changes in the pyroclastic-flow deposit surface were not mapped. No changes in the uplands were mapped.

These two sets of post-eruption DEMs were created from photos in November 1991, October 1992, and March-April 1994. They thus represent the landscape following each of the first three lahar seasons (1991, 1992, and 1993). JICA DEMs (j-series) are only available for 1992 and 1994 (Post-92j, Post-93j). The simplified valley map series (dvw-series) (Daag and van Westen, 1996) is available for all three years (Post-91dvw, Post-92dvw, and Post-93dvw).

There are systematic problems with both DEM sets. The dvw-series does not include any changes across the uplands or on the fan surface. The j-series does include the entire landscape, but has problems with vertical accuracy. I compared the uplands for each year by removing the pyroclastic-flow area and a 300-meter buffer around it and found an offset of 8 meters between 1992 and 1994. Although some discrepancy is expected as hillslope tephra is eroded, an overall change of 8 meters is too high (average airfall tephra deposit depth was 0.5 m). After adjusting for this offset, the volume change from 1992 to 1994 is consistent between the two data sets.

For the latter half of the decade following the eruption, the primary source for elevation data are two TOPSAR (Topographic Synthetic Aperture Radar) DEMs from November 1996 and September 2000. TOPSAR has a resolution of 5 to 10 meters in the horizontal but contains many holes, especially in areas of steep topography, and there are systematic biases in the vertical leading to errors of more than 50 meters at the alluvial fan head. In addition to TOPSAR data, I used an ASTER (Advanced

Spaceborne Thermal Emission and Reflection Radiometer) multispectral image (15-m resolution) and DEM (30-m resolution) from December 28, 2001. Because the DEM had only 30-m resolution, there were inaccuracies in valleys with narrow widths. I used TOPSAR data to map out the edges of valleys in 1996 and 2000, and the TOPSAR data combined with the ASTER imagery to map geomorphic terrain units in 2000-2001.

The ASTER multispectral image from 2001 and a Landsat Thematic Mapper multispectral image from April 2, 1993, were used to compare vegetation recovery across the landscape. Normalized Difference Vegetation Index (NDVI) classifications were computed using the standard formula:

$$NDVI = \left( \frac{IR - R}{IR + R} \right) \quad (2.2)$$

where  $IR$  and  $R$  refer to the near-infrared and red bands, respectively. The NDVI results were subdivided based on terrain boundaries to examine vegetation differences between geomorphic terrains.

### ***Geomorphic classification***

Combining DEMs and vertical and oblique air photos, Daag and van Westen (1996) mapped geomorphic terrain units for conditions pre-eruption, post-eruption, and following the first three lahar seasons. These terrain maps show the location of pyroclastic-flow terraces, valley-bottom deposits, valley slopes, impounded lakes, and secondary-explosion craters or scars. The secondary-explosion terrains represent areas impacted by significant secondary explosions in the pyroclastic-flow deposits that were still discernible at the end of the rainy season, providing a lower bound to the role of secondary explosions in landscape modification.

To compare conditions at the end of the decade with conditions at the end of 1993, I generated another terrain map using the 2000 TOPSAR and 2001 ASTER data (Figure 2.2). This terrain map included an additional unit for lahar terraces stranded well above the active valley bottom. Because the early terrain maps and the later map

were created using different data (air photos vs. multispectral imagery) and by different people, there may be some mapped changes related more to these external factors than in actual changes in the terrain, although all efforts were made to keep these errors to a minimum. Between 1993 and 2001, the area covered by mapped terrain units dropped by  $4.3 \times 10^6 \text{ m}^2$ , a difference of 17%. Of this,  $3.1 \times 10^6 \text{ m}^2$  of the terrain loss occurred in the upper basin, as some area mapped as pyroclastic-flow surface in 1993 was indistinguishable from the vegetated uplands by 2001. Excluding these areas, the total area mapped in terrain units changed by 5%. This is a reasonable minimum bound on errors in the 2001 terrain map due to differences in operator and data source.

Erosion and sediment redistribution led to significant changes in the drainage network and basin boundaries through time. Some of the most significant changes to the drainage network included the capture of the Abacan catchment by the Sacobia River in April 1992, the capture of the upper Sacobia catchment by the Pasig-Potrero River in October 1993, and the redirection of flow from the Papatak branch into the Timbu branch of the Pasig-Potrero River in July 1994 (Figure 2.3) (Punongbayan et al., 1994; Torres et al., 1996; Tuñgol, 2002; Daag, 2003). To standardize between years, I used tributary-basin delineations from spring 1994 for all measurements. For measurements along the mainstem channel, I divided the channel into five segments: Papatak, Timbu, Sacobia, North Upper Basin, and South Upper Basin. These five segments acted as the primary conveyers of water and sediment throughout the decade, although the connections between these channel segments changed from year to year due to stream capture. The entire basin area was subdivided into three units delineating the upper, middle, and lower portions of the Pasig-Potrero/Sacobia basin upstream of the alluvial fan head. These subdivisions best capture the major differences in terms of sediment emplacement and erosional and depositional processes following the eruption. The Abacan basin (as of spring 1994) was excluded from this study; the main sub-basin in the Abacan River watershed with pyroclastic-flow deposits from the 1991 eruption became part of the Sacobia River in April 1992.

### **Sediment yield**

Sediment yields on the entire Sacobia-Pasig-Abacan system were compiled through 1995 by Umbal (1997) and extended on the Pasig-Potrero River through 1997 by Tuñgol (2002). After the stream capture event in October 1993, the Pasig-Potrero River carried the majority of the sediment out of the Sacobia-Pasig-Abacan system, so measurements continued only on the Pasig-Potrero River. I extended the record of sediment yield through 2001 by measuring volume changes on the Pasig-Potrero River given changes in valley area and bed elevation on the upper alluvial fan.

Following the last major lahar in 1997, up through 2001, deposition on the alluvial fan occurred predominantly from normal streamflow within an entrenched valley. Valley area was mapped in 1996 and 2000 using TOPSAR data. Bed elevation changes at Delta 5 and the Mancatian-Manibaug crossing, 7.4 km downstream, were measured through field observations and repeat photography. Using Hayes et al.'s (2002) calculated estimate that 80% of the sediment in transport at Delta 5 deposits before Mancatian, I estimated the volume of sediment transporting past Delta 5 for 1997-2001 from the volume deposited. An additional volume deposited between Delta 5 and the Hanging Sabo site, 2.5 km upstream was calculated to estimate the proportion of sediment leaving the uplands that reached the Delta 5 site.

### **Quantifying rates of erosion by environment**

Total annual erosion in the Pasig-Potrero/Sacobia basin was measured each year from 1991 – 1993 through straightforward subtraction of successive DEMs. Determining where the sediment was derived and what processes were responsible for the erosion required combining DEMs with terrain maps and field observations. Erosion in five different environments was measured including valley-bottom incision, valley-wall retreat, channel network extension, sediment mobilization from secondary explosions, and bulk erosion of the pyroclastic-flow surface through rainsplash, sheetwash, or channelized flow in channels too small to be mapped (< 20 meters). While the main sediment transport mechanism out of the basin was lahars, and many

processes were enhanced during lahars (e.g. valley incision, valley-wall collapse, and secondary explosions), this study does not consider lahars as a separate source.

I used pairs of DEMs, subtracting successive years (PostErupt – Post91, Post91 – Post92, and Post92 – Post93). The “differenced DEMs” display negative values in erosional zones and positive in depositional zones. Terrain maps by Daag and van Westen (1996) were used to delineate geomorphic terrains in the 1991, 1992, and 1993 lahar seasons. All of the area mapped as a single type of geomorphic terrain was used to create a mask layer. This mask was then used with the differenced DEMs to measure volume changes only within the area mapped as a particular terrain. In general, terrain maps for the later year were used, showing erosion that led to the creation of that particular terrain unit. Any exceptions are noted.

For example, to measure erosion on pyroclastic-flow surfaces during the 1993 lahar season, areas mapped as pyroclastic-flow deposit terrain in 1993 were masked over the differenced DEM created by taking Post92j – Post93j. The resulting map shows where and how much erosion occurred in pyroclastic-flow deposit terrains in 1993.

Measuring valley erosion required extra steps to separate out valley widening, valley incision, network extension, and sediment mobilized by large secondary explosions. Erosion from secondary explosions was considered a form of valley erosion because most secondary explosions occurred on the edges of valleys, contributing to changes in valley morphology. Sediment mobilized by large secondary explosions was measured in a similar way to pyroclastic-flow surface erosion by masking 1993 secondary-explosion terrain over a differenced DEM.

Combined erosion from valley incision, widening, and extension was measured by taking area mapped as valley or valley slope terrain in 1993 and masking these areas over the differenced DEM to create a map showing volume change in these terrains. To separate out network extension, area mapped as valley or valley-slope terrain in 1992 was compared to 1993. Any area of network growth was mapped separately and masked over the new valley change map. To measure valley incision, area mapped as valley terrain in 1992 was masked over the valley change map. Any remaining area in

the valley-change map after accounting for valley incision and network extension was attributed to valley widening. Figure 2.4 shows the results for this example, using the j-series DEMs to map erosion in 1993.

Erosion volumes were calculated using both the dvw-series and the j-series DEMs where possible. However, erosion on the pyroclastic-flow surface was only mapped using the j-series DEMs. Erosion of the pyroclastic-flow surface was measured for 1991 and 1992 combined by subtracting Post92j from PostErupt. This volume was then split into individual years, with 67% going to 1991 and 33% to 1992. This 2:1 ratio was based on the ratios of total annual sediment yield as measured by Umbal (1997) (210:110 million m<sup>3</sup>) and JICA (1996) (250:110 million m<sup>3</sup>). All other erosion is categorized as valley erosion, so the dvw-series DEMs were appropriate. In 1993, volume changes were taken as an average of results from the dvw-series and the j-series DEMs. Valley erosion in 1991 and 1992 was measured from dvw-series DEMs only.

A separate measure of valley widening was made through direct measurements of valley width, calculated every 100 meters along all five major river segments for 1991, 1992, 1993, 1996, and 2000. As these width measurements do not include information on valley-wall heights, erosion volumes cannot be measured directly. For 1991 to 1993, valley-wall heights were backcalculated from the volume eroded and the valley width change, and these heights were used to estimate erosion volume from valley widening in later years where adequate repeat DEMs are not available.

## Results

### Sediment yield

In 1997, sediment yield due to low-flow fluvial transport at Delta 5 was estimated at  $11 \pm 3$  Mg/yr, of which 80% was deposited before reaching the Mancatian-Manibaug river crossing, 7.4 km downstream (Hayes et al., 2002). Hayes et al. (2002) estimated 5 m of net aggradation at Delta 5 in the 12 months following the last major lahar on the Pasig-Potrero in August 1997. Based on field observations, the bed at Delta 5 aggraded 15 m from 1998 – 2000 and an additional 2 m during 2000 – 2001. From 2000 – 2001, the bed elevation at Mancatian changed by  $< 1$  m, so I assume zero

aggradation for our estimates. Valley areas calculated off of TOPSAR DEMs were  $2.5 \times 10^6 \text{ m}^2$  in 1996, increasing to  $3.4 \times 10^6 \text{ m}^2$  in 2000. Because the valley actually widened from 1996 – 2000, sediment was generated locally and added to the load in transit. Thus, sediment yield must account for deposition in the valley bottom minus erosion of valley walls. Allowing the width to change linearly from year to year and subtracting the volume eroded at the valley walls from the volume deposited gives sediment yields at Delta 5 ranging from  $5.9 - 7.3 \times 10^6 \text{ m}^3/\text{yr}$  for rainy seasons 1998 – 2000, dropping to  $1.5 \times 10^6 \text{ m}^3/\text{yr}$  in 2001. These volumes have been adjusted to account for throughput at Mancatian, estimated at 20% of the volume measured at Delta 5 by Hayes et al. (2002).

Delta 5 was not the upper end of the depositional regime. The Hanging Sabo site, 2.5 km upstream of Delta 5, aggraded an average of 3 m/yr from 1997 – 2001. From 1998-2000, 27-33% of the sediment in transport at the upstream site was deposited before reaching Delta 5. This number increases to 57% in 2001. Thus, the actual sediment volume in transport from the upper basin was  $7.7 - 10.2 \times 10^6 \text{ m}^3/\text{yr}$  from 1998 – 2000, dropping to  $3.2 \times 10^6 \text{ m}^3/\text{yr}$  in 2001. Since even more aggradation was occurring upstream of the Hanging Sabo, these numbers represent a lower bound for sediment yield over this time period. In addition, these figures account only for sediment transport on the Pasig-Potrero River, not the Sacobia River. The Sacobia River contribution may no longer be negligible.

Sediment yields in both the Pasig-Potrero/Sacobia River basin and the Toutle River basin peaked in the first or second year following the eruption and then declined nonlinearly (Figure 2.5). Given that sediment yields initially declined exponentially, I used an exponential decay function (Equation 2.1) as a base function and then tested if the function worked on a decadal scale to model long-term sediment yields. If not, what variations were required to adequately model sediment yields in the decades following the eruption?

Annual sediment yields on the Toutle River decayed exponentially for 5-6 years, then leveled off at a rate 10-100 times higher than background levels on unaffected rivers (pre-eruption sediment yield was not measured). Thus, a simple exponential

decay function does not fit the data for more than 5-6 years. An exponential function that decays to an elevated plateau does capture the trends in the data ( $R^2 = 0.95$ ,  $P < 0.0001$ ):

$$Q_s = 2.3 \times 10^8 e^{-0.67t} + 2.7 \times 10^6 \quad (2.3)$$

For the Pasig-Potrero/Sacobia River, sediment yields declined exponentially for the entire period of record, thus a simple exponential decay model works well for at least the first ten years ( $R^2 = 0.92$ ):

$$Q_s = 3.7 \times 10^8 e^{-0.41t} \quad (2.4)$$

When the last sediment yield measurements were made in 2001, however, sediment yields were still 20 times higher than pre-eruption yields. A function similar to that on the Toutle River, with yields declining to an elevated plateau works just as well as a simple exponential decline for the ten years of record, so it is impossible to tell which model will best fit the data over the next decade. Sediment yields on the Pasig-Potrero/Sacobia River simply may not have reached the elevated plateau yet. Ten years of sediment yield data are not enough to determine the long-term pattern.

Because sediment yields in the Pasig-Potrero/Sacobia basin declined exponentially, there was also an exponential decay in storage,  $S_t$ , approaching a lower bound of  $5.1 \times 10^8 \text{ m}^3$  ( $R^2 = 0.99$ ) (Figure 2.6):

$$S_t = 7.7 \times 10^8 e^{-0.32t} + 5.1 \times 10^8 \quad (2.5)$$

This lower bound represents the volume of sediment that will remain in place for many decades to come. On the Toutle River, a similar pattern developed with an exponential decline in storage as sediment is removed. However, because sediment yields were still elevated, the volume in storage declined exponentially to a declining background rather than a plateau ( $R^2 = 0.98$ ):



$$S_t = (1.8 \times 10^8 e^{-0.60t}) + (2.66 \times 10^9 - 3 \times 10^6 t) \quad (2.6)$$

After the initial exponential decay, the portion removed from storage each year ( $3 \times 10^6 \text{ m}^3$ ) was the average sediment yield from 1986 - 1999.

In the first three years after the eruption, sediment yields based on total volume removed from the uplands were calculated from DEM subtractions in the Pasig-Potrero/Sacobia basin, as well as for the upper, middle, and lower basin zones individually. Sediment yields for all four catchments decayed exponentially for the first three years. The initial decay rate was inversely correlated with the original volume of eruptive material (Figure 2.7), measured as the average depth of deposit. The Toutle River falls along the same trend. As emplacement depth increases, the decay constant approaches zero, leading to a more prolonged period of high sediment yields.

Because the data are scarce, the relationship between disturbance depth and the decay coefficient could be fit statistically by a number of different regressions. However, the simplest option, a linear regression, works well for combined data from the Pasig-Potrero/Sacobia and the Toutle River. The best-fit linear regression line is

$$\varepsilon = -0.02d + 1.5 \quad (2.7)$$

where  $\varepsilon$  is the exponential decay coefficient for sediment yield and  $d$  is the average deposit depth in the basin ( $R^2 = 0.85$ ,  $P = 0.02$ ). Hillslope tephra was not included in the deposit volume or area. The highest estimates of deposit depth for three other basins at Mount Pinatubo fit well with the regression line in equation 2.7. While the statistical parameters in this regression may vary from eruption to eruption, the inverse relationship between deposit size and decay rate should hold, with larger volumes decaying over a longer time scale.

## Erosion rates

Erosion rates for five different processes were measured in each of the first three rainy seasons following the eruption, with estimates of valley widening continuing through 2000. I first present the total erosion rates, how they changed with time, and how they varied by location within the basin. Next, total erosion rates are divided into valley erosion and surface erosion within each basin zone. Then valley erosion is subdivided further by process (valley incision, valley wall retreat, network extension, and erosion by secondary explosions). Finally, the dominant process of valley wall retreat and widening is explored through 2000.

Total erosion rates, compiled by summing up erosion volumes each year from all five processes compare favorably with previous measurements of total erosion (JICA, 1996; Daag, 2003) and with measurements of sediment yield derived from volumes of lahar deposits (Umbal, 1997) (Table 2.1). The difference between this study and Daag (2003), which used the dvw-series DEMs, is due to erosion on the pyroclastic-flow surface which was measured here using j-series DEMs. Erosion of hillslope tephra in the uplands was not measured, but it was a minor fraction of the total sediment flux. Even if all of the tephra eroded in 1991, it would occupy < 10% of the lahar volume for that year (Tuñgol, 2002).

Total erosion was subdivided by zone within the basin (Table 2.2). The middle basin received the greatest sediment load by volume and per unit area. The material was distributed with 27% of the area of pyroclastic-flow deposit < 25 meters deep, 34% between 26 and 75 meters, and the remaining 39% > 75 meters depth (Figure 2.8). The upper basin had the same distribution but a lower overall sediment load. The lower basin had thinner deposits overall, with 50% of the deposit area < 25 meters deep, and 80% of the deposit < 50 meters deep.

In all areas, deposit depletion due to erosion followed an exponential decline for the first three lahar seasons, but the decay rate differed by a factor of four depending on position within the basin (Figure 2.9). The middle basin, which received the highest volume of sediment in the eruption ( $8.19 \times 10^8 \text{ m}^3$ ), had the lowest decay rate (0.12). The upper basin had a higher decay rate of 0.31 and received less sediment ( $3.27 \times 10^8$

m<sup>3</sup>). The lower basin had the lowest sediment loading ( $1.24 \times 10^8$  m<sup>3</sup>) and the highest decay rate (0.48). While these values do not explicitly account for redeposition of material in lower parts of the basin, net redistribution of sediment was measured in DEM subtractions of successive years. In 1993, for instance, valley incision was positive in the lower basin, indicating net addition rather than removal of material.

As early as the first rainy season after the eruption, channelized flow played a major role in eroding pyroclastic-flow deposits. Erosion on the pyroclastic-flow surface in 1991 was  $8.6 \times 10^7$  m<sup>3</sup>, of which potentially half, or  $4.4 \times 10^7$  m<sup>3</sup> (Tuñgol, 2002), was directly attributable to rill erosion. The remaining 49% was eroded through a mix of rainsplash, sheetwash, and secondary hydroeruptions. Because erosion on the pyroclastic-flow surface only accounted for 34% of all erosion in 1991, non-channelized flow created at most 16% of the total erosion in 1991. Erosion on the pyroclastic-flow surface slowly declined in importance, dropping from 34% of the total erosion volume to 30% by 1993. In early 1993, pyroclastic-flow surfaces were still bare, but by 2001 the NDVI assessment showed substantial vegetation recovery, far exceeding vegetation recovery in the valley bottom (Figure 2.10).

Although channelized flow dominated in all portions of the basin, the balance of pyroclastic-flow surface erosion and valley erosion varied (Figure 2.11). In the upper basin, valley:surface erosion ratios ranged from 0.7 to 2.6 with valley erosion increasing in proportion. Valley erosion in the middle basin was 2.0 to 4.0 times greater than pyroclastic-flow surface erosion, also increasing through time. The lower basin was completely dominated by valley erosion.

Partitioning valley erosion into different processes including valley incision, widening, network extension, and secondary explosions in 1992 and 1993 shows that most valley erosion was achieved through valley widening, particularly in the middle and upper basins where sediment released through valley widening contributed 62-81% of the total valley erosion (Figure 2.12). Valley widening was accomplished through a combination of gravitational mass wasting and secondary explosions too small to be mapped. Erosion from large secondary explosions was measured separately. Network extension played a minor role in all cases, with a maximum contribution of only 5.5%

of the valley erosion. In the lower basin, there was a more even division between valley incision, valley widening, and secondary explosions, with each mechanism causing at least 30% of the valley erosion. Secondary explosions peaked in 1992, when they mobilized and removed at least  $3.1 \times 10^7 \text{ m}^3$  of sediment, although this was still less than half the amount attributed to valley widening ( $6.5 \times 10^7 \text{ m}^3$ ).

Overall, valley widening was responsible for approximately half of all erosion in the Pasig-Potrero/Sacobia system: 43% in 1992 and 52% in 1993. Since valley width was readily measurable off TOPSAR data in 1996 and 2000, changes in valley width could be tracked every 3-4 years for the entire decade to see if valley widening persisted (Figure 2.13). From 1991 to 1993, the middle basin showed the greatest increase in valley width, more than tripling in size. Both 1992 and 1993 show significant increases in valley width. Valley width doubled from 1991 to 1993 in the middle basin, while in the lower basin the width increased 24%. These increases mirror measurements of volume change due to valley widening, with substantial volumes in the middle and upper basins ( $1.7 - 4.1 \times 10^7 \text{ m}^3$ ) and smaller volumes from the lower basin ( $< 1 \times 10^7 \text{ m}^3$ ).

Valleys widths actually narrowed from 1993 through 1996 for all reaches in the upper and middle basins. In the lower basin, the average width decreased, but three reaches widened or had no change in valley width. From 1996 to 2000, the lower basin widened considerably, reaching up to four times the 1991 width. In the middle basin, all areas except the upper Sacobia widened by an average of 29%. The upper basin was mixed with half of the reaches expanding while the other half narrowed. The end result was an average width increase of  $< 5\%$ . Volume estimates based on changes in terrain area multiplied by the average valley height (back-calculated from 1993 erosion volume data), show substantial erosion attributed to valley widening in both the middle and lower basins, with minimal erosion in the upper basin. Although the total volume is less reliable due to the large time gap and the possibility for a change in the average depth eroded, the volume change attributed to valley widening from 1993 to 2000 using this method is  $9.2 \times 10^7 \text{ m}^3$ , which is 31% of the total sediment yield from 1994 – 2000.

## Discussion

### **Erosion patterns in the Pasig-Potrero/Sacobia basins**

Erosional processes varied in importance following the 1991 eruption of Mount Pinatubo. This section covers the evolving spatial and temporal patterns of erosion from different processes including surface erosion on the pyroclastic-flow deposits; valley erosion from widening, incision, and extension; and the role of secondary explosions on valley widening and sediment generation overall.

As early as the first rainy season after the eruption, channelized flow played a major role in eroding pyroclastic-flow deposits. Immediately following the climactic eruption, mainstem channels began to re-establish themselves through headward erosion. Rill networks developing on the surface of new pyroclastic-flow deposits soon linked with main channels, often leading to dramatic head cuts  $> 10$  m in height (Scott et al., 1996a). In 1991, non-channelized flow on the pyroclastic-flow surface contributed at most 16% of the total sediment load. The rest was produced by channelized flow or through mass wasting or secondary explosions along valley walls.

Between 1991 and 1993, erosion on the pyroclastic-flow surface declined 71% in the upper basin and 36% in the middle basin. In the middle basin, this decline can be explained completely by a decrease in the available area as terrain mapped as pyroclastic-flow deposit was converted into valley or valley-slope terrain (Figure 2.14). In the upper basin, the shift from pyroclastic-flow deposit to valley terrain cannot explain the magnitude of the decrease in erosion on the pyroclastic-flow surface. Instead, the decline is due to hydrologic and surface alterations. The first year after the eruption, erosion on the pyroclastic-flow surface occurred through rainsplash and sheetwash as well as rill and gully development as the channel network formed. Rill development proceeds rapidly at first, then slows, as rills armor and rill long profiles adjust (Graf, 1977; Parker, 1977; Howard, 1999). At Mount St. Helens, sediment production from rills in hillslope tephra essentially shut down within two years of the eruption due to rill armoring and hydrologic changes on hillslopes (Collins and Dunne, 1986). Although rill formation on steep hillslopes may differ from network development on the low-gradient flow deposit surface, it shows how rapidly rill

armorings can develop. In the middle basin, incision and aggradation on the mainstem kept tributary gullies active, as gully profiles continued to adjust to changing base level conditions. At the headwaters in the upper basin, however, these base-level fluctuations were less severe, and so rill and gully networks could stabilize more rapidly. In the downstream end of the upper basin, large fluctuations in base level continued, but these areas were mostly converted to valley or valley-slope terrain by 1993.

From 1993 to 2001, area mapped as pyroclastic-flow deposit terrain decreased 33% while vegetation density in the deposits increased. Despite repeated burial from secondary-explosion ash columns, the uplands were thickly vegetated within the first decade after the eruption. By 2001, vegetation density on pyroclastic-flow surfaces was approaching the same vegetation density as the uplands, far exceeding any vegetation growth in the valley bottom (Figure 2.10). Both the loss of area and increasing vegetation density contributed to the declining importance of erosion on the pyroclastic-flow surface.

The role of valley erosion from 1991 to 1993 varied depending on position within the basin and the volume of initial sediment loading. Due to a paucity of initial pyroclastic-flow deposits in the lower basin outside of the main valleys, essentially all of the erosion there was related to valley processes. In the upper basin, near the headwaters, valleys are not as wide, so many channels remained classified as pyroclastic-flow deposits simply because they were not large enough to leave the classification of gully and reach the classification of valley or valley slope. Thus, in the upper basin, the role of valley erosion vs. pyroclastic-flow surface erosion was evenly divided. Valley erosion was gaining in importance through time as network extension and valley growth expanded farther into pyroclastic-flow terrains. In the middle basin, extensive pyroclastic-flow fan deposits led to large areas covered by pyroclastic-flow material away from mainstem valleys. Yet even there, valley erosion outpaced surface erosion on the pyroclastic-flow deposits by a factor of two to four, due to deep entrenchment of valleys followed by valley widening in areas with steep, high cliffs. Sediment released by valley widening accounted for half of all erosion in the middle basin in 1992 and 1993.

From 1994 to 2000, erosion from valley widening contributed as much as 31% of the total sediment yield from the Pasig-Potrero and Sacobia basins. Valley widening will continue to contribute sediment to the fluvial system as long as unstable cliffs remain, although rates should diminish as valleys widen and the channel has less access to talus at the base of cliffs. A simple random-walk model, with periodic resetting events (equivalent to large storms that reset the channel to the middle of the valley) shows a nonlinear decline in valley-channel interactions as valleys widen (Figure 2.15). A survey in 2001 of 9 km of channel upstream from Delta 5 showed that approximately 75% of the valley still contained unstable exposures of pyroclastic-flow or lahar deposits on at least one side of the valley, so as of 2001, valley walls still represented a significant potential sediment source.

Mass wasting of valley walls contributed to a high number of secondary explosions from the hot, pyroclastic-flow deposits, widening valleys further. Secondary explosions continued throughout the entire decade, although they diminished in size and importance after 1994 (Figure 2.16). A simple weighting scheme based on ash column height shows that the importance of secondary explosions declined exponentially through time. In addition to directly mobilizing sediment, secondary explosions also initiated stream captures. The large spike in sediment yield in 1994, up 43% from 1993 (Umbal, 1997), is directly attributable to the October 1993 stream capture initiated by a secondary explosion (Punongbayan et al., 1994) in which the Pasig-Potrero River captured the upper half of the Sacobia River basin. The sudden increase in discharge and sediment supply increased the number and magnitude of lahars in that channel. Estimates of lahar volume on the Pasig-Potrero River in 1994 were 2.5 to 6 times higher than in 1993 (Tuñgol 2002). In this particular case, secondary explosions were indirectly responsible for a dramatic increase in sediment yield. More importantly, the focus of the deposition switched from the lower Sacobia River to the lower Pasig-Potrero River, overwhelming different downstream communities.

Both of the long-term erosional processes: valley-wall retreat and secondary explosions, were important contributors of sediment primarily because of the presence of thick, hot pyroclastic-flow deposits. Mass wasting in deeply entrenched valleys

generated significant volumes of sediment because cliffs were tens of meters high. Secondary explosions triggered by valley wall collapse in hot deposits increased the rate of valley wall retreat. Secondary explosions not only enhanced sediment yields; they also complicated sediment yield predictions and hazard zone delineations.

### **Comparison of the Pasig-Potrero/Sacobia Rivers with the Toutle River**

The Toutle River at Mount St. Helens offers the closest analog to rivers at Mount Pinatubo in terms of sediment loading and basin disturbance during an eruption, coupled with modern measurement techniques. The North Fork Toutle River, in particular, had a similar magnitude of sediment loading although most of it was cold debris-avalanche material rather than hot pyroclastic-flow deposits.

At Mount St. Helens, valley widening and incision were important immediately following the eruption. In 1980, sediment yields from valley processes were dominated by valley incision as main stem channels reestablished (Pearson, 1986). In 1981, hillslope erosion peaked, contributing  $4.7 \times 10^6 \text{ m}^3$  of sediment to the Toutle River, but this was overwhelmed by the  $2.4 \times 10^7 \text{ m}^3$  of material generated in the debris avalanche deposits from valley widening, incision, and network extension (Pearson, 1986). By 1982, most of the sediment being eroded at Mount St. Helens came from in-channel and near-channel sources, with stream bank erosion and streamside debris slides and avalanches being the dominant sediment sources (Janda et al., 1984).

Continued high sediment yields on the Toutle River have been attributed to ongoing channel instability and stream bank collapse in tributaries that had significant channel disturbance during the 1980 eruption like the North Fork Toutle and the South Fork Toutle Rivers (Major et al., 2000). Other channels within the Toutle River basin like the Green River were impacted primarily through the deposition of hillslope tephra rather than significant alterations to the main channel. Sediment yields on the Green River declined exponentially, returning to background levels within five years after the eruption. Major et al. (2000) attribute the difference in long-term sediment yields between the Green River and the North and South Forks of the Toutle River to differences in channel disturbance.



There are some important differences between valley-wall collapse at Mount Pinatubo and channel-bank collapse at Mount St. Helens. Valley-wall collapse mobilized less sediment at Mount St. Helens because deeply entrenched valleys occupy a much smaller area, and valley depths are much less. In addition, most valley growth through new eruptive deposits was in cold debris-avalanche deposits rather than in hot pyroclastic-flow deposits. Thus, secondary explosions from gravitational collapse of valley walls, which were important at Mount Pinatubo and contributed to valley widening there, were not important at Mount St. Helens. Secondary hydroeruptions did occur, primarily along the routes of pre-existing drainages buried by pyroclastic-flows in the North Fork Toutle River basin (Moyer and Swanson, 1987; Simon, 1999). These phreatic eruptions helped initiate the new drainage network, but they were not a major source of erosion. Secondary explosions appear to be an active mechanism for mobilizing sediment post-eruption only in large eruptions with voluminous hot pyroclastic-flow deposits such as the 1991 eruption of Mount Pinatubo or the 1912 eruption at the Valley of Ten Thousand Smokes in Alaska (Hildreth, 1983; Torres et al., 1996).

Channel widening and stream-bank collapse are essentially secondary processes, occurring in the valley bottom, after the valley has been created. At Mount Pinatubo, the valleys were still widening a decade after the eruption. As this process declines in importance, channel-scale processes like stream bank collapse should account for an increasingly greater proportion of the overall sediment load. Observations show that in the dry season, when overall sediment inputs to the Pasig-Potrero River are low, channel consolidation and incision into valley-bottom deposits occurs. The incised channel has loose, unconsolidated, erodible banks that probably contribute the bulk of the sediment load to the channel system at these times.

One last process that contributed significantly to sediment yield in the Pasig-Potrero and Sacobia River basins was stream capture. Often triggered by secondary explosions (Torres et al., 1996), these stream captures ranged from minor rerouting of flow to massive reorganization of the drainage basin. The Toutle River did not experience massive stream captures of this nature. Although stream reorganizations of

the magnitude experienced at Mount Pinatubo are rare, other volcanoes have documented stream captures or watershed reorganizations during or shortly after eruptive episodes. For example, a stream capture at Glacier Peak, Washington, 13,100 yr B.P. caused the upper Sauk River to abandon its course towards the Stillaguamish River, rerouting all flow to the Skagit River (Mastin and Waitt, 2000). Lahar deposits from this time period are found in both rivers (Tabor et al., 2002). Lahars have also been invoked as the cause of a major shift of the Tjimanuk River, Indonesia (Tija, 1965), and shifts in the course of the White River, Washington (Vallance and Scott, 1997).

### **Long-term sediment yield**

Sediment yield following volcanic eruptions is commonly fit to an exponential or nonlinear decay function based on measurements in the first few years after an eruption (Hirao and Yoshida, 1989; Pierson et al., 1992; Punongbayan et al., 1994; Umbal, 1997). Mount Pinatubo was modeled the same way, with two separate assessments made by Pierson et al. (1992) after two rainy seasons and by Punongbayan et al. (1994) after four rainy seasons. If a decay curve is accurate, it offers a good prediction of how much sediment to expect, aiding downstream hazards assessments. Typically left unanswered is how long an initial exponential decay curve applies, or whether long-term sediment yields continue to follow a nonlinear or exponential decay model.

Given sediment yield records from the Pasig-Potrero and Sacobia Rivers, an exponential decay function does appear to fit the data for the entire decade following the 1991 eruption. It is important to note that the tail of this distribution is sensitive to the sediment yield estimates made from volumetric measurements in the upper alluvial fan, on the Pasig-Potrero River only. The last four sediment yield measurements are a conservative estimate of the total yield based on volume deposited in the Pasig-Potrero River only, with minimal throughput. Actual sediment yields may have been even higher.

A simple exponential decay in sediment yield on the Pasig-Potrero/Sacobia basin predicts that it will take approximately 20 years before sediment yields return to pre-eruption values. At that point,  $7.3 \times 10^8 \text{ m}^3$  of sediment will have eroded out of the uplands and been deposited on the alluvial fan or transported out of the system. This volume is equivalent to 60% of the pyroclastic-flow deposits emplaced by the eruption, although it includes hillslope tephra and any pre-eruption sediment mobilized during channel incision.

However, a similar plot showing sediment yield on the Toutle River at Mount St. Helens does not support this simple decay model prediction (Figure 2.5). On the Toutle River, sediment yields decayed more rapidly (decay coefficient of 0.67 vs. 0.41), leveling off after five years at a rate one to two orders of magnitude higher than background rates. The continued high sediment output is attributed to channel instability leading to on-going elevated rates of channel widening and bank collapse (Major et al., 2000). These elevated rates are expected to last until channel mobility decreases, perhaps through the growth of riparian vegetation.

The main difference in the pattern of long-term sediment yield between the Toutle River and the Pasig-Potrero/Sacobia River basins (i.e. the exponential decline to plateau vs. a simple exponential decline) reflects the dominance of different erosional processes leading to different decay rates. On the Toutle River, hillslope erosion, network extension, and valley incision and widening operated in the first few years, rapidly decaying to a background rate largely dependent on channel incision and bank collapse. On the Pasig-Potrero/Sacobia Rivers, the initial exponential decline includes processes with a longer decay time such as secondary explosions and valley widening. As valley widening processes decline in importance, and channel incision and bank collapse take over, it is expected that sediment yields on the Pasig-Potrero/Sacobia River basin will shift to a model similar to the Toutle River. Because the initial sediment loading was greater on the Pasig-Potrero/Sacobia River, and erosional processes with longer decay times dominated, sediment yields had not yet leveled off as of 2001. By analogy to the Toutle River, it is unlikely that sediment yields in the Pasig-Potrero/Sacobia basin will continue to decline exponentially at the same rate until pre-

eruption levels are reached, because channel banks are still unstable, and valley-bottom sources are plentiful.

If the Pasig-Potrero/Sacobia River basin follows the same trend as the Toutle River basin, with sediment yields leveling off at a rate one order of magnitude greater than pre-eruption values (JICA 1978), sediment yield should stabilize around 2005. The resulting sediment output would be  $1.4 \times 10^7 \text{ m}^3$  higher in the second decade after the eruption (2001-2010) compared to a continued exponential decline. Spread over the valley bottom from Hanging Sabo to Mancatian, this represents 3 m of deposition everywhere or a wedge 6 m thick at the Hanging Sabo site, 4.5 m at Delta 5, and 0 m at Mancatian. Observations from repeat photographs at Delta 5 show that 1.5 m of aggradation occurred from 2002 – 2005, which is on pace to reach 4.5 m of deposition by the end of decade.

### **Conclusions**

On the Pasig-Potrero and Sacobia Rivers, sediment yields followed an exponential decline for at least one decade following the 1991 eruption. Decay coefficients for the first three years both on the Pasig-Potrero/Sacobia basins and on the Toutle River at Mount St. Helens were inversely correlated with the initial amount of eruptive material. However, a simple exponential decay function alone is probably not adequate to describe long-term sediment yields in basins with significant channel disturbance. On the Toutle River at Mount St. Helens, for instance, continued channel erosion and bank instability have led to sediment yields that remained elevated one or two orders of magnitude above background rates for at least two decades (Major et al., 2000). This same trend is also anticipated on the Pasig-Potrero/Sacobia River basin, but as of 2001, sediment yields had not yet leveled off. Thick, hot, pyroclastic-flow deposits in the Pasig-Potrero/Sacobia River basins led to high rates of erosion from processes like valley wall retreat and secondary explosions. These erosional processes decay slowly leading to a lower overall decay coefficient and a longer time to transition away from the initial exponential decay as compared to the Toutle River.

The slower decay rate on the Pasig-Potrero and Sacobia Rivers is due to the presence of thick, hot pyroclastic-flow deposits and the ensuing erosional environment following the eruption. Like the Toutle River, erosion of hillslope tephra was minor compared to the volumes of sediment eroded from pyroclastic-flow deposits. Most of the erosion of the pyroclastic-flow deposits was due to valley incision, widening, and extension. At Pinatubo, valley-wall collapse in deeply entrenched valleys released large volumes of sediment. Secondary explosions triggered by gravitational collapse of valley walls were an additional mechanism for mobilizing sediment into the channel network. Both valley-wall collapse and secondary explosions continued for the entire decade after the eruption at Mount Pinatubo, diminishing through time. The importance of both was due to the presence of deep, hot pyroclastic-flow deposits filling major valleys.

As valley widening slows and erosion due to channel instability such as bank collapse grows in importance, sediment yields on the Pasig-Potrero and Sacobia Rivers should transition from an exponential decline to a constant elevated rate of background sediment yield. An elevated background rate only one order of magnitude above pre-eruption levels would lead to an additional 14 million m<sup>3</sup> of sediment transported in the second decade after the eruption. Sediment yields on the Pasig-Potrero and Sacobia Rivers would reach this transition around 2005. This is a fairly conservative estimate, using the lower-end estimate from the North Fork Toutle River, where yields in the 1990s measured 10 – 100 times higher than background rates from unaffected rivers (Major et al., 2000). Observations in the fall of 2005 show continued high rates of aggradation on the upper fan, indicating that sediment yields are still elevated. Long-term planning on the Pasig-Potrero and Sacobia Rivers needs to account for the possibility that sediment yields will probably remain elevated for decades.

**Table 2.1: Annual sediment yield, Pasig-Potrero and Sacobia basins ( $10^6$  m<sup>3</sup>/yr)**

	1991	1992	1993
<b>This study</b>	254	152	131
<b>JICA (1996)</b>	250	120	120
<b>Umbal (1997)</b>	210	110	100
<b>Daag (2003) †</b>	202	122	98
<b>Table 5.6</b>			
<b>Daag (2003) †</b>	202	98	98
<b>Table 5.4, a-series</b>			

†Units were reported as thousand m<sup>3</sup>. I assume units are actually million m<sup>3</sup>/yr.

**Table 2.2: Volume change\* by process, 1991 – 1993, for Pasig-Potrero and Sacobia basins ( $10^6 \text{ m}^3/\text{yr}$ ).**

	<b>Upper</b>	<b>Middle</b>	<b>Lower</b>	<b>Total</b>
<b>PFD Erosion<sup>†</sup></b>				
<b>1991</b>	-52.5	-34.2	0.5	-86.2
<b>1992</b>	-25.9	-16.8	0.3	-42.4
<b>1993</b>	-15.0	-22.0	-2.1	-39.1
<b>Secondary Explosions</b>				
<b>1991</b>	-0.8	-13.7	-1.7	-16.2
<b>1992</b>	-3.1	-18.8	-9.4	-31.3
<b>1993</b>	-3.8	-5.0	-1.4	-10.1
<b>Valley Widening</b>				
<b>1992</b>	-17.3	-40.8	-6.4	-64.6
<b>1993</b>	-27.7	-34.8	-5.9	-68.4
<b>Valley Incision</b>				
<b>1992</b>	-5.6	-3.9	-1.3	-10.8
<b>1993</b>	-5.7	-1.0	-3.0	-9.8
<b>Network Extension</b>				
<b>1992</b>	-0.09	-2.4	0	-2.5
<b>1993</b>	-1.5	-2.4	0.2	-3.7
<b>Valley Incision, Widening, and Extension</b>				
<b>1991</b>	-39.2	-54.4	-58.0	-151.5

\*Negative values indicate net erosion, and positive values indicate net deposition.

<sup>†</sup>Erosion on the pyroclastic-flow deposit (PFD) surface

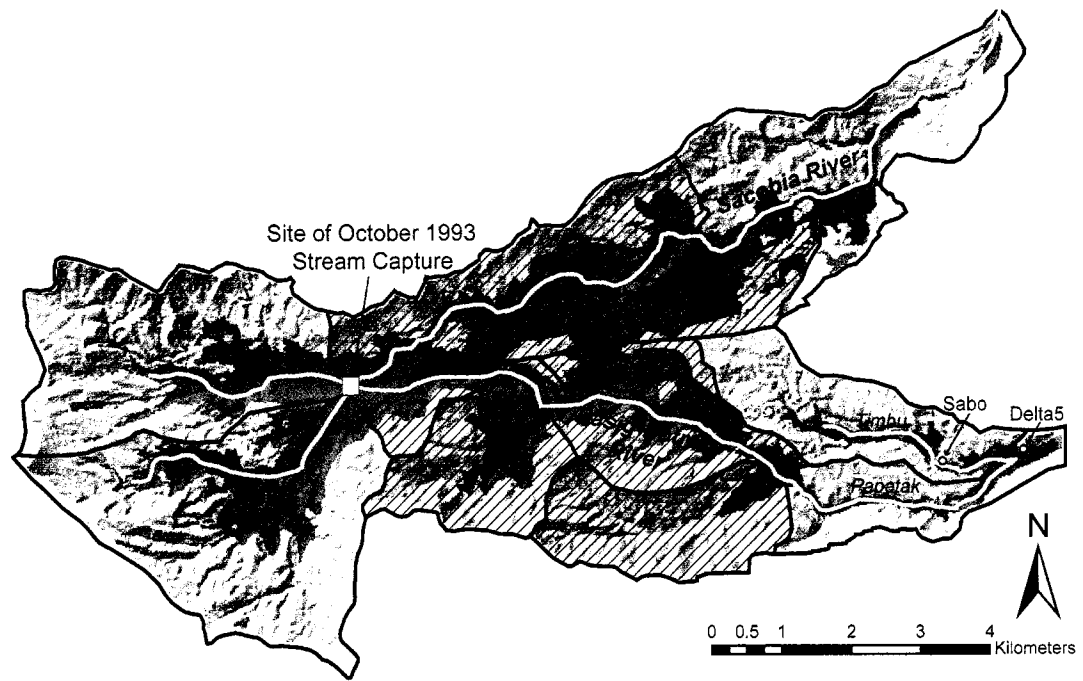


Figure 2.1: Map of Sacobia and Pasig-Potrero basins, with drainage divides and channel locations from spring 1994. Upper, middle, and lower basin divisions are marked, with the middle basin in hatches. The extent of pyroclastic-flow deposits is shown in red.



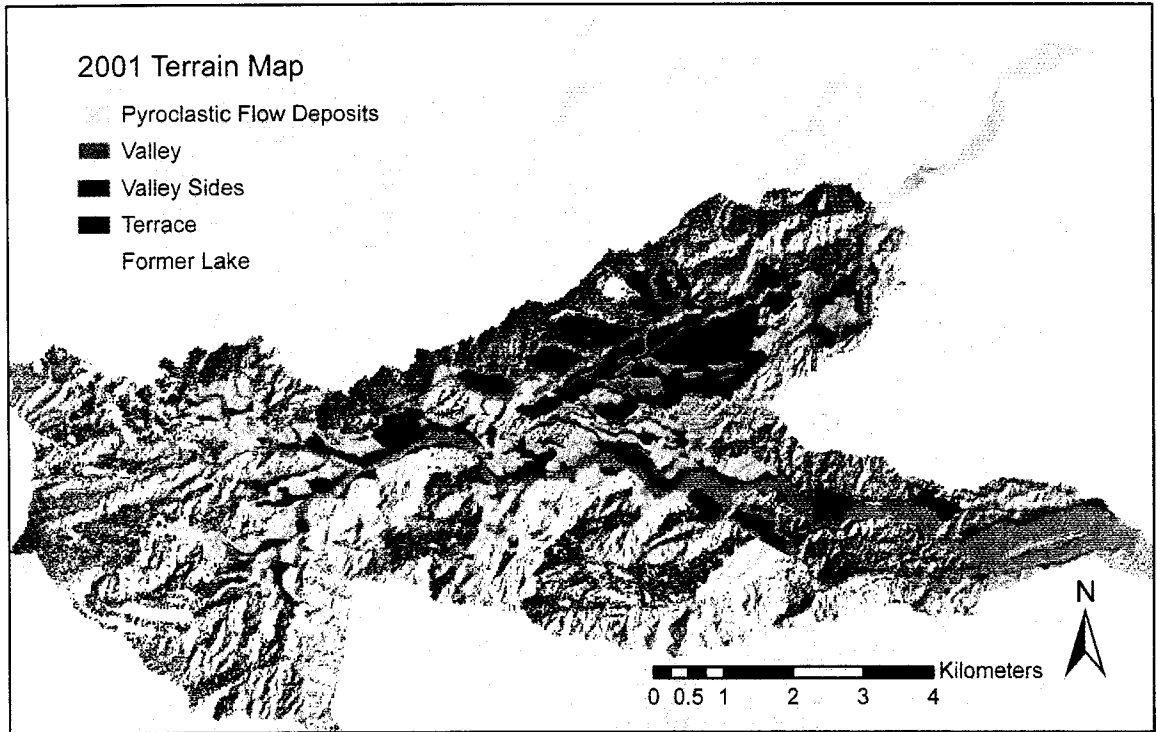


Figure 2.2: Terrain map for 2000-2001 produced from 2000 TOPSAR elevation data and 2001 ASTER multispectral imagery.

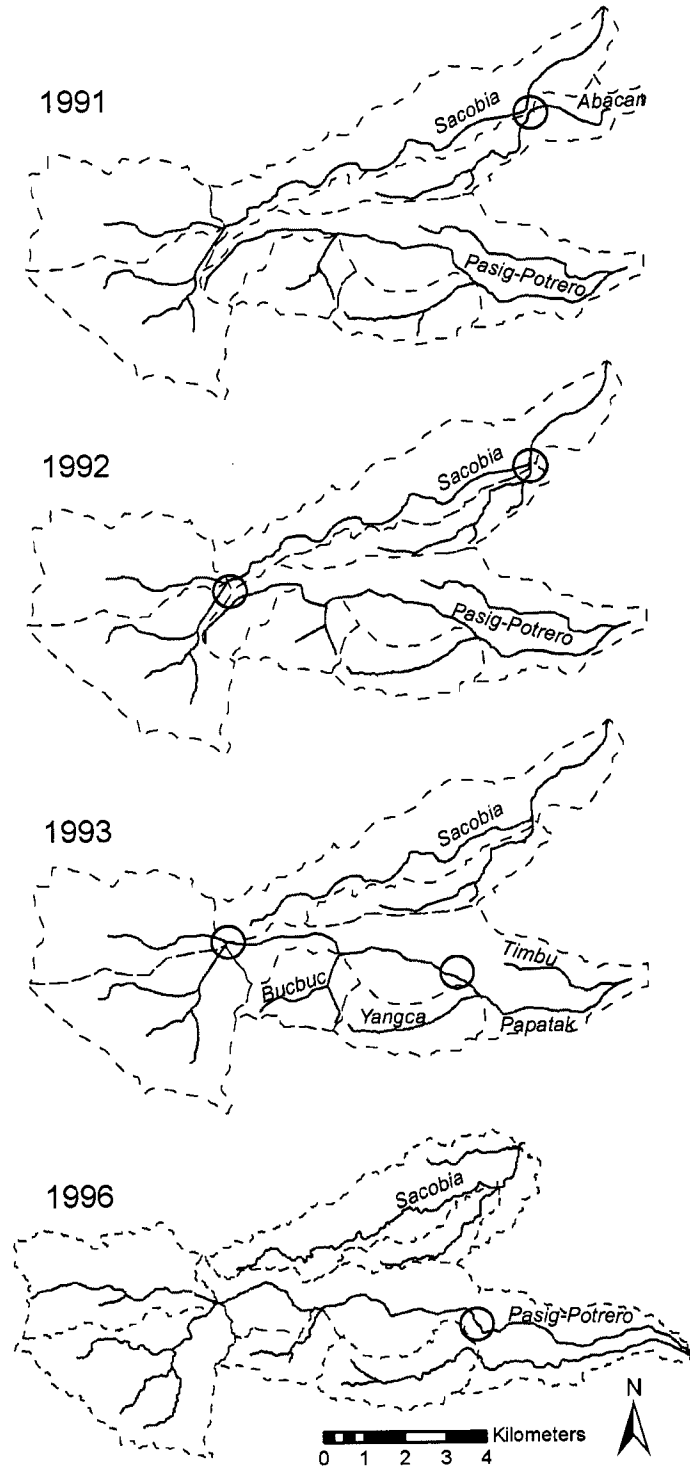


Figure 2.3: Major stream captures in the Pasig-Potrero/Sacobia/Abacan system shown by circles: the April 1992 capture of the upper Abacan by the Sacobia River, the October 1993 capture of the upper Sacobia by the Pasig-Potrero River, and the July 1994 redirection of flow from the Papatak branch into the Timbu branch of the Pasig-Potrero River.

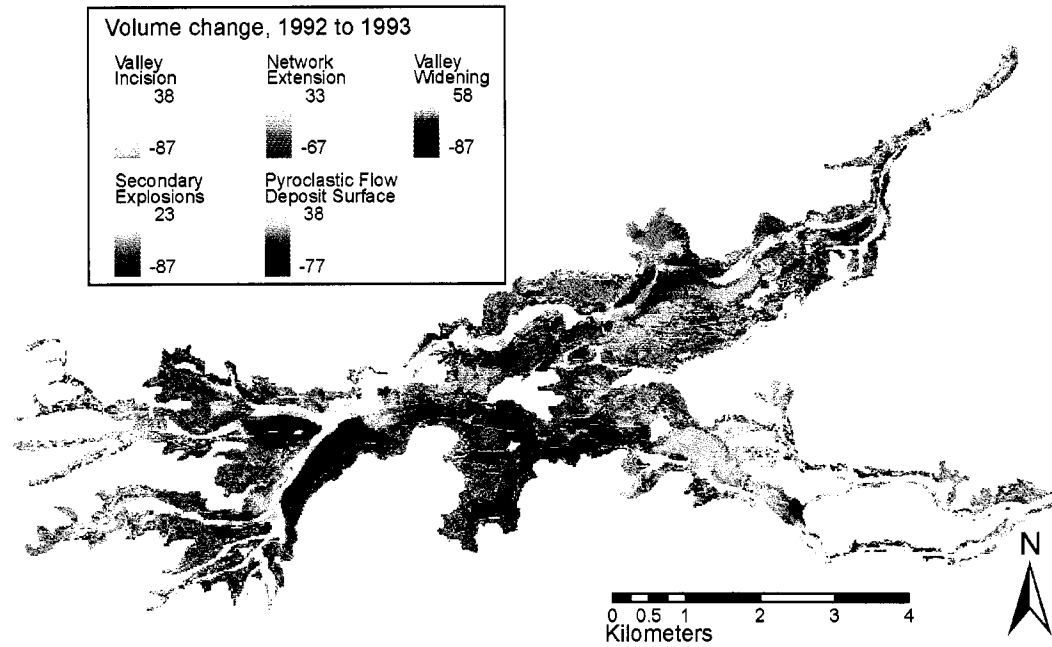


Figure 2.4: Example of erosion volume measurements from differenced DEMs, divided into erosional process based on terrain mapping. Each of five processes is shown, shaded based on depth change from 1992 to 1993. Darker colors represent the greatest depth of erosion. Negative changes indicate erosion, and positive values mean net deposition. Units are meters, calculated over 20-m x 20-m cells.

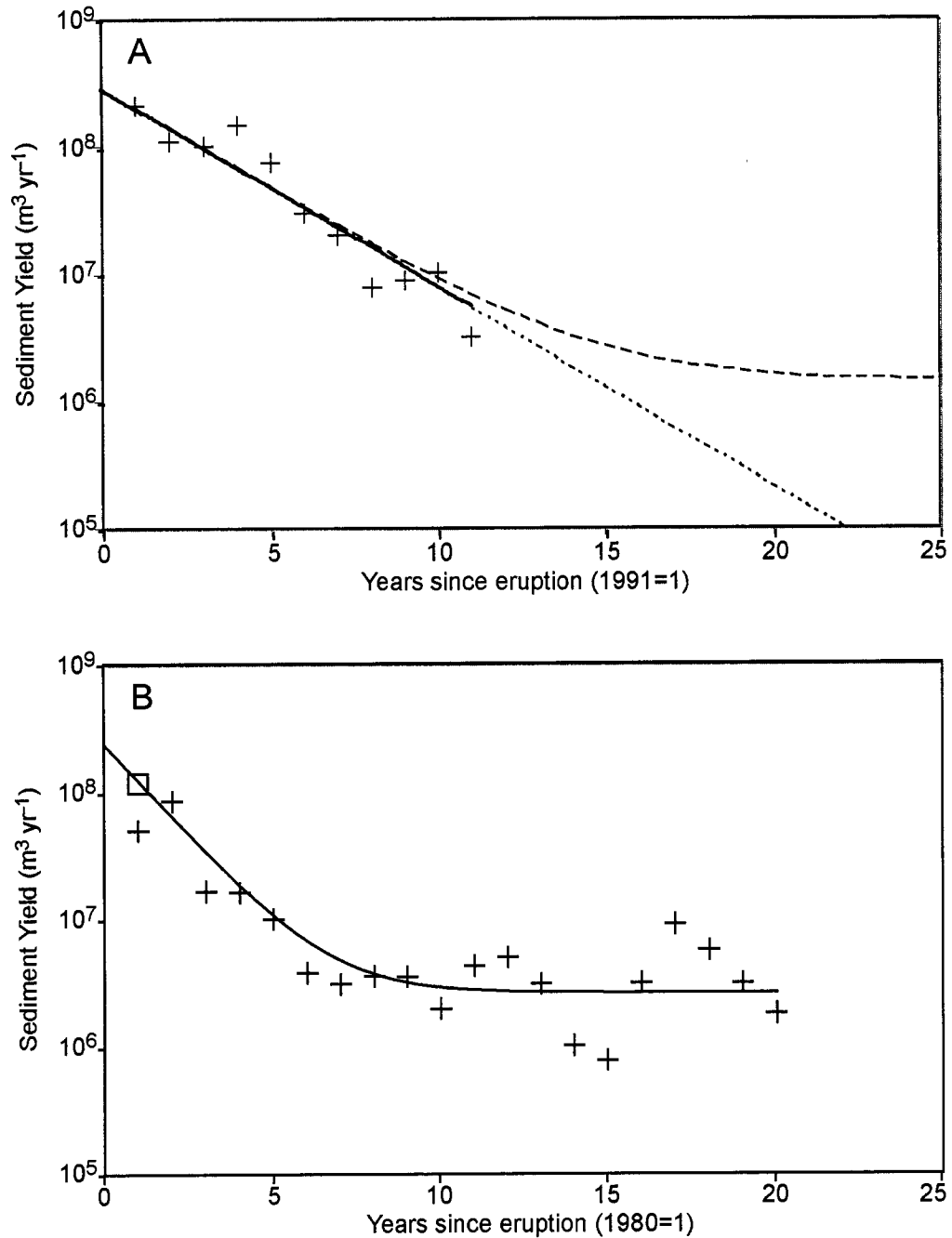


Figure 2.5: Sediment yield from A) Pasig-Potrero/Sacobia Rivers and B) Toutle River following the eruptions of Mount Pinatubo and Mount St. Helens. In (A), data for the first decade are fit well by an exponential decay model (solid line), however, it is unclear which model will fit well in the next decade: a simple exponential decay or an elevated background rate. The Toutle River (B) shows a rapid exponential decay shifting into a stable rate of  $2.7 \times 10^6 \text{ m}^3$ . In computing a best fit curve, sediment yield in 1980 was multiplied by a factor of  $7/3$  (open square) to adjust for the eruption occurring at the end of the 1980 rainy season.

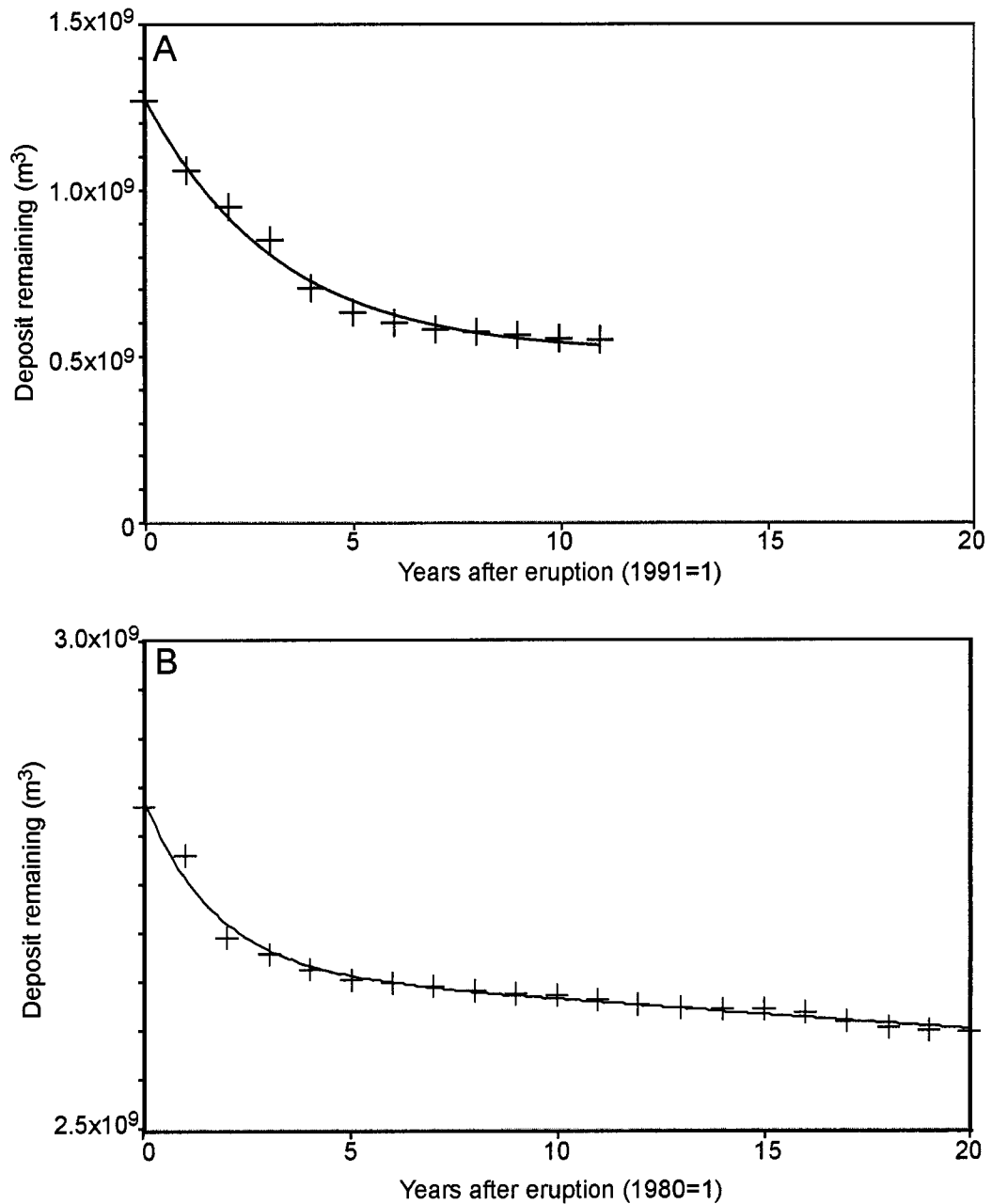


Figure 2.6: Decline in eruptive deposits in A) Pasig-Potrero/Sacobia basins and B) Toulte River basin. Original measurements of deposit volume and sediment yield come from Umbal (1997), Tuñgol (2002), Major et al. (2000), Simon (1999), and this study.

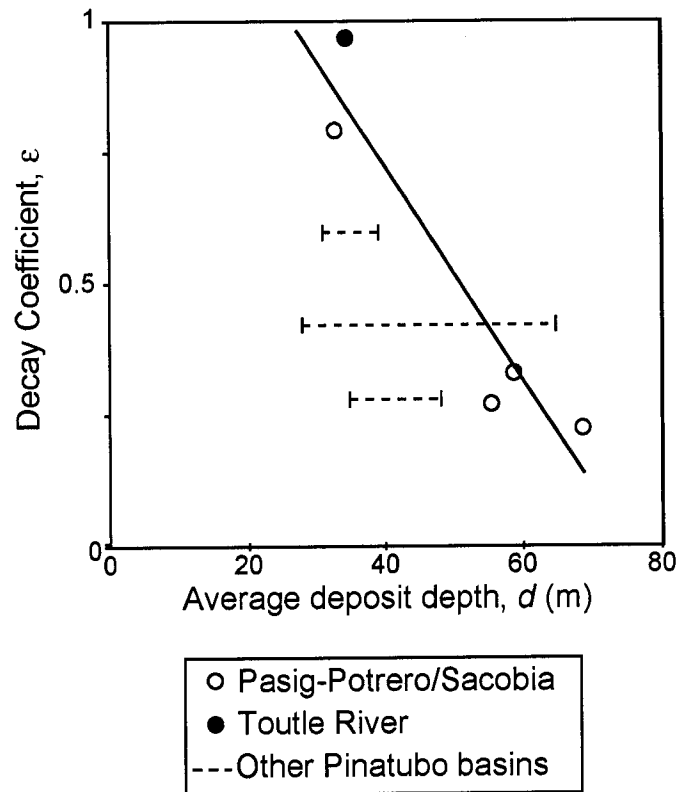


Figure 2.7: The exponential decay coefficient for sediment yield correlates with size of the initial deposit. The decay coefficient was calculated based on the initial exponential decay function for sediment yield in the Pasig-Potrero/Sacobia basin and each of the three sub-basins from this study. The linear regression curve plotted here ( $\epsilon = -0.02d + 1.5$ ,  $R^2=0.85$ ) combines the Pasig-Potrero/Sacobia basins and the Toutle River. Three other basins at Mount Pinatubo (O'Donnell, Bucayo-Balin Buquero, and Marella) are plotted but not included in the regression. Each of these basins had a range of published estimates for eruption volumes, and the range is plotted above. Average deposit depths for the Pasig-Potrero/Sacobia were calculated from DEMs. Other basin deposit depths were derived from published volume and area measurements (Major et al., 1996; Rodolfo et al., 1996; Scott et al., 1996; Simon, 1999). Sediment yields come from Umbal (1997), Major et al. (2000), and Simon (1999).

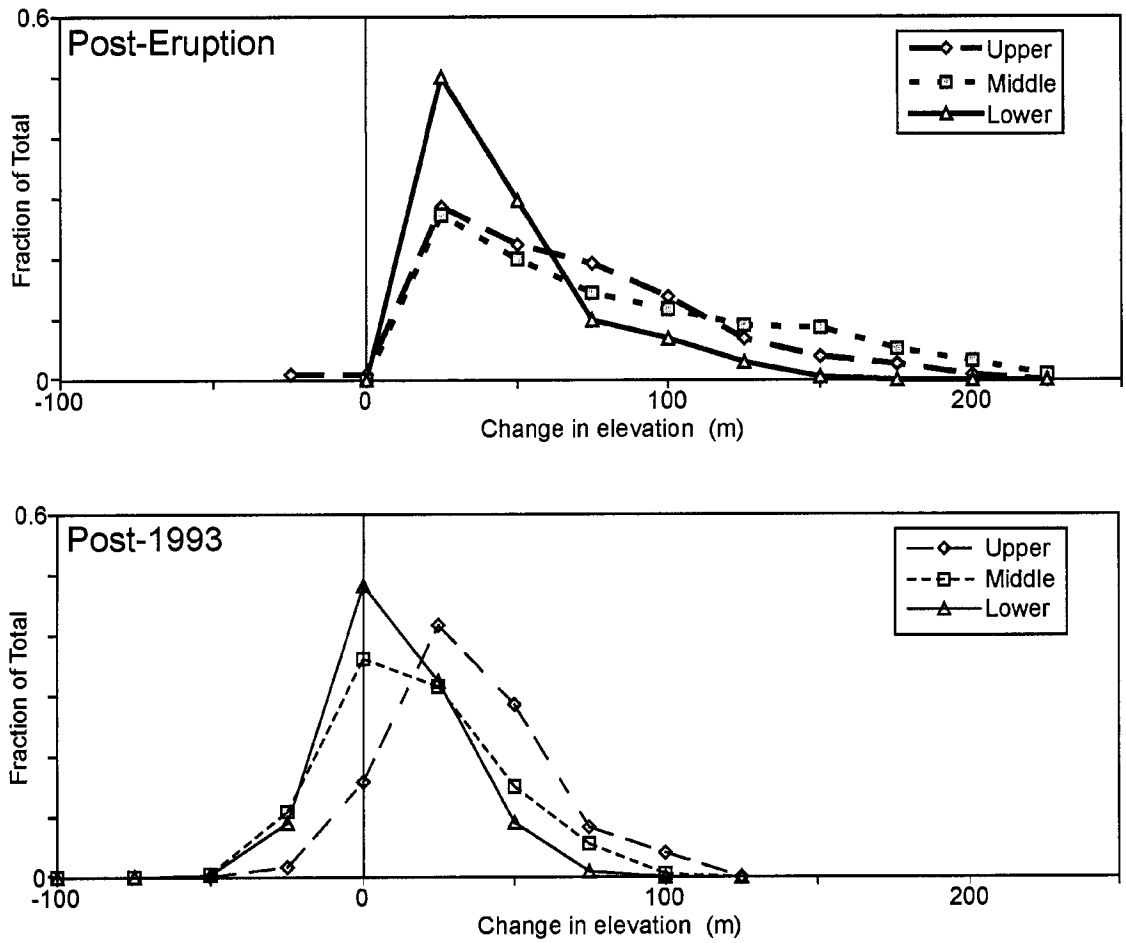


Figure 2.8: Distributions of the depth of initial pyroclastic-flow deposits in each of the three basin zones are shown here, binned in 25-m increments. The same data set was compiled after three rainy seasons (post-1993), showing the change in depth distributions. All three basins had material from the deepest deposits removed (indicated by decrease in upper tail of distribution). The lower and middle basins also show some areas incised into pre-eruption deposits (indicated by negative change in elevation compared with pre-eruption surface).

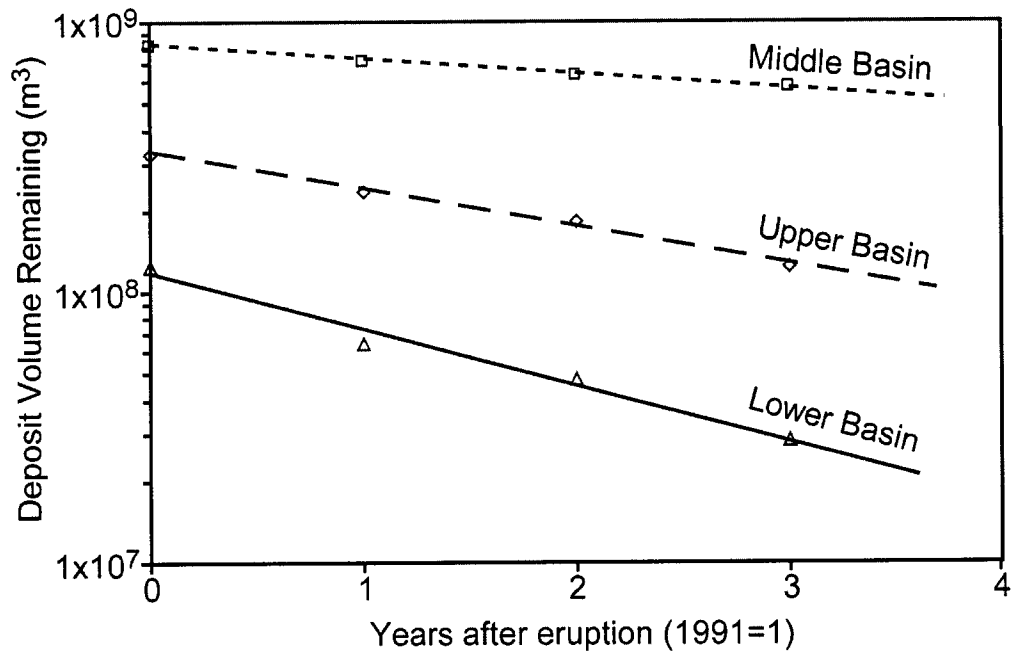


Figure 2.9: In all three basin zones, cumulative erosion followed an exponential decay curve, but each basin zone had a different decay rate that was inversely proportional to the initial volume of sediment loading: upper (0.31), middle (0.12), and lower (0.48).



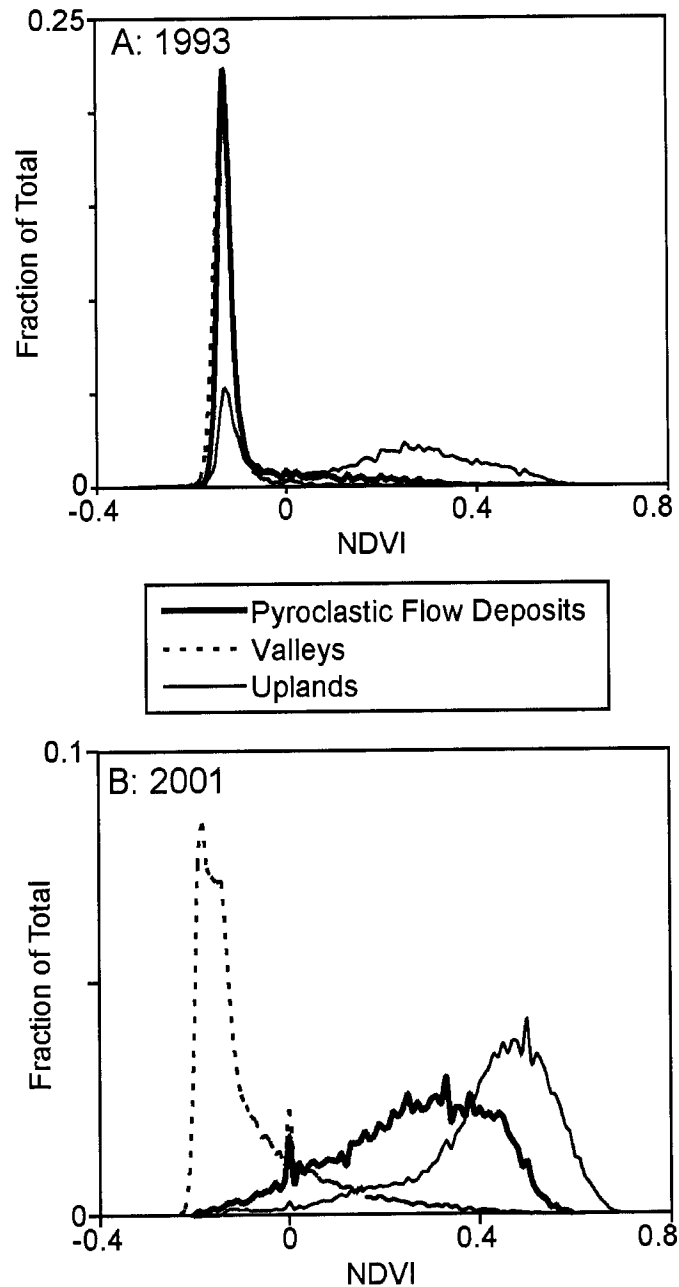


Figure 2.10: Normalized Differenced Vegetation Index (NDVI) provides a standardized measure of vegetation density in an area. The NDVI runs from -1 to 1, with higher values reflecting an increase in vegetation. A) In April 1993, both valleys and pyroclastic-flow deposit terrain were unvegetated, shown by a spike around -0.1. The uplands contained some areas that were vegetated and some that were still bare (note spike at -0.1 plus distribution > 0). B) In 2001, the valleys were still unvegetated, but vegetation regrowth in the pyroclastic-flow deposit terrain was substantial, approaching the same vegetation density as in the uplands.

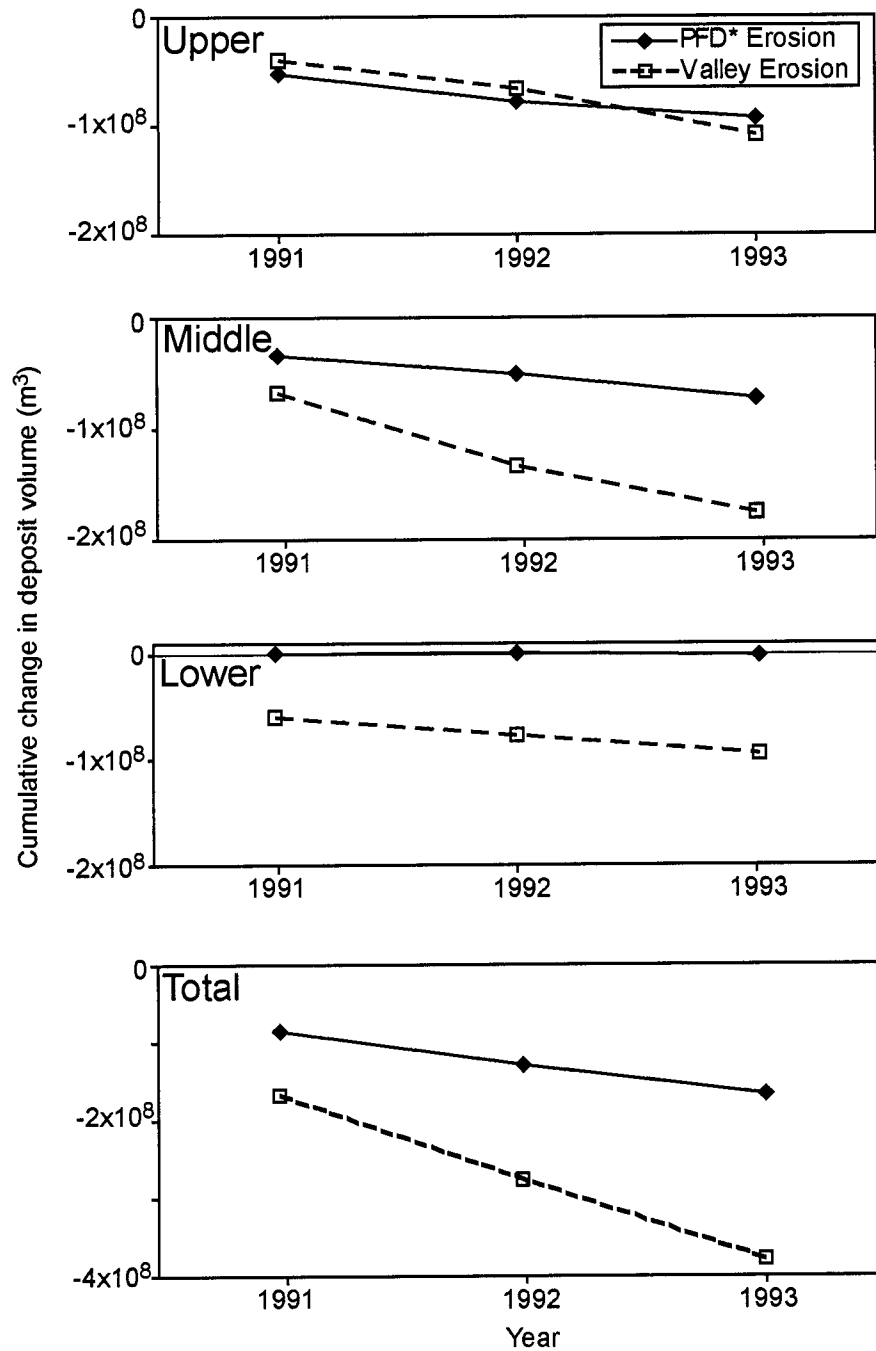


Figure 2.11: Cumulative volume changes in each basin zone due to erosion on the pyroclastic-flow deposit surface vs. valley erosion are compared here for the upper, middle, and lower basin zones, and the entire basin system. Negative volume change indicates net erosion.

\*PFD stands for pyroclastic-flow deposit surface erosion.

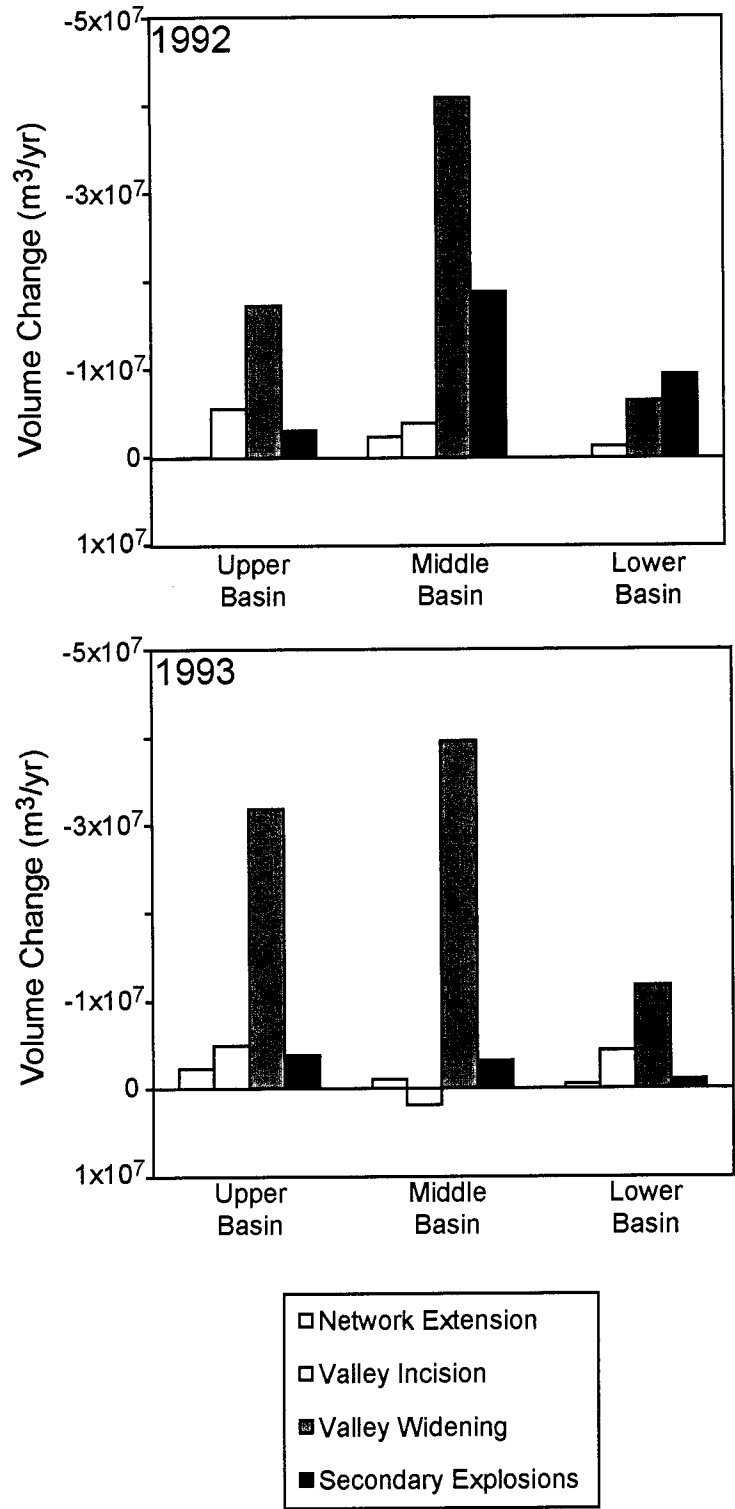


Figure 2.12: Valley erosion is detailed here by process for 1992 and 1993 for each of three basin zones. Negative values for volume change indicate net erosion.

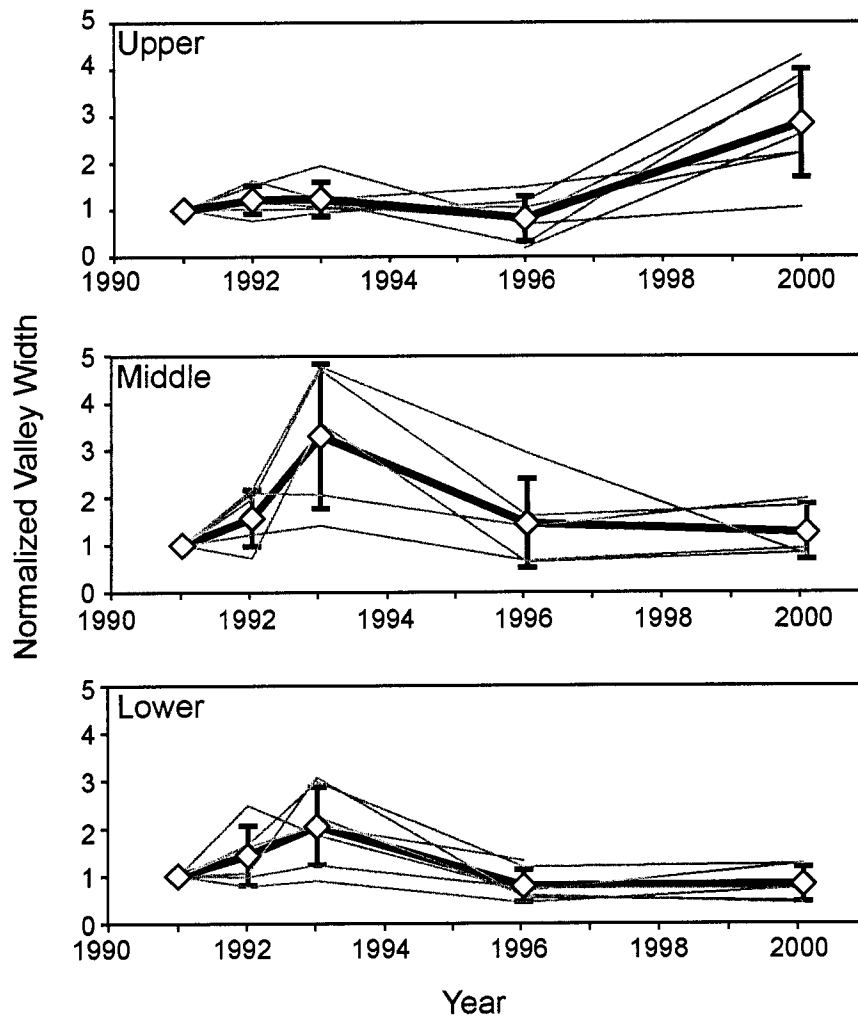


Figure 2.13: Valley width through time for upper, middle, and lower basin zones. Valley widths are normalized to the width measured at the end of 1991. Average valley width for channel sections 1-4 km long are plotted in grey, with the average of all those cross-sections plotted in black. Error bars represent  $1\sigma$  spread in the channel section data.

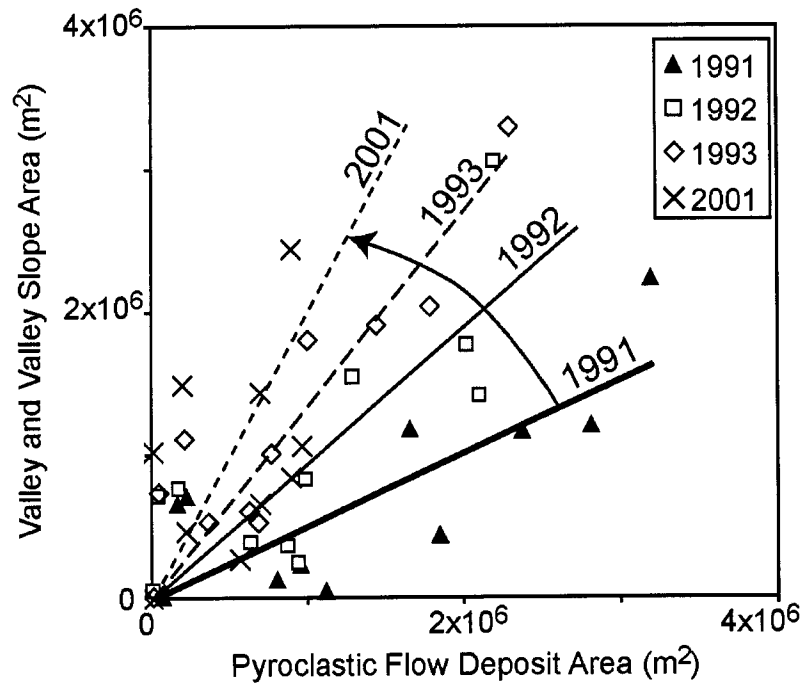


Figure 2.14: Terrain mapped as pyroclastic-flow deposit plotted against combined valley terrains (valley and valley slope), showing the shift through time from pyroclastic-flow deposit terrain to valley terrains. Best fit linear regression curves constrained to go through the origin are shown for 1991, 1992, 1993, and 2001 to illustrate the migration from pyroclastic-flow deposit surface to valley terrain.

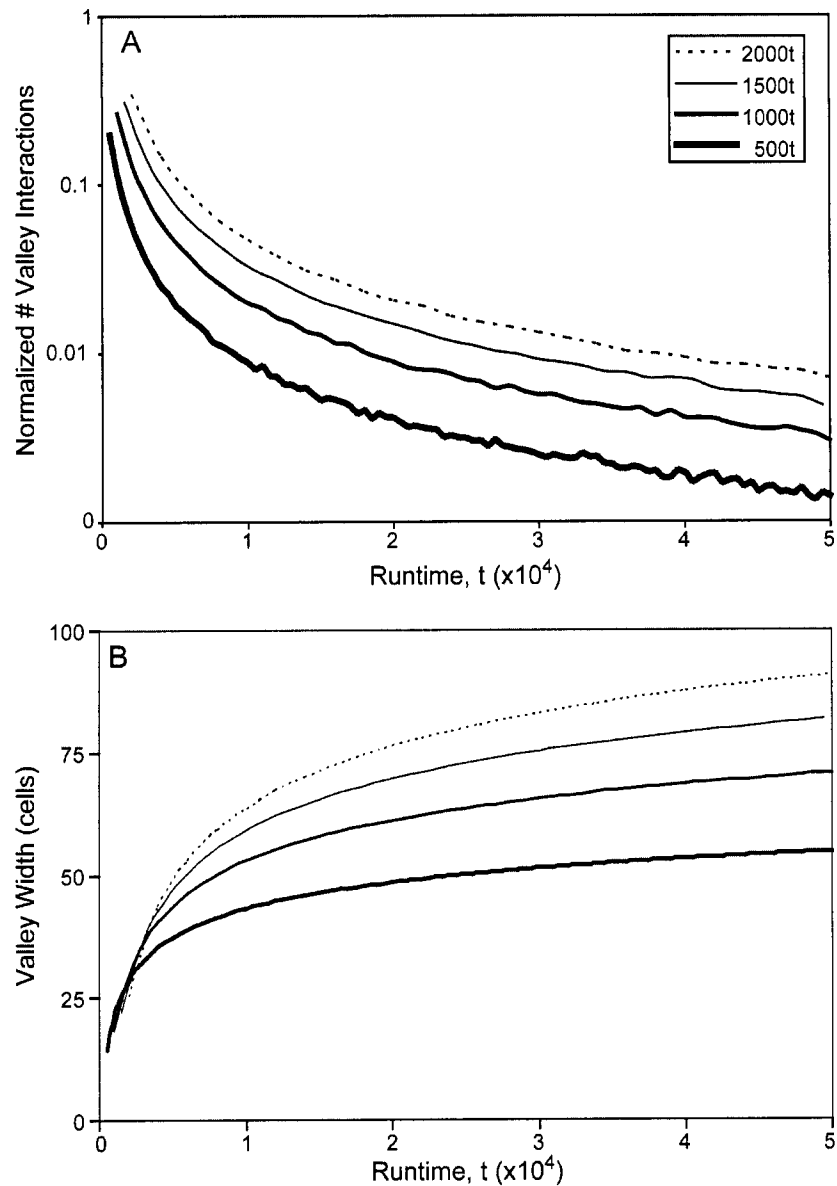


Figure 2.15: Results from a random-walk valley-wall erosion model show nonlinear decay of valley-wall interactions as valleys widen through time (A). The model included a centerline channel in a valley 10 cells wide, with a 10% chance of moving right or left with each time step,  $t$ . If the channel reached the valley wall, the wall moved back one cell, and the interaction was tallied. Periodic resetting events, the equivalent of large storms, moved the channel back to the center of the original valley. Four different runs, with different periods between resetting events (500 – 2000 time steps) show the same nonlinear decay. All four curves are best fit by a power law decay model of the form:  $y = \beta x^{-\epsilon}$  with  $\epsilon = 1.1 - 1.2$ . (B) shows the increase in valley width over time. All runs lasted 50,000 time steps, and each plot here represents a compilation of 50,000 runs.

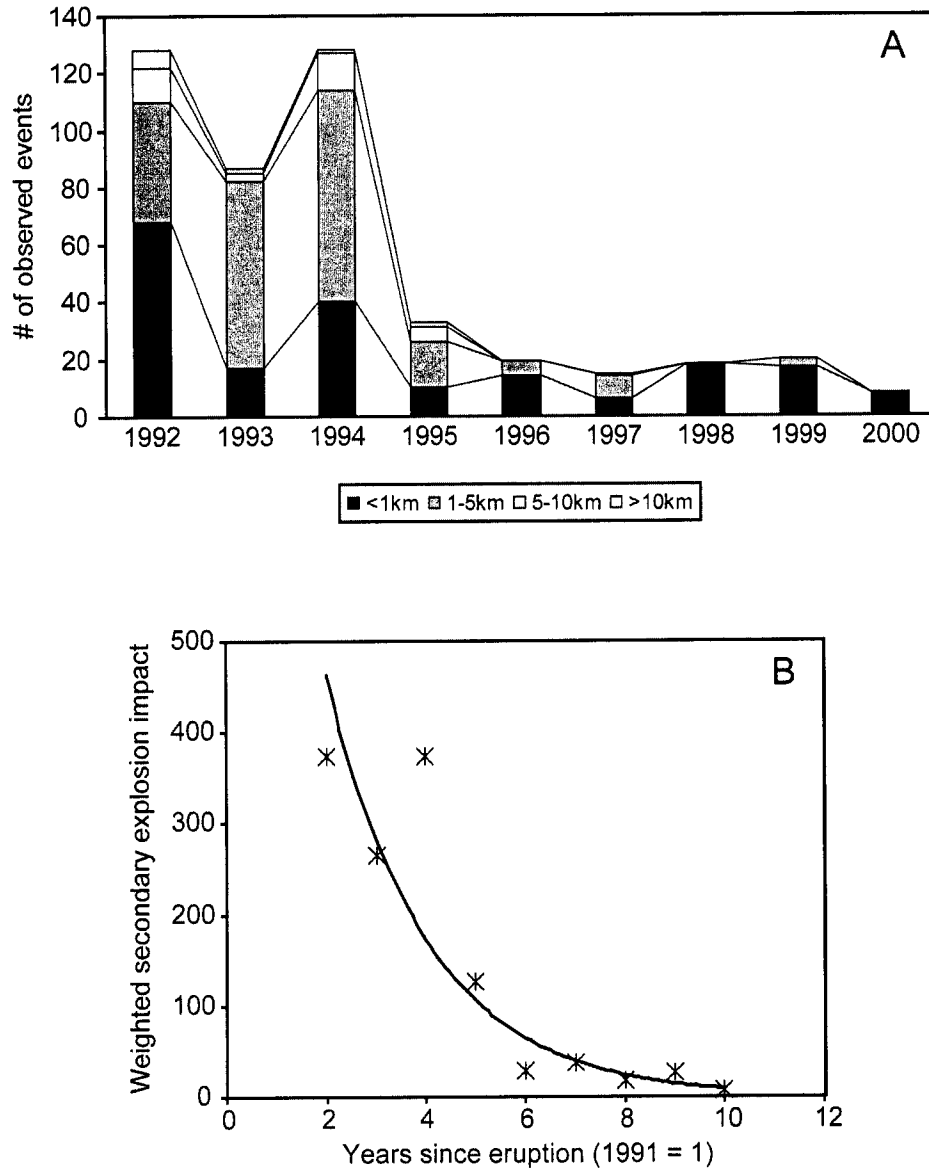


Figure 2.16: (A) Secondary explosions in the decade following the Mount Pinatubo eruption (Tuñgol, 2002, Unpublished PHIVOLCS data). (B) The same data, with each event weighted using the following index based on ash column height: < 1 km = 1; 1-5 km = 3, 5-10 km = 7.5, > 10km = 15. The results can be fit with an exponential decay model, although 1994 is twice what the exponential curve predicts.

### Notes to chapter

- Collins, B. D., and Dunne, T., 1986, Erosion of tephra from the 1980 eruption of Mount St. Helens: Geological Society of America Bulletin, v. 97, p. 896-905.
- Daag, A., and van Westen, C. J., 1996, Cartographic modelling of erosion in pyroclastic flow deposits of Mt. Pinatubo, Philippines: ITC Journal, v. 2, p. 110-124.
- Daag, A. S., 1994, Geomorphic developments and erosion of the Mount Pinatubo 1991 pyroclastic flows in the Sacobia watershed, Philippines: A study using remote sensing and Geographic Information Systems (GIS) [M.S. thesis]: Enschede, Netherlands, International Institute for Geoinformation Science and Earth Observation (ITC), 106 p.
- , 2003, Modelling the erosion of pyroclastic flow deposits and the occurrences of lahars at Mt. Pinatubo, Philippines [Ph.D. thesis]: Enschede, Netherlands, International Institute for Geoinformation Science and Earth Observation (ITC), 232 p.
- Graf, W. L., 1977, The rate law in fluvial geomorphology: American Journal of Science, v. 277, p. 178-191.
- Hayes, S. K., Montgomery, D. R., and Newhall, C. G., 2002, Fluvial sediment transport and deposition following the 1991 eruption of Mount Pinatubo: Geomorphology, v. 45, no. 3-4, p. 211-224.
- Herkelrath, W., and Leavesley, G. H., 1981, Physical properties of volcanic ash from Mount St. Helens -- Relationship to rain infiltration experiments: Agronomy Abstracts, p. 141.
- Hildreth, W., 1983, The compositionally zoned eruption of 1912 in the Valley of Ten Thousand Smokes, Katmai National Park, Alaska: Journal of Volcanology and Geothermal Research, v. 18, no. 1-4, p. 1-56.
- Hirao, K., and Yoshida, M., 1989, Sediment yield of Mt Galunggung after eruption in 1982, *in* International Symposium on Erosion and Volcanic Debris Flow Technology, Yogyakarta, Indonesia, p. V21-1 - V21-22.
- Howard, A., 1999, Simulation of gully erosion and bistable landforms, *in* Darby, S. E., and Simon, A., eds., Incised river channels: processes, forms, engineering and management: Chichester, John Wiley, p. 277-299.



- Janda, R. J., Meyer, D. F., and Childers, D., 1984, Sedimentation and geomorphic changes during and following the 1980-1983 eruptions of Mount St. Helens, Washington (2): *Shin-Sabo*, v. 37, no. 3, p. 5-17.
- JICA, 1978, Planning report on the Pasig-Potrero River flood control and Sabo project: Tokyo, Japan, Japan International Cooperation Agency, 133 p.
- , 1996, The study on flood and mudflow control for Sacobia-Bamban/Abacan River draining from Mt. Pinatubo: Japan International Cooperation Agency (JICA) and Department of Public Works and Highways, Philippines, 45 p.
- Kadomura, H., Imagawa, T., and Yamamoto, H., 1983, Eruption-induced rapid erosion and mass movements on Usu Volcano, Hokkaido: *Zeitschrift für Geomorphologie N. F. Suppl. Bd.*, v. 46, p. 123-142.
- Major, J. J., 2004, Posteruption suspended sediment transport at Mount St. Helens: Decadal-scale relationships with landscape adjustments and river discharges: *Journal of Geophysical Research*, v. 109, p. 1-22.
- Major, J. J., Janda, R. J., and Daag, A. S., 1996, Watershed disturbance and lahars on the east side of Mount Pinatubo during the mid-June 1991 eruptions, *in* Newhall, C. G., and Punongbayan, R. S., eds., *Fire and mud: eruptions and lahars of Mount Pinatubo, Philippines*: Quezon City, Philippine Institute of Volcanology and Seismology, and Seattle, University of Washington Press, p. 895-919.
- Major, J. J., Pierson, T. C., Dinehart, R. L., and Costa, J. E., 2000, Sediment yield following severe volcanic disturbance -- A two-decade perspective from Mount St. Helens: *Geology*, v. 28, no. 9, p. 819-822.
- Mastin, L., and Waitt, R., 2000, Glacier Peak -- History and hazards of a Cascade volcano: U.S. Geological Survey Fact Sheet, v. 058-00.
- Mizuyama, T., and Kobashi, S., 1996, Sediment yield and topographic change after major volcanic activity, *in* *Erosion and Sediment Yield: Global and Regional Perspectives (Exeter Symposium)*, p. 295-301.
- Moyer, T., and Swanson, D., 1987, Secondary hydroeruptions in pyroclastic-flow deposits: examples from Mount St. Helens: *Journal of Volcanology and Geothermal Research*, v. 32, no. 4, p. 299-319.
- Paladio-Melosantos, M. L. O., Solidum, R. O., Scott, W. E., Quiambao, R. B., Umbal, J. V., Rodolfo, K. S., Tubianosa, B. S., de los Reyes, P. J., Alonso, R. A., and Ruelo, H. B., 1996, Tephra falls of the 1991 eruptions of Mount Pinatubo, *in* Newhall, C. G., and Punongbayan, R. S., eds., *Fire and Mud: Eruptions and*

- lahars of Mount Pinatubo, Philippines: Quezon City, Philippine Institute of Volcanology and Seismology, and Seattle, University of Washington Press, p. 513-535.
- Parker, R. S., 1977, Experimental study of basin evolution and its hydrologic implications [Ph.D. thesis]: Colorado State University, 331 p.
- Pearson, M. L., 1986, Sediment yields from the debris avalanche for water years 1980-1983, *in* Keller, S. A. C., ed., Mount St. Helens: Five Years Later, Eastern Washington University Press, p. 87-107.
- Pierson, T. C., Janda, R. J., Umbal, J. V., and Daag, A. S., 1992, Immediate and long-term hazards from lahars and excess sedimentation in rivers draining Mt. Pinatubo, Philippines: U. S. Geological Survey, 92-4039, 35 p.
- Punongbayan, R. S., Tuñgol, N. M., Arboleda, R. A., Delos Reyes, P. J., Isada, M., Martinez, M. M. L., Melosantos, M. L. P., Puertollano, J. R., Regalado, M. T. M., Solidum, R. U., Jr., Tubianosa, B. S., Umbal, J. V., Alonso, R. A., and Remotigue, C. T., 1994, Impacts of the 1993 lahars, and long-term lahar hazards and risks around Pinatubo Volcano, PHIVOLCS, Pinatubo Lahar Studies 1993: Final Report of the UNESCO-funded lahar studies program: PHIVOLCS Press, p. 1-40.
- Rodolfo, K. S., Umbal, J. V., Alonso, R. A., Remotigue, C. T., Paladio-Melosantos, M. L. O., Salvador, J. H. G., Evangelista, D., and Miller, Y., 1996, Two years of lahars on the western flank of Mount Pinatubo: Initiation, flow processes, deposits, and attendant geomorphic and hydraulic changes, *in* Newhall, C. G., and Punongbayan, R. S., eds., Fire and Mud: Eruptions and lahars of Mount Pinatubo, Philippines: Quezon City, Philippine Institute of Volcanology and Seismology, and Seattle, University of Washington Press, p. 989-1013.
- Scott, K. M., Janda, R. J., de la Cruz, E. G., Gabinete, E., Eto, I., Isada, M., Sexton, M., and Hadley, K., 1996a, Channel and sedimentation responses to large volumes of 1991 volcanic deposits on the east flank of Mount Pinatubo, *in* Newhall, C. G., and Punongbayan, R. S., eds., Fire and mud: eruptions and lahars of Mount Pinatubo, Philippines: Quezon City, Philippine Institute of Volcanology and Seismology, and Seattle, University of Washington Press, p. 971-988.
- Scott, W. E., Hoblitt, R. P., Torres, R. C., Self, S., Martinez, M. M. L., and Nillos, T., 1996b, Pyroclastic flows of the June 15, 1991, climactic eruption of Mount Pinatubo, *in* Newhall, C. G., and Punongbayan, R. S., eds., Fire and mud: eruptions and lahars of Mount Pinatubo, Philippines: Quezon City, Philippine Institute of Volcanology and Seismology, and Seattle, University of Washington Press, p. 545-570.

- Segerstrom, K., 1950, Erosion studies at Parícutin, State of Michoacan, Mexico: U.S. Geological Survey Bulletin, v. 965-A, 64 p..
- Simon, A., 1999, Channel and drainage-basin response of the Toutle River system in the aftermath of the 1980 eruption of Mount St. Helens, Washington: U. S. Geological Survey Open-File Report, v. 96-633, 130 p..
- Tabor, R. W., Booth, D. B., Vance, J. A., and Ford, A. B., 2002, Geologic map of the Sauk River 30- by 60-minute quadrangle, Washington: U. S. Geological Survey Geologic Investigations Series, 67 p. + 2 sheets.
- Tija, H., 1965, Course-changes in the lower Tjimanuk river, west Java.: Contributions from the Department of Geology, Institute Technology Bandung, v. 62, p. 75-82.
- Torres, R. C., Self, S., and Martinez, M. M. L., 1996, Secondary Pyroclastic Flows from the June 15, 1991, Ignimbrite of Mount Pinatubo, *in* Newhall, C. G., and Punongbayan, R. S., eds., *Fire and Mud: Eruptions and lahars of Mount Pinatubo*, Philippines: Quezon City, Philippine Institute of Volcanology and Seismology, and Seattle, University of Washington Press, p. 665-678.
- Tuñgol, N. M., 2002, Lahar initiation and sediment yield in the Pasig-Potrero River basin, Mount Pinatubo, Philippines [Ph.D. thesis]: Canterbury, New Zealand, University of Canterbury, 172 p.
- Umbal, J. V., 1997, Five years of lahars at Pinatubo volcano: Declining but still potentially lethal hazards: *Journal of the Geological Society of the Philippines*, v. 52, no. 1, p. 1-19.
- Vallance, J. W., and Scott, K. M., 1997, The Osceola mudflow from Mount Rainier: Sedimentology and hazard implications of a huge clay-rich debris flow: *Geological Society of America Bulletin*, v. 109, no. 2, p. 143-163.
- Waldron, H. H., 1967, Debris flow and erosion control problems caused by the ash eruptions of Irazu Volcano, Costa Rica: U. S. Geological Survey Bulletin, v. 1241-I, p. I1-I37.

### CHAPTER 3

#### **Spatial and temporal patterns in fluvial recovery following volcanic eruptions: Channel response to basin-wide sediment loading at Mount Pinatubo, Philippines**

##### **Summary**

The June 1991 eruption of Mount Pinatubo, Philippines, was one of the largest volcanic eruptions of the 20<sup>th</sup> century, emplacing 5-6 km<sup>3</sup> of pyroclastic-flow material on the flanks of the volcano. The combination of abundant, relatively fine-grained, easily erodible material and intense tropical rainfall led to numerous lahars immediately following the eruption. Even after major lahars ended, sediment yields in some basins remained orders of magnitude above pre-eruption levels. Using data collected from 1996 through 2003, we investigated five basins that experienced varying amounts of sediment loading in the 1991 eruption, from 1% to 33% of the basin area covered by valley-filling pyroclastic-flow deposits. From measurements of flow and bed characteristics made through time, we developed a general conceptual model for channel recovery following basin-wide sediment loading. Initially, finer-grained sediment and pumice are mobilized preferentially through selective transport. Once the bed is coarse enough for gravel-size clasts to interact with one another, clast structures develop, increasing form roughness and critical shear stress and inhibiting initial clast mobility. As sediment inputs continue to decline, the channel incises into valley-bottom sediments, progressively armoring through winnowing. At Pinatubo, incision and armoring occur first as dry season phenomena due to reduced sediment inputs, eventually moving to year-round low-flow bed stability. Observed timing of the onset of in-channel biological recovery suggests that re-establishment of channel stability helps catalyze aquatic ecosystem recovery. The text of this paper was published in *GSA Bulletin*, v. 117, n. 1/2, pp. 195 – 211 (Gran and Montgomery, 2005), with minor updates here.

## Introduction

Hazards from volcanic eruptions with abundant fine-grained pyroclastic-flow material last well beyond the actual eruptive event. Following an eruption, easily erodible sediment and greater surface runoff create extremely high sediment yields in rivers draining active volcanoes. Sediment yields orders of magnitude higher than average world rivers have been measured at Mount St. Helens (Pearson, 1986; Dinehart, 1998; Major et al., 2000; Major, 2004), Mount Usu (Kadomura et al. 1983), Galunggung (Hirao and Yoshida, 1989), and Mount Pinatubo (Umbal, 1997; Tuñgol, 2002) in years immediately following major eruptions (Figure 3.1). Much of the initial high sediment yield can be attributed to lahars, but even after lahar activity has ceased, sediment yields may remain elevated (Major et al., 2000; Hayes et al., 2002).

Pyroclastic-flow and tephra-fall material inundating the surrounding landscape can severely impact watersheds. On hillslopes, loss of vegetation and blanketing by tephra leads to reduced infiltration rates and flashier responses to storms (Segerstrom, 1950; Waldron, 1967; Kadomura et al., 1983; Janda et al., 1984a; Yamamoto, 1984; Leavesley et al., 1989; Shimokawa et al., 1989). Abundant fine-grained material is easily mobilized from hillslopes into rills and channels. In valleys, pyroclastic flows can temporarily bury pre-existing drainage networks or permanently reorganize drainage basin boundaries. In addition, abundant erodible material coupled with greater surface runoff often leads to the development of volcanic debris flows and hyperconcentrated flows, referred to collectively as lahars.

Watershed recovery from volcanic disturbance represents an important process, yet only a few studies were conducted on the hydrologic effects of eruptions prior to the May 1980 eruption of Mount St. Helens. One of the first comprehensive studies of long-term geomorphic recovery of an eruptive landscape was on Parícutin Volcano in Mexico (Segerstrom, 1950; 1960; 1966). Parícutin first erupted in 1943, with activity continuing through 1952. At Parícutin, many features described in later eruptions were documented including destruction of vegetation, reduced infiltration rates related to ash crusting, increased mass movements, extensive rill erosion, and development of debris-laden stream flows. Like lahars at other volcanoes (Janda et al., 1984b; Tuñgol, 2002),

many debris flows scoured down below the pre-eruption surface, incorporating older sediments with new eruptive materials. By 1965, the area achieved relative stability, and farmers reoccupied most low-lying areas around the edifice. Landscape stability and recovery in these lower areas was attributed primarily to revegetation.

Irazú Volcano in Costa Rica erupted ash from 1963 to 1965. Waldron (1967) documented erosion of ash deposits with particular emphasis on debris flow hazards and mitigation efforts. Similar to Parícutin, ash surfaces crusted, reducing infiltration rates and increasing runoff rates to as high as 95-100% during high-intensity rainfall events. Initially most ash erosion occurred through rilling and headward erosion of gullies. In the second year, channel erosion became more severe, leading to oversteepened banks, which reactivated old landslides and formed new ones. Debris flows were common, with more than 90 during the 1964 rainy season alone. Much of Waldron's work focuses on these flows, downstream hazards associated with them, and mitigation efforts.

The May 1980 eruption of Mount St. Helens generated some of the first comprehensive, long-term, detailed studies of geomorphic impact of volcanic eruptions on neighboring watersheds, with continued monitoring to the present. During the May 18<sup>th</sup> eruption, a lateral blast denuded over 550 km<sup>2</sup>, and 0.19 km<sup>3</sup> of easily erodible tephra was deposited over relatively steep terrain. In addition, 2.8 km<sup>3</sup> of debris avalanche material composed mostly of sand and fine gravel was emplaced in the North Fork Toutle River basin (Janda et al., 1984b). Detailed studies documented intense sheet wash and rill erosion on hillslopes in the year following the eruption. By the second year, sheet and rill erosion had dramatically declined due to changes in hillslope hydrology (Collins et al., 1983; Lehre et al., 1983; Collins and Dunne, 1986). In river valleys, lahars moved through many major tributaries of the Toutle and Lewis Rivers, transporting sediment from low-order watersheds, scouring the bed, and eroding main channel banks. Much of the sediment eroded from channels was pre-eruption alluvium and colluvium (Janda et al., 1984b). In the debris avalanche valley fill, the newly forming channel network went through four stages: 1) headward extension of the

channel network, 2) incision, 3) channel widening and aggradation, and 4) alternating periods of aggradation and scour (Janda et al., 1984b; Pearson, 1986).

Since Mount St. Helens, studies on Mount Usu, Unzen, and Sakurajima in Japan (Kadomura et al., 1983; Shimokawa and Taniguchi, 1983; Chinen and Kadomura, 1986; Mizuyama and Kobashi, 1996), Mount Galunggung in Indonesia (Hamidi, 1989; Hirao and Yoshida, 1989), and Mayon Volcano and Mount Pinatubo in the Philippines (Rodolfo, 1989; Rodolfo and Arguden, 1991; Newhall and Punongbayan, 1996) have addressed landscape disturbance and recovery from volcanic eruptions. A significant fraction of this research concentrates on the time immediately following eruptions, when disturbance to the hydrologic system is greatest. In many cases, reduced infiltration rates and excess sediment contributed to lahar activity and immediate downstream hazards for the local populace. At Mount Pinatubo, for example, major lahars in the first year affected 364 villages, home to 2.1 million people (Mercado et al., 1996).

Relatively little research has focused on the time after the initial lahar phase has passed and sediment transport is controlled by non-lahar fluvial processes. During this period rivers may no longer be dominated by lahar activity, but sediment yields remain far above pre-eruption levels. Sediment yields on the Pasig-Potrero River at Mount Pinatubo six years after the eruption were still two orders of magnitude higher than pre-eruption yields (JICA, 1978; Hayes et al., 2002). Almost 20 years after the eruption of Mount St. Helens, suspended sediment yields in the area draining the debris avalanche deposit remained two orders of magnitude higher than pre-eruption background values (Major et al., 2000). At both volcanoes, hydrologic hazards including excess sedimentation and downstream flooding are still concerns years to decades after major eruptions. The time scale over which fluvial recovery will occur is still not well constrained. Long after the initial eruption, volcanically-disturbed rivers can continue to be a significant threat to communities.

Our study investigates watershed recovery on the east flank of Mount Pinatubo following the June 1991 eruption, focusing on the time after major lahar activity ceased. Not only does Pinatubo offer an excellent opportunity to study fluvial recovery from an

eruption, but it also offers a unique window into dynamics of sediment-laden rivers in general. Many mountain watersheds in tectonically active areas are dominated by discrete, often substantial, inputs of sediment from hillslope disturbances. These landslide-derived sediment pulses can constitute a major portion of the sediment budget (Dietrich and Dunne, 1978; Swanson et al., 1982; Pearce and Watson, 1986; Benda and Dunne, 1987). Sediment loading also occurs from anthropogenic sources, such as mining debris or sediment released during dam removal (Gilbert, 1917; Pickup et al., 1983; Knighton, 1989). However, the dynamics of how a large sediment input is processed and moved downstream are still being studied (Meade, 1985; Knighton, 1989; Madej and Ozaki, 1996; Lisle et al., 1997; Lisle et al., 2001; Cui et al., 2003a; Cui et al., 2003b).

In the case of Mount Pinatubo, the excess sediment load is extreme. The behavior of a system when subjected to such an intense disturbance should help elucidate the relationships important in systems with less intense disturbances. By studying how a volcanically-impacted landscape is affected by a substantial increase in sediment load and how the geomorphic systems process, remove, or stabilize that excess sediment, we are better able to infer how watersheds experiencing episodic sediment loading may behave.

We examined a series of watersheds with varying amounts of sediment loading, and thus different rates of sediment remobilization and eventual recovery and stabilization of the watershed. Recovery can take on many forms and is subject to many definitions. Here, we are concerned mostly with the physical recovery of the stream channel. We consider a channel recovered when it can support the re-establishment of an aquatic ecosystem of pre-eruption complexity. In some cases, the channel will be able to return to pre-eruption conditions (similar grain size, roughness, and lateral mobility rates) although perhaps with more terrace or valley-bottom storage than before. In other cases, a new equilibrium condition may be reached. In both cases, however, physical recovery implies a degree of channel stability which requires evacuation or stabilization of the bulk of the excess sediment load and the reduction of significant lateral and vertical channel adjustments.



We begin by reviewing the potential response of fluvial systems to the introduction of abundant fine-grained sediment and how channels might adjust as sediment input declines. We then describe recovery processes at Pinatubo, drawing on data and observations from five basins with varying impact from the eruption. This multi-basin approach is used both to illustrate the importance of the degree of initial impact and as a form of space-for-time substitution. We also use one basin as a case study, following the Pasig-Potrero River from 1996 through 2003. Based on the parallel implications of these two approaches, we propose a conceptual framework to explain trends in channel recovery following massive sedimentation events.

### **Theoretical context**

As sediment inputs increase, a fluvial system can adjust by increasing storage through channel or valley-bottom aggradation or by increasing sediment transport rates. If the river is supply-limited and able to transport all sediment that enters the system, then an increase in sediment input can directly translate into an increase in sediment transport without necessitating adjustments in storage. If the sediment load far exceeds the transport capacity, as it did at Pinatubo after the eruption, then adjustments in geometry or substrate within the channel or valley bottom will result in changes in sediment storage or transport or both. We consider here the case of increased sediment transport.

Sediment transport is a function of excess basal shear stress which is the total basal shear stress generated by a flow minus the portion removed through turbulent dissipation from roughness elements. The portion of the excess shear stress available to move sediment may be reduced further by a critical value that must be overcome to initiate motion. The remaining effective shear stress will increase if either the total shear stress increases, through an increase in depth, slope, or discharge, or if the critical shear stress or roughness decreases. Sediment transport rates can also change if the sediment being transported has a different grain size distribution than the substrate before sediment loading. Under conditions of selective transport, finer sediments mobilize at lower flow conditions than coarser clasts, and thus can be evacuated at

higher rates than coarser material (Komar, 1987). In addition, as sand content in mixtures increases, transport rates of both sand and gravel may increase by orders of magnitude (Wilcock et al., 2001; Wilcock and Kenworthy, 2002). Thus, the addition of large amounts of sand may enhance overall sediment transport.

After an initial sediment loading event, as sediment inputs decline through time, the reverse conditions apply and either a decrease in storage or transport rates must occur. In order to decrease the sediment transport rate, the effective shear stress should decrease, either through lower total basal shear stress or higher critical shear stress or roughness. Channel widening, increased sinuosity, slope adjustments through downstream aggradation and upstream incision, or lower discharge can all reduce total basal shear stress. An increase in surface grain size or the introduction of bedforms, pebble clusters, or obstructions like vegetation or large woody debris will increase the roughness. All of these factors will lower the excess shear stress. The effective shear stress can be reduced further by raising the critical shear stress. Increasing surface grain size and particle interactions can raise the critical shear stress. Because of all the degrees of freedom outlined above, it is hard to predict from first principles exactly how a channel will accommodate decreasing sediment inputs and the order and sequencing of expected changes. We do, however, have an idea of what types of changes to expect in a system under a decreasing sediment supply.

### **Study area**

Mount Pinatubo is located approximately 100 km northwest of Manila on the island of Luzon, Philippines. In June 1991, Mount Pinatubo erupted, emplacing 5-6 km<sup>3</sup> of pyroclastic-flow material on the volcanic flanks. River valleys were partially buried with as much as 200 meters of loose pyroclastic debris (Scott et al., 1996b).

The climate at Mount Pinatubo is tropical and monsoonal, with distinct rainy and dry seasons. Clark Air Base on the lower east flank of the volcano receives an average annual rainfall of 1950 mm, 60% of which falls during the summer months of July, August, and September (Scott et al., 1996a). This rainfall often comes in very intense storms, which, coupled with loose sediment deposited during the eruption, led to

major lahars following the eruption on all rivers draining the volcano. Over time, the threshold rainfall necessary to trigger a lahar has risen, reducing lahar frequency (Tuñgol, 2002).

Sediment yields immediately following the eruption were several orders of magnitude higher than normal (Figure 3.1). Initial estimates of total sediment yield made using standard techniques (United States Army Corps of Engineers, 1994) were lower than actual yields, by close to an order of magnitude. Initial U.S. Geological Survey estimates were closer but were still approximately 50% too low (Pierson et al., 1992). Yields declined non-linearly during the first four years following the eruption, with minor variations to the overall declining trend occurring due to local events such as stream captures or lake break-out floods (Umbal, 1997; Tuñgol, 2002) (Figure 3.2). Measurements of sediment volume deposited in the Pasig-Potrero River on the upper alluvial fan head show that sediment yields continued to decline exponentially for at least the first decade following the eruption.

East flank basins were variably affected, with 1% to 33% of each basin covered with pyroclastic-flow deposits. Our study focuses on five rivers on the east side of the volcano which are, in order from the most impacted to the least, the Sacobia, Pasig-Potrero, O'Donnell, Gumain, and Porac Rivers (Figure 3.3). Table 3.1 shows the size and relative volcanic impact in terms of the percent area covered by valley-filling primary pyroclastic-flow deposits.

The Pasig-Potrero and Sacobia Rivers have a unique history involving a massive stream capture event in October 1993. At the time of the eruption, the Sacobia River basin extended into the area now occupied by the 1991 crater. The Pasig-Potrero River initiated several kilometers downstream. In October 1993, the Pasig-Potrero River captured the upper half of the Sacobia basin, doubling the basin area of the Pasig-Potrero while halving that of the Sacobia (Punongbayan et al., 1994). Since this capture occurred after three rainy seasons, a substantial amount of sediment had already left the upper Sacobia River basin (Daag, 1994), and the Pasig-Potrero inherited transport capacity (increased discharge) without a commensurate increase in sediment load from the upper watershed. At the end of the 1992 lahar season, the upper Sacobia basin had

an estimated  $1.2 \times 10^7$  m<sup>3</sup> of sediment per km<sup>2</sup> of basin area, while the Pasig-Potrero basin had  $1.8 \times 10^7$  m<sup>3</sup>/km<sup>2</sup> (Daag, 1994). Although the Pasig-Potrero River did have a sharp increase in sediment yield immediately following the stream capture event, the increase was transient, and now the Pasig-Potrero River is adjusting more rapidly than the Sacobia River.

The sediment-laden rivers of Pinatubo have several interesting features (Figure 3.4). During the rainy season they are shallow and highly braided, with braids ranging in size from a few centimeters in width to tens of meters, all of which actively transport sediment. Transport occurs as a moving carpet of sand and fine gravel over a smooth bed. Gravel clasts roll or slide independently over the predominantly sand bed. Any clast that becomes stationary in an active channel is quickly scoured around, sinks into the bed, and is buried, thus maintaining a smooth bed. Flow is often super-critical, and transient antidunes are present. During high flows, the water level may rise high enough to completely fill the valley bottom, and channel-spanning roll waves pulse downstream. Many of these characteristics are beginning to change, and it is these adjustments that we are seeking to document and understand.

### **Methods**

We use data collected from 1996 through 2003 to examine evidence of sediment removal and document channel response in each basin (Table 3.2). We focus on adjustments in the channel bed including grain size, roughness, and the presence/absence of bedforms or clast structures. In some rivers we are tracking changes in low-flow sediment mobility or transport through time. Although our focus is on the physical recovery of the channel system, we noted signs of ecologic recovery – or lack thereof – within the channel and valley bottom.

#### **Cross-sectional surveys**

Survey lines were established in 1997 at or near the alluvial fan head in four of the five basins in our study area (Hayes et al., 2002). We established an additional cross-section upstream of the fan head on the O'Donnell River in 2001. Table 3.2 shows

when cross-sections were established and reoccupied for each river. During each survey, we measured bed topography across the valley bottom using an auto level and stadia rod. Depth and mean downstream velocity were measured at equally spaced intervals in active channels. We measured mean velocity using a Swoffer current meter in later surveys. Early surveys used a stopwatch to measure surface velocity from which we approximated mean velocity as 80% of the surface velocity. At each survey site we measured water surface slope using the level and stadia. Surface grain size distributions were obtained through Wolman pebble counts (Wolman, 1954). To track bed surface composition, clasts  $\geq 4\text{mm}$  in diameter were categorized as lithic or pumice.

### **Longitudinal surveys**

On the three rivers with the most sediment loading we measured bed surface long profiles from the alluvial fan head as far upstream as possible. These data were coupled with a reconnaissance survey done in 1996 on the Pasig-Potrero River by J. Stock. We used a laser rangefinder with built-in inclinometer to measure bed elevation and slope at points spaced 50-100 m apart along the river. With this spacing, the rangefinder has uncertainties of  $\pm 0.06$  m in the horizontal and  $\pm 0.14$  m in the vertical. Given this, we do not use the profile elevation data to show absolute changes in bed elevation, but we do consider that slopes integrated over several hundred meters are accurate and can be compared between years.

In addition to measuring longitudinal bed elevation, we also conducted Wolman pebble counts every 1-2 km. We noted clast type (lithic vs. pumice) for all clasts  $\geq 4\text{mm}$  diameter to document lithologic composition of the bed surface.

On the O'Donnell River we surveyed 10.9 km upstream, all the way to the headwaters of the channel at the crater wall. On the Sacobia River, we could survey 8.0 km upstream of the alluvial fan head in the dry season, to a spring emanating from a cliff, but in the rainy season we were limited to the lower 5 km. A 16.0 km stretch of the Pasig-Potrero River was surveyed, including 7.3 km on the alluvial fan for comparison.

### **Sediment mobility and transport**

In channels with highly mobile clasts, we conducted surveys to quantify conditions necessary for sediment mobility. We surveyed four sites on the Pasig-Potrero and Sacobia Rivers repeatedly from 1997 through 2002 (Table 3.2). Surveys from 1997 are presented in Montgomery et al. (1999). In these surveys, we measured the diameter of clasts that were either mobile or stationary, noted clast composition (lithic or pumice), and measured water depth. Clasts were designated as mobile only if they were actively moving at the time of measurement. Although these surveys neglect variations in important parameters like flow velocity, we sampled across entire braids to ensure a range of flow conditions.

By 2000, low bars within the active braidplain were becoming weakly armored, leading to more grain interactions in channels flowing across bars. To assess the importance of these clast interactions, we surveyed braids flowing across bars separately from braids not associated with bars. During the winter of 2001, we also conducted a clast mobility survey in what we termed “clear-water channels”. These braids had visibly low suspended sediment concentrations and few mobile clasts  $\geq 4$ mm. Many were groundwater-fed, and we could trace them to their source in the river bed. The average velocity measured in one of these braids was 0.4 m/s, swift enough to mobilize and transport coarser sediment in exposed positions, but only small amounts of sand were mobile.

On the Pasig-Potrero River, we also measured sediment transport rates during low-flow conditions in the rainy season of 2001. We compare sediment transport rating curves with a similar study undertaken by Hayes et al. (2002) during the 1997 and 1998 rainy seasons. Bedload and suspended load were measured over the course of a four week period in August and September 2001. We sampled both suspended load and bedload using the equal-width increment technique as outlined in Edwards and Glysson (1999). For suspended load, we obtained vertically-integrated bulk samples with a U. S. Geological Survey DH-48 sampler with a  $\frac{1}{4}$  inch (0.64 cm) opening. Bedload was measured using a handheld modified U. S. Geological Survey Elwha pressure-

difference sampler with a 200 mm x 100 mm opening and 1 mm mesh bag. Bedload transport was computed assuming a 100% sampler efficiency (Hayes et al., 2002).

For each suspended load sample, we used the average of three separate passes across the channel. For bedload discharge, we collected samples on two separate passes across the channel. One of the two samples was dried, weighed, and sieved. We measured discharge immediately before and after sample collection to ensure flow conditions remained constant. If the discharge changed more than 30%, transport data were discarded.

## **Results**

The degree of channel response and timescale of channel recovery varied directly with the initial sediment loading. Below we examine and review changes in the five study basins, with particular emphasis on 1997 through 2002. It is important to note that the basins were at different phases in the recovery process in 1997, a result of variations in initial sediment loading. Those basins with the least sediment loading had recovered more than those with more severe sediment loading. We discuss our observations on the bed surface, channel form, and flow and sediment transport processes in order from basins with the least to the greatest impact, or those farthest along the recovery process to those with less progress. All our results focus on the portion of the basin upstream of the alluvial fan head. In this context, references to the lower and upper basin are the lower and upper half of the basin upstream of the alluvial fan head. In some cases, river kilometers are used to denote locations within the basin upstream of the fan head. An overview of the results for each basin is given in Tables 1.3 and 1.4.

### **Porac River**

The Porac River had only 1% of its basin covered by pyroclastic-flow deposits (Major et al., 1996), although > 0.4 m of ash and tephra-fall blanketed upper basin hillslopes (Paladio-Melosantos et al., 1996). Lahars occurred in the summer of 1991. Helicopter flights in September 1991 found practically all pyroclastic-flow deposits

gone by the end of the first rainy season (Pierson et al., 1992). Cross-sectional surveys at two sites upstream of the alluvial fan head on the Porac River began in August of 1997. On August 20, 1997, a storm with a 100-year recurrence interval occurred on the east flank of Pinatubo (Tuñgol, 2002). Repeat surveys after the storm showed only minor changes in bed topography (Figure 3.5a). In August 2000, surveys of site P1 found almost no changes in bed topography since 1997. Site P2 could not be compared directly to 1997 data due to the construction of a small dam below the site. In 1997, the P1 site was dominated by very coarse pebble gravel (average  $D_{50}$  of  $-5.5\phi$  (45 mm)) and had high roughness values with an average Manning's  $n$  value of 0.08. Site P2 had a mean grain size in the granule range, with a  $D_{50}$  of  $-1.9\phi$  (4 mm), and a Manning's  $n$  value of 0.03. By 2000, both cross-sections had coarsened, with  $D_{50}$  values in the very coarse pebble to cobble range:  $-6.7\phi$  (104 mm) and  $-5.6\phi$  (49 mm) at sites P1 and P2, respectively. By 1997, the banks were fully vegetated. By 2000, algae, macroinvertebrates, snails, and fish had returned to the main channel.

### **Gumain River**

The Gumain River had 5% of its basin area covered by pyroclastic-flow deposits (Janda et al., 1996). Lahars occurred during the 1991 rainy season. Helicopter flights in September 1991 showed only 20-40% of the pyroclastic-flow deposits remaining in the upper Gumain valley (Pierson et al., 1992). No lahars were reported during the 1992 or 1993 rainy seasons (Janda et al., 1996).

Cross-sectional survey lines were established on three sites upstream of the alluvial fan head in August 1997. Repeat surveys at sites G1 and G3 after the storm of August 20, 1997, show substantial incision and lateral movement of the channel (Figure 3.5b). In 2000 and 2001, repeat surveys were conducted on the same two sites. Site G1 had stabilized and showed little change other than some deepening of the thalweg from September 1997 through 2001. At site G3, the channel continued to migrate rapidly across the floodplain, moving by at least 18 meters from 2000 to 2001.

The Gumain River bed is dominated by coarse pebble gravel to large cobbles. In 1997, surface  $D_{50}$  values measured on three cross-sections ranged from  $-4.5$  to  $-7.0\phi$  (23



– 128 mm). Surface  $D_{50}$  values in 2000 and 2001 at sites G1 and G3 were coarser than 1997 values by an average of  $-1.1\phi$ . Backcalculated Manning's  $n$  values ranged from 0.041 to 0.050 in 1997, and rose to 0.07 in 2001. We were unable to get accurate flow measurements on site G1 in 2001 due to backwater effects from a small dam erected just downstream from the site.

By 2000, sparse vegetation occupied a terrace formed during the August 20, 1997, event. The river bed was armored and rough with fairly clear water. In 2000, there was no evidence of either macroinvertebrates or fish in the river, but by 2001 locals reported that fish had returned to the main channel.

### **O'Donnell River**

The O'Donnell River drains the north flank of Mount Pinatubo. The 1991 eruption covered 18% of the basin with pyroclastic-flow deposits. Major lahars occurred through 1994 (N. Tuñgol, personal communication). The channel was not surveyed until 2000, at which point it was still wide, turbid, and braided at the fan head. The upper basin had coarsened considerably, leading to noticeable downstream fining (average  $D_{50}$  of  $-4.4\phi$  (21mm) in the upper 5 km versus  $-2.7\phi$  (6 mm) in the lower 5 km). The channel bed is still very active during the rainy season, with a highly mobile bed. In summer 2001, bed elevation changes of at least 0.5 meters were observed during a single storm.

During the 2001 dry season, reaches of the O'Donnell shifted from wide, shallow, and braided to a single, incised, armored channel. The reaches where this incision occurred stretched as far downstream as 2 km above the alluvial fan head. The flow had visibly low suspended sediment concentrations. In places where the valley constricts to a width of less than 12 meters, the channel had cut down to bedrock. Algae were present in the main channel during the dry season but were confined mostly to hot springs in the upper basin. In the headwaters (uppermost 2 km), vegetation was present in the valley bottom, and several aquatic species were found including algae, macroinvertebrates, and frogs. In the lower basin, vegetation was limited to a few high

terraces and rill fields, and no aquatic flora or fauna were observed in the main channel or valley bottom.

### **Pasig-Potrero River**

Of the five study basins, the Pasig-Potrero River had the greatest sediment cover with approximately 33% of the basin area covered by valley-filling pyroclastic-flow deposits (Major et al., 1996) to depths as great as 200 meters in the valley bottom (Scott et al., 1996b). The Pasig-Potrero River is currently wide, shallow, and braided with high sediment loads even at low flow. It is incised into its alluvial fan and continues to aggrade near the fan head (Figure 3.6). By 2000, the long profile had developed a fairly consistent curvature upstream of the alluvial fan head. This is a change from 1996 when a segment 5-9 km above the fan head had a steady 3.5% gradient and no apparent curvature (Figure 3.7).

Major lahars continued on the Pasig-Potrero River through 1997. Hayes et al. (2002) measured sediment yield from non-lahar fluvial transport in 1997 and found that it was quite substantial, equal to one quarter of the total annual sediment yield. In 1997, the sediment yield was still two orders of magnitude higher than pre-eruption sediment yields measured at a sediment control (sabo) dam at site PP2, 2.5 km upstream of the alluvial fan head (JICA, 1978; Hayes et al., 2002). Estimates based on valley-bottom deposition show that sediment yields in 2001 were still 20 times higher than pre-eruption yields.

Sediment yields from lahar volumes and valley-bottom deposition show that yields declined exponentially during the entire first decade after the eruption. In addition, there is indirect evidence of ongoing sediment evacuation from the upper Pasig-Potrero River. If pumice content is treated as a tracer of eruptive material, then by measuring pumice content along the length of the river through time, we can determine whether or not eruptive sediment being transported out of the basin is being replenished from the hillslopes. We found a distinct decrease in pumice content for clasts  $\geq 4$  mm, starting in the upper basin. By 2001 pumice content at the alluvial fan head had dropped to  $<30\%$ , down from  $>95\%$  in 1996 (Figure 3.8a).

Surveys of surface grain size in the channel bottom show an overall increase in median grain size through time, starting in the upper basin (Figure 3.8b). This pattern of a coarser upper basin and finer lower basin has led to systematic downstream fining, even though the channel overall is coarsening through time. Coupled with coarser surface grain size is an increase in bed organization. There are more pebble clusters and armor patches present within the Pasig-Potrero River now than there were at the end of the lahar phase. However, reach-averaged Manning's  $n$  roughness values did not change substantially from 1997 through 2001 (Table 3.3).

The effect of the pebble clusters and armor patches on sediment mobility is evident from the results of channel mobility surveys. In 1997, there was a fairly sharp delineation between mobility and stability for sediment in the active channel network (Figure 3.9). Clasts were stable in water less than half their grain diameters, and any flow deeper than that would mobilize clasts (Montgomery et al., 1999). By 1998, there was some overlap between stable and mobile regions. The region of mobility did not change: clasts in water depths greater than approximately half their diameter could mobilize. However, the range of depths over which clasts could remain stable increased, and clasts could remain stable in water depths up to approximately one grain diameter. Thus, for many clasts there was a greater barrier to overcome for initiating mobility. In surveys after 1998, channels running across low bars with greater concentrations of pebble clusters and armor patches showed an even greater barrier to initial mobility. In these partially armored channels, clasts could remain stable at any depth, although the conditions under which clasts could mobilize were the same as in unarmored channels.

There were differences between lithic and pumice clast mobility in main channels from summer 2000 and winter 2001 surveys. In the transition zone between stability and mobility, there tend to be more mobile pumice than lithic clasts and more stable lithic than pumice clasts. The summer 2001 and 2002 surveys show no apparent lithologic differences.

The increase in clast stability also affects overall low-flow sediment transport. We found an increase in the critical shear stress, from  $<0.02$  Pa in 1997-98 to 5 Pa in 2001.

Otherwise, the bedload transport rating curves remained similar. Chapter 4 goes into more detail on bedload and suspended load rating curves from both 1997-98 and 2001. It is difficult to compare suspended load measurements between 1997-98 and 2001 due to sparse overlap in data. During the 1997 and 1998 field seasons, several large storms occurred, allowing Hayes et al. (2002) to measure suspended load at much higher discharges than occurred in August and September 2001. In the range where measurements do overlap, between 1-5 m<sup>3</sup>/s, the average concentration was higher in 1997-98 than in 2001 (24 kg/m<sup>3</sup> versus 15 kg/m<sup>3</sup>), although this is somewhat misleading due to the skew in the samples. In 1997-98 only 6 of 20 samples were collected at discharges from 1-3 m<sup>3</sup>/s, while in 2001, 16 out of 22 were collected over this range. Even during the storms in 1997 and 1998, concentrations did not reach hyperconcentrated flow levels, with a maximum sediment concentration by weight of less than 30%. Hyperconcentrated flows occur with sediment concentrations of greater than 40% by weight (Beverage and Culbertson 1964). Hyperconcentrated flow probably did occur during the 1997 Typhoon Ibiang lahar on the Pasig-Potrero River.

In winter 2001, the flow condensed into a single armored channel incised into valley-bottom sediments in the upper basin, 5.5 kilometers upstream of Delta 5. Incision greater than 3 meters had occurred in some reaches before an armored, stable bed developed (Figure 3.10). The channel bed appeared much less mobile, and there were lower suspended sediment concentrations. Unfortunately, no direct measurements were made. Repeat observations were made in June of 2003, near the beginning of the rainy season. Even after one typhoon, river consolidation and incision were still present starting 6.9 km upstream of Delta 5. Flow in the single-thread channel was measured along two cross-sections. The average unit discharge was 1.3 m<sup>2</sup>/s, which is higher than any measurement made from active braids during the rainy season of 2001. Even though discharge was so high, sediment mobility was visibly lower than during the rainy season.

During the dry season in 2001, small clear-water channels also developed at the fan head. These channels were armored, much less mobile than main braids,

groundwater-fed, and able to support algae growth. We have seen no other evidence of aquatic life in the lower Pasig-Potrero River through 2002.

### **Sacobia River**

The Sacobia River had 29% of its basin inundated with pyroclastic-flow deposits (Major et al., 1996). Numerous lahars occurred following the eruption which lessened when the channel was beheaded in 1993. However, a lahar that left deposits greater than 2 meters thick at the alluvial fan head occurred as recently as July 2002. The Sacobia River remains fully braided, wide, and shallow, with high sediment transport rates.

There are fewer pebble clusters visible than on the Pasig-Potrero River. Patches of armor appear on low bar surfaces, but the “armor” is generally composed of small pumice clasts which offer little resistance to movement as shown by clast mobility surveys. Mobility surveys had similar results to the Pasig-Potrero in 1997 and 1998 (Figure 3.9). By 2000, clasts were slightly more stable in channels on bar tops than in main channels, but the difference was not as evident as on the Pasig-Potrero River. Surveys in winter 2001, summer 2001, and summer 2002 found little difference between channels and bar tops in terms of clast mobility. There were differences between lithic and pumice clasts in winter and summer 2001, with lithic clasts stabilizing at greater depths than pumice clasts. These lithologic variations were not evident in summer 2002 surveys.

We see no significant changes in surface grain size or pumice content from 1997 through 2002 (Figure 3.11). There is some evidence of a downstream decrease in grain size and pumice content during the dry season of 2001, but there are no temporal trends. Despite the lack of measurable grain size adjustments, roughness values have increased from 1997 through 2002 (Table 3.3, Figure 3.12). No seasonal incision was observed in winter 2001 like that on the Pasig-Potrero and O’Donnell Rivers. In 2000, the channel upstream of the alluvial fan head was essentially a ramp with a slope just over 2% (Figure 3.13). By 2001, this ramp area developed a distinct concavity. Sparse grassy

vegetation was starting to grow in rill fields and on high terraces by 2001, but we saw no evidence of vegetation or aquatic life in the active braidplain.

### **Discussion**

Because of the magnitude of sediment loading at Pinatubo, stream recovery has been prolonged, allowing us to observe adjustments to the fluvial system over a number of years. Initially, lahars occurred in all basins, lasting just one rainy season in low-impact basins, while continuing for more than a decade in some high-impact basins. Following the lahar phase, sediment inputs to the system have declined as upland sources are depleted or stabilized. A simplistic way to envision this fluvial recovery phase is as a large flume with steadily decreasing sediment feed rate. As sediment inputs decline, channel and valley-bottom adjustments occur that lower sediment storage volume and reduce the effective shear stress available to transport sediment. Given the difficulty in predicting the timing and sequencing of these adjustments from first principles in field situations, we made observations and measurements in basins with a range of initial sediment loading conditions to document adjustments during fluvial recovery. We focus first on changes over half a decade in the heavily impacted Pasig-Potrero River and then expand our view to include four other basins. Finally, we synthesize our observations to formulate a general conceptual model for channel recovery following basin-wide sediment loading. Differences in the style and rate of fluvial recovery between basins illustrates the importance of local sediment budget context on the pace of recovery.

#### **Fluvial recovery on the Pasig-Potrero River**

Measurements of sediment yield at Pinatubo in the first few years after the eruption show an exponential decline (Figure 3.2) (Umbal, 1997), although further studies on the Pasig-Potrero River show that a non-linear power function decay may be more appropriate (Tuñgol, 2002). It is unclear whether sediment yields will continue declining non-linearly, or if they will stabilize at a higher level. Climatic shifts or high

magnitude precipitation events could act to reset recovery rates, producing and possibly maintaining sediment yields above predicted rates (Major et al. 2000; Major 2004).

Throughout the first decade, sediment yields were still declining on the Pasig-Potrero River. This is supported by changes in bed surface composition. The 1991 pyroclastic-flow material is sandier (70-85% by weight) and more pumice-rich than the original channel bed material (Scott et al., 1996b). A steady decline in pumice content on the Pasig-Potrero River indicates hillslope inputs to the river valley are not keeping pace with sediment evacuation. These observations are compatible with declining sediment inputs to the river valley. It is possible that the decrease in the percentage of pumice on the bed is related not to a removal of pumice, but rather to an increase of lithics as channels in the upper basin incise and expand into pre-eruption valley fill. However, the amount of incision into the pre-eruption bed would have to be far greater and more widespread than observed to compare with the volume of continuing inputs from recent eruptive material.

Sources of replenishment for sediment in the channel include mass wasting from high lahar and pyroclastic-flow terraces, runoff from gullied terraces (referred to as “rill fields”), and mining of the valley floor (Figure 3.14). The high terraces are a finite source which becomes less accessible as the valley widens and the channel comes into contact less frequently with valley walls. The rill fields are starting to revegetate which may slow inputs from them, although many still have no vegetation and remain an active sediment source. During high precipitation events, debris torrents pour from the rill fields, forming fans in the valley bottom which are then removed during high flows. The valley bottom represents the most accessible source of storage in the system. It still has abundant sediment, but channel incision is required to access the sediment, and this incision can be self-limiting due to bed surface armoring and stabilization.

As sediment inputs decline, the bed is coarsening and developing more pebble clusters and armor patches (Figure 3.15). Clast structures create more form drag, directly increasing roughness. Clast structures like pebble clusters have been shown to increase bed stability, increasing the critical shear stress required to move individual particles within the cluster (Brayshaw et al., 1983). Field observations elsewhere show

that particles in cluster bedforms can remain stable longer and under higher velocity conditions than isolated particles when subjected to rising flow conditions (Brayshaw et al., 1983; Brayshaw, 1985). Clast structures like clusters and stone lines can provide enough stability in some gravel-bed channels to reduce sediment transport rates by orders of magnitude (Church et al., 1998).

The increase in cluster bedforms is coincident with decreasing clast mobility on the Pasig-Potrero River. Mobility studies from braids with and without large densities of pebble clusters clearly show that in areas with more grain interactions, gravel clasts can remain stable under greater flow conditions. This reduction in clast mobility appears to be increasing the critical shear stress necessary to mobilize clasts which could reduce overall low-flow sediment transport. Critical shear stress is still quite low, however, and the bulk of the overall sediment yield is moved during high flows, well above the critical shear stress. Thus, the current bed configuration may not be affecting overall sediment yields during the rainy season. These high flows are capable of mobilizing all grain sizes, and may destroy any cluster bedforms or armor patches present at low flow.

During the dry season, more dramatic changes were seen, with reaches in the upper basin consolidating into one main channel, incising, and armoring. Both suspended and bedload transport rates appeared much smaller. Even though there is still sediment available to these incised channels from the banks and bed, the process of incision and armoring appears to be self-limiting. As the channel incises, finer grains are winnowed away leading to the development of a surface armor. This armor layer makes it more difficult for the bed to mobilize, essentially shutting down sediment transport in the upper basin during the dry season. Even though low dry season transport rates may not profoundly affect annual sediment yields, dry season behavior may be a preview of future year-round behavior as rainy season sediment sources are stabilized or depleted.



### **Neighboring basins**

Even though we have an 8-year record on the Pasig-Potrero River, it still offers a limited view into the full spectrum of channel recovery following volcanic eruptions. We use other basins at Pinatubo to expand the model in time, including three (Porac, Gumain, and O'Donnell) that had less sediment loading and are therefore farther along in the recovery process, and one basin (Sacobia) that is progressing slower due to a substantial loss of transport capacity. It is important to keep in mind that although the Porac and Gumain Rivers received a far lesser impact than the Pasig-Potrero River and we doubt ever reached the wide, shallow, braided state that the Pasig-Potrero River is in currently, we believe they represent reasonable end members for channel recovery.

The Porac and Gumain Rivers evacuated pyroclastic-flow material early, with most or all of it moving through lahars to the alluvial fan in the first year. Both rivers are now gravel-bedded and incised, with relatively stable beds year-round. The Porac River, which had the least impact, recovered the fastest. By 1997, it withstood a 100-year precipitation event without substantial bank scour. By 2000, aquatic algae, macroinvertebrates, and fish had returned to the river. The Gumain River was subjected to slightly more sediment loading. It appears to have reached relative stability in terms of local bed elevation, but some reaches are still quite mobile laterally. The bed has become stable enough to support an aquatic ecosystem that includes fish as of 2001. In the Gumain, base level stability and the initiation of ecosystem recovery have preceded a substantial decrease in lateral mobility rates.

By 2001, the O'Donnell River was gravel-bedded and armored in the headwaters year-round with a re-developing aquatic ecosystem as evidenced by the presence of aquatic plants, insects, and amphibians. Farther downstream, the river is wide, shallow, and braided all the way to the alluvial fan head during the rainy season. Because the upper few km of the basin remains gravel-bedded and armored throughout the entire year, the lower basin must be receiving sediment primarily from local sources including adjacent rill fields and high terraces or the valley bottom. During the dry season, sediment production from rill fields and high terraces shuts down due to a lack of high precipitation and high flow events necessary to mobilize sediment into the

valley bottom. Some reaches consolidate and incise into the valley-bottom sediments. Other reaches actually cut down to bedrock.

We believe the O'Donnell best represents the state the Pasig-Potrero River is evolving toward within the next five to ten years. The area which is seasonally incised and armored should shift downstream through time. The reaches which remain armored year-round also should expand downstream as more rill fields and high terraces are stabilized or depleted. In the lower basin, inputs from unvegetated rill fields will continue to be a significant sediment source as long as base level continues to fluctuate, and incision on the mainstem propagates up into the rill fields.

The Sacobia River characterizes the opposite end of the spectrum from the Porac and Gumain Rivers. Although it is similar to the Pasig-Potrero in many respects, being wide, shallow, braided, and sediment-laden, many features indicate that it has not progressed as far towards recovery as the Pasig-Potrero River. The Sacobia still has a pumice-rich granule to fine pebble bed, with no temporal or longitudinal trends in surface grain size or pumice content. The only exception to this is a downstream gradient in grain size during the dry season in 2001. Pumice "armor" develops on bars, but this armor provides little resistance to motion. Clast mobility surveys on bar tops and channels show little difference between the two environments, in contrast with conditions on the Pasig-Potrero River.

It could be that channel recovery will get no further on the Sacobia. Due to low transport capacity, the channel may not flush excess sediment from the system leaving it sediment-choked for many years. This could be seen as a form of recovery to a new equilibrium state. However, because the eruptive sediment sources are finite and still not stabilized, we believe the Sacobia will continue to evolve, but over a longer time scale than the Pasig-Potrero River. The Sacobia may appear stable over a time frame of 2-3 years, but that does not represent recovery. As of 2002, the basin was still subject to lahars during high precipitation events, and there were no signs of any aquatic plants or animals in the valley bottom. As sediment sources are depleted or as vegetation becomes more established, slowing sediment inputs from rill fields, we expect the

Sacobia River to begin showing more of the signs of recovery now apparent on the Pasig-Potrero River.

### **Conceptual model for fluvial recovery**

Based on temporal monitoring on the Pasig-Potrero and a space-for-time substitution with four other basins on the east flank of Pinatubo, we propose a general conceptual model for recovery of fluvial systems following basin-wide volcanic sediment loading (Figure 3.16). The first stage in recovery is characterized by instability laterally, vertically, and in bed surface form and composition. At Pinatubo, this phase involved widespread lahars. These flows mobilized vast amounts of sediment, contributing to record sediment yields. They also led to wild fluctuations in base level on the main stem, which in turn created instability on adjoining tributaries (Tuñgol, 2002). Only after major lahars end can the fluvial system begin to process and adjust to the excess sediment load without big disturbances to base level. It is this phase, termed the fluvial recovery phase, wherein the channel bed can begin to adjust to changing input conditions without every lahar completely resetting the bed.

Following cessation of widespread lahars, stabilization or removal of upland sediment sources eventually allows sediment evacuation through the channel network to exceed sediment inputs from hillslopes. Pumice clasts and sand are removed preferentially through selective transport, first in the upper basin and then expanding downstream. This coincides with the establishment of downstream fining and the development of long profile curvature.

Once enough sand has been removed that gravel clasts begin to interact with one another, clast structures like pebble clusters and armor patches begin to form (Figure 3.15). They are found initially on low-amplitude bars and the edges of primary braids. These structures, coupled with increasing surface grain size, act to increase form roughness, lowering the effective shear stress available for transporting sediment. In addition, the critical shear stress increases from an overall increase in grain size and development of cluster bedforms. These clusters create hiding effects making it more difficult to mobilize sediment.

From our observations, clast structure development appears to be a precursor to full surface armor. Looking from one rainy season to the next, we see an increased density of clast structures and armor patches. During the dry season, low sediment inputs lead to winnowing through selective transport, substantially increasing gravel interactions, and leading to the development of a surface armor layer in the active channel. Sediment transport in the incised, armored dry season channel is much lower than in braids with similar discharge during the rainy season. These incised reaches represent areas with decreasing sediment in storage, as the channel mines the valley bottom, flushing sediment from the upper basin into the lower basin and alluvial fan. This process may act to keep sediment yields high early in the dry season, as incision occurs, but after the channel has incised, sediment transport rates appear to be dramatically reduced from the highly mobile braided state seen in the lower basin and during the rainy season. We predict that this zone of incision will shift downstream through time, until all of the channel upstream of the alluvial fan is incised during the dry season. Eventually, as rainy season sediment sources are evacuated or stabilized, the channel may remain incised and armored year-round.

Ecological recovery does not appear to begin until some degree of bed stability exists. Thus the pace of ecological recovery is tied to the pace of channel recovery. Stable bed sediment helps maintain habitat for higher-order species like invertebrates (Townsend et al., 1997). Eventually the presence of clast structures like pebble clusters may help maintain ecological diversity in a stream by offering refugia to aquatic organisms during flood events (Biggs et al., 1997; Biggs et al., 2001). At Pinatubo, channels with more stable beds also have lower suspended sediment concentrations, aiding the return of photosynthetic organisms.

Even after base level stabilizes, the channel armors, ecological recovery begins, and the river has recovered, lateral migration rates may remain high, as observed on the Gumain River. This condition may continue as long as sediment transport rates remain high or lessen as riparian vegetation is established along river banks and bars as seen on the Porac River.

The pace of channel recovery is tied to the rate of sediment evacuation or stabilization. How and when upland sediment sources are evacuated or stabilized depends on the source and delivery processes. Although rill fields and valley-bottom sediment may be stabilized by vegetation, high terraces are essentially immune to any stabilizing effects of vegetation. These high terraces can form shear cliffs tens of meters in height, well above the rooting depth of most plants. However, access to high terraces by active channels is reduced through valley widening. Valley-bottom sediments are the most accessible source, but entrainment is self-limiting due to sediment transport feedbacks that result in bed armoring. In terms of seasonal variations, valley-bottom sediments and some high terraces can be accessed year-round, but rill fields are only important sediment sources during high precipitation events which are limited to the rainy season. This seasonal difference in sediment supply leads to the observed seasonal recovery patterns, as sediment contributions from the rill fields are essentially shut off during the dry season.

The time scale over which adjustments occur depends fundamentally on the nature and volume of local sediment sources, and this can vary not only between eruptions, but between individual river basins for a single eruption. Following the 1980 Mount St. Helens eruption, for example, hillslope sediment sources shut down rapidly and were relatively insignificant after only a few years (Collins et al., 1983; Lehre et al., 1983; Collins and Dunne, 1986). Revegetation was not a significant factor in reducing sediment yields. At Mount Pinatubo, however, sediment production from rill fields remains an important sediment source, and it probably will take revegetation of these deposits before they are stabilized. Local context must be considered when assessing the lingering effects of volcanic sediment loading. Figure 3.16 offers a conceptual framework for the sequencing of events in channel recovery following widespread sediment loading, but post-eruption valley-bottom context is important for interpreting recovery time scales.

### Conclusions

Using observations from a suite of basins with variable sediment loading from the 1991 Mount Pinatubo eruption, we propose a conceptual model for channel recovery following extreme basin-wide sediment loading. After an initial period of widespread instability (characterized at Mount Pinatubo by lahars and base level fluctuations), the fluvial recovery phase begins. Upland sediment inputs decrease as sediment sources stabilize or are evacuated. In channels, sediment is mobilized preferentially through selective transport, starting in the upper basin and leading to downstream fining. Once the bed is coarse enough for gravel-size clasts to interact, clast structures develop, first on low bar tops and edges of channels, and finally within the main flow. These clast structures act to increase form roughness and critical shear stress. Both of these effects lead to a decrease in initial clast mobility, which can result in bed armoring. Eventually, sediment inputs from hillslopes can no longer keep pace with transport capacity, and the channel can incise into valley-bottom sediments. During incision, armoring through selective transport acts to limit overall incision and eventually stabilize the channel. After base level within the channel has stabilized, high lateral mobility rates can continue until banks are stabilized.

This conceptual model can apply to basin-wide sediment loading from numerous mechanisms, from single large landslides or regional episodes of extensive landsliding to volcanic eruptions. The time scale of recovery and details of specific stages are dependent on the climate and nature of sediment sources. At Pinatubo, for example, sediment sources are strongly seasonal, so incision and armoring are occurring first as a dry season phenomenon. In locations with different climates and sediment sources, incision and armoring may occur following the clustering stage without the initial seasonal component. While some sediment sources may decrease according to the classic exponential decline in sediment yield following an eruption, active sediment production from others may linger for years to decades while still supplying the fluvial system with excess sediment.

In many cases, the desired goal of river recovery is the re-establishment of an aquatic ecosystem of pre-disturbance complexity. Although the model above does not

include the additional process of ecosystem recovery, channel bed recovery is an important precursor to the return of aquatic species. While widespread fluctuations in base level remain, or while the channel still maintains high suspended load concentrations and a highly mobile bed, it will be difficult for anything to live in the river. Thus, the time scale for ecological recovery is fundamentally dependent on the pace of physical channel recovery.

**Table 3.1: Basin characteristics**

Basin	Basin Area <sup>†</sup> in 1991 (km <sup>2</sup> )	Area <sup>†</sup> covered by pyroclastic-flow deposits <sup>‡</sup> (km <sup>2</sup> )	% Basin covered by pyroclastic- flow deposits <sup>‡</sup>
Sacobia	42.5 (19) <sup>§</sup>	12.3	29%
Pasig-Potrero	22.7 (45) <sup>§</sup>	7.5	33%
O'Donnell <sup>#</sup>	37	6.8	18%
Gumain <sup>#</sup>	41	2.0	5%
Porac	30.8	0.3	1%

<sup>†</sup>Data are from Daag 1994, Major et al. 1996, Janda et al. 1996, and Scott et al. 1996b. Basin areas are for post-eruption conditions in 1991 upstream of alluvial fan heads: Pasig-Potrero River above 240m (PP1 site), Sacobia River above 200m (S1 site), O'Donnell River above 240m, Gumain River above 60 m (G3 site), and Porac River above 120 m (P1 site).

<sup>‡</sup> Area and percent basin covered by pyroclastic-flow deposits refers specifically to valley-filling primary pyroclastic-flow deposits.

<sup>§</sup>In October 1993, a stream capture event occurred, diverting the upper Sacobia River basin into the Pasig-Potrero River basin. Drainage areas following the capture are given in parentheses.

<sup>#</sup>We considered only the west fork of the O'Donnell River and the north fork of the Gumain River.



**Table 3.2: Data summary**

Survey and Year <sup>†</sup>	Porac	Gumain	O'Donnell	Pasig-Potrero	Sacobia
<b>Cross-section surveys</b>					
(# sites) <sup>‡</sup>					
1997	2	3		2	5
1998				2	
2000	2	2		2	4
2001 winter		2	1	2	5
2001		2	1	2	4
2002				2	3
<b>Long profile surveys<sup>§</sup></b>					
1996				•	
1997 (grain size only)				•	•
2000			•	•	•
2001 winter			•	•	•
2001			•	•	•
2002 (limited)					•
2003 <sup>†</sup> (grain size only)				•	
<b>Sediment mobility</b>					
(# surveys) <sup>#</sup>					
1997				2	2
1998				2	2
2000 (bars and channels)				4	4
2001 winter (bars, channels, and clear channels)				5	4
2001 (bars and channels)				4	4
2002 (bars and channels)				4	4
<b>Low-flow sediment transport<sup>††</sup></b>					
1997-98				•	
2001				•	

<sup>†</sup>Surveys were conducted during the rainy season, in August and September of the year listed unless otherwise noted. 2001 winter surveys were conducted in January and February 2001. Surveys in 2003 were done in June.

<sup>‡</sup>Cross-sections were established just upstream of alluvial fan heads. Listed are the number of sites established or reoccupied that year.

<sup>§</sup>Bed slope was measured as far upstream as possible during long profile surveys. Surface grain size was sampled every 1-2 km during surveys. In 1997 and 2003, only surface grain size data were collected.

<sup>#</sup>The number of sediment mobility surveys conducted on each river are listed.

<sup>††</sup>Bedload and suspended load measurements were collected to establish rating curves.

**Table 3.3: Summary of basin results: 1997-98 and 2000-02**

	Porac	Gumain	O'Donnell	Pasig-Potrero	Sacobia
<b>% Pumice<sup>†</sup></b>					
1997-98	4%	0%	N.D.	75%	86%
2000-02	1%	0%	68%	53%	93%
<b>Surface Grain Size<sup>†</sup></b>					
<i>D</i> <sub>50</sub> 1997-98	-3.7 ϕ (13 mm)	-5.9 ϕ (60 mm)	N.D.	-2.8 ϕ (7 mm)	-2.3 ϕ (5 mm)
<i>D</i> <sub>50</sub> 2000-02	-6.2 ϕ (74 mm)	-6.6 ϕ (97 mm)	-2.3 ϕ (5 mm)	-1.8 ϕ (3 mm)	-1.3 ϕ (2.5 mm)
<i>D</i> <sub>90</sub> 1997-98	-7.6 ϕ (194 mm)	-8.2 ϕ (294 mm)	N.D.	-5.3 ϕ (39 mm)	-5.0 ϕ (32 mm)
<i>D</i> <sub>90</sub> 2000-02	-7.9 ϕ (239 mm)	-8.3 ϕ (315 mm)	-5.1 ϕ (34 mm)	-5.2 ϕ (37 mm)	-4.6 ϕ (24 mm)
<b>Roughness<sup>‡</sup></b>					
<i>n</i> 1997-98 <sup>§</sup>	0.078	0.064	N.D.	0.024	0.013
<i>n</i> 2000-02	N.D.	0.067	0.035	0.023	0.023
<i>C<sub>f</sub></i> 1997-98 <sup>§</sup>	19	17	N.D.	82	288
<i>C<sub>f</sub></i> 2000-02	N.D.	16	28	90	85
<b>Aggradation/Degradation (m)<sup>#</sup></b>					
August 1997 storm	<0.5	<0.5	N.D.	-12.6 (-7.9 to -17.3)	-2.1 (-1.6 to +2.3)
1997-2000	<0.5	-1.7 (-1.5 to -1.8)	N.D.	+12.7 (8.9 to 16.5)	+3.1 (+2.6 to +3.5)
2000-2001	N.D.	-0.9 (-0.8 to -1.0)	N.D.	+2.6 (2.0 to 3.1)	-0.1 (-0.5 to +0.8)

*Notes:* Values listed are averages for all cross-sections near the alluvial fan head measured during the given time interval. N.D. – no data.

<sup>†</sup>Surface grain size and % pumice come from Wolman surface pebble counts.

<sup>‡</sup>Roughness parameters (Manning's *n*,  $n = R_h^{2/3} S^{1/2} v^{-1}$ , and coefficient of friction,  $C_f = \rho v^2 \tau_b^{-1}$ ) were backcalculated from flow measurements at each cross-section. Here,  $R_h$  is the hydraulic radius,  $S$  is water surface slope,  $v$  is mean velocity,  $\rho$  is water density, and  $\tau_b$  is the total basal shear stress.

<sup>§</sup>Velocities from 1997 and 1998 were adjusted to shift from measured thalweg to mean cross-sectional values.

<sup>#</sup>Valley-bottom aggradation/degradation refers to the overall change in the thalweg or active braidplain elevation between cross-sections. The number listed is an average of all cross-sections with the range from all cross-sections given in parentheses.

**Table 3.4: Summary of basin observations**

	Lateral Mobility <sup>†</sup>	Bed morphology/ Clast interactions <sup>‡</sup>	Signs of ecological recovery <sup>§</sup>
Porac	Low mobility: Channel cross-sections stable from 1997-2000; stable during 1997 storm event	Armored Bed	Vegetated banks; fish and macroinvertebrates present by 2000
Gumain	High mobility during 1997 storm event; Low to moderate mobility 1997-2001	Armored Bed	Light vegetation on 1997 terrace surfaces by 2000; Fish returned by 2001
O'Donnell	High mobility during rainy season – wide, shallow, and braided; As of 2001, many reaches have moderate mobility during dry season	Pebble clusters and patchy armor in rainy season; Some reaches fully armored during dry season	Very light vegetation in rill fields and terrace surfaces by 2001; some algae in river during dry season; upper 2 km have valley-bottom vegetation, frogs and macroinvertebrates
Pasig-Potrero	High mobility during rainy season – wide, shallow, and braided; As of 2001, many upper basin reaches have moderate mobility in dry season	Pebble clusters and patchy armor in rainy season; Some upper basin reaches armored during dry season	Very light vegetation in rill fields and terrace surfaces by 2001; some algae in river during dry season; nothing in active channel area during rainy season by 2002
Sacobia	High mobility year-round – wide, shallow, and braided	Patchy armor on bars composed mostly of pumice – fairly ineffective when flow reaches bar tops	Light vegetation in rill fields and terrace surfaces by 2001; nothing in active channel area during rainy season by 2002

<sup>†</sup>Lateral mobility is assessed based both on repeat surveys of cross-sections and observations made during both the rainy and dry seasons. Lateral mobility is classified as low (incised and fairly stable), moderate (incised but still migrating rapidly across the valley bottom), and high (braided or incised but migrating tens of meters in a single event).

<sup>‡</sup>Bed morphology and clast interactions encompasses observations of the presence or absence of surface armor, clast structures like pebble clusters or patches of armor, and variations between the rainy and dry seasons as of 2002.

<sup>§</sup>Signs of ecological recovery include observations of vegetation in the valley and within the active channel and the presence or absence of macroinvertebrates. Presence or absence of fish was usually assessed through conversations with local residents.

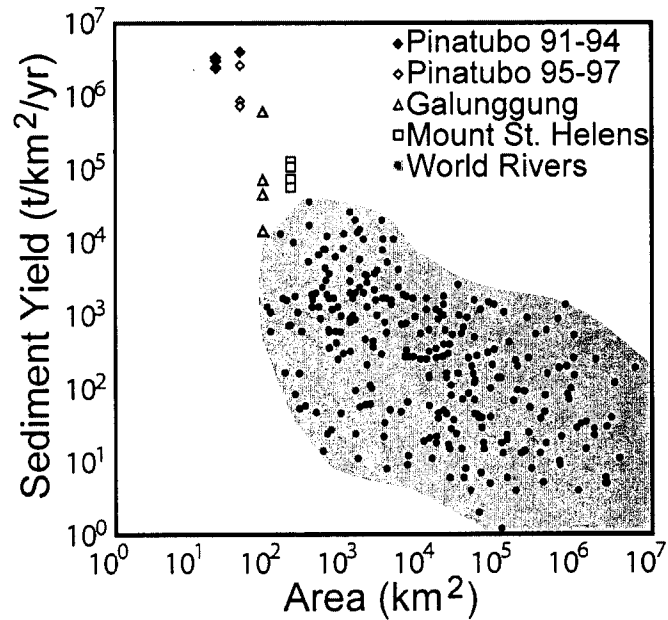


Figure 3.1: Sediment yields on volcanically disturbed rivers as compared to normal world rivers. Shown here are sediment yields from Galunggung Volcano in Indonesia (Hirao and Yoshida, 1989), the North Fork Toutle River at Mount St. Helens (Pearson, 1986), and the Pasig-Potrero River at Mount Pinatubo (Umbal, 1997; Tuñgol, 2002) in the four years following a major eruption. Pinatubo also has years 1995-1997 plotted to show how sediment yields are declining. Sediment yields from world rivers comes from Milliman and Syvitski (1992).

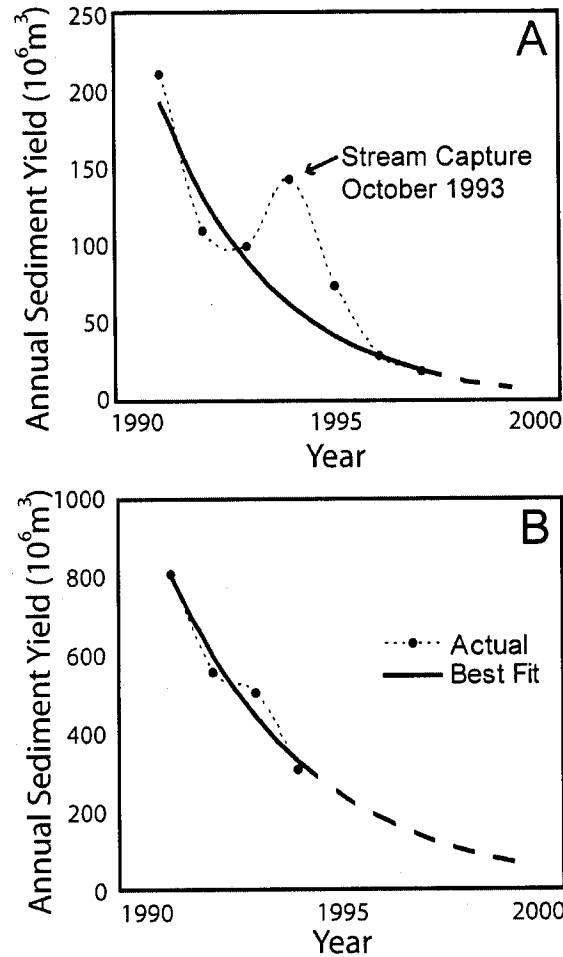


Figure 3.2. Sediment yields from (A) the Sacobia-Pasig-Abacan River system and (B) Mount Pinatubo overall. Yields generally followed an exponential decline in the years following the eruption. Data for 1991-1994 and the “best fit” exponential line estimating future yields are from Umbal (1997). Data from 1995-1997 come from Tuñgol (2002) and are for the Pasig-Potrero River system only. All data are based on mapping of lahar deposits. On the Sacobia-Pasig-Abacan, a stream capture event in October 1993 led to temporarily elevated sediment yields in 1994. Pre-eruption sediment yields on the Pasig-Potrero River were  $<1 \times 10^6 \text{ m}^3/\text{yr}$  (JICA, 1978).

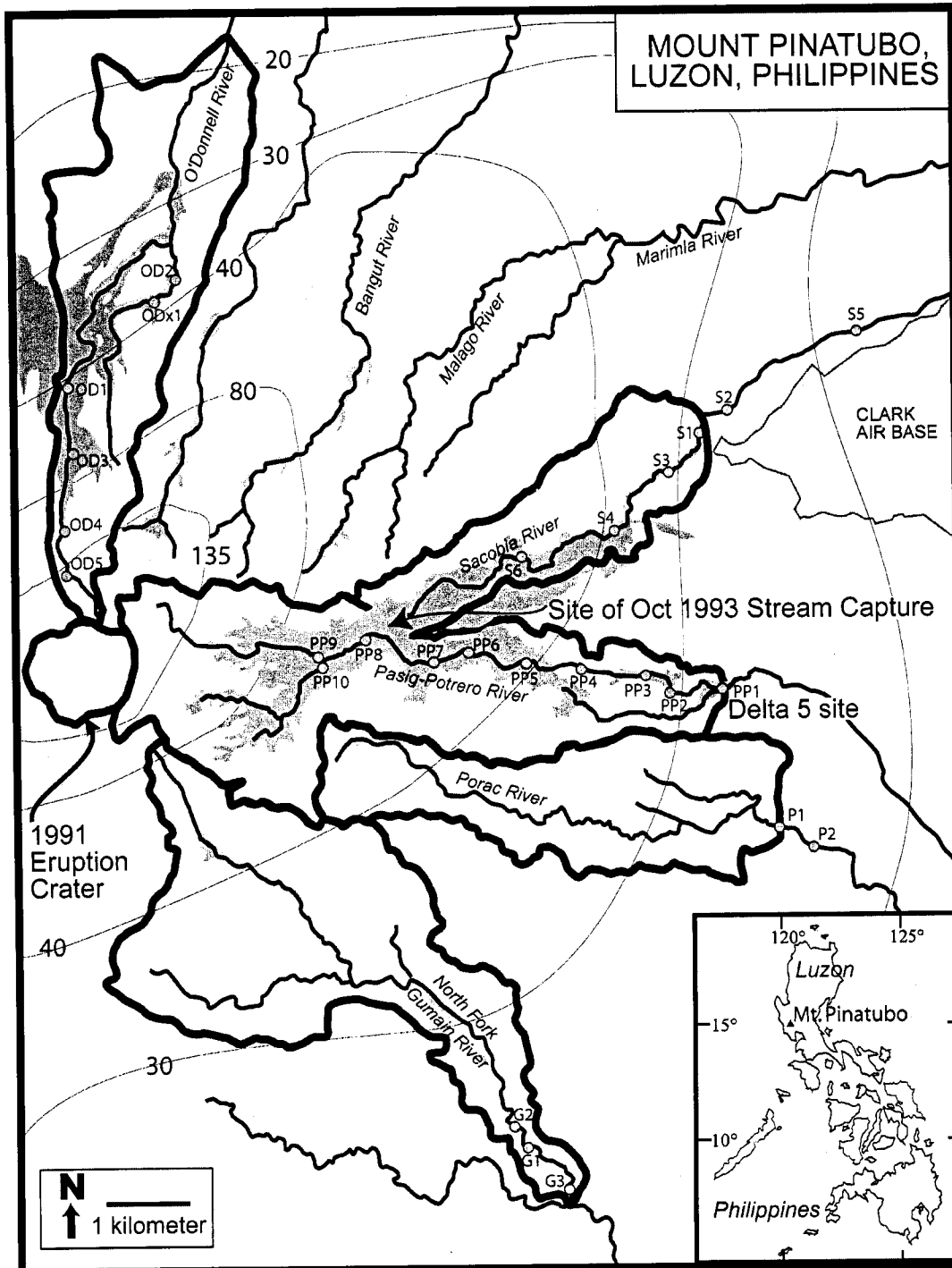


Figure 3.3. Eastern half of Mount Pinatubo showing major rivers draining the east and north flanks of the volcano. Watershed boundaries for the five study basins are delineated. Circles mark field sites. Massive valley-filling primary pyroclastic-flow deposits from the June 1991 eruption are shaded (Scott et al. 1996b), and isopach lines represent cumulative tephra fall deposits in centimeters (Paladio-Melosantos et al. 1996).

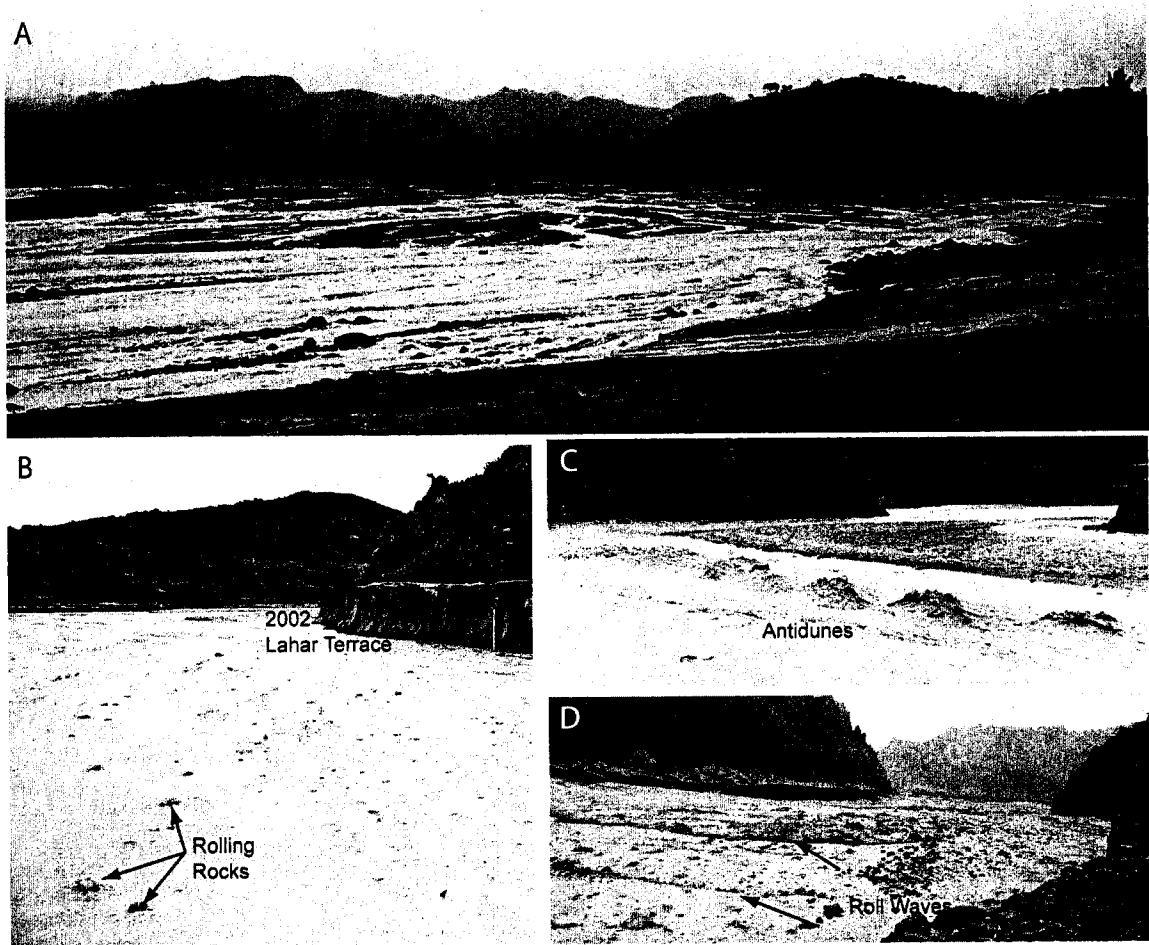


Figure 3.4. Photos from the (A) Pasig-Potrero, (B) and (C) Sacobia, and (D) O'Donnell Rivers illustrating several of the unique features of rivers which were severely impacted in the 1991 eruption. (A) Channels are often wide and braided with dozens of active braids from widths of a few centimeters up to tens of meters all transporting sediment. (B) Many of the larger clasts can be seen sticking up out of the flow and rolling or sliding across a smooth carpet of moving sand and fine pebbles. (C) Flow is often supercritical, and antidunes are common. (D) Roll waves can be seen moving downstream under all flow conditions, although they become larger and more frequent during high flow events. This event had roll waves with amplitudes up to one meter.

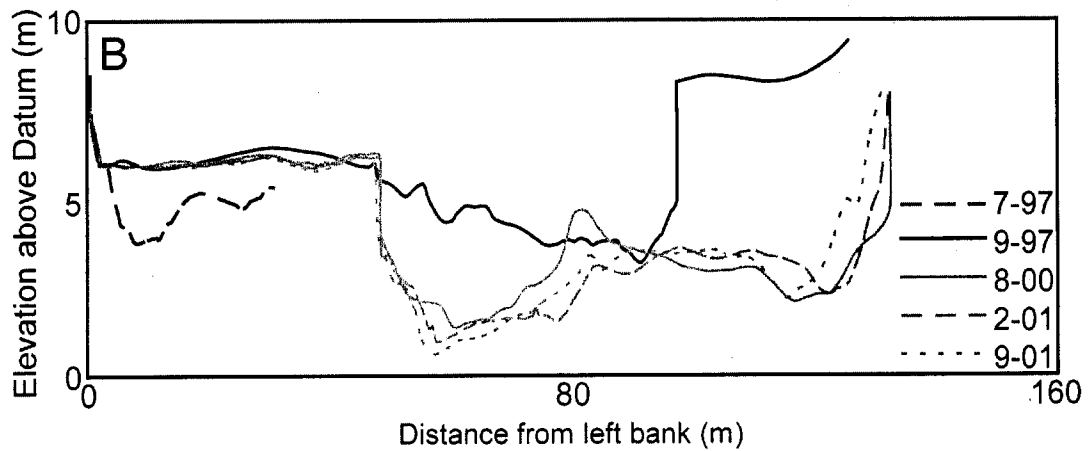
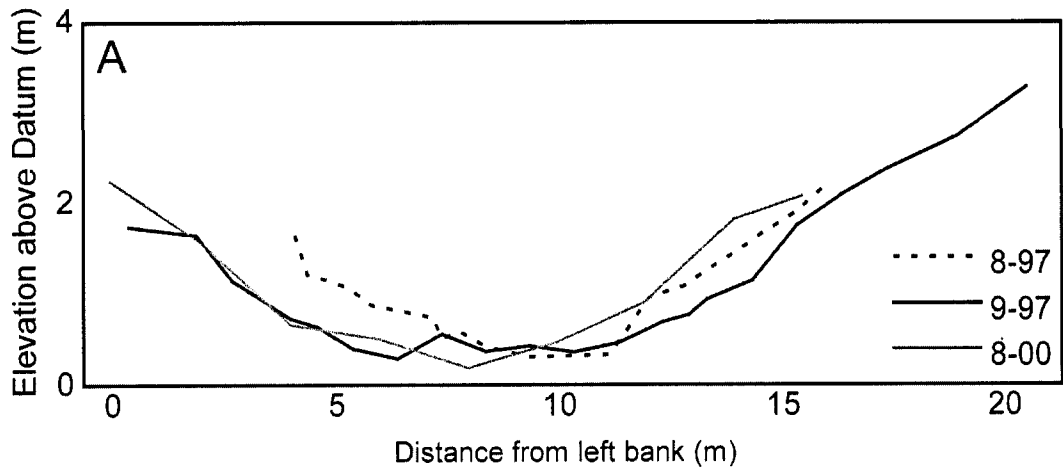


Figure 3.5. Cross-sectional surveys from the (A) Porac and (B) Gumain Rivers. Surveys of the Porac River site P1 taken before and after a 100-year storm event in August 1997 with an additional survey taken in August 2000, show little lateral movement during either time period. Surveys of the Gumain River site G1 show substantial lateral movement and vertical incision during the same storm event in August 1997. Between August 1997 and August 2000, the channel continued to deepen and widen, but the cross-section remained fairly stable both laterally and vertically from August 2000 through September 2001.



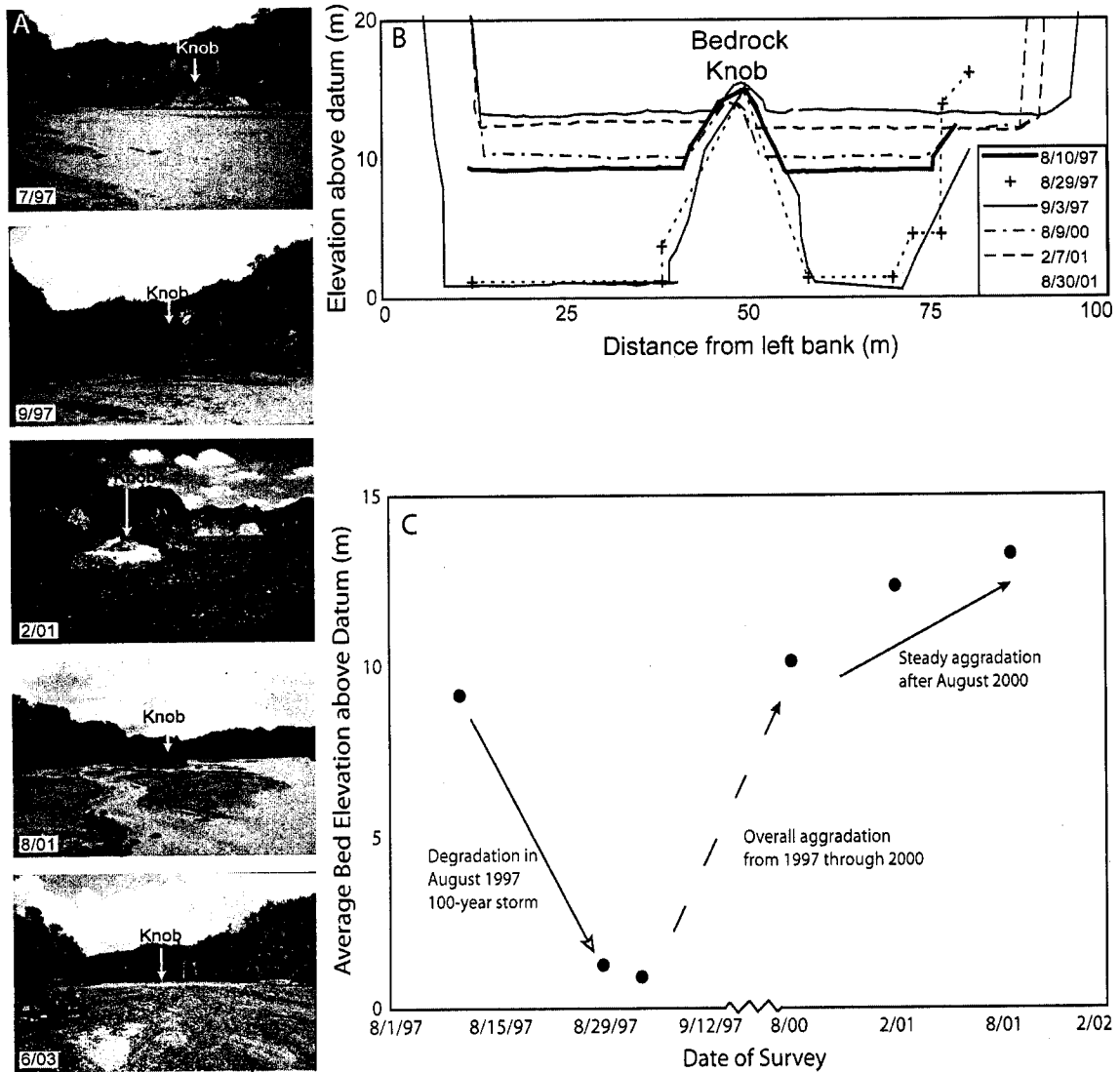


Figure 3.6. Pasig-Potrero River site PP2 (“Hanging Sabo”). PP2 has had steady aggradation following a 100-year storm in August 1997 (Tuñgol, 2002) which caused at least 8 meters of degradation. Since then, the bed has aggraded 12 meters. (A) Photo series showing scour and aggradation around a bedrock knob (“Hanging Sabo Rock”). There are people for scale in the 9/97 photo. (B) Surveys of the same river cross-section from 1997-2001. (C) Detail of the bed elevation changes through time. Note the scale change between 1997 and 2000.

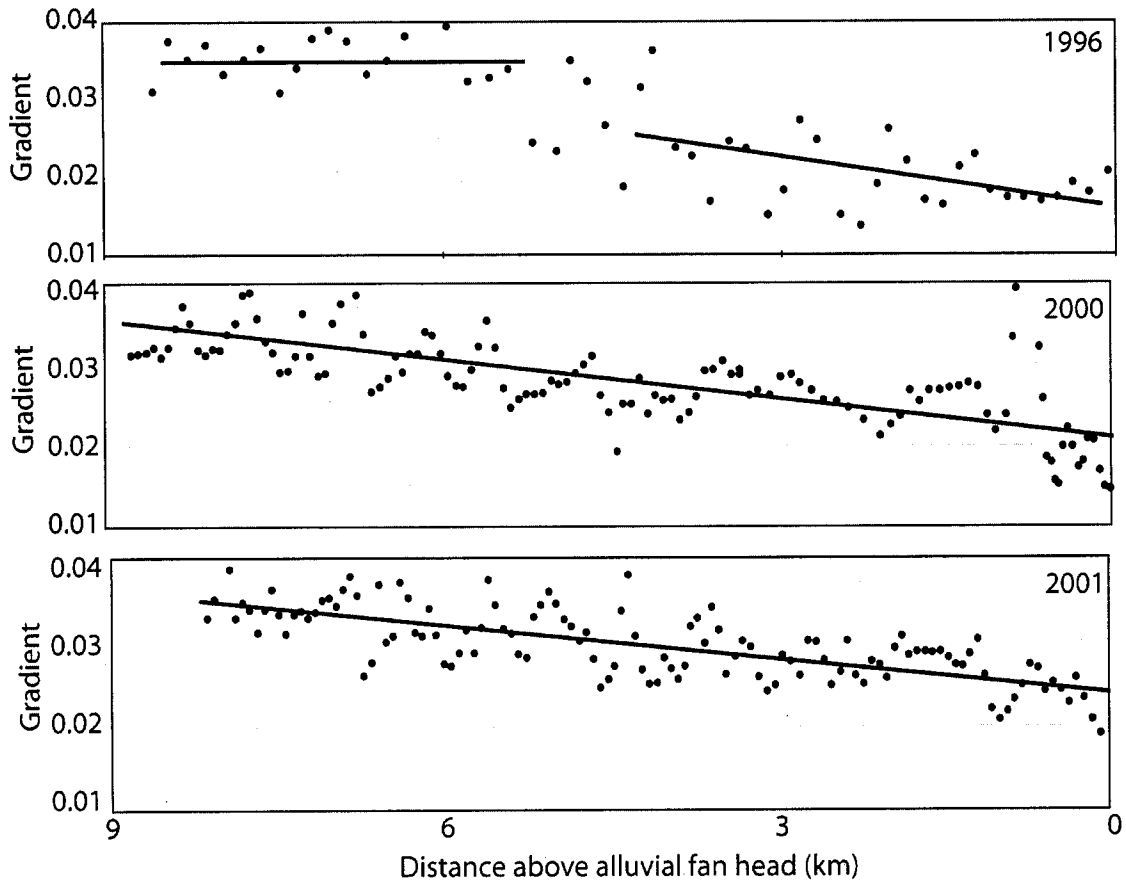


Figure 3.7. Longitudinal bed gradients on the Pasig-Potrero River. (A) In 1996, a reconnaissance survey was completed by J. Stock. Gradients were calculated an average of every 140 meters, and a two-point moving average of those gradient data are plotted here. (B) In 2000, and (C) 2001, stream gradient was calculated every 75-100 m. Plotted here are three-point moving averages. In 1996, upper reaches had almost no curvature, as shown by a constant 3.5% slope. By 2000, a fairly consistent curvature had developed.

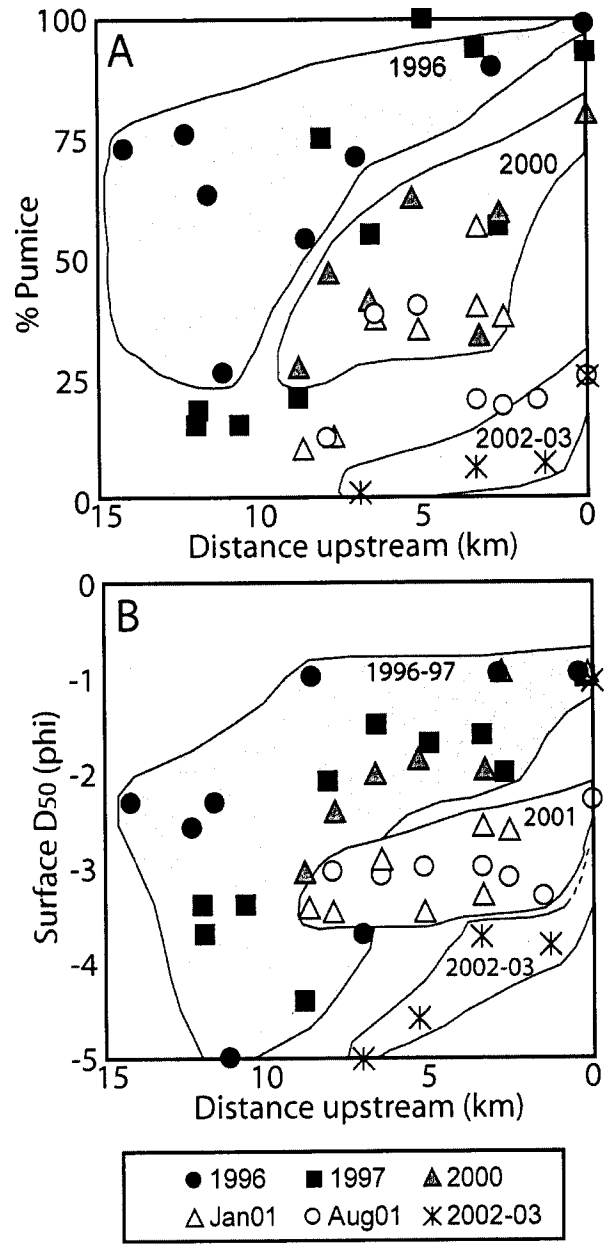


Figure 3.8. Bed surface surveys of (A) pumice content and (B) median grain size along the Pasig-Potrero River. Data plotted as  $-1\phi$  are  $\geq -1\phi$ . Pumice content decreased and median grain size increased through time. The changes occur first in the upper basin, setting up longitudinal gradients.

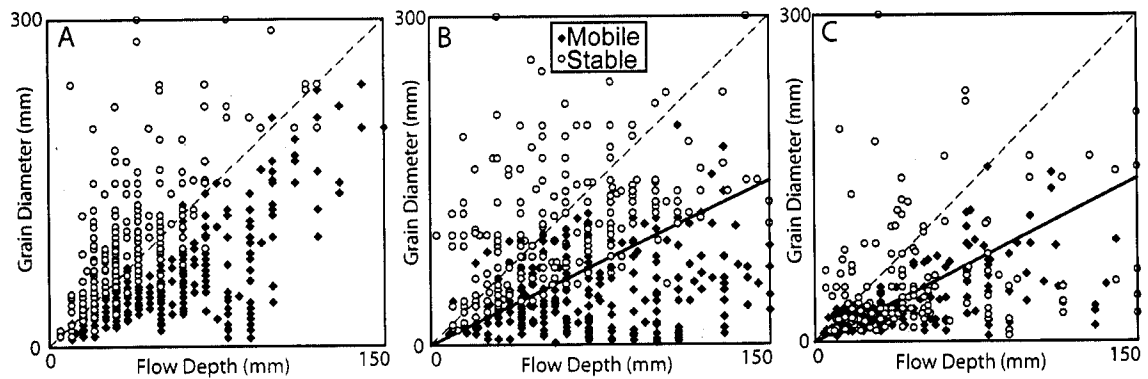


Figure 3.9. Grain mobility plots from 1997 and 2000 on the Pasig-Potrero River. (A) In 1997, there was a distinct break between mobility and stability at just below a 1:2 ratio of flow depth: grain diameter (Montgomery et al., 1999). (B) By 2000, a definite transition zone was present between the 1:2 ratio line and a 1:1 ratio over which grains could be either mobile or stable. (C) In braids running along low bar tops with concentrations of gravel clasts, grain interactions were more common. The mobility zone was the same as in the unarmored channels, but clasts could remain stable at any depth. Dashed lines are at a 1:2 ratio, and solid lines are at a 1:1 ratio.

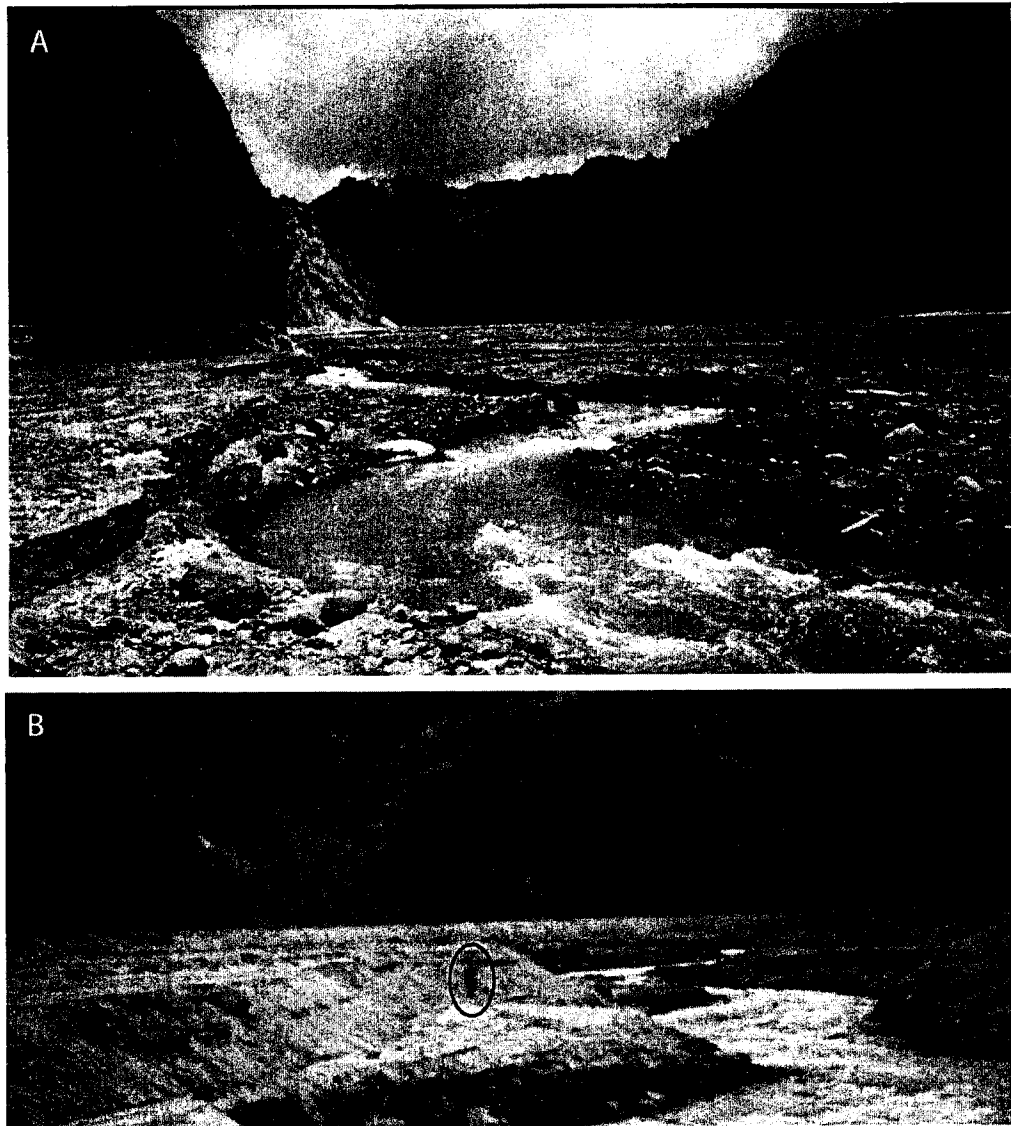


Figure 3.10. Photos of stream incision on the Pasig-Potrero River. During the dry season, upper reaches of the Pasig-Potrero River incise into the valley-bottom sediments, armoring in the process. These photos show the upper Pasig-Potrero River during (A) the very beginning of the rainy season in 2003 and (B) in the middle of the dry season in 2001. Incision during the dry season in 2001 exceeded 3 meters in some places (circled person for scale).

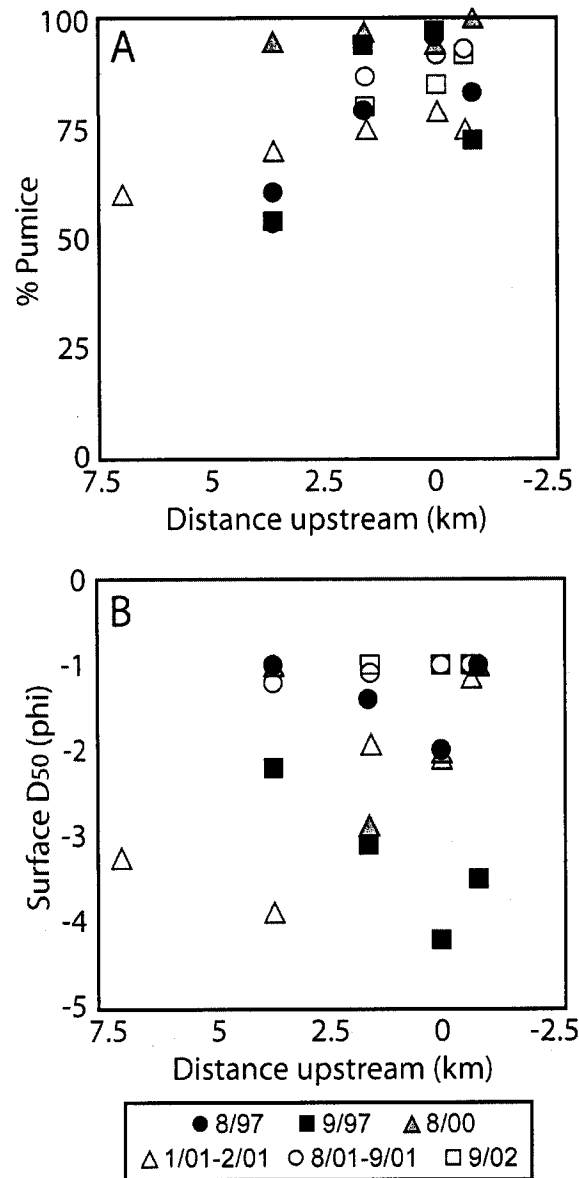


Figure 3.11. Bed surface surveys of (A) pumice content and (B) median grain size along the Sacobia River. Data plotted as  $-1\phi$  are  $\geq -1\phi$ . There were no noticeable patterns either longitudinally or through time in either pumice content or surface grain size during the rainy seasons. During the dry season in 2001, a slight downstream fining gradient developed.

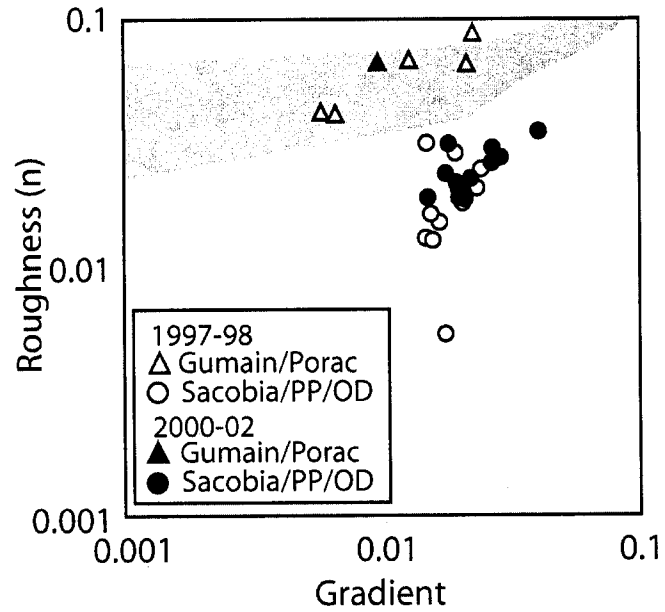


Figure 3.12. Manning's  $n$  roughness values. Roughness was backcalculated from hydrologic surveys from 1997 through 2002. Roughness increased through time on heavily impacted basins (circles), approaching values seen in the lesser impacted basins (triangles) and in mountain rivers worldwide (shaded area) (Barnes, 1967; Marcus et al., 1992).

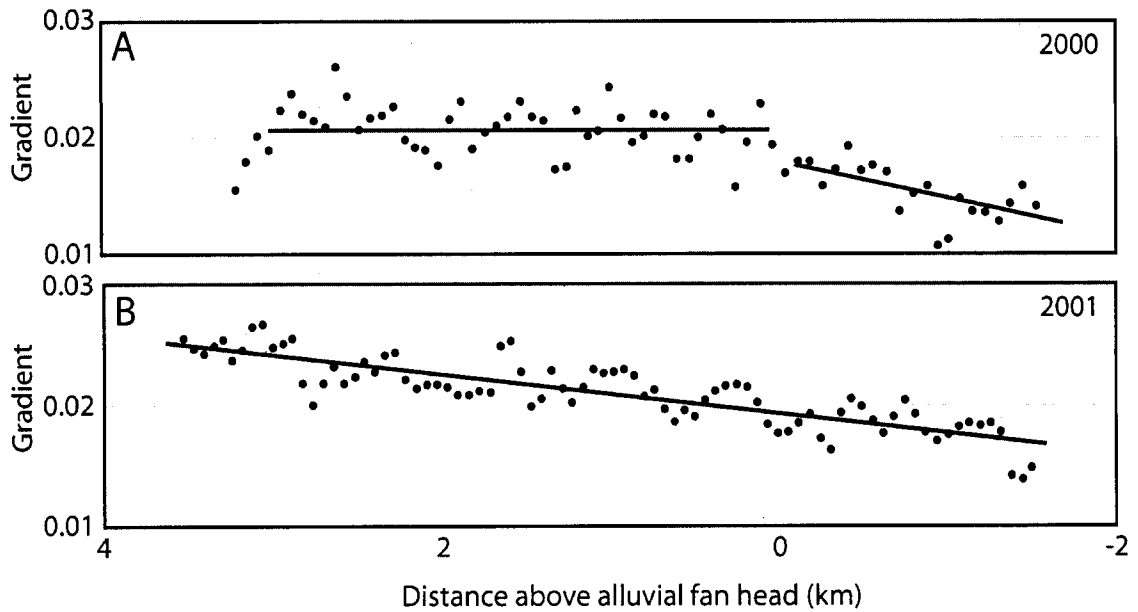


Figure 3.13. Longitudinal bed gradients on the Sacobia River. Stream gradient was calculated every 75-100 m along the accessible length of the Sacobia River. Plotted here are three-point moving averages for each of those gradient values. (A) In 2000, most of the river upstream of the alluvial fan head had no concavity, remaining at a slope just over 2% for almost 4 km before developing concavity downstream of the alluvial fan head. (B) By 2001, this reach had developed uniform concavity, with gradients steadily rising upstream.





Figure 3.14. Primary sediment sources at Mount Pinatubo. There are three main sediment sources for rivers draining Mount Pinatubo: rill fields, high terraces, and the valley bottom. The “rill fields” are gullied out terraces. They supply sediment to the channel during high precipitation events and potentially can be stabilized by vegetation. The high terraces can form shear cliffs. They erode through mass wasting, forming talus cones at the base of cliffs which are then removed during high discharge events. They cannot be stabilized by vegetation, but as valleys widen, they become less accessible. The valley bottom represents a vast reservoir of sediment, but erosion of the valley bottom is self-limiting since the channel armors and stabilizes during incision.

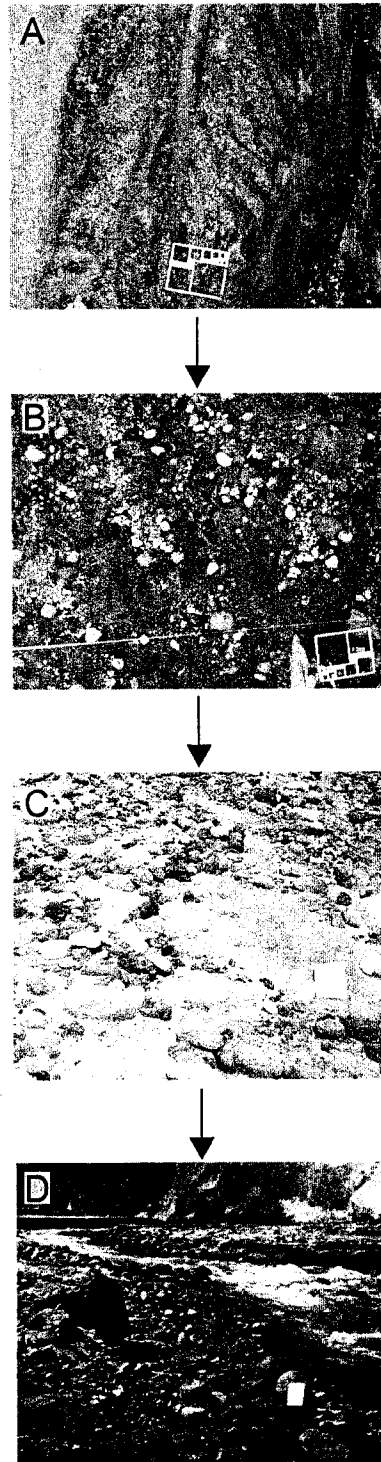


Figure 3.15. Development of bed armor in Pinatubo channels from (A) unarmored through (B) development of pebble clusters to (C) partial armor layer covering active channel surface as pebble clusters begin to interact to (D) fairly complete armor layer following incision during the dry season. Gravelometer for scale in (A) and (B) is 340 x 280 mm. Field book for scale in (C) and (D) is 120 x 195 mm.

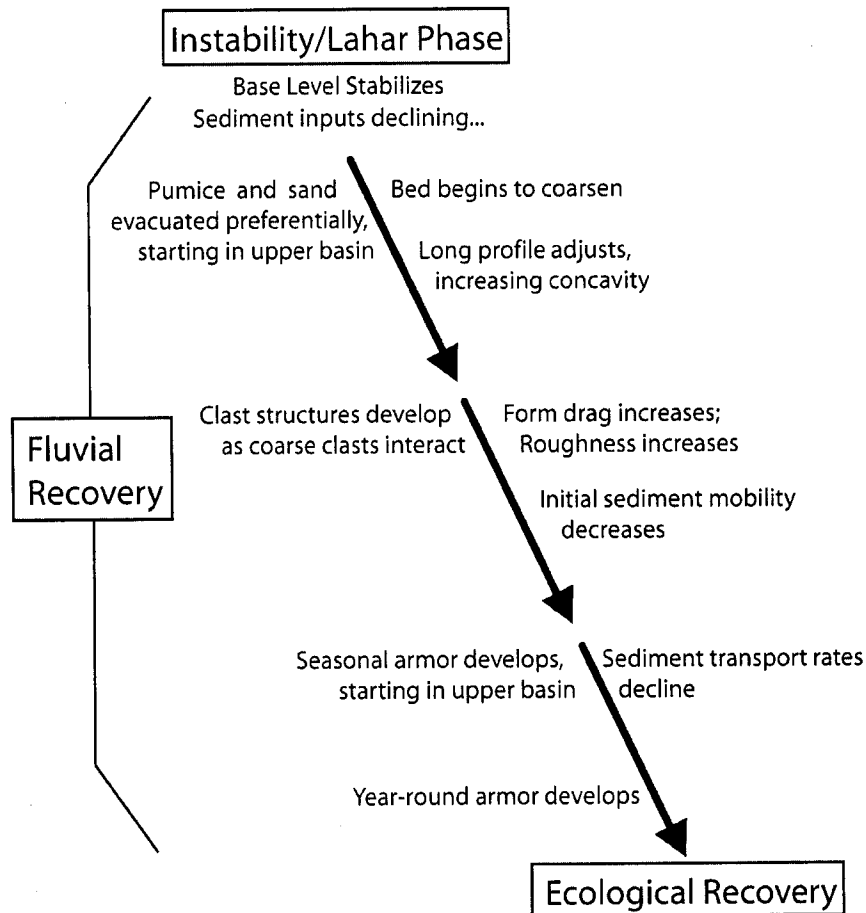


Figure 3.16. A general time line for channel recovery following extreme sediment loading. There are three basic phases: the initial instability phase, the fluvial recovery phase, and the ecological recovery phase. The initial instability phase at Pinatubo was characterized by numerous lahars leading to fluctuating base levels. The channel bed was smooth and unarmored, fine-grained, and highly mobile with high sediment transport rates. By the end of the fluvial recovery phase, the channel bed is coarse and armored, with much lower sediment transport rates and decreased channel mobility. These conditions allow ecological recovery to proceed.

**Notes to chapter**

- Barnes, H. H., 1967, Roughness characteristics of natural channels: U. S. Geological Survey Water Supply Paper 1849, 213 p.
- Benda, L., and Dunne, T., 1987, Sediment routing by debris flow, *in* Erosion and Sedimentation in the Pacific Rim, Corvallis, OR: International Association of Hydrological Sciences, v. 165, p. 213-223.
- Beverage, J. P., and Culbertson, J. K., 1964, Hyperconcentrations of suspended sediment: Journal of the Hydraulics Division, American Society of Civil Engineers, v. 90, no., HY6, p. 117-128.
- Biggs, B. J. F., Duncan, M. J., Farancoeur, S. N., and Meyer, W. D., 1997, Physical characterisation of microform bed cluster refugia in 12 headwater streams, New Zealand: New Zealand Journal of Marine and Freshwater Research, v. 31, p. 413-422.
- Biggs, B. J. F., Duncan, M. J., Suren, A. M., and Holomuzki, J. R., 2001, The importance of bed sediment stability to benthic ecosystems of streams, *in* Mosley, M. P., ed., Gravel-Bed Rivers V: Wellington, New Zealand Hydrological Society Inc., p. 423-449.
- Brayshaw, A. C., 1985, Bed microtopography and entrainment thresholds in gravel-bed rivers: Geological Society of America Bulletin, v. 96, p. 218-223.
- Brayshaw, A. C., Frostick, L. E., and Reid, I., 1983, The hydrodynamics of particle clusters and sediment entrainment in coarse alluvial channels: Sedimentology, v. 30, p. 137-143.
- Chinen, T., and Kadomura, H., 1986, Post-eruption sediment budget of a small catchment on Mt. Usu, Hokkaido: Zeitschrift für Geomorphologie N. F. Suppl. Bd., v. 60, p. 217-232.
- Church, M., Hassan, M. A., and Wolcott, J. F., 1998, Stabilizing self-organized structures in gravel-bed stream channels: Field and experimental observations: Water Resources Research, v. 31, no. 11, p. 3169-3179.
- Collins, B. D., and Dunne, T., 1986, Erosion of tephra from the 1980 eruption of Mount St. Helens: Geological Society of America Bulletin, v. 97, p. 896-905.
- Collins, B. D., Dunne, T., and Lehre, A. K., 1983, Erosion of tephra-covered hillslopes north of Mount St. Helens, Washington: May 1980 - May 1981: Zeitschrift für Geomorphologie N. F. Suppl. Bd., v. 46, p. 103-121.

- Cui, Y., Parker, G., Lisle, T. E., Gott, J., Hansler, M. E., Pizzuto, J. E., Allmendinger, N. E., and Reed, J. M., 2003a, Sediment pulses in mountain rivers: I. Experiments: *Water Resources Research*, v. 39, no. 9, p. ESG\_3-1 to 3-12.
- Cui, Y., Parker, G., Pizzuto, J. E., and Lisle, T. E., 2003b, Sediment pulses in mountain rivers: 2. Comparison between experiments and numerical predictions: *Water Resources Research*, v. 39, no. 9, p. ESG\_4-1 to 4-11.
- Daag, A. S., 1994, Geomorphic developments and erosion of the Mount Pinatubo 1991 pyroclastic flows in the Sacobia watershed, Philippines: A study using remote sensing and Geographic Information Systems (GIS) [M.S. thesis]: Enschede, Netherlands, International Institute for Geoinformation Science and Earth Observation (ITC), 106 p.
- Dietrich, W. E., and Dunne, T., 1978, Sediment budget for a small catchment in mountainous terrain: *Zeitschrift für Geomorphologie N. F. Suppl Bd.*, v. 29, p. 191-206.
- Dinehart, R. L., 1998, Sediment transport at gauging stations near Mount St. Helens, Washington, 1980-90. Data collection and analysis: U. S. Geological Survey Professional Paper 1573, 105 p.
- Edwards, T. K., and Glysson, G. D., 1999, Field methods for measurement of fluvial sediment: U. S. Geological Survey, Techniques of Water-Resources Investigations Reports, TWRI-3-C2, 89 p.
- Gilbert, G. K., 1917, Hydraulic mining debris in the Sierra Nevada: U.S. Geological Survey Professional Paper, v. 105, 154 p..
- Gran, K. B., and Montgomery, D. R., 2005, Spatial and temporal patterns in fluvial recovery following volcanic eruptions: Channel response to basin-wide sediment loading at Mount Pinatubo, Philippines: *Geological Society of America Bulletin*, v. 117, n. 1/2, p. 195-211.
- Hamidi, S., 1989, Lahar of Galunggung Volcano from 1982 through 1986, *in* International Symposium on Erosion and Volcanic Debris Flow Technology, Yogyakarta, Indonesia, p. VP1-1 - VP1-23.
- Hayes, S. K., Montgomery, D. R., and Newhall, C. G., 2002, Fluvial sediment transport and deposition following the 1991 eruption of Mount Pinatubo: *Geomorphology*, v. 45, no. 3-4, p. 211-224.

- Hirao, K., and Yoshida, M., 1989, Sediment yield of Mt Galunggung after eruption in 1982, *in* International Symposium on Erosion and Volcanic Debris Flow Technology, Yogyakarta, Indonesia, p. V21-1 - V21-22.
- Janda, R. J., Daag, A. S., de los Reyes, P. J., and Newhall, C., 1996, Assessment and response to lahar hazard around Mount Pinatubo, 1991 to 1993, *in* Newhall, C., G., and Punongbayan, R. S., eds., Fire and mud: eruptions and lahars of Mount Pinatubo, Philippines: Quezon City, Philippine Institute of Volcanology and Seismology, and Seattle, University of Washington Press, p. 107-139.
- Janda, R. J., Meyer, D. F., and Childers, D., 1984a, Sedimentation and geomorphic changes during and following the 1980-1983 eruptions of Mount St. Helens, Washington (1): *Shin-Sabo*, v. 37, no. 2, p. 10-21.
- , 1984b, Sedimentation and geomorphic changes during and following the 1980-1983 eruptions of Mount St. Helens, Washington (2): *Shin-Sabo*, v. 37, no. 3, p. 5-17.
- JICA, 1978, Planning report on the Pasig-Potrero River flood control and Sabo project: Tokyo, Japan, Japan International Cooperation Agency, 133 p.
- Kadomura, H., Imagawa, T., and Yamamoto, H., 1983, Eruption-induced rapid erosion and mass movements on Usu Volcano, Hokkaido: *Zeitschrift für Geomorphologie N. F. Suppl. Bd.*, v. 46, p. 123-142.
- Knighton, A. D., 1989, River adjustment to changes in sediment load: The effects of tin mining on the Ringarooma River, Tasmania, 1875-1984: *Earth Surface Processes and Landforms*, v. 14, p. 333-359.
- Komar, P. D., 1987, Selective grain entrainment by a current from a bed of mixed sizes: A reanalysis: *Journal of Sedimentary Petrology*, v. 57, no. 2, p. 203-211.
- Leavesley, G. H., Lusby, G. C., and Lichty, R. W., 1989, Infiltration and erosion characteristics of selected tephra deposits from the 1980 eruption of Mount St. Helens, Washington, USA: *Hydrological Sciences Journal*, v. 34, no. 3, p. 339-353.
- Lehre, A. K., Collins, B. D., and Dunne, T., 1983, Post-eruption sediment budget for the North Fork Toutle River Drainage, June 1980 - June 1981: *Zeitschrift für Geomorphologie N. F. Suppl. Bd.*, v. 46, p. 143-163.
- Lisle, T. E., Cui, Y., Parker, G., Pizzuto, J. E., and Dodd, A., 2001, The dominance of dispersion in the evolution of bed material waves in gravel-bed rivers: *Earth Surface Processes and Landforms*, v. 26, p. 1409-1420.

- Lisle, T. E., Pizzuto, J. E., Ikeda, H., Iseya, F., and Kodama, Y., 1997, Evolution of a sediment wave in an experimental channel: *Water Resources Research*, v. 33, no. 8, p. 1971-1981.
- Madej, M. A., and Ozaki, V., 1996, Channel response to sediment wave propagation and movement, Redwood Creek, California, USA: *Earth Surface Processes and Landforms*, v. 21, p. 911-927.
- Major, J. J., 2004, Posteruption suspended sediment transport at Mount St. Helens: Decadal-scale relationships with landscape adjustments and river discharges: *Journal of Geophysical Research*, v. 109, p. F01002.
- Major, J. J., Janda, R. J., and Daag, A. S., 1996, Watershed disturbance and lahars on the east side of Mount Pinatubo during the mid-June 1991 eruptions, *in* Newhall, C. G., and Punongbayan, R. S., eds., *Fire and mud: eruptions and lahars of Mount Pinatubo, Philippines*: Quezon City, Philippine Institute of Volcanology and Seismology, and Seattle, University of Washington Press, p. 895-919.
- Major, J. J., Pierson, T. C., Dinehart, R. L., and Costa, J. E., 2000, Sediment yield following severe volcanic disturbance -- A two-decade perspective from Mount St. Helens: *Geology*, v. 28, no. 9, p. 819-822.
- Marcus, W. A., Roberts, K., Harvey, L., and Tackman, G., 1992, An evaluation of methods for estimating Manning's n in small mountain streams: *Mountain Research and Development*, v. 12, p. 227-239.
- Meade, R. H., 1985, Wavelike movement of bedload sediment, East Fork River, Wyoming: *Environmental Geology and Water Science*, v. 7, no. 4, p. 215-225.
- Mercado, R. A., Lacsamana, J. B. T., and Pineda, G. L., 1996, Socioeconomic impacts of the Mount Pinatubo eruption, *in* Newhall, C. G., and Punongbayan, R. S., eds., *Fire and Mud: Eruptions and Lahars of Mount Pinatubo, Philippines*: Quezon City, Philippine Institute of Volcanology and Seismology, and Seattle, University of Washington Press, p. 1063-1069.
- Milliman, J. D., and Syvitski, J. P. M., 1992, Geomorphic/tectonic control of sediment discharge to the ocean: the importance of small mountainous rivers: *Journal of Geology*, v. 100, no. 5, p. 525-544.
- Mizuyama, T., and Kobashi, S., 1996, Sediment yield and topographic change after major volcanic activity, *in* *Erosion and Sediment Yield: Global and Regional Perspectives (Exeter Symposium)*, p. 295-301.

- Montgomery, D. R., Panfil, M. S., and Hayes, S. K., 1999, Channel-bed mobility response to extreme sediment loading at Mount: *Geology*, v. 27, no. 3, p. 271-274.
- Newhall, C. G., and Punongbayan, R. S., 1996, Fire and mud: eruptions and lahars of Mount Pinatubo, Philippines: Quezon City, Philippine Institute of Volcanology and Seismology, and Seattle, University of Washington Press, 1115 p.
- Paladio-Melosantos, M. L. O., Solidum, R. O., Scott, W. E., Quiambao, R. B., Umbal, J. V., Rodolfo, K. S., Tubianosa, B. S., de los Reyes, P. J., Alonso, R. A., and Ruelo, H. B., 1996, Tephra falls of the 1991 eruptions of Mount Pinatubo, *in* Newhall, C. G., and Punongbayan, R. S., eds., Fire and Mud: Eruptions and lahars of Mount Pinatubo, Philippines: Quezon City, Philippine Institute of Volcanology and Seismology, and Seattle, University of Washington Press, p. 513-535.
- Pearce, A. J., and Watson, A. J., 1986, Effects of earthquake-induced landslides on sediment budget and transport over a 50-year period: *Geology*, v. 14, p. 52-55.
- Pearson, M. L., 1986, Sediment yields from the debris avalanche for water years 1980-1983, *in* Keller, S. A. C., ed., Mount St. Helens: Five Years Later: Spokane, Eastern Washington University Press, p. 87-107.
- Pickup, G., Higgins, R. J., and Grant, I., 1983, Modelling sediment transport as a moving wave -- The transfer and deposition of mining waste: *Journal of Hydrology*, v. 60, p. 281-301.
- Pierson, T. C., Janda, R. J., Umbal, J. V., and Daag, A. S., 1992, Immediate and long-term hazards from lahars and excess sedimentation in rivers draining Mt. Pinatubo, Philippines: U. S. Geological Survey Water Resources Investigation, 92-4039, 35 p.
- Punongbayan, R. S., Tuñgol, N. M., Arboleda, R. A., Delos Reyes, P. J., Isada, M., Martinez, M. M. L., Melosantos, M. L. P., Puertollano, J. R., Regalado, M. T. M., Solidum, R. U., Jr., Tubianosa, B. S., Umbal, J. V., Alonso, R. A., and Remotigue, C. T., 1994, Impacts of the 1993 lahars, and long-term lahar hazards and risks around Pinatubo Volcano, PHIVOLCS, Pinatubo Lahar Studies 1993: Final Report of the UNESCO-funded lahar studies program: PHIVOLCS Press, 40 p.
- Rodolfo, K. S., 1989, Origin and early evolution of lahar channel at Mabinit, Mayon Volcano, Philippines: *Geological Society of America Bulletin*, v. 101, p. 414-426.



- Rodolfo, K. S., and Arguden, A. T., 1991, Rain-lahar generation and sediment-delivery systems at Mayon Volcano, Philippines, *in* Fisher, R. V., and Smith, G. A., eds., *Sedimentation in Volcanic Settings*: Tulsa, Oklahoma, SEPM Special Publication 45, p. 71-87.
- Scott, K. M., Janda, R. J., de la Cruz, E. G., Gabinete, E., Eto, I., Isada, M., Sexton, M., and Hadley, K., 1996a, Channel and sedimentation responses to large volumes of 1991 volcanic deposits on the east flank of Mount Pinatubo, *in* Newhall, C. G., and Punongbayan, R. S., eds., *Fire and mud: eruptions and lahars of Mount Pinatubo, Philippines*: Quezon City, Philippine Institute of Volcanology and Seismology, and Seattle, University of Washington Press, p. 971-988.
- Scott, W. E., Hoblitt, R. P., Torres, R. C., Self, S., Martinez, M. M. L., and Nillos, T., 1996b, Pyroclastic flows of the June 15, 1991, climactic eruption of Mount Pinatubo, *in* Newhall, C. G., and Punongbayan, R. S., eds., *Fire and mud: eruptions and lahars of Mount Pinatubo, Philippines*: Quezon City, Philippine Institute of Volcanology and Seismology, and Seattle, University of Washington Press, p. 545-570.
- Segerstrom, K., 1950, Erosion studies at Parícutin, State of Michoacan, Mexico: U.S. Geological Survey Bulletin 965-A, 64 p..
- , 1960, Erosion and related phenomena at Parícutin in 1957: U.S. Geological Survey Bulletin 1104-A, 18 p..
- , 1966, Parícutin, 1965 -- Aftermath of eruption: U.S. Geological Survey Professional Paper 550-C, p. C93-C101.
- Shimokawa, E., Jitousono, T., Yazawa, A., and Kawagoe, R., 1989, An effect of tephra cover on erosion processes of hillslopes in and around Sakurajima Volcano, *in* International Symposium on Erosion and Volcanic Debris Flow Technology, Yogyakarta, Indonesia, Ministry of Public Works, p. V32-1 - V32-21.
- Shimokawa, E., and Taniguchi, Y., 1983, Sediment yield from hillside slope of active volcanoes, *in* Symposium on erosion control in volcanic areas, Seattle and Vancouver, Washington and Tsukuba, Japan, Sabo Division, Erosion Control Department p. 155-181.
- Swanson, F. J., Fredrickson, R. L., and McCorison, F. M., 1982, Material transfer in a western Oregon forested watershed, *in* Edmonds, R. L., ed., *Analysis of Coniferous Forest Ecosystems in the Western United States*: Stroudsburg, PA, Hutchinson Ross, p. 233-266.

- Townsend, C. R., Scarsbrook, M. R., and Doledec, S., 1997, Quantifying disturbance in streams: Alternative measures of disturbance in relation to macroinvertebrate species traits and species richness: *Journal of the North American Benthological Society*, v. 16, p. 531-544.
- Tuñgol, N. M., 2002, Lahar initiation and sediment yield in the Pasig-Potrero River basin, Mount Pinatubo, Philippines [Ph.D. thesis]: Canterbury, New Zealand, University of Canterbury, 172 p.
- Umbal, J. V., 1997, Five years of lahars at Pinatubo volcano: Declining but still potentially lethal hazards: *Journal of the Geological Society of the Philippines*, v. 52, no. 1, p. 1-19.
- United States Army Corps of Engineers, 1994, Mount Pinatubo Recovery Action Plan: Long Term Report: Portland, Oregon, U. S. Army Corps of Engineers, 162 p. and 5 Appendices.
- Waldron, H. H., 1967, Debris flow and erosion control problems caused by the ash eruptions of Irazu Volcano, Costa Rica: *U. S. Geological Survey Bulletin* 1241-I, p. 11-137.
- Wilcock, P. R., and Kenworthy, S. T., 2002, A two fraction model for the transport of sand/gravel mixtures: *Water Resources Research*, v. 38, p. 12-1 - 12-12.
- Wilcock, P. R., Kenworthy, S. T., and Crowe, J. C., 2001, Experimental study of the transport of mixed sand and gravel: *Water Resources Research*, v. 37, no. 12, p. 3349-3358.
- Wolman, M. G., 1954, A method of sampling coarse river-bed material: *Transactions of the American Geophysical Union*, v. 35, no. 6, p. 951-956.
- Yamamoto, H., 1984, Erosion of the 1977-1978 tephra layers on a slope of Usu Volcano, Hokkaido: *Transactions of the Japanese Geomorph. Union*, v. 5, no. 2, p. 111-124.

## CHAPTER 4

### Channel bed evolution and sediment transport under declining sand inputs

#### Summary

Coupled field and laboratory investigations explore links between bed surface structure development and sediment transport as sand inputs decline. On the Pasig-Potrero River, we investigated channel recovery following emplacement of sand-rich pyroclastic deposits in the 1991 eruption of Mount Pinatubo, Philippines. As sediment inputs declined from 1996-2003, surface grain size increased, clast structures formed, and sediment mobility and bedload transport rates declined. Our field results parallel those from flume experiments studying highly energetic channels with similar sand contents. As sand content declined from 70% to 40% of the feed, surface grain size and gravel interactions increased, forming clusters and armor patches. Bed reorganization into patches initially accommodated coarsening with minimal effect on bedload transport rates, roughness, or critical shear stress within sandy transport zones. As sand declined further, gravel jams interrupted the connectivity of sandy transport zones, lowering transport rates. Patch development lowered the threshold for the transition from sand-dominated to gravel-dominated transport, focusing this transition into a narrow range of sand content. This chapter was submitted for publication to *Water Resources Research* in June 2005 (Gran et al., in review).

#### Introduction

Sediment transport in river systems involves important interactions between sand and gravel fractions. At low sand content, the bed is gravel-dominated, and sand transport is a function of the mobilization and removal of surface gravels. As sand content increases, sand fills the interstices between gravel clasts, eventually leading to sand-dominated transport where gravel clasts move independently over a smooth sand bed. Experimental studies find sand contents as low as 10-30% enhance gravel transport rates (Wilcock et al., 2001) and affect bed structure and organization (Ikeda and Iseya, 1988). The transition between sand and gravel beds may be characterized by

bimodal grain size distributions (Sambrook Smith and Ferguson, 1995; Sambrook Smith, 1996), grain size patchiness (Seal and Paola, 1995), and gravel jams forming over an otherwise sandy transport zone (Ikeda and Iseya, 1988).

The June 1991 eruption of Mount Pinatubo covered one third of the Pasig-Potrero watershed (Figure 4.1) with loose pyroclastic-flow deposits containing 70-85% sand (Major et al., 1996; Scott et al., 1996b). The abrupt basin-wide increase in sand loading on the previously gravel-bedded Pasig-Potrero River created a smooth, highly mobile, sand-bedded channel. Most gravel-bed rivers that experience basin-wide sediment loading (Gilbert, 1917; Knighton, 1989; Maita, 1991; Madej and Ozaki, 1996) receive less sand than the disturbed Pasig-Potrero River and may never complete the shift from gravel-bedded to sand-bedded. Because sand loading was so intense, the Pasig-Potrero River is an ideal field site for examining the role of sand content on bed development and sediment transport and how highly energetic, sand-rich channels adjust as sand inputs decline. The Pasig-Potrero River is adjusting to a decline in overall sediment supply coupled with a changing sediment mixture as the sand-rich eruptive material is removed and mixed with coarser pre-eruption deposits.

In this paper, we use field surveys of bed and flow characteristics combined with measurements of sediment mobility and transport on the Pasig-Potrero River to examine bed structure development and the associated feedbacks with sediment transport. These measurements and observations are combined with flume experiments modeling highly energetic, sand-rich systems as sand content declines. The initial conditions are based upon measurements from the Pasig-Potrero River in 2000-2001, with additional runs designed to emulate future conditions as sand is removed from the system, with sand inputs declining from 70% to 40% of the feed mixture. We examine the role of bed structure development on sediment transport as the bed coarsens and reorganizes, forming discrete coarse patches. These patches accommodate bed coarsening while still maintaining a smooth high transport zone, minimizing the effect of sand depletion on bedload transport, and restricting the transition from sand- to gravel-dominated transport to a narrow range of sand content.

## Background

Transient sediment loading in rivers can arise from many sources including landsliding, volcanic eruptions, dam removal, mining operations, forest clearing, and agricultural practices. In gravel-bed channels, sand loading can affect sediment transport beyond the simple addition of more material through feedbacks between sand content and the transport of both sand and gravel fractions. The Pasig-Potrero River is one of the few places where a wide range of sand and gravel mixtures can be observed in transit at a single site, because the sand supply varies through time. The Pasig-Potrero River thus offers an on-going natural experiment on the effects of sand content on bed development and sediment transport.

The Pasig-Potrero River is responding to both a reduction in overall sediment supply and a change in the sediment mixture as sandy pyroclastic deposits are removed or stabilized. Experiments have shown that a decrease in sediment supply can lead to surface coarsening, channel narrowing, and/or incision (Dietrich et al., 1989; Lisle et al., 1993). Because the 1991 pyroclastic-flow deposits are predominantly sand, but the pre-eruption fluvial deposits are predominantly gravel, the ratio of sand to gravel in active transport should shift as pyroclastic material is removed and mixed with pre-eruption sediment. This decline in sand content should affect bed surface structure and sediment transport rates in addition to any effects from a decline in sediment supply.

The role of sand content in the transport of sand/gravel mixtures has been the subject of several field studies (Whiting et al., 1988; Ferguson et al., 1989) and experiments (Iseya and Ikeda, 1987; Ikeda and Iseya, 1988; Whiting et al., 1988; Wilcock and McArdell, 1993; Wilcock et al., 2001). Ferguson et al. (1989) measured sediment transport in a bimodal, braided, pro-glacial stream and found that the channel bed organized into coarse and fine flow-parallel patches, with the majority of the transport moving through fine-grained "sand ribbons". Similar flow-parallel patches observed on the North Fork Toutle River were invoked as a means to enhance transport rates and create rapid downstream fining (Seal and Paola, 1995).

In some moderately to poorly sorted beds with both sand and gravel fractions, bedload moves as migrating bedload sheets (Whiting et al., 1988). In these flow-

perpendicular patches, coarse grains detach, move over a transitional zone, and then transport rapidly over a smooth sand bed to the next coarse patch. Transport rates fluctuate greatly during the passage of coarse and fine patches (Iseya and Ikeda, 1987; Kuhnle and Southard, 1988; Whiting et al., 1988; Dietrich et al., 1989). Time-integrated transport rates are higher for the mixture than for a uniform bed due to rapid transport in the fine-grained patches (Iseya and Ikeda, 1987). In experiments by Dietrich et al. (1987), bedload sheets developed only after adding sand to a fine gravel bed.

Ikeda and Iseya (1988) conducted flume experiments with different sand and gravel mixtures, tracking the shift from gravel- to sand-dominated transport as sand content increased. Initially, the bed was gravel-dominated, with sand hidden in the interstices between gravel clasts. Transport rates were thus controlled by mobility of the surface gravel layer, and sand entered into transport through removal of surface gravels. As sand contents increased, sand filled the interstices and began forming patches on the surface. Eventually, the bed surface became smooth, transport was sand-dominated, and isolated gravel clasts rolled over a sandy bed. Ikeda and Iseya observed bedload sheets, also called “gravel jams”, forming during the transition between gravel-dominated and sand-dominated beds.

Experiments on mixtures with varying sand contents also show an increase in the total sediment transport rate with increasing sand content (Ikeda and Iseya, 1988; Wilcock et al., 2001). An increase in the total transport rate is expected for mixtures with increasing sand content simply because the grain size distribution is finer overall, but transport rates increased as shear stress decreased. In addition, gravel transport rates increased even as the percentage of gravel in the mixture declined (Wilcock et al., 2001). Wilcock et al. (2001) place the transition between gravel- and sand-dominated transport at 10-30% sand. Based on these observations, Wilcock and Kenworthy (2002) developed a two-fraction sediment transport model that explicitly accounts for sand content in the bed by incorporating sand content into an incipient motion function.

Nonlinearities in the transport of different mixtures of sand and gravel may influence larger channel morphology, including the relatively common gravel-sand

transition that typically occurs longitudinally rather than temporally. River beds often become finer downstream as a result of abrasion and size selective transport and deposition. In contrast with gradual downstream fining, the gravel-sand transition is abrupt, with a decrease of several phi sizes over short distances compared to the overall channel length: 20 km in an 1100 km long channel (Shaw and Kellerhals, 1982), 250 m in a 3 km channel (Yatsu, 1955; Sambrook Smith and Ferguson, 1995), or <1 m in a 21 m laboratory flume (Paola et al., 1992). The abrupt decline in grain size at the gravel-sand transition has been explained through enhanced abrasion of fine gravels (Yatsu, 1955; Wolcott, 1988; Kodama, 1994), changes in sediment supply (Knighton, 1991; Sambrook Smith and Ferguson, 1995; Knighton, 1999), or changes in local base level (Pickup, 1984; Sambrook Smith and Ferguson, 1995; Ferguson, 2003). While multiple factors may be involved in different rivers, Ferguson (2003) found the nonlinear effects of interaction between sand and gravel transport coupled with a steadily decreasing slope are enough to trigger an abrupt gravel-sand transition without invoking external forcing like changes in base level or sediment supply.

The abrupt nature of the longitudinal gravel-sand transition is important when considering the recovery of a transiently sand-loaded system. Since an abrupt transition can arise without external forcing, a rapid transition from sand-dominated to transitional to gravel-dominated may be expected as sand contents decline during channel recovery. Even if sand inputs decline steadily, major effects on sediment transport may be concentrated into a narrow range of sand contents as the bed transitions from sand- to gravel-dominated transport.

## **Methodology**

### **Field site and methods**

The Pasig-Potrero River drains the east flank of Mount Pinatubo on the island of Luzon, Philippines (Figure 4.1). In 1991, Mount Pinatubo erupted, emplacing 5-6 km<sup>3</sup> of pyroclastic-flow material on the volcano's flanks. Over 1 km<sup>3</sup> of that material was deposited in the Sacobia-Pasig-Abacan basins (Scott et al., 1996; Daag, 2003). Areal, 33% of the Pasig-Potrero basin was covered with valley-filling primary pyroclastic-flow

deposits to depths as great as 200 meters. The pyroclastic-flow material was 70-85% sand by volume (Scott et al., 1996).

The climate at Mount Pinatubo is tropical and monsoonal, with distinct rainy and dry seasons. Intense storms, coupled with loose sediment deposited during the eruption, led to the generation of numerous lahars, volcanic debris-flows and hyperconcentrated flows. Sediment yields peaked in 1991, then declined nonlinearly (Umbal, 1997; Tuñgol, 2002). In October 1993, the Pasig-Potrero River captured the upper Sacobia River basin, nearly doubling its basin area, from 23 to 45 km<sup>2</sup> (Daag, 1994; Major et al., 1996) and generating a second peak in sediment yield. In 1997, the year of the last major lahar on the Pasig-Potrero River, sediment yields were still two orders of magnitude higher than pre-eruption values (JICA, 1978; Tuñgol, 2002). In summer 2000, the Delta 5 site at the alluvial fan head (Figure 4.1) was incised approximately 20 meters into the alluvial fan, and the channel was aggrading ~2-3 m yr<sup>-1</sup>.

Low-flow sediment transport was measured at Delta 5 over a four week period in August and September 2001. We sampled both suspended load and bedload using the equal-width increment technique as outlined in Edwards and Glysson (1999). For suspended load, we obtained vertically-integrated bulk samples with a U. S. Geological Survey DH-48 sampler with a ¼ inch (0.64 cm) opening. Bedload was measured using a handheld modified U. S. Geological Survey Elwha pressure-difference sampler with a 200 mm x 100 mm opening and 1 mm mesh bag. All samples were dried, sieved, and weighed in whole phi increments. All sand < 1mm (mesh size) was removed from bedload samples, since any sediment < 1mm was considered part of the suspended load fraction. Bedload transport was computed assuming a 100% sampler efficiency to compare sediment transport rating curves with a similar study undertaken by Hayes et al. (2002) during the 1997 and 1998 rainy seasons. We also calculated discharge-weighted average particle size distributions for each year using a technique outlined in Lisle (1995).

Sediment mobility was surveyed periodically from 1997-2002 at two sites near the fan head by comparing grain size distributions in motion under different flow



conditions. Results from these surveys are presented elsewhere (Montgomery et al., 1999; Gran and Montgomery, 2005). We also measured surface grain size distributions and lithologic content using point count surveys (Wolman, 1954) at a total of eight additional sites upstream of Delta 5. These data track changes in the upper basin from 1996-2003 in conjunction with the more detailed surveys at the fan head.

### **Experimental methods**

Four experiments designed to study channel recovery under declining sand input were conducted at the experimental flume facility at Humboldt State University. Initial conditions were based on measurements from the Pasig-Potrero River near the alluvial fan head in 2001. The initial slope was 2%, and the grain size distribution in the bed was a 1:4 size ratio of the average subsurface grain size distribution in 2000 - 2001. Water and sediment discharge rates were established such that all size fractions were visibly mobile, with large clasts rolling or sliding downstream over a moving carpet of sand, similar to low-flow conditions on the Pasig-Potrero River. Discharge was  $9.5 \times 10^{-3} \pm 1.0 \times 10^{-3} \text{ m}^3 \text{ s}^{-1}$ , and sediment feed averaged  $181 \pm 15 \text{ g s}^{-1}$ .

The goal of these experiments was to investigate the role of sand content on bed structure and sediment transport under conditions similar to those on the Pasig-Potrero River. Care was taken to ensure Froude similarity with field conditions and that flow was turbulent. Reynolds numbers ranged from 13,000 - 20,000 in the flume. Flow was supercritical in both the flume and field; Froude numbers (Fr) ranged from 1.1 to 1.6 with a mean of 1.3 for the flume experiments, and in the field  $Fr = 0.9 - 1.7$  with a mean of 1.4.

There are several distinct ways to create sand depletion in a feed flume. The gravel feed can be held constant while the sand is lowered, the feed mixture can be adjusted to accommodate both a decrease in sand and an increase in gravel while maintaining a constant total feed rate, or the feed rate can be reduced without altering the mix ratio. The advantage of the first method is that it most closely models selective transport and depletion of a sand reservoir. The advantage of the second is the overall feed rate does not change between runs, eliminating an extra variable. The third

method, with a reduction in the total feed rate, could result in degradation and armoring related more to loss of sediment input than to loss of sand. We chose the second technique, and altered the feed mixture to reflect decreasing sand content while maintaining a constant feed rate.

We conducted four runs, with 70%, 60%, 50%, and 40% sand content in the feed mix. References to each run as the X% run refer specifically to the sand content in the feed. The first run (70%) was initialized by screeding a bed composed of 70% sand at a 2% slope. The second (50%) and third (40%) runs began on the bed from the previous run. Following the 40% run, we rescreeded the bed, ran at 70% sand to establish a water-worked surface, and then dropped the feed to 60% sand and began the last run. Each run lasted from 94-140 minutes.

During each run, we measured water surface elevations and surface velocities. Sediment exiting the flume was collected, dried, sieved, and weighed to compute transport rates and distributions. The frequency of sediment collection varied depending on transport rate, from 25-279 seconds. The average collection time per run was 78 seconds/sample. Every 15 minutes, we stopped the run and measured bed elevations along cross-sections using a point gage. Every 30 minutes, we scanned the bed topography at 1 mm resolution with a laser scanner and took vertical photographs of the bed.

Only data in the middle portion of the flume were used in analyses. Water surface slopes and depths were calculated using data between 4 and 8 m (upstream of the outlet). Topographic scans and bed photos were analyzed between 6.75 and 2.75 m, excluding the outer 15 cm on either side of the flume to avoid zones directly affected by roughness elements added to prevent the flow from hugging the walls.

Bed structure development is a function of grain size distribution and flow conditions. One potential pitfall of studying bed structure development in a flume is that the coarse grains pivotal to formation of clast structures are difficult to move under many experimental conditions. We kept the grain size distribution as coarse as possible while still ensuring that all grain sizes were mobile. The relative roughness, calculated as  $D_{50}^* = D_{50}/h$ , where  $h$  is flow depth, and  $D_{50}$  is the median bedload grain size, was

slightly higher in channels on the Pasig-Potrero River than in the flume. The mean  $D_{50}^*$  of the flume was  $0.07 \pm 0.04$ , and the mean  $D_{50}^*$  of the Pasig-Potrero channels was  $0.04 \pm 0.03$ . Dimensionless explicit particle Reynold's numbers ( $R_{ep} = \sqrt{(\rho_s / \rho_w - 1)gD^3 / \nu}$ ) were similar for  $D_{50}$  clasts in the bedload on both the flume and the Pasig-Potrero River. Here,  $\rho_s$  and  $\rho_w$  are the sediment and water densities,  $g$  is the acceleration due to gravity,  $\nu$  is the kinematic viscosity, and  $D$  is the grain size of interest. Mean  $R_{ep(50)}$  values for  $D_{50}$  in the bedload were  $520 \pm 470$  in flume runs and  $410 \pm 190$  on the Pasig-Potrero River. In the coarse end of the distribution, the relative roughness of  $D_{84}$  clasts in the bedload had a mean of  $0.46 \pm 0.11$  in the flume compared to  $0.19 \pm 0.11$  on the Pasig-Potrero River. For the same clasts,  $R_{ep(84)}=7060 \pm 2080$  in the flume, while on the Pasig-Potrero River,  $R_{ep(84)}=4960 \pm 4140$ . The difference in the  $D_{84}$  parameters between flume and field may have enhanced the influence of the coarsest clasts under our experimental conditions.

## Results and analyses

### Pasig-Potrero River

Observations compiled from 1996-2003 indicate that the Pasig-Potrero River is undergoing a transition from a completely unarmored, sand-bedded channel towards a gravel-bedded one (Gran and Montgomery, 2005). As of 2003, gravel-bedded reaches were confined to the upper basin during the dry season. Near the alluvial fan head, pebble clusters and armor patches were prevalent year round, particularly on low bar complexes and along the edges of major braids.

During the rainy season, braids with widths ranging from a few centimeters to tens of meters actively transport sediment with gravel, cobbles, and boulders rolling or sliding independently over a moving carpet of sand and fine gravel. During low flow conditions, average water depths are often  $< 10$  cm, yet the flow transports clasts with diameters twice the flow depth (Montgomery et al., 1999; Gran and Montgomery, 2005). Flow is often supercritical, and transient antidunes are common. During high

flow events, channel-spanning roll waves pulse downstream. Small roll waves 1-5 cm in height occur during low flow.

Sand and pumice depletion has begun in the upper basin and is extending downstream through time. From 1997 through 2001, average pumice contents at sites near the alluvial fan head dropped from 75% to 53%. Sand content on the bed surface ranged from 39-57% sand. Five kilometers upstream of the alluvial fan head, average pumice contents dropped from 83% to 43%,  $D_{50}$  increased from 3mm to 8mm, and % sand on the bed decreased from 40-50% to 20-30% (Figure 4.2). Because the primary source for both pumice and sand is the 1991 pyroclastic-flow deposits, we interpret the decline in pumice and sand content as indicating that inputs of eruptive material to the channel network are no longer keeping pace with sediment evacuation. Selective transport is enhancing evacuation of the lighter, finer-grained bedload. Increased mixing of coarser, pre-eruptive deposits is contributing to the increase in grain size and decrease in pumice in the upper basin.

The effects of surface coarsening are evident as more gravel clasts begin to interact, forming clast structures like pebble clusters and armor patches (Figure 4.3). On low bar complexes with the highest density of clast structures and armor patches, gravel clasts are able to remain stable under greater flow depths than in major braids (Gran and Montgomery, 2005).

### **Sediment transport on the Pasig-Potrero River**

Rainy season low-flow suspended load and bedload transport data from the Pasig-Potrero River in summer 2001 were compared to 1997-1998 transport data (Hayes et al., 2002). All suspended load samples in 2001 had concentrations (0.1 to 3.4% sediment by weight) well below the threshold for hyperconcentrated flow of 40% sediment by weight (Beverage and Culbertson, 1964). In 1998, Hayes (1999) measured two storm events that reached concentrations at peak discharge that were close, but all other low flow measurements were well below hyperconcentrated flow levels (0.9 to 8.4% sediment by weight). There was little change in low-flow suspended load

concentrations from 1997 to 2001, so a single suspended load rating curve ( $R^2 = 0.68$ ,  $n = 92$ ) was created using the 2001 data and the 1997-98 data from Hayes (1999):

$$C = 12.0 \times Q_w^{0.70} \quad (4.1)$$

where  $C$  is the concentration and  $Q_w$  is the water discharge (Figure 4.4a). This curve excludes data with  $Q_w < 1 \text{ m}^3 \text{ s}^{-1}$ , which were collected primarily from individual braids in 2001. Below this discharge, there is a kink in the curve, and concentrations flatten out with considerable scatter.

Bedload made up an average of 38% ( $\sigma = 15\%$ ) of the total load (suspended load plus bedload). Comparing samples collected over the same discharge range in 1997-98 and 2001 ( $0.05 < q_w < 2.0$ ), we found no significant changes in the discharge-weighted bedload grain size distributions. We do not have bedload samples taken at high discharges to compare between years.

Rating curves comparing low-flow bedload transport,  $Q_b$ , were developed for 2001 and compared with rating curves from measurements made by Hayes et al. (2002) in 1997-1998. The curves are similar and can be described by a single linear curve ( $R^2 = 0.85$ ,  $n = 80$ ) (Figure 4.4b):

$$Q_b = 0.0043 \times Q_w \quad (4.2)$$

A comparison of unit discharge,  $q_w$ , and unit bedload transport,  $q_b$ , gives a similar result ( $R^2 = 0.69$ ,  $n = 80$ ):

$$q_b = 0.0042 \times q_w \quad (4.3)$$

Bedload transport is also a function of excess shear stress available to move sediment, which is the effective basal shear stress,  $\tau'$ , imposed by the flow minus a critical value,  $\tau_c$ , that must be overcome prior to initiation of motion:

$$q_b = f(\tau' - \tau_c)^\beta \quad (4.4)$$

Values of  $\beta$  generally fall in the range of 1.5 to 2.5 (Meyer-Peter and Müller, 1948; Engelund and Hansen, 1967), but on the Pasig-Potrero River, in both 1997-1998 and 2001, a well-defined linear relationship exists between low-flow  $q_b$  and total basal shear stress,  $\tau_b$  (Figure 4.5a). The slopes are statistically similar, but differences between intercepts are significant ( $p < 0.0001$ ). In 1997-1998, the best-fit linear regression ( $R^2 = 0.67$ ,  $n = 48$ ) is

$$q_b = 3.6 \times 10^{-5} \tau_b - 3.8 \times 10^{-7} \quad (4.5)$$

giving a  $\tau_c = 0.01$  Pa. For 2001,  $\tau_c$  increases to 3.5 Pa and the best-fit linear regression ( $R^2 = 0.55$ ,  $n = 32$ ) is

$$q_b = 2.8 \times 10^{-5} \tau_b - 9.6 \times 10^{-5} \quad (4.6)$$

Using the above values for  $\tau_c$ , the dimensionless critical Shield's parameter can be calculated:

$$\tau_c^* = \frac{\tau_c}{\rho_w \mathcal{R} g D} \quad (4.7)$$

where  $\mathcal{R} = (\rho_s - \rho_w) / \rho_w$  and  $D = D_{50}$ . In 1997-1998,  $\tau_c^* = 0.0003$ , increasing to  $\tau_c^* = 0.04$  in 2001. Most critical Shield's stress values lie within the range of 0.030 – 0.086 for gravel-bed rivers (Buffington and Montgomery, 1997), and a  $\tau_c^*$  of 0.0003 indicates there is essentially no barrier to incipient motion.

To compare the Pasig-Potrero River data to other rivers, we computed a dimensionless unit bedload transport rate,  $q_b^*$ :

$$q_b^* = \frac{q_b}{\rho_s \sqrt{\mathcal{R}gD^3}} \quad (4.8)$$

and compared it to  $\tau^*$  as computed using  $\tau_b$  instead of  $\tau_c$  in equation 4.7 (Figure 4.5b). The two data sets separate into two distinct fields along a similar curve. The separation is due in part to an increase in  $\rho_s$ . As pumice is depleted from the system,  $\rho_s$  increased from an average of  $1500 \text{ kg m}^{-3}$  in 1997 to  $2300 \text{ kg m}^{-3}$  in 2001. While the channels are still carrying the same mass for a given shear stress, they now move a lower volume of sediment.

### **Flume results and analyses**

Water surface slope, bed slope, and  $\tau_b$  all increased as sand content in the feed declined. Bedload fined during aggradation, although bed surface textures rapidly adjusted to changes in feed distribution. Bed surface structure developed, but the initial effect on sediment mobility was minimal. Armor patches formed, partitioning the flow into low and high transport zones, thereby maintaining high transport rates despite overall bed coarsening.

### ***Description of runs***

As sand contents declined, equilibrium slopes doubled from 0.02 with 70% sand to 0.04 with 40% sand (Table 4.1). This led to an overall increase in reach-average  $\tau_b$  from 5.3 Pa to 13.0 Pa. Both the surface grain size ( $D_{50}$  and  $D_{84}$  values) and the degree of armoring increased with decreasing sand content (Table 4.2). The grain size distribution on the bed surface became increasingly bimodal (Figure 4.6).

In the highest sand run (70%), the bed was sandy and unarmored with very few coarse clast structures (Figure 4.7). Isolated gravel clasts moved over a smooth sand

bed. At 60% sand, gravel interactions became more prevalent, and pebble clusters developed. In some cases, pebble clusters merged to form short-lived armor patches. At 50% sand, armor patches developed, with a sand ribbon running between them. Within the sand ribbon, transport appeared to be primarily sand-dominated with some gravel jams moving through the system. The number and size of gravel jams increased in the 40% run, slope and shear stress continued to increase, and armor patches became more dense.

The 70% run was in dynamic equilibrium with a constant slope and no significant aggradation or degradation. There was no significant coarsening of the bed. Under equilibrium conditions the sediment transport rate should match the feed rate. However, measured transport rates were lower due to sediment losses while changing the sample bag and from splash out of the trap. The initial trap efficiency was estimated at 63%. Improvements to the sediment trap design increased the trap efficiency to an average of 75% for later runs. Sediment transport results were corrected for trap efficiency.

For the other three runs, disequilibrium occurred while the bed aggraded and the slope increased to move sediment of a higher caliber. Equilibrium conditions were met in the runs with 60% and 50% sand, as the slope stabilized and grain size distributions and sediment transport rates increased back to match feed rates. In the run with 40% sand, the slope and sediment transport rates did not stabilize until the very end of the run, so it is less clear if dynamic equilibrium was achieved. However, the bedload grain size distribution did adjust to match the feed distribution within the first 50 minutes of the run.

### ***Bed structure***

The term “bed structure” refers to the arrangement and sorting of clasts on the channel bed. A bed with structure may exhibit sorting into grain size patches, clustering of coarse clasts into well-defined clast structures like pebble clusters or transverse ribs, or armoring of the bed with respect to the subsurface. Differences in bed structure between runs were visually striking, from unarmored in the 70% sand run, through



cluster-dominated under 60% sand, to armor patches with sand ribbon structure in the 50% and 40% sand runs (Figure 4.7). Differences in grain size metrics of  $D_{50}$ ,  $D_{84}$ , and  $D_{90}$  show the expected trends of increasing grain size with decreasing sand loading, as do ratios of surface to bedload grain size (Table 4.2). As the sand content declined, the bed coarsened with respect to the bedload.

Figure 4.7 shows images of the four runs illustrating the development of bed structure. In all runs, the edges of the flume coarsened, due to roughness elements placed along the walls. Our discussion here focuses on the middle 0.4 m of the flume. In the 70% run, the flume had an unarmored sand bed with isolated gravel clasts. About half of the gravel present on the bed was arranged into loose clusters. The bed surface had 79% sand cover.

The 60% run was dominated by the formation of pebble clusters, often occupying the entire width of the flume in dense packing. Many of these clusters linked together forming discrete transverse structures 10-15 cm in length. In a few areas, clusters joined together to form a weak armor patch, leaving an open sand ribbon next to the patch. Overall, the bed surface had 60% sand, the same sand content as the sediment feed.

The bed surface in the 50% run was dominated by armor patches with a narrow sand ribbon running between them. Most of the sediment transport occurred within this sand ribbon rather than on the armor patches. Within the high transport zone, 63% of the bed surface was covered by sand, compared to only 31% sand cover in the armor patches. The  $D_{50}$  in the sand ribbon ( $0.8 \phi$ ; 0.6 mm) was similar to the 70% run ( $0.9 \phi$ ; 0.5 mm), but the  $D_{50}$  over the armor patches was substantially greater ( $-2.8 \phi$ ; 7.1 mm). Sediment transport in the sand ribbon was primarily sand-dominated, although some gravel jams did form, clogging the otherwise highly mobile transport zone.

In the 40% run, gravel packing on the armor patches was more dense, with only 18% sand cover, compared to 51% sand cover in the high transport zone running between the armor patches. Transport within the sand ribbon was transitional, with numerous gravel jams. The  $D_{84}$  and  $D_{90}$  in the high transport zone ( $D_{84} = -3.5 \phi$ ; 11.2 mm;  $D_{90} = -3.9 \phi$ ; 14.8 mm) were closer to the distribution in the armor patches from

the 50% run ( $D_{84} = -3.7 \phi$ ; 12.9 mm;  $D_{90} = -3.9 \phi$ ; 14.6 mm) than in the sandy bed in the 70% run ( $D_{84} = -2.1 \phi$ ; 4.4 mm;  $D_{90} = -3.2 \phi$ ; 9.1 mm).

### ***Friction angle and roughness***

Initiation of mixed grain sediment transport is a function of the surface grain size distribution and bed structure. A clast tends to mobilize in the direction of least resistance, overcoming the lowest angle in the downstream direction. This angle of least resistance is defined as the friction angle,  $\alpha$ . Previous studies on water-worked sediments have measured  $\alpha$  by fixing a bed, placing grains on top of it, and then tilting the bed and tracking when grains mobilize (Kirchner et al., 1990; Buffington et al., 1992). These studies show a dependence of  $\alpha$  on both the individual grain size and the grain size distribution of the bed surface. Comparisons between water-worked beds and unworked beds indicate that  $\alpha$  increases substantially due to the sorting and organization associated with flowing water (Kirchner et al., 1990).

Since  $\alpha$  is a primary control on  $\tau_c$  necessary to initiate motion, we investigated how the distribution of  $\alpha$  on the bed changes with decreasing sand content and increasing bed structure. We measured a proxy for  $\alpha$  using the scanned bed topography to determine the angle a clast needs to overcome to mobilize downstream. At each pixel, we calculated the average local slope using a least squares algorithm of a small wedge facing downstream, thus allowing for the possibility of a clast mobilizing slightly off-center rather than only directly downstream. The wedge width was  $36^\circ$ , or the equivalent of 3 pixels down and 1 over. This span is similar to the average path traversed by flow in an unvegetated braided stream of  $\pm 22^\circ$  from the centerline (Gran and Paola, 2001). Three different wedge lengths were compared: 3mm, 6mm, and 9mm, simulating the friction angle that three different grain sizes would experience. Full distributions of positive  $\alpha$  for each run are given in Figure 4.8. The 70% run distribution has a strong peak at  $0^\circ$ , in keeping with observations of a dominant sand bed with isolated gravel clasts. There is a dramatic shift to a flat distribution at 60% sand, and then to a distribution with a peak in higher angles at 50% and 40% sand. Mean friction angles,  $\bar{\alpha}$ , for each run were determined from angles  $\geq 0^\circ$  (Figure 4.9).

These values ranged from  $\bar{\alpha} = 23^\circ \pm 3^\circ$  for 70% sand to  $\bar{\alpha} = 56^\circ \pm 2^\circ$  for 40% sand. Between 70% and 60% sand,  $\bar{\alpha}$  almost doubled.

Because most of the transport was confined to the fine-grained sand ribbon running between armored patches in the 50% and 40% runs, we partitioned the bed into armor patches and transport zones, and recalculated  $\alpha$  in each zone. An example from the 50% run is shown in Figure 4.10. The average  $\bar{\alpha}$  for transport zones ( $\bar{\alpha} = 39^\circ$  for 50% run and  $\bar{\alpha} = 47^\circ$  in the 40% run) were substantially lower than  $\bar{\alpha}$  for the entire bed (Table 4.3, Figure 4.9). In the armor patches,  $\bar{\alpha}$  were higher with an average  $\bar{\alpha} = 56^\circ$  and  $60^\circ$  in the 50% and 40% runs, respectively.

Roughness was computed as Manning's  $n$  using reach-averaged quantities. Roughness increased from 0.024 to 0.06 from the 70% to the 40% run. However, because most of the flow and sediment transport was confined to the sand ribbon, we recomputed the roughness within the width of the sand ribbon for the 40% and 50% runs. The roughness in these high transport zones changed little between the runs, varying from 0.024 to 0.032 (Table 4.1).

### ***Sediment transport and critical shear stress***

The water surface slope increased with decreasing sand content, increasing  $\tau_b$  from 5.3 Pa to 13.0 Pa. This increase in  $\tau_b$  is expected in order to move sediment of greater caliber. To compare  $\tau_b$  and sediment transport rates to measured values from the Pasig-Potrero River, we computed dimensionless variables  $\tau^*$  and  $q_b^*$ , as defined in equations 7 and 8 (Figure 4.11). The flume data span the range of conditions measured on the Pasig-Potrero River from 1997 through 2001 and appear to cluster into two distinct groups based on sand content.

The measured  $\tau_c^*$  values on the Pasig-Potrero River were low, with  $\tau_c^* = 0.0003$  in 1997-98 and  $\tau_c^* = 0.04$  in 2001. Because we set the sediment transport rate in the experiments, we cannot back-calculate  $\tau_c^*$  in the same way from sediment transport rating curves. We can, however, use the transport data to estimate the  $\tau_c^*$  required to match predicted transport rates given the grain size composition in the feed and flume

conditions. A simple approach to this is to use a standard sediment transport formula, that of Meyer-Peter and Müller (1948) (MPM), that was developed in a flume setting:

$$q_b^* = 5.7(\tau_b^* - \tau_c^*)^{1.5} \quad (4.9)$$

Rather than compute a single sediment transport rate on the entire distribution using the  $D_{50}$  grain size, we calculated the predicted transport rate for individual grain size bins, weighted by the composition of that fraction in the sediment feed. Using our calculated values of  $q_b^*$  and  $\tau_b^*$ , we used a least squares approach to determine which  $\tau_c^*$  would best fit the full grain size distribution of the bedload binned at 1 phi intervals. The best fit value for the 70% and 60% runs was  $\tau_c^* = 0$ . For 50% and 40% sand, the best-fit  $\tau_c^* = 0.01$ . Plotting sand vs. gravel transport rates (Figure 4.12), the best-fit value for the 70% and 60% runs is still  $\tau_c^* = 0$ . A  $\tau_c^* = 0.003$  best fit both the 50% and 40% runs. These low  $\tau_c^*$  values lead to predicted grain size distributions matching those measured in the bedload, but the actual transport rates were overpredicted in the lower sand content runs. In these runs hiding effects become important, and these effects are not accounted for in equation 9.

Another potential problem with the MPM approach is that  $\tau_b^*$  is calculated using the  $D_{50}$  of the bulk bed distribution, which can be misleading in a bimodal system where the  $D_{50}$  often lies between modes. The model of Wilcock and Kenworthy (2002) predicts bedload transport rates for the sand and gravel fractions independently, based on the median grain size of each mode and the distribution of sand vs. gravel on the bed surface or subsurface. The sand content on the bed surface ( $F_s$ ) in our runs ranged from 0.32 to 0.77, mostly above the range of influence of the sand-gravel transition in the Wilcock-Kenworthy model. Thus, the reference shear stress values for sand ( $\tau_{rs}^*$ ) and gravel ( $\tau_{rg}^*$ ) fractions are at or close to the limiting values found in high sand environments ( $\tau_{rg}^* = 0.011$ ;  $\tau_{rs}^* = 0.065$ ). These  $\tau_{ri}^*$  values are similar to  $\tau_c^*$ . The main difference is that  $\tau_{ri}^*$  is used to calculate the  $\tau$  at which transport rates reach a small

reference value ( $W_i^* = 0.002$ ) rather than the  $\tau$  at which motion begins. Here,  $i$  refers to the fraction (sand or gravel), and  $W^*$  is a dimensionless sediment transport rate (see Wilcock and Kenworthy (2002) for a full explanation of the model).

Bedload transport predictions using the Wilcock-Kenworthy model are fairly good, although the model tends to underpredict gravel transport in the high sand runs ( $F_s \geq 0.6$ ) and overpredict sand transport in the moderate sand runs ( $0.3 \geq F_s \geq 0.5$ ) by a factor of 5 to 10. A five-fold decrease in  $\tau_{rg}^*$  for the 70% and 60% runs and a five-fold increase in  $\tau_{rs}^*$  for the 50% and 40% runs match predicted and measured bedload transport rates.

An alternate way to assess  $\tau_c^*$  is through a force balance of a grain resting on the bed. Kirchner et al. (1990) explored a simplified version of a force balance on a spherical grain originally developed by Wiberg and Smith (1987). They used measured values of  $\alpha$ , grain exposure, and grain protrusion to estimate  $\tau_c^*$  and found a strong dependence of  $\tau_c^*$  on  $\alpha$ , grain protrusion, and grain diameter. A variation in  $\alpha$  of  $\pm 15 - 20^\circ$  led to a roughly twofold variation in  $\tau_c^*$ . The variation in  $\bar{\alpha}$  from 70% sand to 40% sand in our experiments was  $33^\circ$ .

We used Kirchner et al. (1990)'s approach to determine how  $\tau_c^*$  varies between our experimental runs based on bed grain size distributions and  $\alpha$  for several protrusion and exposure ratios. We found that  $\tau_c^*$  increased 2.5 to 3 times from 70% sand to 40% sand (Table 4.3). Comparing 70% to 60% runs, for fine to medium pebbles (5-16 mm in diameter) with moderate exposure and protrusion the average ratio of  $\tau_{c(60)}^* / \tau_{c(70)}^* = 1.9 - 2.1$ . From 60% to 40% the ratio  $\tau_{c(40)}^* / \tau_{c(60)}^*$  was only 1.3 - 1.4, meaning that most of the increase in  $\tau_c^*$  occurred between 70% and 60% sand.

The same force balance analysis was conducted in separate areas of the bed in the 50% and 40% runs, to determine the difference in  $\tau_c^*$  between the armor patches and the high transport zones, as well as how  $\tau_c^*$  from each patch compared with the 70% run. Figure 4.13 shows the results from the 40% run. For the 50% run,  $\tau_{c(50Armor)}^* / \tau_{c(50Transport)}^* = 1.5 - 2.2$  in fine to medium pebbles with moderate exposure and protrusion. This ratio was similar in the 40% run (1.2 - 2.4). Comparing the armor

patches in the 50% run to the 70% run,  $\tau_{c(50Armor)}^* / \tau_{c(70)}^* = 1.8 - 2.0$ , while the transport zones had ratios of  $\tau_{c(50Transport)}^* / \tau_{c(70)}^* = 0.9 - 1.3$ . The 40% run had higher  $\tau_c^*$  values, with  $\tau_{c(40Armor)}^* / \tau_{c(70)}^* = 2.1 - 3.2$  and  $\tau_{c(40Transport)}^* / \tau_{c(70)}^* = 1.1 - 2.0$ .

## Discussion

### Bed development

Both the Pasig-Potrero River and the flume experiments show a transition from a completely sand-dominated, unstructured bed surface to a coarser, more organized bed. In the experiments, the driving force behind the transition is a reduction in sand input. On the Pasig-Potrero River, it is most likely a reduction in sand input combined with an overall reduction in sediment load. During the dry season, reaches in the upper half of the Pasig-Potrero River basin consolidate, narrow, incise, and armor. The main driving force is a sharp reduction in sediment supply, and these observations are consistent with experimental studies (Dietrich et al., 1989; Lisle et al., 1993). During the rainy season, however, the Delta 5 site is still transport-limited and aggrading at a rate of 2 - 3 m yr<sup>-1</sup>. There have been no reductions in rainy season active channel width from 1997 to 2001. Although we found no measurable change in low-flow discharge-weighted grain size distributions between 1997 and 2001, these other observations make it difficult to ascribe bed coarsening solely to supply reduction. We conclude that although supply reduction is the driving force during the dry season, a combination of supply reduction and sand depletion govern bed coarsening during the rainy season. Our experiments show that sand depletion alone can create bed coarsening, clustering, and armor patch development.

In our experiments, as sand declined from 70% to 60%, bed coarsening was accommodated through formation of pebble clusters, some of which merged to form weak armor patches. From 60% to 50% sand, distinct armor patches developed, leaving a smooth sand ribbon able to maintain high transport rates. As the percentage of sand declined further, there was not enough sand to maintain the smooth transport zone, and gravel jams began disrupting the longitudinal connectivity of the sand ribbon. The gravel jams became more dominant as sand inputs declined to 40%. In the 40% run, the

bed surface had only 32% sand, consistent with the transition between sand-dominated and gravel-dominated transport as measured by Wilcock et al. (2001) and Ikeda and Iseya (1988).

The Pasig-Potrero River is on a similar trajectory to the experiments although sand contents in 2001 were still higher in the low-flow bedload and on the surface (70% and 39%, respectively) than in the lowest sand run. Following the cessation of major lahars in 1997, the rainy season bed of the Pasig-Potrero River has developed an increasing density of clast structures and armor patches, particularly on low bar complexes within the active braidplain and at the edge of major braids. Similar to bimodal reaches on other rivers (Sambrook Smith, 1996), the bed of the Pasig-Potrero River is sorted into distinctly bimodal grain size patches. At the alluvial fan head in 2002, sandy transport zones running between armor patches still dominated the bed area. Even if equal mobility of grains is maintained within each patch, the overall effect may be enhanced transport of sand, leading to longitudinal sorting and downstream fining (Paola and Seal, 1995).

Given the sand content on the bed surface at the head of the alluvial fan on the Pasig-Potrero River (39%), the bimodal grain size distribution, and the observed development of grain size patchiness, this reach should be nearing the threshold between sand-dominated and transitional transport that we observed in our experiments. Reaches > 5km upstream of the fan head cross that threshold during the dry season, when sediment inputs to the mainstem channel network are reduced. Selective transport winnows the bed during this transition, leading to depletion of the sandy bedload from the surface. The end result is incision coupled with bed armoring and greatly reduced sediment mobility. Other volcanically-loaded rivers like the O'Donnell River at Mount Pinatubo and the North Fork Toutle River at Mount St. Helens show a similar shift from multiple-thread, highly mobile channels in the rainy season to single-thread, incised and armored channels in the dry season throughout the watershed. Armored reaches on the Pasig-Potrero River form predominantly in the upper basin, but are expanding downstream as more sediment is removed from the system.

### Sediment transport

How does the development of bed structure affect sediment transport? The development of clast structures and armor patches from a previously unarmored bed should increase bed roughness and lower the effective shear stress. In addition, as the density of coarse particles on the bed increases, they could form a greater topographic barrier to motion, increasing  $\alpha$  on the bed. Either of these effects may reduce sediment transport rates for a given  $\tau_b$ . However, we found that reorganization of the bed structure into armor patches and sandy high transport zones allows the flow to maintain high transport rates while accommodating bed coarsening down to ~40% sand on the bed surface.

On the Pasig-Potrero River, armor patches and zones with a high density of pebble clusters had lower gravel mobility compared to major braids (Gran and Montgomery, 2005). Although clast structures delay entrainment, their main effect on total sediment transport rates may be to narrow the width of active transport. Sediment transport rating curves within zones of active transport indicate a slightly greater barrier to incipient motion, with higher  $\tau_c^*$  in 2001, although Manning's  $n$  roughness values remained essentially constant. The increase in  $\tau_c^*$  can decrease initial mobility, thus lowering low flow sediment transport, but it should not have much effect on high flow sediment transport rates. Almost all clasts were mobile once fully submerged in unarmored braids.

In our flume experiments, sand ribbons remained highly active, transporting the bulk of the sediment load as coarse patches formed. Abundant sand tends to enhance transport of both sand and gravel. Organization into flow-parallel patches helped maintain these high transport rates even as armor developed and the bed coarsened overall. As sand content declined, gravel jams formed in the sand ribbon and bedload was transported in sheets rather than as a continuous strip of moving sediment.

If the entire wetted width of the flume is considered, Manning's  $n$  values more than doubled as sand content dropped from 70% to 40%. Likewise,  $\bar{\alpha}$  values more than doubled, leading to a 2.5–3-fold increase in  $\tau_c^*$ . However, these analyses incorporate the entire bed, while most of the transport occurred in the sand ribbon. If



only the active transport zone is considered, analogous to considering only the major braids on the Pasig-Potrero River, we find little effect of the decreasing sand content on parameters affecting sediment transport. Considering only the high transport zones, we find little change in roughness, a doubling of  $\bar{\alpha}$ , and only a small (<30%) increase in  $\tau_c^*$  between 70% and 50% sand.

Estimates of  $\tau_c^*$  from sediment transport data show that  $\tau_c^*$  remained low throughout the flume runs, with only a slight increase in  $\tau_c^*$  from the 70% and 60% runs to the 50% and 40% runs. This agrees more with results from the sand ribbon than from the entire wetted width, which is not surprising as the bulk of the transport occurred within this narrow zone. The increase in  $\tau_c^*$  from the 60% run to the 50% run may be related to the development of gravel jams within the sand ribbon, shifting from sand-dominated to transitional transport. The transverse sorting associated with gravel jams disrupts the longitudinal connectivity and essentially shuts down the moving carpet of sand, leading to reductions in overall transport. The sand content of the bed surface (42% sand in the 50% run and 32% sand in the 40% run) was low enough for these runs to be within the transition zone from sand-dominated to gravel-dominated transport (Ikeda and Iseya, 1988; Wilcock et al., 2001).

### **Current and future conditions on the Pasig-Potrero River**

Immediately following a volcanic eruption like that at Mount Pinatubo, rivers are able to convey extremely high sediment yields compared to most rivers (Kadomura et al., 1983; Pearson, 1986; Hirao and Yoshida, 1989; Umbal, 1997; Dinehart, 1998; Major et al., 2000; Tuñgol, 2002; Major, 2004). Even following the cessation of major lahars, some volcanic rivers can retain high transport rates for decades (Major et al., 2000; Major, 2004). Hayes et al. (2002) demonstrated that, for a given  $\tau^*$ , low-flow  $q_b^*$  rates on the Pasig-Potrero River were similar to those found in the Nahal Yatir, an arid ephemeral stream measured during flash floods (Reid et al., 1995). Hayes et al. (2002) also compared the Pasig-Potrero River to the volcanically-loaded North Fork Toutle River, Washington; gravel-bedded Oak Creek, Oregon; and sand-bedded East Fork

River, Wyoming. We extend this comparison to include five additional rivers: three gravel-bedded rivers, one sand-bedded river, and one bimodal braided river (Figure 4.14).

Sand-dominated rivers and gravel-dominated rivers separate into two different portions of the plot, with the bimodal braided Tanana River in between. In Figure 4.14, data from volcanic and arid rivers lie above the data from sand-bedded rivers, with sediment transport rates one to two orders of magnitude higher for a given  $\tau^*$ . Interestingly, as sand inputs drop on the Pasig-Potrero River, the data are shifting towards the bimodal and gravel-bedded channels while maintaining high transport rates rather than dropping into the sand-bedded regime. Even though transport is currently sand-dominated on the Pasig-Potrero River, gravel clasts, rolling or sliding independently over the mobile sand bed are able to maintain higher transport rates than in a sand-bedded channel. The flume data show the same shift towards gravel-bedded channels with decreasing sand content.

This shift in bedload transport regime is important, particularly during post-eruption hazard assessment. The effect of high sand content increasing the rates of gravel transport could lead to higher sediment yields immediately after a sand loading event than predicted by current sediment transport relations.

Future sediment yields at Mount Pinatubo will depend explicitly on sediment inputs from remaining deposits of sand-rich eruptive material. Already, seasonal patterns in sediment inputs are reflected in the changing bed structure and sediment transport rates between the rainy season and the dry season. We expect transitional transport to dominate in the sand ribbons during the rainy season once rainy season sediment sources are evacuated or stabilized enough that sand contents on the bed drop below 30%. Given that the eruptive sediment is mostly sand, and the pre-eruption sediment is mostly gravel, we expect to see a shift towards coarser bedload coincident with a drop in sediment supply, further enhancing bed coarsening, armoring, and structure development. The shift to transitional and eventually to gravel-dominated transport should lower bedload transport rates. Observations from other volcanic rivers

show that suspended load yields may remain high for much longer, until upland sediment sources are stabilized or evacuated (Major et al., 2000; Major, 2004).

### **Conclusions**

Extreme sand loading in the Pasig-Potrero River altered the bed and transport conditions from gravel-dominated to sand-dominated and greatly increased sediment yields. Even after lahars ceased, sediment yields remained two orders of magnitude above pre-eruption levels. As sediment inputs decline, bed reorganization into flow-parallel patches is maintaining high transport rates while accommodating bed coarsening. We observed the same patterns in our flume experiments, as the bed developed armor patches while maintaining high sediment transport rates in the fine-grained zones. In these sand ribbons, roughness, critical shear stress, and grain size distributions remained similar from 70% down to 50% sand content, despite large increases in average values for all three parameters over the entire bed. Once gravel jams formed in the sand ribbon, the highly mobile channel became choked, and sediment transport rates declined. This transitional transport phase started at 50% sand, with gravel jams becoming more prominent in the 40% run. The shift from sand-dominated to transitional transport occurred at bed surface sand contents consistent with those measured by Ikeda and Iseya (1988) and Wilcock et al. (2001). This transition should be reached in the future on the Pasig-Potrero River. In 2001, sand contents on the bed surface of the Pasig-Potrero River (39% sand) were nearing the transitional range, but transport remained sand-dominated in major braids.

Because the channel bed tends to sort into armor patches prior to development of full bed armor, significant bed coarsening can be accommodated with little impact on sediment transport as long as sand ribbons remain connected. Patch development thus compresses the transition from sand to gravel into a narrow range of sand content rather than a continuous, smooth transition over a wide range of sand content. This effect helps explain why, in general, most channels are sand-bedded or gravel-bedded, with fewer bimodal or transitional channels. Even in channels with downstream gravel to sand transitions, transitional reaches are relatively short. The shift in transport regime

as sand inputs decline is important for hazards assessment, and predictions of future sediment yield need to accommodate the changing nature of the bed surface and sediment transport regime.

**Table 4.1:** Basic flow conditions for flume runs.

	Run Time (min)	Average Depth <sup>a</sup> (mm)	Water Surface Slope <sup>a</sup>	Shear Stress <sup>b</sup> (Pa)	Manning's n <sup>c</sup>	
					Full Flume <sup>c</sup>	Transport Zone <sup>c</sup>
70% Run	140	0.026	0.021	5.3	0.024	0.024
60% Run	94	0.034	0.025	8.3	0.034	0.027
50% Run	118	0.037	0.027	9.8	0.044	0.023
40% Run	129	0.030	0.040	11.8	0.060	0.032

<sup>a</sup> Depth and slope measurements are average values from the portion of the run after equilibrium conditions were met. For the 40% run, we used the last 60 minutes of runtime.

<sup>b</sup> Shear stress was calculated as  $\tau = \rho ghS$  using reach-averaged values.

<sup>c</sup> Manning's n roughness was calculated using two different widths: the entire wetted with (Full Flume) and the width of the transport zone only (Transport Zone).

**Table 4.2a:** Surface grain size distributions for flume runs.

	Sand on Surface (%)	Surface D <sub>50</sub> (φ / mm)	Surface D <sub>84</sub> (φ / mm)	Surface D <sub>90</sub> (φ / mm)
70% Run	78	0.9 / 0.5	-0.6 / 1.5	-2.3 / 5
60% Run	60	0.8 / 0.6	-3.3 / 10	-3.8 / 14
50% Run	42	-1.8 / 3	-3.3 / 10	-3.7 / 13
Armor <sup>a</sup>	63	-2.8 / 7	-3.7 / 13	-3.9 / 15
Transport <sup>a</sup>	31	0.8 / 0.6	-3.1 / 8	-3.5 / 11
40% Run	32	-2.8 / 7	-4.0 / 16	-4.2 / 18
Armor <sup>a</sup>	18	-3.3 / 10	-4.0 / 16	-4.2 / 18
Transport <sup>a</sup>	51	-0.9 / 2	-3.5 / 11	-3.9 / 15

<sup>a</sup> For the 50% and 40% runs, the bed was subdivided into two zones: armor patches and sandy transport zones. Grain size distributions within each zone were then measured separately.

**Table 4.2b:** Bedload grain size distributions for flume runs.

	Sand in Bedload (%)	Bedload D <sub>50</sub> (φ / mm)	Bedload D <sub>84</sub> (φ / mm)	Bedload D <sub>90</sub> (φ / mm)
70% Run	69	-0.5 / 1.4	-3.5 / 11	-4.1 / 17
60% Run	59	-1.2 / 2.3	-4.0 / 16	-4.1 / 17
50% Run	52	-1.3 / 2.4	-4.0 / 16	-4.2 / 18
40% Run	42	-2.3 / 5.0	-4.1 / 18	-4.3 / 19

**Table 4.3:** Mean friction angles and critical shear stress ratios for flume runs.

	$\alpha$ , 3mm <sup>b</sup> (degrees)	$\alpha$ , 6mm <sup>b</sup> (degrees)	$\alpha$ , 9mm <sup>b</sup> (degrees)	$\bar{\alpha}$ (degrees)	$\tau_{c(\#)}^* / \tau_{c(70)}^*$
70% Run	24.6	23.7	21.9	23.4	1
60% Run	43.5	42.0	39.4	41.6	1.9-2.1
50% Run	49.1	50.5	48.4	49.3	2.1-2.3
Armor <sup>a</sup>			56.3		1.8-2.0
			39.3		0.9-1.3
Transport <sup>a</sup>					
40% Run	56.2	57.0	55.2	56.1	2.5-2.8
Armor <sup>a</sup>			60.2		2.1-3.2
			47.4		1.1-2.0
Transport <sup>a</sup>					

<sup>a</sup> For the 50% and 40% runs, the bed was subdivided into two zones: armor patches and sandy transport zones. Friction angle measurements were made separately in each zone.

<sup>b</sup> Friction angles were computed by measuring the angle of a wedge facing downstream. Three wedge lengths were used: 3mm, 6mm, and 9mm.

<sup>c</sup> The critical shear stress ratio comes from  $\tau_c^*$  values computed using a force balance of a grain resting on the bed (Kirchner et al., 1990). The data listed are the range of values for grain size of 5 - 15mm, with an exposure to protrusion ratio of 0.5.

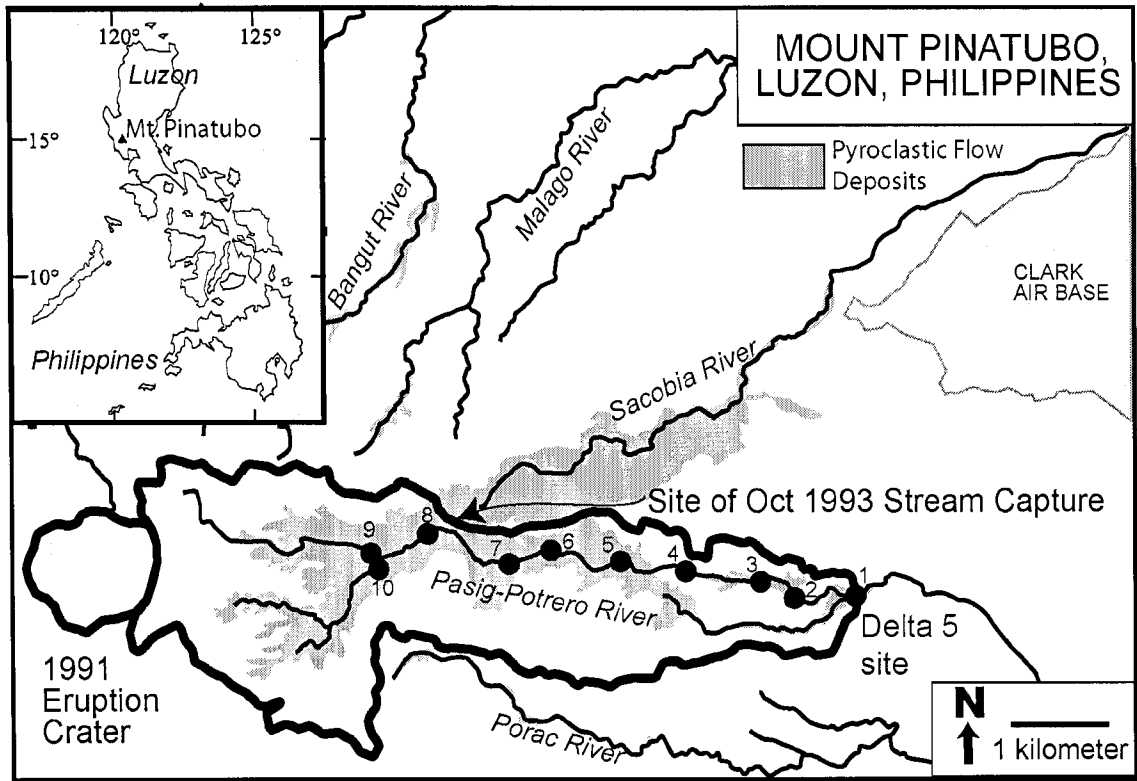


**Figure 4.1:** The Pasig-Potrero River drains the east flank of Mount Pinatubo on the island of Luzon, Philippines. Circles denote study sites.



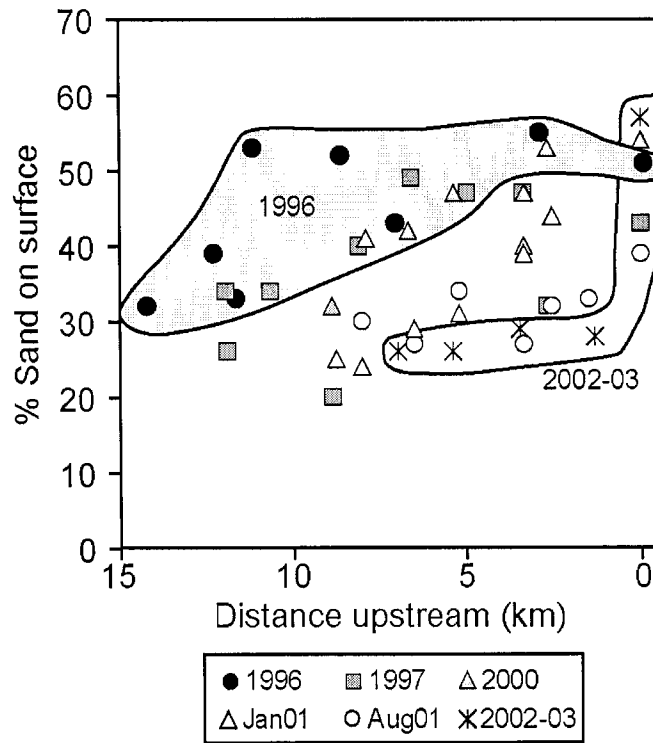


**Figure 4.2:** Sand content on the bed surface was measured through point count surveys periodically from 1996 through 2003 on the Pasig-Potrero River, plotted here against distance upstream of the alluvial fan head. The first and last data sets (1996 and 2002-03) have been shaded to highlight the changes between them.

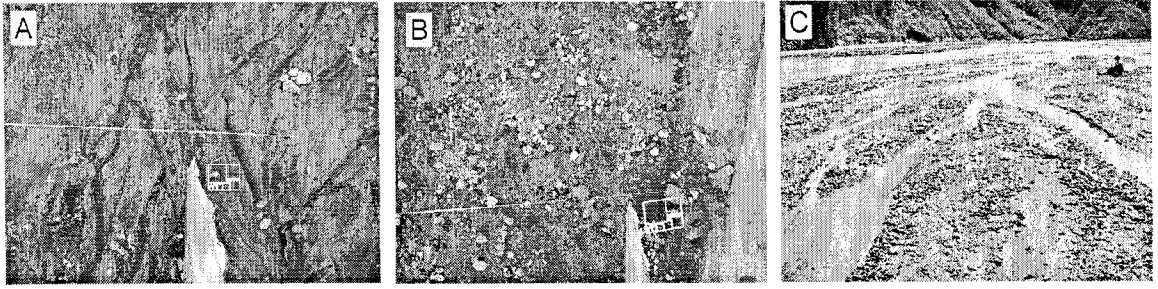


**Figure 4.3:** Stages of bed structure development on the Pasig-Potrero River from A) unarmored to B) clustered to C) armor patches with sandy transport zones.

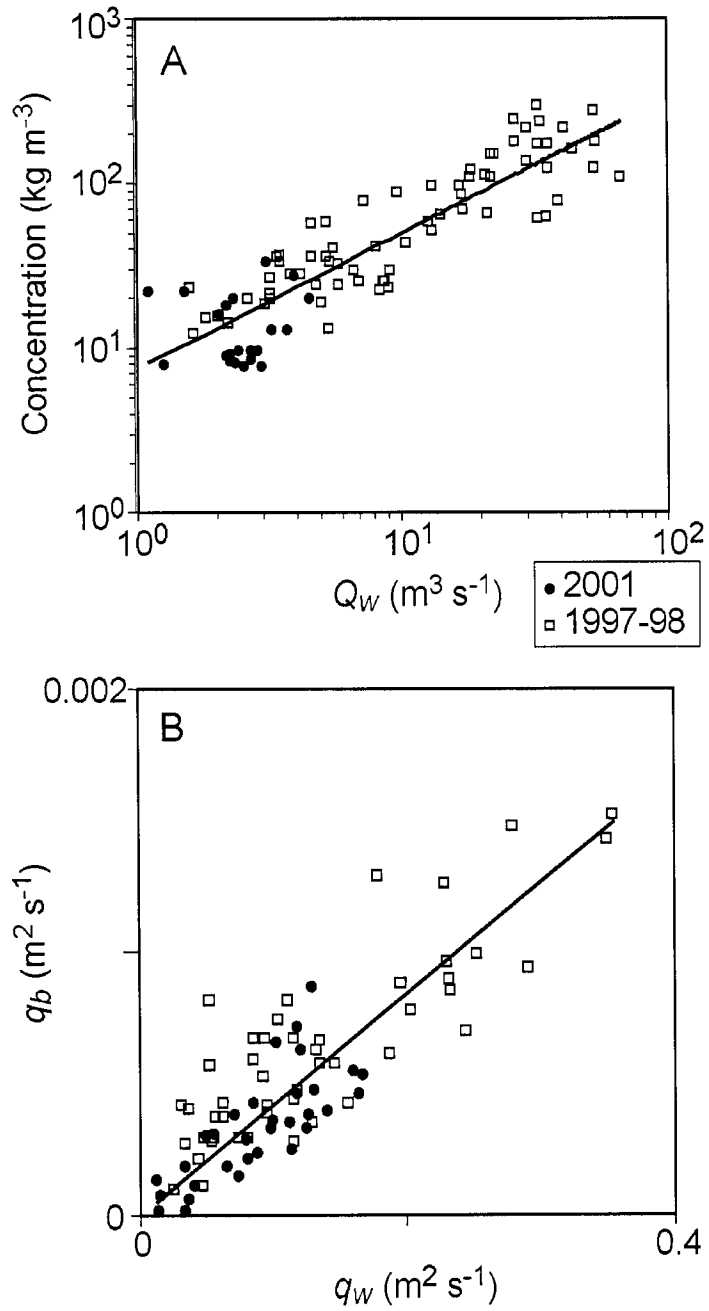


**Figure 4.4:** Sediment transport rating curves developed on the Pasig-Potrero River from data in 1997-98 (Hayes, 1999; Hayes et al., 2002) and 2001 [this study] including A) suspended load and B) bedload. Concentration data in (A) are truncated at  $Q_w = 1 \text{ m}^3 \text{ s}^{-1}$ .

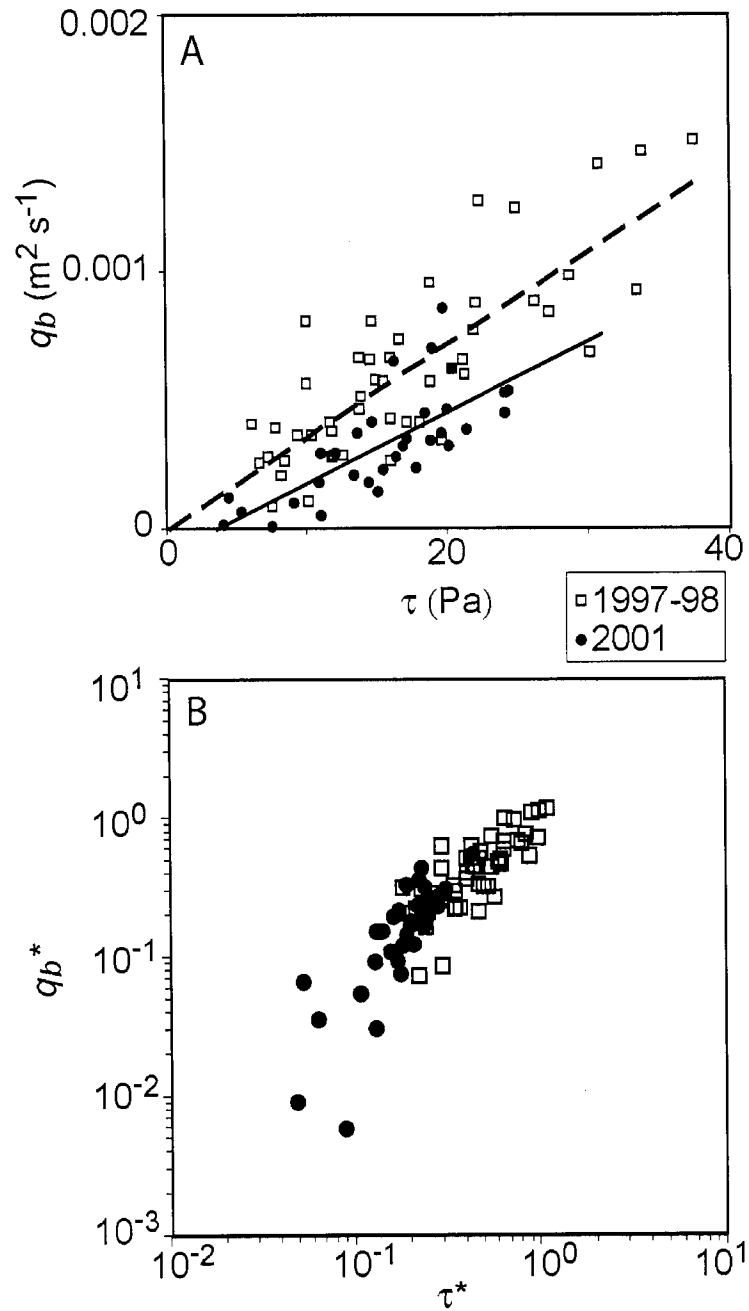


**Figure 4.5:** Bedload transport versus basal shear stress on the Pasig-Potrero River in 1997-98 (Hayes, 1999; Hayes et al., 2002) and 2001 [this study]. A) Unit bedload transport ( $q_b$ ) rates were higher in 1997-98 for a given shear stress ( $\tau$ ). B) Dimensionless bedload ( $q_b^*$ ) versus dimensionless shear stress ( $\tau^*$ ) show a shift in the distributions from 1997-98 to 2001.

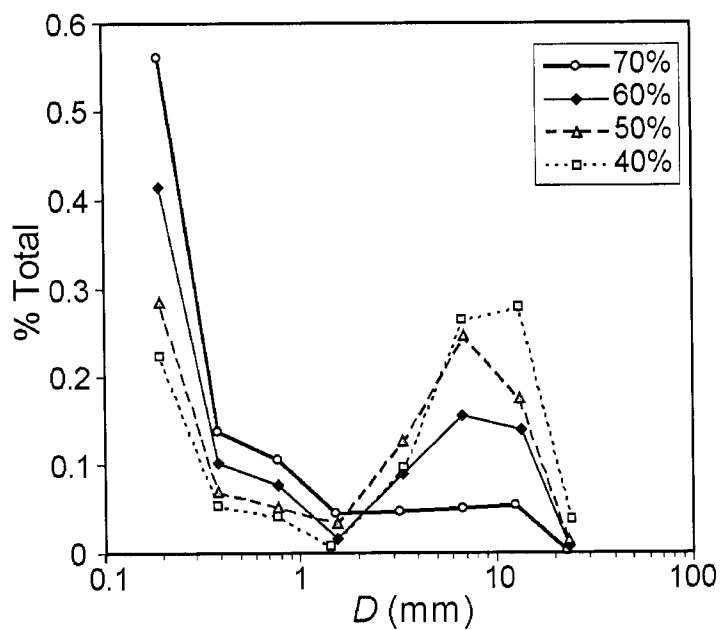


**Figure 4.6:** Surface grain size distributions on the four flume runs. Distributions were obtained from point counts on bed photos taken every thirty minutes during the course of each run.

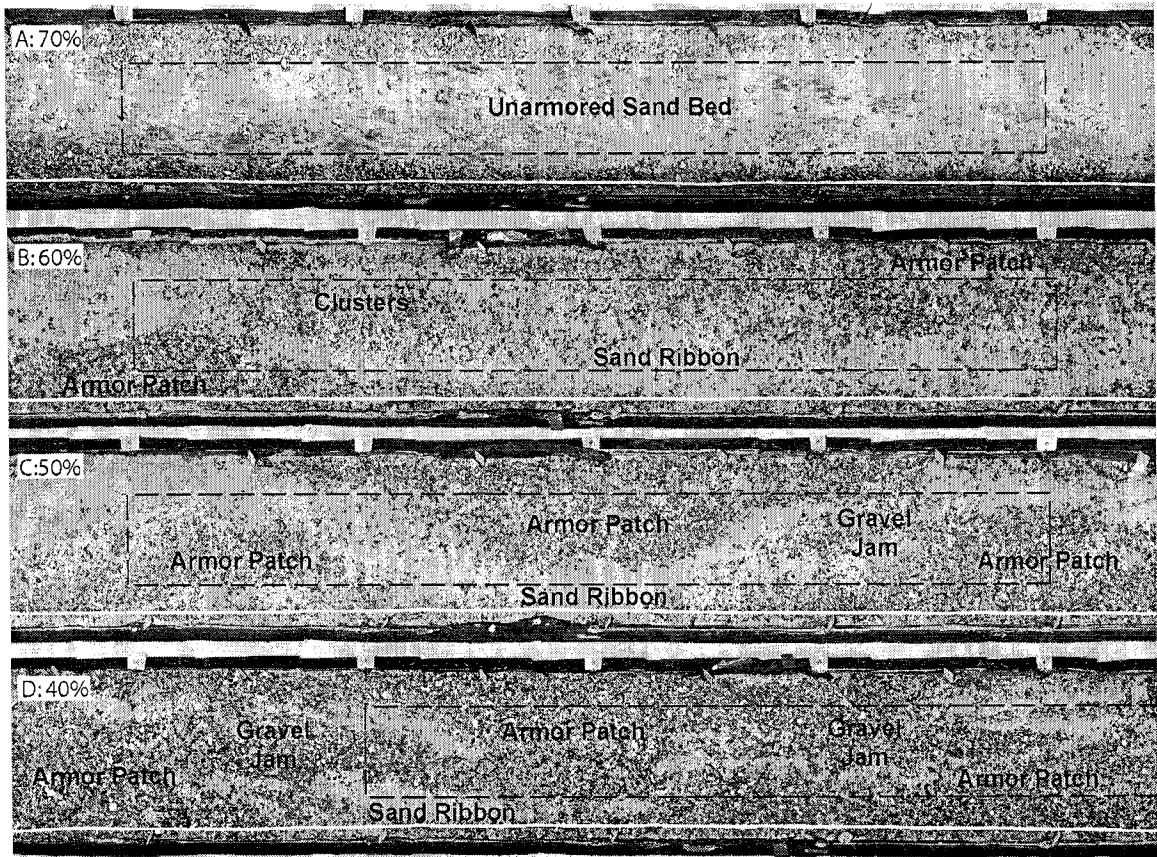


**Figure 4.7:** Photographs of the bed surface during each of four flume runs with different feed mixtures: A) 70% sand, B) 60% sand, C) 50% sand, and D) 40% sand. The black boxes denote study patches for photo and topographic scan analyses. The bed progressed from (A) sandy and unarmored with isolated gravel clasts and few clusters to (B) mostly clustered over sand bed with a few weak armor patches to (C and D) structured with armor patches and a highly mobile sand ribbon. In (D), large gravel jams can be seen in the otherwise sandy transport zone between armor patches.

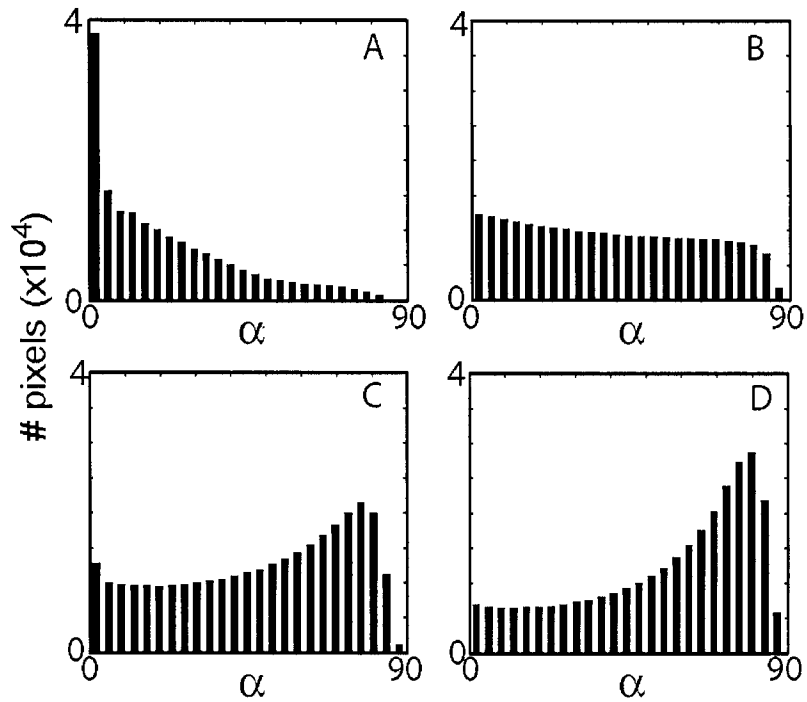


**Figure 4.8:** Histograms of friction angles ( $\alpha$ ) for a wedge 6 mm in length for each run: A) 70% run, B) 60% run, C) 50% run, and D) 40% run. Note the progressive shift from a peak at 0° to a peak at higher angles as sand content decreases.

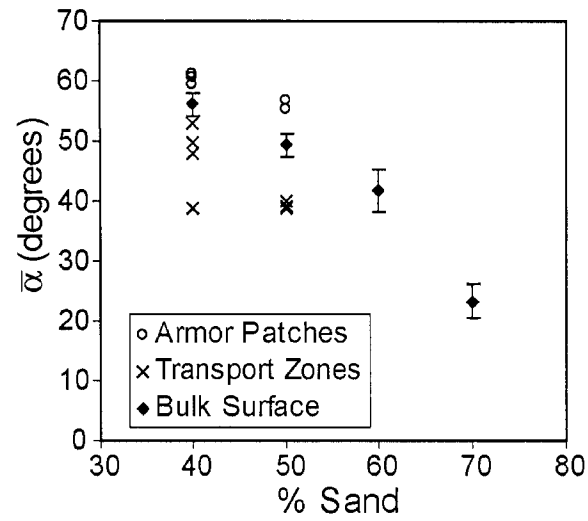


**Figure 4.9:** Mean friction angles ( $\bar{\alpha}$ ) calculated for all  $\alpha > 0^\circ$  for each topographic scan, for three different wedge lengths (3, 6, and 9 mm). The  $\bar{\alpha}$  plotted here is the average of  $\bar{\alpha}$  for all measurements for a given run. For the 50% and 40% runs, the bed was mapped into armor patches and sandy transport zones, and  $\bar{\alpha}$  were calculated separately in each zone.



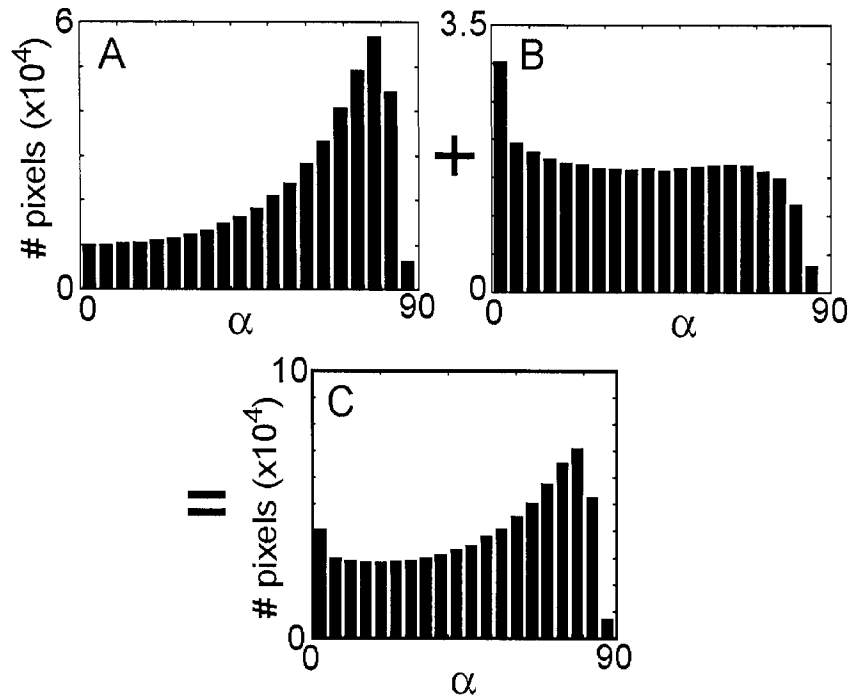


**Figure 4.10:** Friction angle histograms for the 40% run showing the distributions in A) armor patches, B) sandy transport zones, and C) both combined. The mean friction angle in each zone varied from  $\bar{\alpha} = 57^\circ$  in the armor patches to  $\bar{\alpha} = 39^\circ$  in the transport zones with an overall mean of  $\bar{\alpha} = 49^\circ$  for the entire swath.

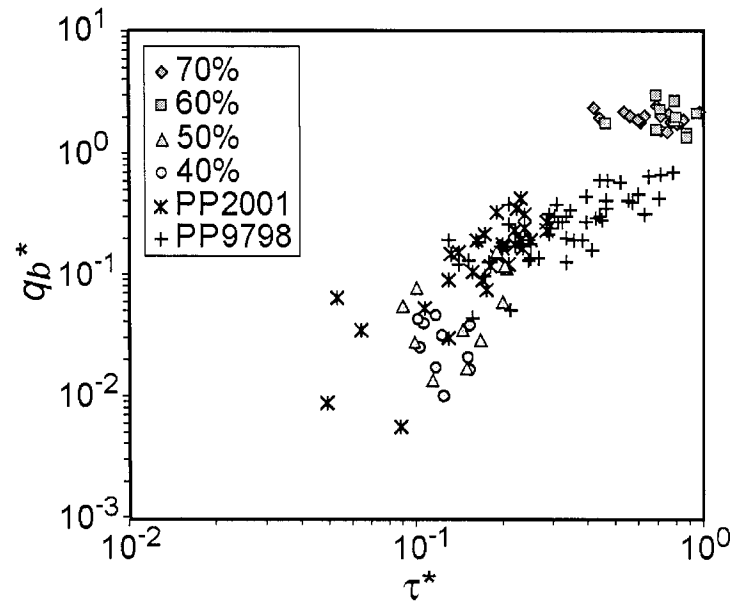


**Figure 4.11:** Dimensionless bedload transport ( $q_b^*$ ) and dimensionless shear stress ( $\tau^*$ ) for the Pasig-Potrero River and the flume data combined. The flume data span the range of conditions measured on the Pasig-Potrero River, separating into two zones based on sand content in the feed.

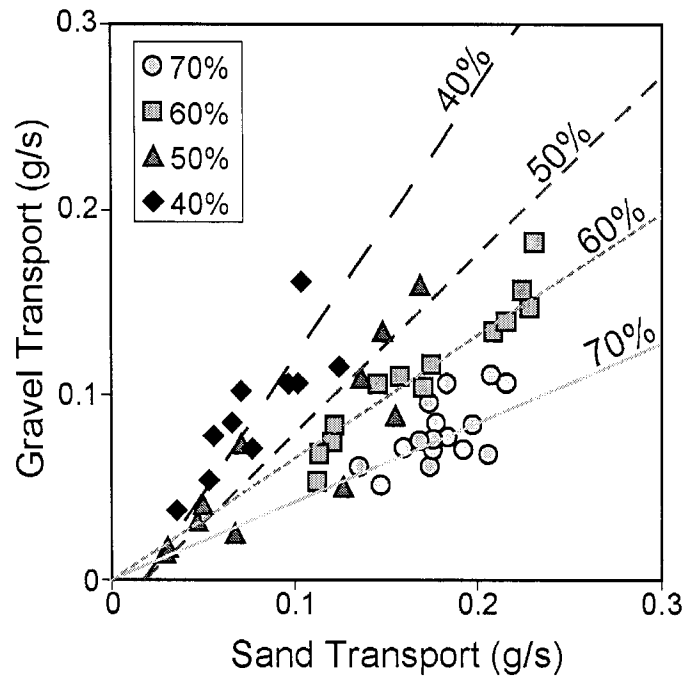


**Figure 4.12:** Fractional bedload transport rates for each flume run, plotted as sand vs. gravel transport. The solid lines represent estimated fractional transport rates (sand vs. gravel) using MPM with the  $\tau_c^*$  that best fits these fractional transport data. For the 70% and 60% runs, the best-fit  $\tau_c^* = 0$ . For the 50% and 40% runs, the best-fit  $\tau_c^* = 0.003$ .

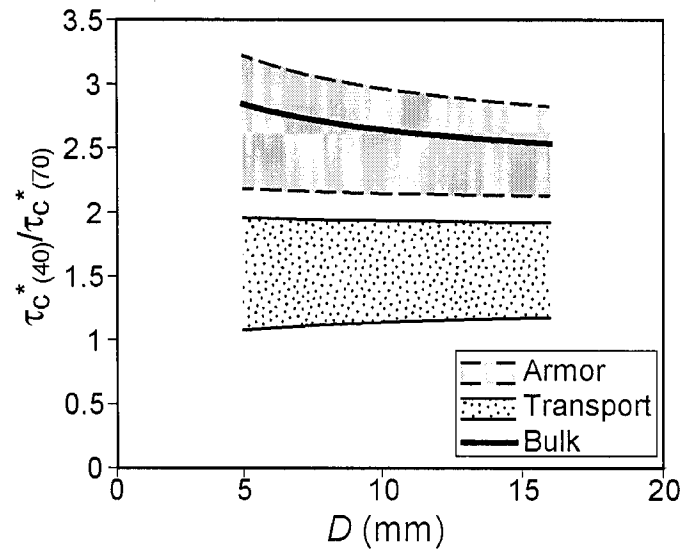


**Figure 4.13:** Ratios of  $\tau_c^*$ , comparing the 40% run to the base line  $\tau_c^*$  of the 70% run. A  $\tau_c^*$  ratio of 1 indicates no significant increase in  $\tau_c^*$  compared to the 70% run. The graph illustrates the differences in  $\tau_c^*$  ratios between the armor patches and the sandy transport zones. All  $\tau_c^*$  values were computed using a force balance outlined in Kirchner et al. (1990).

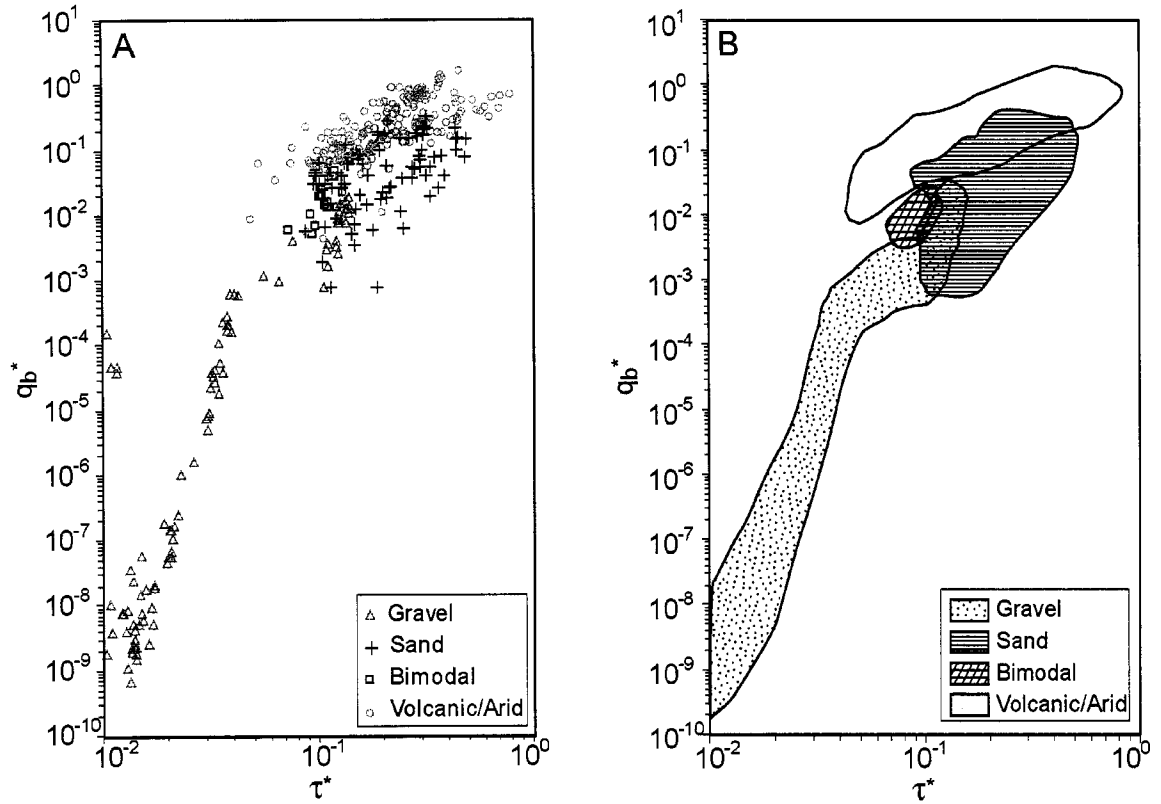


**Figure 4.14:** Dimensionless bedload transport ( $q_b^*$ ) and dimensionless shear stress ( $\tau^*$ ) for the Pasig-Potrero River (Hayes et al., 2002) as compared to other world rivers (Milhous, 1973; Leopold and Emmett, 1976; Emmett et al., 1985; Gomez and Church, 1988; Pitlick, 1992; Reid et al., 1995). Here, rivers are plotted based on river type (gravel ( $\Delta$ ), sand (+), bimodal ( $\square$ ), and volcanic / arid ephemeral (o)). Plot (A) shows the data, and (B) summarizes the general range covered by each river type.

### Notes to chapter

- Beverage, J. P., and Culbertson, J. K., 1964, Hyperconcentrations of suspended sediment: *Journal of the Hydraulics Division, American Society of Civil Engineers*, v. 90, no. HY6, p. 117-128.
- Buffington, J. M., Dietrich, W. E., and Kirchner, J. W., 1992, Friction angle measurements on a naturally formed gravel streambed: Implications for critical boundary shear stress: *Water Resources Research*, v. 28, no. 2, p. 411-425.
- Buffington, J. M., and Montgomery, D. R., 1997, A systematic analysis of eight decades of incipient motion studies, with special reference to gravel-bedded rivers: *Water Resources Research*, v. 33, no. 8, p. 1993-2029.
- Daag, A. S., 1994, Geomorphic developments and erosion of the Mount Pinatubo 1991 pyroclastic flows in the Sacobia watershed, Philippines: A study using remote sensing and Geographic Information Systems (GIS) [M.S. thesis]: Enschede, Netherlands, International Institute for Geoinformation Science and Earth Observation (ITC), 106 p.
- , 2003, Modelling the erosion of pyroclastic flow deposits and the occurrences of lahars at Mt. Pinatubo, Philippines [Ph.D. thesis]: Enschede, Netherlands, International Institute for Geoinformation Science and Earth Observation (ITC), 232 p.
- Dietrich, W. E., Kirchner, J. W., Ikeda, H., and Iseya, F., 1987, The origin of the coarse surface layer in gravel-bedded streams: The role of sediment supply: *Geological Society of America Abstracts with Programs*, v. 19, p. 642.
- , 1989, Sediment supply and the development of the coarse surface layer in gravel-bedded rivers: *Nature*, v. 340, p. 215-217.
- Dinehart, R. L., 1998, Sediment transport at gauging stations near Mount St. Helens, Washington, 1980-90. Data collection and analysis: U.S. Geological Survey Professional Paper 1573, p. 105.
- Edwards, T. K., and Glysson, G. D., 1999, Field methods for measurement of fluvial sediment: U. S. Geological Survey, Techniques of Water-Resources Investigations Report, v. 3-C2, 89 p..
- Emmett, W. W., Myrick, R. M., and Martinson, R. H., 1985, Hydraulic and sediment-transport data, East Fork River, Wyoming, 1978: U. S. Geological Survey Open-File Report 85-486, 37 p..

- Engelund, F., and Hansen, E., 1967, A Monograph on Sediment Transport in Alluvial Streams: Copenhagen, Teknisk Forlag, 62 p.
- Ferguson, R. I., 2003, Emergence of abrupt gravel to sand transitions along rivers through sorting processes: *Geology*, v. 31, no. 2, p. 159-162.
- Ferguson, R. I., Prestegard, K. L., and Ashworth, P. J., 1989, Influence of sand on hydraulics and gravel transport in a braided gravel bed river: *Water Resources Research*, v. 25, no. 4, p. 635-643.
- Gilbert, G. K., 1917, Hydraulic mining debris in the Sierra Nevada: U.S. Geological Survey Professional Paper 105, p. 154.
- Gomez, B., and Church, M., 1988, A catalogue of equilibrium transport data for coarse sand and gravel-bed channels: University of British Columbia, Vancouver, BC, 90 p.
- Gran, K. B., and Montgomery, D. R., 2005, Spatial and temporal patterns in fluvial recovery following volcanic eruptions: Channel response to basin-wide sediment loading at Mount Pinatubo, Philippines: *Geological Society of America Bulletin*, v. 117, no. 1/2, p. 195-211.
- Gran, K. B., Montgomery, D. R., and Sutherland, D. G., in review, Channel bed evolution and sediment transport under declining sand inputs: *Water Resources Research*, p. 48 ms.
- Gran, K. B., and Paola, C., 2001, Riparian vegetation controls on braided stream dynamics: *Water Resources Research*, v. 37, no. 12, p. 3275-3283.
- Hayes, S. K., 1999, Low-flow sediment transport on the Pasig-Potrero alluvial fan, Mount Pinatubo, Philippines [M.S. thesis]: Seattle, University of Washington, 73 p.
- Hayes, S. K., Montgomery, D. R., and Newhall, C. G., 2002, Fluvial sediment transport and deposition following the 1991 eruption of Mount Pinatubo: *Geomorphology*, v. 45, no. 3-4, p. 211-224.
- Hirao, K., and Yoshida, M., 1989, Sediment yield of Mt Galunggung after eruption in 1982, *in* International Symposium on Erosion and Volcanic Debris Flow Technology, Yogyakarta, Indonesia, p. V21-1 - V21-22.
- Ikeda, H., and Iseya, F., 1988, Experimental study of heterogeneous sediment transport: The University of Tsukuba, Environmental Research Center Report 12, 50 p.

- Iseya, F., and Ikeda, H., 1987, Pulsations in bedload transport rates induced by a longitudinal sediment sorting: A flume study using sand and gravel mixtures: *Geografiska Annaler A*, v. 69, no. 1, p. 15-27.
- JICA, 1978, Planning report on the Pasig-Potrero River flood control and Sabo project: Tokyo, Japan, Japan International Cooperation Agency, 133 p.
- Kadomura, H., Imagawa, T., and Yamamoto, H., 1983, Eruption-induced rapid erosion and mass movements on Usu Volcano, Hokkaido: *Zeitschrift für Geomorphologie N. F. Suppl. Bd.*, v. 46, p. 123-142.
- Kirchner, J. W., Dietrich, W. E., Iseya, F., and Ikeda, H., 1990, The variability of critical shear stress, friction angle, and grain protrusion in water-worked sediments: *Sedimentology*, v. 37, p. 647-672.
- Knighton, A. D., 1989, River adjustment to changes in sediment load: The effects of tin mining on the Ringarooma River, Tasmania, 1875-1984: *Earth Surface Processes and Landforms*, v. 14, p. 333-359.
- , 1991, Channel bed adjustment along mine-affected rivers of northeast Tasmania: *Geomorphology*, v. 4, p. 205-219.
- , 1999, The gravel-sand transition in a disturbed catchment: *Geomorphology*, v. 27, p. 325-341.
- Kodama, Y., 1994, Experimental study of abrasion and its role in producing downstream fining in gravel-bed rivers: *Journal of Sedimentary Research*, v. 64, p. 76-85.
- Kuhnle, R. A., and Southard, J. B., 1988, Bed load transport fluctuations in a gravel bed laboratory channel: *Water Resources Research*, v. 24, no. 2, p. 247-260.
- Leopold, L. B., and Emmett, W. W., 1976, Bedload measurements, East Fork River, Wyoming: *National Academy of Sciences (USA) Proceedings*, v. 73, p. 1000-1004.
- Lisle, T. E., 1995, Particle size variations between bed load and bed material in natural gravel bed channels: *Water Resources Research*, v. 31, no. 4, p. 1107-1118.
- Lisle, T. E., Iseya, F., and Ikeda, H., 1993, Response of a channel with alternate bars to a decrease in supply of mixed-size bed load: A flume experiment: *Water Resources Research*, v. 29, no. 11, p. 3623-3629.



- Madej, M. A., and Ozaki, V., 1996, Channel response to sediment wave propagation and movement, Redwood Creek, California, USA: *Earth Surface Processes and Landforms*, v. 21, p. 911-927.
- Maita, H., 1991, Sediment dynamics of a high gradient stream in the Oi River Basin of Japan, USDA Forest Service General Technical Report, PSW-GTR-130, p. 56-64.
- Major, J. J., 2004, Posteruption suspended sediment transport at Mount St. Helens: Decadal-scale relationships with landscape adjustments and river discharges: *Journal of Geophysical Research*, v. 109, p. 1-22.
- Major, J. J., Janda, R. J., and Daag, A. S., 1996, Watershed disturbance and lahars on the east side of Mount Pinatubo during the mid-June 1991 eruptions, *in* Punongbayan, R. S., ed., *Fire and mud: eruptions and lahars of Mount Pinatubo, Philippines*: Quezon City, Philippine Institute of Volcanology and Seismology, and Seattle, University of Washington Press, p. 895-919.
- Major, J. J., Pierson, T. C., Dinehart, R. L., and Costa, J. E., 2000, Sediment yield following severe volcanic disturbance -- A two-decade perspective from Mount St. Helens: *Geology*, v. 28, no. 9, p. 819-822.
- Meyer-Peter, E., and Müller, R., 1948, Formulas for bed-load transport, *in* 2nd Meeting International Association for Hydraulic Structures Research, Stockholm, p. 39-64.
- Milhous, R. T., 1973, Sediment transport in a gravel-bottomed stream [Ph.D. thesis]: Corvallis, Oregon State University, 232 p.
- Montgomery, D. R., Panfil, M. S., and Hayes, S. K., 1999, Channel-bed mobility response to extreme sediment loading at Mount: *Geology*, v. 27, no. 3, p. 271-274.
- Paola, C., Parker, G., Seal, R., Sinha, S. K., and Southard, J. B., 1992, Downstream fining by selective deposition in a laboratory flume: *Science*, v. 258, no. 5089, p. 1757-1760.
- Paola, C., and Seal, R., 1995, Grain size patchiness as a cause of selective deposition and downstream fining: *Water Resources Research*, v. 31, no. 5, p. 1395-1407.
- Pearson, M. L., 1986, Sediment yields from the debris avalanche for water years 1980-1983, *in* Keller, S. A. C., ed., *Mount St. Helens: Five Years Later*: Spokane, Eastern Washington University Press, p. 87-107.

- Pickup, G., 1984, Geomorphology of tropical rivers. 1. Landforms, hydrology, and sedimentation in the Fly and lower Purari, Papua New Guinea: *Catena Supplement*, v. 5, p. 1-17.
- Pitlick, J., 1992, Flow resistance under conditions of intense gravel transport: *Water Resources Research*, v. 28, no. 3, p. 891-903.
- Reid, I., Laronne, J. B., and Powell, D. M., 1995, The Nahal Yatir bedload database: Sediment dynamics in a gravel-bed ephemeral stream: *Earth Surface Processes and Landforms*, v. 20, p. 845-857.
- Sambrook Smith, G. H., 1996, Bimodal fluvial bed sediments: origin, spatial extent and processes: *Progress in Physical Geography*, v. 20, no. 4, p. 402-417.
- Sambrook Smith, G. H., and Ferguson, R. I., 1995, The gravel-sand transition along river channels: *Journal of Sedimentary Research*, v. A65, no. 2, p. 423-430.
- Scott, W. E., Hoblitt, R. P., Torres, R. C., Self, S., Martinez, M. M. L., and Nillos, T., 1996, Pyroclastic flows of the June 15, 1991, climactic eruption of Mount Pinatubo, *in* Punongbayan, R. S., ed., *Fire and mud: eruptions and lahars of Mount Pinatubo*, Philippines: Quezon City, Philippine Institute of Volcanology and Seismology, and Seattle, University of Washington Press, p. 545-570.
- Seal, R., and Paola, C., 1995, Observations of downstream fining on the North Fork Toutle River near Mount St. Helens, Washington: *Water Resources Research*, v. 31, no. 5, p. 1409-1419.
- Shaw, J., and Kellerhals, R., 1982, The composition of recent alluvial gravels in Alberta river beds: *Alberta Research Council Bulletin*, v. 41, p. 151 p.
- Tuñgol, N. M., 2002, Lahar initiation and sediment yield in the Pasig-Potrero River basin, Mount Pinatubo, Philippines [Ph.D. thesis]: Canterbury, New Zealand, University of Canterbury, 172 p.
- Umbal, J. V., 1997, Five years of lahars at Pinatubo volcano: Declining but still potentially lethal hazards: *Journal of the Geological Society of the Philippines*, v. 52, no. 1, p. 1-19.
- Whiting, P. J., Dietrich, W. E., Leopold, L. B., Drake, T. G., and Shreve, R. L., 1988, Bedload sheets in heterogeneous sediment: *Geology*, v. 16, p. 105-108.
- Wiberg, P. J., and Smith, J. D., 1987, Velocity distribution and bed roughness in high-gradient streams: *Water Resources Research*, v. 27, p. 825-838.

- Wilcock, P. R., and Kenworthy, S. T., 2002, A two fraction model for the transport of sand/gravel mixtures: *Water Resources Research*, v. 38, p. 12-1 - 12-12.
- Wilcock, P. R., Kenworthy, S. T., and Crowe, J. C., 2001, Experimental study of the transport of mixed sand and gravel: *Water Resources Research*, v. 37, no. 12, p. 3349-3358.
- Wilcock, P. R., and McArdell, B. W., 1993, Surface-based fractional transport rates: Mobilization thresholds and partial transport of a sand-gravel sediment: *Water Resources Research*, v. 29, no. 4, p. 1297-1312.
- Wolcott, J. F., 1988, Non-fluvial control of bimodal grainsize distributions in river bed gravels: *Journal of Sedimentary Petrology*, v. 58, p. 979-84.
- Wolman, M. G., 1954, A method of sampling coarse river-bed material: *Transactions of the American Geophysical Union*, v. 35, no. 6, p. 951-956.
- Yatsu, E., 1955, On the longitudinal profile of the graded river: *Transactions of the American Geophysical Union*, v. 36, no. 4, p. 655-663.

## CHAPTER 5

### Conclusions

Studies of the erosional response to the 1991 eruption of Mount Pinatubo show that landscape response to and recovery from a volcanic eruption will depend on the size of the eruption and the type of deposits emplaced over the surrounding landscape. The June 1991 eruption of Mount Pinatubo was a large Plinian eruption, with voluminous pyroclastic-flow deposits that filled valleys with as much as 200 meters of hot, sandy, easily erodible sediment. In the most disturbed basins, average pyroclastic-flow deposit depths ranged from ~30-70 m (Major et al., 1996; Rodolfo et al., 1996; Scott et al., 1996b). Thus, erosion of pyroclastic-flow material and erosion in valleys, in particular, dominated sediment yields. Specific processes like secondary explosions and valley-wall retreat were important specifically because of the presence of thick, hot deposits. These processes erode over a longer time period than the initial period of network integration, valley incision, and hillslope-tephra erosion, leading to elevated sediment yields throughout the entire first decade.

Other rivers at Mount Pinatubo, like the Porac River, were affected primarily by the emplacement of air-fall tephra, rather than voluminous pyroclastic flows. These hillslope deposits were removed rapidly, leading to lahar generation and high sediment yields that declined rapidly back to pre-eruption yields. This was the same situation in basins like the Green River basin at Mount St. Helens that were affected primarily by hillslope tephra (Major et al., 2000). Basin response to a large eruption is not just a function of the overall size and volume of the eruption but also of the distribution of tephra on the landscape. Climate also plays a role, although this is not explored in depth here. The intense, tropical rainfall at Mount Pinatubo was an important factor in mobilizing and transporting such high volumes of sediment, leading to removal of ~60% of the eruptive material from basins like the Pasig-Potrero/Sacobia.

Ten years after the eruption, sediment yields from the Pasig-Potrero/Sacobia River basins were still 20 times higher than pre-eruption levels and were declining exponentially. Based on long-term sediment yields from the Toutle River at Mount St.

Helens, I expect that sediment yields will level off before reaching pre-eruption values. If sediment yields level off at a rate 10 times higher than pre-eruption levels, it will send an addition 14 million m<sup>3</sup> of sediment down the Pasig-Potrero and Sacobia Rivers in the second decade after the eruption. This is a fairly conservative estimate given the extent of valley and channel disturbance on the Pasig-Potrero and Sacobia Rivers. At Mount St. Helens, channels with significant channel disturbance, like the Toutle River, had sediment yields 10 – 100 times higher than background levels for at least two decades due to continued instability in the channel and high rates of bank collapse.

Initially after the eruption, sediment yields were dominated by lahars. As sediment sources stabilized or were evacuated, lahars ceased to be the dominant conveyers of sediment. Sediment transport became dominated by normal streamflow processes, and the fluvial network could adjust to the imposed sediment load without large fluctuations in base level during the passage of each lahar. Throughout the fluvial recovery period, channels adjusted to continuing declines in sediment yield.

Field observations revealed the effects of declining sediment yields in channels, where sediment was mobilized preferentially through selective transport leading to downstream gradients in grain size and pumice content. As the bed coarsened enough for gravel-size clasts to interact, clast structures developed, first on low bar tops and edges of channels, and finally within the main flow. Clast structures increased form roughness and critical shear stress. Both of these effects led to a decrease in initial clast mobility, enhancing bed armoring.

Further exploration of clast structure development and bed organization under conditions of declining sand content shows that bed reorganization provides a mechanism for accommodating significant bed coarsening with little impact on sediment transport as long as sand ribbons remain connected. Patch development thus compresses the transition from a sand- to gravel-bed into a narrow range of sand content rather than a continuous, smooth transition over a wide range of sand content. This effect helps explain why, in general, most channels are sand-bedded or gravel-bedded, with fewer bimodal or transitional channels. Even in channels with downstream gravel to sand transitions, transitional reaches are relatively short.

On the Pasig-Potrero River in 2001, clast structure development and bed armoring occurred during the dry season when sediment inputs to channels were lower and the channel incised into valley-bottom sediments. During incision, armoring through selective transport limited overall incision, adding some stability to the channel surface. Even after base level within the channel stabilizes, high lateral mobility rates can continue, maintaining high sediment yields until banks stabilize, similar to the pattern seen on the Toutle River at Mount St. Helens. Bank stabilization may not occur until vegetation becomes established on the valley floor. As of 2001, valley floors were still mostly bare. Although the tropical climate has led to rapid vegetation growth in the uplands, the intense tropical storms also create flashy floods capable of scouring most vegetation attempting to grow in the valley bottom.

In many cases, the desired goal of river recovery is the re-establishment of an aquatic ecosystem of pre-disturbance complexity. Although this thesis does not address the additional process of ecosystem recovery, channel bed recovery is an important precursor to the return of aquatic species. While widespread fluctuations in base level remain, or while the channel still maintains high suspended load concentrations and a highly mobile bed, it will be difficult for anything to live in the river. Observed timing of the onset of in-channel biological recovery suggests that re-establishment of channel bed stability helps catalyze aquatic ecosystem recovery.

### **Directions for future research**

In the future, an expansion of both spatial and temporal scales would help add more insight into the processes involved in landscape recovery from basin-wide sediment loading. Continued monitoring of sediment yield on the Pasig-Potrero and Sacobia Rivers can determine whether sediment yields will continue to decay exponentially or decay to an elevated tail as predicted here and as seen on the Toutle River at Mount St. Helens. It should be clear by the end of the current decade which route the Pasig-Potrero/Sacobia Rivers are taking. In addition, continued monitoring of both systems (Pasig-Potrero/Sacobia and Toutle) in the ensuing decades will help determine how long sediment yields remain elevated, and what changes to the

landscape are necessary to finally bring sediment yields back down to pre-eruption levels. For instance, channel stability may not be achieved until vegetation becomes established in the valley-bottom.

Spatially, I would like to take the investigations from chapter 4 down another scale to look at exactly how cluster formations on the bed surface are perturbing the flow field actually experienced by particles on the bed. This was not something I was able to address, and most of the parameters measured or back-calculated in my study were average values (average shear stress, friction angle, roughness, etc.). In many cases, it is the fluctuations in shear stress driven by turbulence that initiates motion of particles on the bed. I would like to have a more clear understanding of the role of cluster formations on turbulent fluctuations and how much shielding particles receive once clusters develop.

Many of the processes seen in the latter half of the decade at Mount Pinatubo are not specific to volcanic eruptions, but instead could apply to any system that is currently overloaded with sediment. I think it would be worthwhile to move into other systems that experience single-event, large-scale sediment loading. Both large landslides and dam removals have the effect of immediately inundating a channel with an abundant source of sediment, often fine-grained. While studies have been conducted on how small pulses of sediment translate or disperse downstream (e.g. Cui et al. 2003a, b; Lisle et al. 2003), Mount Pinatubo offered a case study of a system that was forced to process the sediment in place, leaving large volumes that may never be removed from the system.

Lastly, I would look to the next major eruption as an opportunity to test the generality of the patterns and processes seen here. Hopefully, comparisons of eruptions like Mount Pinatubo and Mount St. Helens, with growing records of long-term sediment yield and patterns of landscape recovery, will help in long-term hazards management following future eruptions.

**BIBLIOGRAPHY**

- Arboleda, R. A., and Martinez, M. M. L., 1996, 1992 lahars in the Pasig-Potrero River system, *in* Newhall, C. G., and Punongbayan, R. S., eds., Fire and mud: eruptions and lahars of Mount Pinatubo, Philippines: Quezon City, Philippine Institute of Volcanology and Seismology, and Seattle, University of Washington Press, p. 1045-1052.
- Barnes, H. H., 1967, Roughness characteristics of natural channels: U. S. Geological Survey Water Supply Paper 1849, 213 p.
- Bautista, C. B., 1996, The Mount Pinatubo disaster and the people of Central Luzon *in* Newhall, C. G., and Punongbayan, R. S., eds., Fire and mud: eruptions and lahars of Mount Pinatubo, Philippines: Quezon City, Philippine Institute of Volcanology and Seismology, and Seattle, University of Washington Press, p. 151-161.
- Benda, L., and Dunne, T., 1987, Sediment routing by debris flow, *in* Erosion and Sedimentation in the Pacific Rim, Corvallis, OR, International Association of Hydrologic Sciences, v. 165, p. 213-223.
- Beverage, J. P., and Culbertson, J. K., 1964, Hyperconcentrations of suspended sediment: Journal of the Hydraulics Division, American Society of Civil Engineers, v. 90, no. HY6, p. 117-128.
- Biggs, B. J. F., Duncan, M. J., Farancoeur, S. N., and Meyer, W. D., 1997, Physical characterisation of microform bed cluster refugia in 12 headwater streams, New Zealand: New Zealand Journal of Marine and Freshwater Research, v. 31, p. 413-422.
- Biggs, B. J. F., Duncan, M. J., Suren, A. M., and Holomuzki, J. R., 2001, The importance of bed sediment stability to benthic ecosystems of streams, *in* Mosley, M. P., ed., Gravel-Bed Rivers V: Wellington, New Zealand Hydrological Society Inc., p. 423-449.
- Brayshaw, A. C., 1985, Bed microtopography and entrainment thresholds in gravel-bed rivers: Geological Society of America Bulletin, v. 96, p. 218-223.
- Brayshaw, A. C., Frostick, L. E., and Reid, I., 1983, The hydrodynamics of particle clusters and sediment entrainment in coarse alluvial channels: Sedimentology, v. 30, p. 137-143.



- Buffington, J. M., Dietrich, W. E., and Kirchner, J. W., 1992, Friction angle measurements on a naturally formed gravel streambed: Implications for critical boundary shear stress: *Water Resources Research*, v. 28, no. 2, p. 411-425.
- Buffington, J. M., and Montgomery, D. R., 1997, A systematic analysis of eight decades of incipient motion studies, with special reference to gravel-bedded rivers: *Water Resources Research*, v. 33, no. 8, p. 1993-2029.
- Chinen, T., and Kadomura, H., 1986, Post-eruption sediment budget of a small catchment on Mt. Usu, Hokkaido: *Zeitschrift für Geomorphologie N. F. Suppl. Bd.*, v. 60, p. 217-232.
- Church, M., Hassan, M. A., and Wolcott, J. F., 1998, Stabilizing self-organized structures in gravel-bed stream channels: Field and experimental observations: *Water Resources Research*, v. 31, no. 11, p. 3169-3179.
- Collins, B. D., and Dunne, T., 1986, Erosion of tephra from the 1980 eruption of Mount St. Helens: *Geological Society of America Bulletin*, v. 97, p. 896-905.
- Collins, B. D., Dunne, T., and Lehre, A. K., 1983, Erosion of tephra-covered hillslopes north of Mount St. Helens, Washington: May 1980 - May 1981: *Zeitschrift für Geomorphologie N. F. Suppl. Bd.*, v. 46, p. 103-121.
- Cui, Y., Parker, G., Lisle, T. E., Gott, J., Hansler, M. E., Pizzuto, J. E., Allmendinger, N. E., and Reed, J. M., 2003a, Sediment pulses in mountain rivers: I. Experiments: *Water Resources Research*, v. 39, no. 9, p. ESG\_3-1 to 3-12.
- Cui, Y., Parker, G., Pizzuto, J. E., and Lisle, T. E., 2003b, Sediment pulses in mountain rivers: 2. Comparison between experiments and numerical predictions: *Water Resources Research*, v. 39, no. 9, p. ESG\_4-1 to 4-11.
- Daag, A., and van Westen, C. J., 1996, Cartographic modelling of erosion in pyroclastic flow deposits of Mt. Pinatubo, Philippines: *ITC Journal*, v. 2, p. 110-124.
- Daag, A. S., 1994, Geomorphic developments and erosion of the Mount Pinatubo 1991 pyroclastic flows in the Sacobia watershed, Philippines: A study using remote sensing and Geographic Information Systems (GIS) [M.S. thesis]: Enschede, Netherlands, International Institute for Geoinformation Science and Earth Observation (ITC), 106 p.
- , 2003, Modelling the erosion of pyroclastic flow deposits and the occurrences of lahars at Mt. Pinatubo, Philippines [Ph.D. thesis]: Enschede, Netherlands, International Institute for Geoinformation Science and Earth Observation (ITC), 232 p.

- Dietrich, W. E., and Dunne, T., 1978, Sediment budget for a small catchment in mountainous terrain: *Zeitschrift für Geomorphologie N. F. Suppl Bd.*, v. 29, p. 191-206.
- Dietrich, W. E., Kirchner, J. W., Ikeda, H., and Iseya, F., 1987, The origin of the coarse surface layer in gravel-bedded streams: The role of sediment supply: *Geological Society of America Abstracts with Programs*, v. 19, p. 642.
- , 1989, Sediment supply and the development of the coarse surface layer in gravel-bedded rivers: *Nature*, v. 340, p. 215-217.
- Dinehart, R. L., 1998, Sediment transport at gauging stations near Mount St. Helens, Washington, 1980-90. Data collection and analysis: U.S. Geological Survey Professional Paper, v. 1573, p. 105.
- Doyle, M. W., Stanley, E. H., and Harbor, J. M., 2002a, Channel adjustments following two dam removals in Wisconsin: *Water Resources Research*, v. 39, no. 1, p. ESG 2-1 - 2-15.
- , 2002b, Geomorphic analogies for assessing probably channel response to dam removal: *Journal of the American Water Resources Association*, v. 38, no. 6, p. 1567-1579.
- Edwards, T. K., and Glysson, G. D., 1999, Field methods for measurement of fluvial sediment: U. S. Geological Survey, *Techniques of Water-Resources Investigations Report*, TWRI-3-C2, 89 p.
- Emmett, W. W., Myrick, R. M., and Martinson, R. H., 1985, Hydraulic and sediment-transport data, East Fork River, Wyoming, 1978: U. S. Geological Survey Open-File Report 85-486, p. 37.
- Engelund, F., and Hansen, E., 1967, *A Monograph on Sediment Transport in Alluvial Streams*: Copenhagen, Teknisk Forlag, 62 p.
- Fahnestock, R. K., and Haushild, W. L., 1962, Flume studies of the transport of pebbles and cobbles on a sand bed: *Geological Society of America Bulletin*, v. 73, p. 1431-1436.
- Ferguson, R. I., 2003, Emergence of abrupt gravel to sand transitions along rivers through sorting processes: *Geology*, v. 31, no. 2, p. 159-162.

- Ferguson, R. I., Prestegard, K. L., and Ashworth, P. J., 1989, Influence of sand on hydraulics and gravel transport in a braided gravel bed river: *Water Resources Research*, v. 25, no. 4, p. 635-643.
- Gilbert, G. K., 1917, Hydraulic mining debris in the Sierra Nevada: U.S. Geological Survey Professional Paper 105, p. 154.
- Gomez, B., and Church, M., 1988, A catalogue of equilibrium transport data for coarse sand and gravel-bed channels: University of British Columbia, Vancouver, BC, 90 p.
- Graf, W. L., 1977, The rate law in fluvial geomorphology: *American Journal of Science*, v. 277, p. 178-191.
- Gran, K. B., and Montgomery, D. R., 2005, Spatial and temporal patterns in fluvial recovery following volcanic eruptions: Channel response to basin-wide sediment loading at Mount Pinatubo, Philippines: *Geological Society of America Bulletin*, v. 117, no. 1/2, p. 195-211.
- Gran, K. B., Montgomery, D. R., and Sutherland, D. G., in review, Channel bed evolution and sediment transport under declining sand inputs: *Water Resources Research*, p. 48 ms.
- Gran, K. B., and Paola, C., 2001, Riparian vegetation controls on braided stream dynamics: *Water Resources Research*, v. 37, no. 12, p. 3275-3283.
- Hamidi, S., 1989, Lahar of Galunggung Volcano from 1982 through 1986, *in* International Symposium on Erosion and Volcanic Debris Flow Technology, Yogyakarta, Indonesia, p. VP1-1 - VP1-23.
- Hayes, S. K., 1999, Low-flow sediment transport on the Pasig-Potrero alluvial fan, Mount Pinatubo, Philippines [M.S. thesis]: Seattle, University of Washington, 73 p.
- Hayes, S. K., Montgomery, D. R., and Newhall, C. G., 2002, Fluvial sediment transport and deposition following the 1991 eruption of Mount Pinatubo: *Geomorphology*, v. 45, no. 3-4, p. 211-224.
- Herkelrath, W., and Leavesley, G. H., 1981, Physical properties of volcanic ash from Mount St. Helens -- Relationship to rain infiltration experiments: *Agronomy Abstracts*, p. 141.

- Hildreth, W., 1983, The compositionally zoned eruption of 1912 in the Valley of Ten Thousand Smokes, Katmai National Park, Alaska: *Journal of Volcanology and Geothermal Research*, v. 18, no. 1-4, p. 1-56.
- Hirao, K., and Yoshida, M., 1989, Sediment yield of Mt Galunggung after eruption in 1982, *in* International Symposium on Erosion and Volcanic Debris Flow Technology, Yogyakarta, Indonesia, p. V21-1 - V21-22.
- Howard, A., 1999, Simulation of gully erosion and bistable landforms, *in* Simon, A., ed., *Incised river channels: processes, forms, engineering and management*: Chichester, John Wiley, p. 277-299.
- Ikeda, H., and Iseya, F., 1988, Experimental study of heterogeneous sediment transport: The University of Tsukuba, Environmental Research Center Report 12, 50 p.
- Iseya, F., and Ikeda, H., 1987, Pulsations in bedload transport rates induced by a longitudinal sediment sorting: A flume study using sand and gravel mixtures: *Geografiska Annaler A*, v. 69, no. 1, p. 15-27.
- Janda, R. J., Daag, A. S., de los Reyes, P. J., and Newhall, C., 1996, Assessment and response to lahar hazard around Mount Pinatubo, 1991 to 1993, *in* Newhall, C., G., and Punongbayan, R. S., eds., *Fire and mud: eruptions and lahars of Mount Pinatubo, Philippines*: Quezon City, Philippine Institute of Volcanology and Seismology, and Seattle, University of Washington Press, p. 107-139.
- Janda, R. J., Meyer, D. F., and Childers, D., 1984a, Sedimentation and geomorphic changes during and following the 1980-1983 eruptions of Mount St. Helens, Washington (1): *Shin-Sabo*, v. 37, no. 2, p. 10-21.
- , 1984b, Sedimentation and geomorphic changes during and following the 1980-1983 eruptions of Mount St. Helens, Washington (2): *Shin-Sabo*, v. 37, no. 3, p. 5-17.
- JICA, 1978, Planning report on the Pasig-Potrero River flood control and Sabo project: Tokyo, Japan, Japan International Cooperation Agency, 133 p.
- , 1996, The study on flood and mudflow control for Sacobia-Bamban/Abacan River draining from Mt. Pinatubo: Japan International Cooperation Agency (JICA) and Department of Public Works and Highways, Philippines, 45 p.
- Kadomura, H., Imagawa, T., and Yamamoto, H., 1983, Eruption-induced rapid erosion and mass movements on Usu Volcano, Hokkaido: *Zeitschrift für Geomorphologie N. F. Suppl. Bd.*, v. 46, p. 123-142.

- Kirchner, J. W., Dietrich, W. E., Iseya, F., and Ikeda, H., 1990, The variability of critical shear stress, friction angle, and grain protrusion in water-worked sediments: *Sedimentology*, v. 37, p. 647-672.
- Knighton, A. D., 1989, River adjustment to changes in sediment load: The effects of tin mining on the Ringarooma River, Tasmania, 1875-1984: *Earth Surface Processes and Landforms*, v. 14, p. 333-359.
- , 1991, Channel bed adjustment along mine-affected rivers of northeast Tasmania: *Geomorphology*, v. 4, p. 205-219.
- , 1999, The gravel-sand transition in a disturbed catchment: *Geomorphology*, v. 27, p. 325-341.
- Kodama, Y., 1994, Experimental study of abrasion and its role in producing downstream fining in gravel-bed rivers: *Journal of Sedimentary Research*, v. 64, p. 76-85.
- Komar, P. D., 1987, Selective grain entrainment by a current from a bed of mixed sizes: A reanalysis: *Journal of Sedimentary Petrology*, v. 57, no. 2, p. 203-211.
- Kuhle, R. A., and Southard, J. B., 1988, Bed load transport fluctuations in a gravel bed laboratory channel: *Water Resources Research*, v. 24, no. 2, p. 247-260.
- Leavesley, G. H., Lusby, G. C., and Lichty, R. W., 1989, Infiltration and erosion characteristics of selected tephra deposits from the 1980 eruption of Mount St. Helens, Washington, USA: *Hydrological Sciences Journal*, v. 34, no. 3, p. 339-353.
- Lehre, A. K., Collins, B. D., and Dunne, T., 1983, Post-eruption sediment budget for the North Fork Toutle River Drainage, June 1980 - June 1981: *Zeitschrift für Geomorphologie N. F. Suppl. Bd.*, v. 46, p. 143-163.
- Leopold, L. B., and Emmett, W. W., 1976, Bedload measurements, East Fork River, Wyoming: *National Academy of Sciences (USA) Proceedings*, v. 73, p. 1000-1004.
- Lisle, T. E., 1995, Particle size variations between bed load and bed material in natural gravel bed channels: *Water Resources Research*, v. 31, no. 4, p. 1107-1118.
- Lisle, T. E., Cui, Y., Parker, G., Pizzuto, J. E., and Dodd, A., 2001, The dominance of dispersion in the evolution of bed material waves in gravel-bed rivers: *Earth Surface Processes and Landforms*, v. 26, p. 1409-1420.

- Lisle, T. E., Iseya, F., and Ikeda, H., 1993, Response of a channel with alternate bars to a decrease in supply of mixed-size bed load: A flume experiment: *Water Resources Research*, v. 29, no. 11, p. 3623-3629.
- Lisle, T. E., Pizzuto, J. E., Ikeda, H., Iseya, F., and Kodama, Y., 1997, Evolution of a sediment wave in an experimental channel: *Water Resources Research*, v. 33, no. 8, p. 1971-1981.
- Madej, M. A., and Ozaki, V., 1996, Channel response to sediment wave propagation and movement, Redwood Creek, California, USA: *Earth Surface Processes and Landforms*, v. 21, p. 911-927.
- Maita, H., 1991, Sediment dynamics of a high gradient stream in the Oi River Basin of Japan, USDA Forest Service General Technical Report, PSW-GTR-130, p. 56-64.
- Major, J. J., 2004, Posteruption suspended sediment transport at Mount St. Helens: Decadal-scale relationships with landscape adjustments and river discharges: *Journal of Geophysical Research*, v. 109, p. F01002.
- Major, J. J., Janda, R. J., and Daag, A. S., 1996, Watershed disturbance and lahars on the east side of Mount Pinatubo during the mid-June 1991 eruptions, *in* Newhall, C. G., and Punongbayan, R. S., eds., *Fire and mud: eruptions and lahars of Mount Pinatubo, Philippines*: Quezon City, Philippine Institute of Volcanology and Seismology, and Seattle, University of Washington Press, p. 895-919.
- Major, J. J., Pierson, T. C., Dinehart, R. L., and Costa, J. E., 2000, Sediment yield following severe volcanic disturbance -- A two-decade perspective from Mount St. Helens: *Geology*, v. 28, no. 9, p. 819-822.
- Marcus, W. A., Roberts, K., Harvey, L., and Tackman, G., 1992, An evaluation of methods for estimating Manning's n in small mountain streams: *Mountain Research and Development*, v. 12, p. 227-239.
- Martinez, M. M. L., Arboleda, R. A., Delos Reyes, P. J., Gabinete, E., and Dolan, M. T., 1996, Observations of 1992 lahars along the Sacobia-Bamban River system, *in* Newhall, C. G., and Punongbayan Raymundo, S., eds., *Fire and mud: eruptions and lahars of Mount Pinatubo, Philippines*: Quezon City, Philippine Institute of Volcanology and Seismology, and Seattle, University of Washington Press, p. 1033-1043.
- Mastin, L., and Waitt, R., 2000, Glacier Peak -- History and hazards of a Cascade volcano: U.S. Geological Survey Fact Sheet, v. 058-00.

- Meade, R. H., 1985, Wavelike movement of bedload sediment, East Fork River, Wyoming: *Environmental Geology and Water Science*, v. 7, no. 4, p. 215-225.
- Mercado, R. A., Lacsamana, J. B. T., and Pineda, G. L., 1996, Socioeconomic impacts of the Mount Pinatubo eruption, *in* Newhall, C. G., and Punongbayan, R. S., eds., *Fire and Mud: Eruptions and Lahars of Mount Pinatubo, Philippines: Quezon City, Philippine Institute of Volcanology and Seismology, and Seattle, University of Washington Press*, p. 1063-1069.
- Meyer-Peter, E., and Müller, R., 1948, Formulas for bed-load transport, *in* 2nd Meeting International Association for Hydraulic Structures Research, Stockholm, p. 39-64.
- Milhous, R. T., 1973, Sediment transport in a gravel-bottomed stream [Ph.D. thesis]: Corvallis, Oregon State University, 232 p.
- Milliman, J. D., and Syvitski, J. P. M., 1992, Geomorphic/tectonic control of sediment discharge to the ocean: the importance of small mountainous rivers: *Journal of Geology*, v. 100, no. 5, p. 525-544.
- Mizuyama, T., and Kobashi, S., 1996, Sediment yield and topographic change after major volcanic activity, *in* *Erosion and Sediment Yield: Global and Regional Perspectives (Exeter Symposium)*, International Association of Hydrological Sciences (IAHS) Publication 236, p. 295-301.
- Montgomery, D. R., Panfil, M. S., and Hayes, S. K., 1999, Channel-bed mobility response to extreme sediment loading at Mount: *Geology*, v. 27, no. 3, p. 271-274.
- Moyer, T., and Swanson, D., 1987, Secondary hydroeruptions in pyroclastic-flow deposits: examples from Mount St. Helens: *Journal of Volcanology and Geothermal Research*, v. 32, no. 4, p. 299-319.
- Newhall, C. G., Daag, A. S., Delfin, F. G., Jr., Hoblitt, R. P., McGeehin, J., Pallister, J. S., Regalado, M. T. M., Rubin, M., Tubianosa, B. S., Tamayo, R. A., Jr., and Umbal, J. V., 1996, Eruptive history of Mount Pinatubo, *in* Newhall, C. G., and Punongbayan Raymundo, S., eds., *Fire and mud: eruptions and lahars of Mount Pinatubo, Philippines: Quezon City, Philippine Institute of Volcanology and Seismology, and Seattle, University of Washington Press*, p. 165-195.
- Newhall, C. G., and Punongbayan, R. S., 1996, *Fire and mud: eruptions and lahars of Mount Pinatubo, Philippines: Quezon City, Philippine Institute of Volcanology and Seismology, and Seattle, University of Washington Press*, 1115 p.

- Paladio-Melosantos, M. L. O., Solidum, R. O., Scott, W. E., Quiambao, R. B., Umbal, J. V., Rodolfo, K. S., Tubianosa, B. S., de los Reyes, P. J., Alonso, R. A., and Ruelo, H. B., 1996, Tephra falls of the 1991 eruptions of Mount Pinatubo, *in* Newhall, C. G., and Punongbayan, R. S., eds., *Fire and Mud: Eruptions and lahars of Mount Pinatubo*, Philippines: Quezon City, Philippine Institute of Volcanology and Seismology, and Seattle, University of Washington Press, p. 513-535.
- Paola, C., Parker, G., Seal, R., Sinha, S. K., and Southard, J. B., 1992, Downstream fining by selective deposition in a laboratory flume: *Science*, v. 258, no. 5089, p. 1757-1760.
- Paola, C., and Seal, R., 1995, Grain size patchiness as a cause of selective deposition and downstream fining: *Water Resources Research*, v. 31, no. 5, p. 1395-1407.
- Parker, R. S., 1977, Experimental study of basin evolution and its hydrologic implications [Ph.D. thesis]: Fort Collins, Colorado State University, 331 p.
- Pearce, A. J., and Watson, A. J., 1986, Effects of earthquake-induced landslides on sediment budget and transport over a 50-year period: *Geology*, v. 14, p. 52-55.
- Pearson, M. L., 1986, Sediment yields from the debris avalanche for water years 1980-1983, *in* Keller, S. A. C., ed., *Mount St. Helens: Five Years Later*: Spokane, Eastern Washington University Press, p. 87-107.
- Pickup, G., 1984, Geomorphology of tropical rivers. 1. Landforms, hydrology, and sedimentation in the Fly and lower Purari, Papua New Guinea: *Catena Supplement*, v. 5, p. 1-17.
- Pickup, G., Higgins, R. J., and Grant, I., 1983, Modelling sediment transport as a moving wave -- The transfer and deposition of mining waste: *Journal of Hydrology*, v. 60, p. 281-301.
- Pierson, T. C., Janda, R. J., Umbal, J. V., and Daag, A. S., 1992, Immediate and long-term hazards from lahars and excess sedimentation in rivers draining Mt. Pinatubo, Philippines: U. S. Geological Survey Water Resources Investigations 92-4039, 35 p.
- Pitlick, J., 1992, Flow resistance under conditions of intense gravel transport: *Water Resources Research*, v. 28, no. 3, p. 891-903.
- Pizzuto, J. E., 2002, Effects of dam removal on river form and process: *BioScience*, v. 52, no. 8, p. 683-691.



- Punongbayan, R. S., Tuñgol, N. M., Arboleda, R. A., Delos Reyes, P. J., Isada, M., Martinez, M. M. L., Melosantos, M. L. P., Puertollano, J. R., Regalado, M. T. M., Solidum, R. U., Jr., Tubianosa, B. S., Umbal, J. V., Alonso, R. A., and Remotigue, C. T., 1994, Impacts of the 1993 lahars, and long-term lahar hazards and risks around Pinatubo Volcano, PHIVOLCS, Pinatubo Lahar Studies 1993: Final Report of the UNESCO-funded lahar studies program: PHIVOLCS Press, 40 p.
- Reid, I., Laronne, J. B., and Powell, D. M., 1995, The Nahal Yatir bedload database: Sediment dynamics in a gravel-bed ephemeral stream: *Earth Surface Processes and Landforms*, v. 20, p. 845-857.
- Rodolfo, K. S., 1989, Origin and early evolution of lahar channel at Mabinit, Mayon Volcano, Philippines: *Geological Society of America Bulletin*, v. 101, p. 414-426.
- Rodolfo, K. S., and Arguden, A. T., 1991, Rain-lahar generation and sediment-delivery systems at Mayon Volcano, Philippines, *in* Smith, G. A., ed., *Sedimentation in Volcanic Settings*: Tulsa, Oklahoma, SEPM Special Publication 45, p. 71-87.
- Rodolfo, K. S., Umbal, J. V., Alonso, R. A., Remotigue, C. T., Paladio-Melosantos, M. L. O., Salvador, J. H. G., Evangelista, D., and Miller, Y., 1996, Two years of lahars on the western flank of Mount Pinatubo: Initiation, flow processes, deposits, and attendant geomorphic and hydraulic changes, *in* Newhall, C. G., and Punongbayan, R. S., eds., *Fire and Mud: Eruptions and lahars of Mount Pinatubo*, Philippines: Quezon City, Philippine Institute of Volcanology and Seismology, and Seattle, University of Washington Press, p. 989-1013.
- Roque, V. P., Jr., Reyes, B. P., and Gonzales, B. A., 1972, Report on the comparative stratigraphy of the east and west of the mid-Luzon Central Valley, Philippines: *Mineral Engineering Magazine*, Philippine Society of Mining, Metallurgical, and Geological Engineers, v. 24, p. 11-62.
- Sambrook Smith, G. H., 1996, Bimodal fluvial bed sediments: origin, spatial extent and processes: *Progress in Physical Geography*, v. 20, no. 4, p. 402-417.
- Sambrook Smith, G. H., and Ferguson, R. I., 1995, The gravel-sand transition along river channels: *Journal of Sedimentary Research*, v. A65, no. 2, p. 423-430.
- Scott, K. M., Janda, R. J., de la Cruz, E. G., Gabinete, E., Eto, I., Isada, M., Sexton, M., and Hadley, K., 1996a, Channel and sedimentation responses to large volumes of 1991 volcanic deposits on the east flank of Mount Pinatubo, *in* Newhall, C. G., and Punongbayan, R. S., eds., *Fire and mud: eruptions and lahars of Mount*

- Pinatubo, Philippines: Quezon City, Philippine Institute of Volcanology and Seismology, and Seattle, University of Washington Press, p. 971-988.
- Scott, W. E., Hoblitt, R. P., Torres, R. C., Self, S., Martinez, M. M. L., and Nillos, T., 1996b, Pyroclastic flows of the June 15, 1991, climactic eruption of Mount Pinatubo, *in* Newhall, C. G., and Punongbayan, R. S., eds., Fire and mud: eruptions and lahars of Mount Pinatubo, Philippines: Quezon City, Philippine Institute of Volcanology and Seismology, and Seattle, University of Washington Press, p. 545-570.
- Seal, R., and Paola, C., 1995, Observations of downstream fining on the North Fork Toutle River near Mount St. Helens, Washington: Water Resources Research, v. 31, no. 5, p. 1409-1419.
- Segerstrom, K., 1950, Erosion studies at Parícutin, State of Michoacan, Mexico: U.S. Geological Survey Bulletin 965-A, 64 p..
- , 1960, Erosion and related phenomena at Parícutin in 1957: U.S. Geological Survey Bulletin 1104-A, 18 p..
- , 1966, Parícutin, 1965 -- Aftermath of eruption: U.S. Geological Survey Professional Paper 550-C, p. C93-C101.
- Shaw, J., and Kellerhals, R., 1982, The composition of recent alluvial gravels in Alberta river beds: Alberta Research Council Bulletin, v. 41, 151 p.
- Shimokawa, E., Jitousono, T., Yazawa, A., and Kawagoe, R., 1989, An effect of tephra cover on erosion processes of hillslopes in and around Sakurajima Volcano, *in* International Symposium on Erosion and Volcanic Debris Flow Technology, Yogyakarta, Indonesia, Ministry of Public Works, p. V32-1 - V32-21.
- Shimokawa, E., and Taniguchi, Y., 1983, Sediment yield from hillside slope of active volcanoes, *in* Symposium on erosion control in volcanic areas, Seattle and Vancouver, Washington, and Tsukuba, Japan, Sabo Division, Erosion Control Department, p. 155-181.
- Simon, A., 1999, Channel and drainage-basin response of the Toutle River system in the aftermath of the 1980 eruption of Mount St. Helens, Washington: U. S. Geological Survey Open-File Report 96-633, 130 p.
- Swanson, F. J., Fredrickson, R. L., and McCorison, F. M., 1982, Material transfer in a western Oregon forested watershed, *in* Edmonds, R. L., ed., Analysis of Coniferous Forest Ecosystems in the Western United States: Stroudsburg, PA, Hutchinson Ross, p. 233-266.

- Tabor, R. W., Booth, D. B., Vance, J. A., and Ford, A. B., 2002, Geologic map of the Sauk River 30- by 60-minute quadrangle, Washington: U. S. Geological Survey Geologic Investigations Series, 67 p. + 2 sheets.
- Tija, H., 1965, Course-changes in the lower Tjimanuk river, west Java.: Contributions from the Department of Geology, Institute Technology Bandung, v. 62, p. 75-82.
- Torres, R. C., Mouginis, M. P. J., Garbeil, H., Kallianpur, K., Self, S., and Quiambao, R. B., 2004, Monitoring the evolution of the Pasig-Potrero alluvial fan, Pinatubo volcano, using a decade of remote sensing data: *Journal of Volcanology and Geothermal Research*, v. 138, no. 3-4, p. 371-392.
- Torres, R. C., Self, S., and Martinez, M. M. L., 1996, Secondary Pyroclastic Flows from the June 15, 1991, Ignimbrite of Mount Pinatubo, *in* Newhall, C. G., and Punongbayan, R. S., eds., *Fire and Mud: Eruptions and lahars of Mount Pinatubo, Philippines*: Quezon City, Philippine Institute of Volcanology and Seismology, and Seattle, University of Washington Press, and Seattle, University of Washington Press, p. 665-678.
- Townsend, C. R., Scarsbrook, M. R., and Doledec, S., 1997, Quantifying disturbance in streams: Alternative measures of disturbance in relation to macroinvertebrate species traits and species richness: *Journal of the North American Benthological Society*, v. 16, p. 531-544.
- Tuñgol, N. M., 2002, Lahar initiation and sediment yield in the Pasig-Potrero River basin, Mount Pinatubo, Philippines [Ph.D. thesis]: Canterbury, New Zealand, University of Canterbury, 172 p.
- Umbal, J. V., 1997, Five years of lahars at Pinatubo volcano: Declining but still potentially lethal hazards: *Journal of the Geological Society of the Philippines*, v. 52, no. 1, p. 1-19.
- United States Army Corps of Engineers, 1994, Mount Pinatubo Recovery Action Plan: Long Term Report: Portland, Oregon, U. S. Army Corps of Engineers Long Term Report, 162 p. and 5 Appendices.
- Vallance, J. W., and Scott, K. M., 1997, The Osceola mudflow from Mount Rainier: Sedimentology and hazard implications of a huge clay-rich debris flow: *Geological Society of America Bulletin*, v. 109, no. 2, p. 143-163.

- Villones, R., 1980, The Aksitero Formation: Its implications and relationship with respect to the Zambales ophiolite: Philippine Bureau of Mines and Geosciences, Technical Information Series, v. 16-80, p. 21.
- Waldron, H. H., 1967, Debris flow and erosion control problems caused by the ash eruptions of Irazu Volcano, Costa Rica: U. S. Geological Survey Bulletin 1241-I, p. 11-137.
- Whiting, P. J., Dietrich, W. E., Leopold, L. B., Drake, T. G., and Shreve, R. L., 1988, Bedload sheets in heterogeneous sediment: *Geology*, v. 16, p. 105-108.
- Wiberg, P. J., and Smith, J. D., 1987, Velocity distribution and bed roughness in high-gradient streams: *Water Resources Research*, v. 27, p. 825-838.
- Wilcock, P. R., and Kenworthy, S. T., 2002, A two fraction model for the transport of sand/gravel mixtures: *Water Resources Research*, v. 38, p. 12-1 - 12-12.
- Wilcock, P. R., Kenworthy, S. T., and Crowe, J. C., 2001, Experimental study of the transport of mixed sand and gravel: *Water Resources Research*, v. 37, no. 12, p. 3349-3358.
- Wilcock, P. R., and McArdell, B. W., 1993, Surface-based fractional transport rates: Mobilization thresholds and partial transport of a sand-gravel sediment: *Water Resources Research*, v. 29, no. 4, p. 1297-1312.
- Wolcott, J. F., 1988, Non-fluvial control of bimodal grain size distributions in river bed gravels: *Journal of Sedimentary Petrology*, v. 58, p. 979-84.
- Wolman, M. G., 1954, A method of sampling coarse river-bed material: *Transactions of the American Geophysical Union*, v. 35, no. 6, p. 951-956.
- Yamamoto, H., 1984, Erosion of the 1977-1978 tephra layers on a slope of Usu Volcano, Hokkaido: *Transactions of the Japanese Geomorph. Union*, v. 5, no. 2, p. 111-124.
- Yatsu, E., 1955, On the longitudinal profile of the graded river: *Transactions of the American Geophysical Union*, v. 36, no. 4, p. 655-663.

## APPENDIX A

## Variable list

$\alpha$	friction angle
$\bar{\alpha}$	mean friction angle
$\beta$	transport exponent, coefficient
$C$	concentration
$C_f$	coefficient of friction
$d$	depth of deposit
$D$	grain size
$D_{50}$	median grain size
$D_{84}$	grain size coarser than 84% of distribution
$D^*$	relative roughness
$\varepsilon$	exponential decay coefficient
$g$	acceleration due to gravity
$h$	flow depth
$IR$	near-infrared band of multispectral image
$n$	Manning's n roughness
$NDVI$	Normalized Difference Vegetation Index
$\nu$	kinematic viscosity
$q_b$	unit bedload discharge
$q_b^*$	dimensionless unit bedload discharge
$q_w$	unit water discharge
$Q_b$	bedload discharge
$Q_s$	sediment discharge or yield
$Q_w$	water discharge
$R$	red wavelength band of multispectral image
$R_h$	hydraulic radius
$\rho_s$	sediment density
$\rho_w$	water density
$\mathcal{R}$	specific gravity of submerged sediment (excess specific gravity...?)
$R_{ep}$	dimensionless explicit particle Reynold's number
$S$	slope
$S_t$	storage
$t$	time
$\tau$	shear stress
$\tau_b$	total basal shear stress
$\tau_c$	critical shear stress
$\tau'$	effective shear stress
$\tau_b^*$	dimensionless basal shear stress
$\tau_c^*$	dimensionless critical Shields parameter
$\tau_{rg}^*$	reference shear stress for gravel

$\tau_{rs}^*$	reference shear stress for sand
$v$	mean velocity
$W^*$	dimensionless shear stress

## APPENDIX B

## Pasig-Potrero River, sediment transport 2001

Date	Sample	$Q_w$ ( $m^3/s$ )	width (m)	depth (m)	$v$ (m/s)	$Q_b$ ( $m^3/s$ )	$q_b$ ( $m^2/s$ )	C ( $kg/m^3$ )	$\tau$ ( $N/m^2$ )
08/26/01	A - a*	2.5	14.7	0.12	1.38	9.0E-03	6.1E-04	10.0	26.7
08/26/01	A - c*	7.1	20.5	0.18	1.96	2.3E-02	1.1E-03		38.0
08/26/01	B	0.2	6.1	0.06	0.68			33.0	13.2
08/26/01	C	0.1	3.7	0.04	0.96	4.3E-05	1.2E-05	4.0	7.6
08/28/01	D1	0.2	5.1	0.05	1.01			15.0	9.9
08/28/01	D2	0.6	11.3	0.07	0.76			20.0	14.6
08/28/01	D3	1.5	7.8	0.12	1.65			22.0	26.0
08/28/01	D12	0.8	16.4	0.06	0.82			19.0	13.1
08/28/01	D123	2.3	24.2	0.08	1.22			20.0	17.3
08/29/01	E - b	4.5	37.1	0.09	1.27	2.3E-02	6.3E-04	20.0	20.5
08/29/01	E - c	4.5	35.5	0.09	1.48	1.3E-02	3.8E-04	20.0	19.7
08/29/01	F - a	1.1	15.8	0.06	1.13	6.0E-03	3.8E-04	22.1	13.8
08/29/01	F - b	0.9	14.6	0.06	1.06				
08/29/01	F - c	0.7	13.4	0.05	0.99	4.0E-03	3.0E-04	22.1	11.2
09/01/01	G	3.2	19.2	0.11	1.54	1.0E-02	5.3E-04	13.0	24.3
09/04/01	J - a	0.9	9.4	0.08	1.28	3.1E-03	3.3E-04	23.7	17.0
09/04/01	K - a	0.8	12.6	0.07	0.98	2.3E-03	1.8E-04	14.3	14.6
09/04/01	L - a	0.2	5.05	0.04	0.97	5.4E-04	1.1E-04	12.0	9.2
09/06/01	M1 - a	0.1	6.7	0.02	0.58	8.7E-04	1.3E-04	10.0	4.5
09/06/01	M2 - a	2.4	21.6	0.09	1.29	7.6E-03	3.5E-04	16.0	18.9
09/06/01	M12 - a	2.5	28.3	0.07	1.25	6.7E-03	2.4E-04	18.0	15.6
09/06/01	N1	3.1	23.5	0.09	1.45	1.1E-02	4.7E-04	33.0	20.1
09/06/01	N2	0.8	9.75	0.07	1.27	4.1E-03	4.2E-04	14.0	14.8
09/06/01	N12	3.9	33.25	0.08	1.41	1.5E-02	4.6E-04	27.0	18.6
09/07/01	P1	1.3	11.2	0.08	1.38	2.7E-03	2.4E-04	8.0	18.0
09/07/01	P2	0.1	7.95	0.03	0.67	5.6E-04	7.0E-05	6.0	5.5
09/07/01	P3 - b*	1.6	14.3	0.07	1.49	4.5E-02	3.1E-03		16.0
09/07/01	P123	2.7	33	0.06	1.32	7.1E-03	2.1E-04	8.5	13.4
09/10/01	Q1	2.3	17.5	0.09	1.43	1.5E-02	8.7E-04	8.2	19.8
09/10/01	Q2	0.1	5.6	0.02	0.75	1.0E-04	1.8E-05	1.3	4.2
09/10/01	Q12	2.4	22.85	0.08	1.38	1.5E-02	6.5E-04	8.1	16.4
09/10/01	R	2.9	17.95	0.11	1.42	9.7E-03	5.4E-04	9.5	24.5
09/11/01	S1	2.2	15.5	0.10	1.43	6.1E-03	3.9E-04	9.0	21.5
09/11/01	S2	0.8	13.75	0.06	0.99	4.2E-03	3.0E-04	6.5	12.2
09/11/01	S12	3.0	29.65	0.08	1.25	1.1E-02	3.6E-04	7.7	17.3
09/11/01	T	2.6	31.75	0.08	1.07	9.1E-03	2.9E-04	7.7	16.5
09/13/01	V	2.2	30	0.07	1.07	4.5E-03	1.5E-04	9.1	15.2
09/13/01	W	0.1	2.4	0.05	0.67	4.4E-04	1.8E-04	8.9	11.1
09/14/01	X1	2.4	14.85	0.11	1.47	6.8E-03	4.6E-04	9.7	24.3
09/14/01	X2	0.2	6.7	0.05	0.68	4.0E-04	6.0E-05	8.5	11.2
09/14/01	X12	2.7	21.55	0.09	1.34	7.1E-03	3.3E-04	9.5	20.3
09/14/01	Z	3.7	31.5	0.09	1.35	2.2E-02	7.1E-04	13.0	19.1

Data listed include water discharge ( $Q_w$ ), channel width, mean depth, mean velocity ( $v$ ), bedload discharge ( $Q_b$ ), unit bedload discharge ( $q_b$ ), concentration ( $C$ ), and basal shear stress ( $\tau$ ). During this time period, the bed slope was measured at 0.022,  $D_{50}$  on the bed surface was 0.0068 m, and the bulk sediment density was 2300 kg/m<sup>3</sup>.

\*Not used in analyses due to fluctuations in water discharge during measurements.



## APPENDIX C

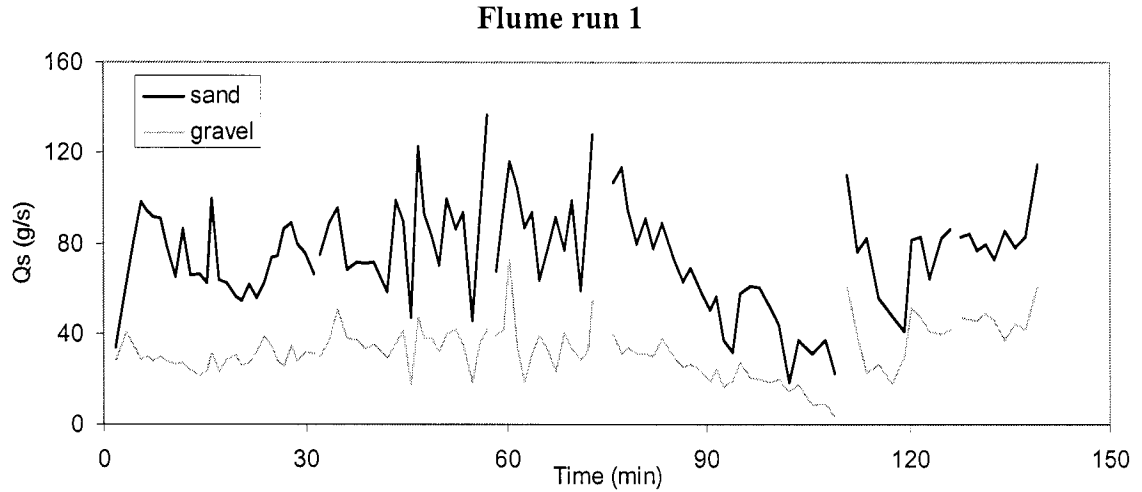
## Grain size distributions of bedload samples, Pasig-Potrero River 2001

Sample	Sieve size ( $\phi$ ); Sample mass (kg)										
	-5.5	-5	-4.5	-4	-3.5	-3	-2	-1	-0.5	0	>0
A3	0.18	0.10	0.44	0.51	0.64	0.65	1.97	2.60	2.15	0.65	2.69
C	0.00	0.00	0.10	0.17	0.22	0.21	0.56	0.69	0.74	0.19	1.58
E3	0.00	1.53	0.81	0.59	0.42	0.28	0.65	0.85	1.00	0.37	1.89
F3	0.00	0.08	0.31	0.14	0.26	0.20	0.52	0.91	1.25	0.26	2.37
J	0.00	2.68	1.15	1.39	0.66	1.30	2.44	3.10	4.70	2.25	16.52
K	0.00	0.25	0.07	0.48	0.68	0.64	1.24	1.13	1.10	0.44	1.32
L	0.00	0.06	0.07	0.05	0.28	0.24	0.70	0.75	0.90	0.46	1.56
M1	0.00	0.00	0.10	0.12	0.15	0.22	0.56	0.65	0.57	0.15	0.20
M2	0.00	0.46	0.18	0.40	0.60	0.56	2.05	3.40	4.83	1.79	5.19
M12	0.00	0.46	0.28	0.52	0.75	0.78	2.61	4.05	5.40	1.94	5.39
N1	0.00	0.94	1.50	2.02	2.91	2.11	7.33	6.35	4.03	1.49	7.18
N2	0.00	0.02	0.20	0.40	0.70	0.70	1.35	2.40	3.59	1.60	6.76
N12	0.00	0.96	1.70	2.42	3.61	2.81	8.68	8.75	7.62	3.09	13.95
P1	0.00	0.37	0.32	0.52	0.65	0.70	1.75	2.45	2.45	0.66	4.86
P2	0.00	0.00	0.02	0.03	0.03	0.06	0.30	0.50	0.63	0.13	0.30
P3	0.00	0.43	0.53	0.76	1.05	1.02	2.13	1.84	1.84	0.35	0.88
P123	0.00	0.80	0.87	1.31	1.73	1.78	4.18	4.79	4.92	1.14	6.04
Q1	0.00	2.27	1.48	2.22	3.34	2.57	7.28	6.72	6.67	2.59	11.25
Q2	0.00	0.00	0.00	0.00	0.03	0.02	0.03	0.06	0.08	0.03	0.03
Q12	0.00	2.27	1.48	2.22	3.37	2.59	7.31	6.78	6.75	2.62	11.28
R	0.00	2.90	0.80	1.06	1.21	1.48	3.65	4.96	5.32	0.93	6.92
S1	0.00	2.15	1.30	1.10	1.32	0.95	2.12	3.07	3.07	0.87	5.36
S2	0.00	0.03	0.20	0.18	0.42	0.55	1.42	1.89	3.15	0.44	3.63
S12	0.00	2.18	1.50	1.28	1.74	1.50	3.54	4.96	6.22	1.31	8.99
T	0.00	1.71	0.93	1.39	1.70	1.28	3.05	3.65	4.59	1.25	5.74
V	0.00	0.32	0.47	0.69	0.76	0.74	1.73	2.22	2.54	0.52	4.97
W	0.00	0.30	0.19	0.20	0.19	0.25	0.30	0.35	0.42	0.21	1.13
X1	0.00	0.45	0.40	0.78	1.08	1.08	3.17	5.15	5.79	0.51	5.16
X2	0.00	0.00	0.04	0.05	0.10	0.10	0.25	0.26	0.21	0.05	0.17
X12	0.00	0.45	0.44	0.83	1.18	1.18	3.42	5.41	6.00	0.56	5.33
Z	0.00	0.90	1.30	1.40	1.78	1.96	4.46	6.18	6.64	1.30	6.98

Grain size distributions of bedload samples from August-September 2001 on the Pasig-Potrero River. Samples were dried, sieved, and weighed in whole  $\phi$  and half  $\phi$  increments. Weights are listed in kilograms. The mesh size for the bedload sampler was 1 mm (0  $\phi$ ).

## APPENDIX D

## Flume experiment sediment transport data



Run 1 contained 70% sand and 30% gravel. Feed rate =  $181 \pm 15$  g/s; Initial slope = 0.021; Final slope = 0.021;  $Q_w = 0.0095 \pm 0.001$  m<sup>3</sup>/s. Feeder jammed from 73.7 – 108.8 min runtime. These data were not included in analyses. Measured sand and gravel transport rates ( $Q_s$ ) are plotted above and listed below.

Sample	Time (min)	$Q_s$ (g/s)	% Total Bedload Composition (mm)*							
			16	8	4	2	1	0.5	0.25	
1	1.9	62.1	0.00	0.12	0.20	0.14	0.13	0.16	0.26	
2	3.4	102.3	0.00	0.13	0.16	0.10	0.17	0.22	0.22	
3	4.5	115.5	0.00	0.12	0.11	0.07	0.14	0.20	0.36	
4	5.5	126.9	0.00	0.09	0.08	0.05	0.11	0.17	0.49	
5	6.5	124.4	0.00	0.11	0.08	0.05	0.12	0.17	0.47	
6	7.5	119.5	0.00	0.10	0.07	0.06	0.12	0.17	0.48	
7	8.5	121.1	0.00	0.10	0.08	0.06	0.11	0.15	0.49	
8	9.5	107.3	0.00	0.11	0.09	0.07	0.12	0.17	0.44	
9	10.8	91.6	0.00	0.12	0.10	0.07	0.13	0.18	0.41	
10	11.9	113.7	0.00	0.09	0.09	0.07	0.14	0.19	0.43	
11	13.0	89.6	0.01	0.11	0.08	0.07	0.14	0.18	0.41	
12	14.3	87.4	0.00	0.10	0.07	0.06	0.14	0.18	0.44	
13	15.5	86.4	0.00	0.12	0.09	0.06	0.12	0.15	0.46	
14	15.9	131.1	0.00	0.11	0.07	0.07	0.14	0.17	0.45	
15	17.1	87.2	0.00	0.10	0.11	0.06	0.13	0.17	0.44	
16	18.3	90.9	0.00	0.14	0.10	0.07	0.11	0.14	0.43	
17	19.5	87.6	0.00	0.15	0.11	0.08	0.15	0.17	0.34	
18	20.6	80.0	0.00	0.15	0.10	0.07	0.14	0.16	0.37	

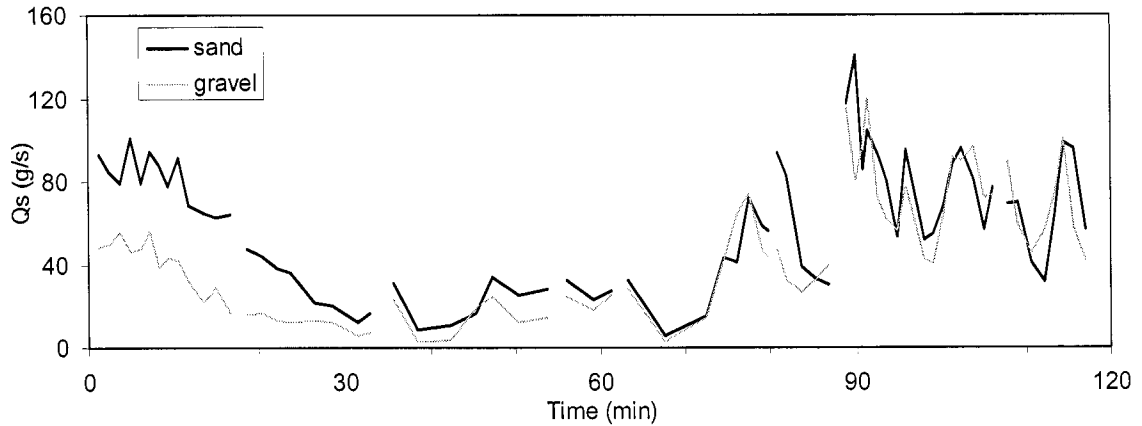
19	21.5	89.3		0.01	0.12	0.10	0.07	0.14	0.16	0.39
20	22.6	87.6		0.00	0.18	0.10	0.07	0.13	0.19	0.32
21	23.8	101.1		0.01	0.16	0.14	0.08	0.14	0.17	0.30
22	24.8	108.4		0.00	0.15	0.09	0.07	0.17	0.21	0.31
23	25.9	102.1		0.00	0.10	0.10	0.07	0.17	0.22	0.35
24	26.8	112.5		0.00	0.09	0.08	0.06	0.13	0.18	0.46
25	27.8	123.7		0.00	0.12	0.10	0.06	0.11	0.14	0.47
26	28.8	107.1		0.01	0.12	0.08	0.06	0.14	0.19	0.41
27	29.8	107.2		0.00	0.13	0.10	0.06	0.12	0.15	0.43
28	31.2	97.7		0.01	0.14	0.11	0.07	0.14	0.17	0.39
30	32.0	104.7		0.01	0.12	0.09	0.07	0.14	0.17	0.41
31	33.4	126.5		0.00	0.12	0.10	0.07	0.14	0.17	0.37
32	34.8	145.9		0.00	0.16	0.10	0.07	0.13	0.15	0.37
33	36.1	106.1		0.00	0.15	0.12	0.09	0.15	0.15	0.34
34	37.6	109.4		0.00	0.14	0.13	0.08	0.16	0.17	0.33
35	38.8	104.2		0.00	0.13	0.11	0.08	0.17	0.19	0.32
36	40.2	107.0		0.00	0.14	0.11	0.07	0.15	0.17	0.35
37	42.0	87.5		0.01	0.16	0.10	0.07	0.15	0.17	0.34
38	43.4	134.8		0.01	0.12	0.08	0.05	0.14	0.14	0.46
39	44.5	130.5		0.00	0.14	0.10	0.07	0.15	0.16	0.38
40	45.6	64.5		0.00	0.13	0.08	0.06	0.14	0.15	0.44
41	46.7	170.0		0.00	0.14	0.08	0.06	0.14	0.16	0.43
42	47.7	130.4		0.00	0.15	0.08	0.06	0.12	0.14	0.45
43	48.8	120.8		0.00	0.17	0.08	0.06	0.13	0.13	0.43
44	49.8	101.8		0.01	0.15	0.09	0.07	0.16	0.18	0.36
45	51.0	139.3		0.00	0.14	0.07	0.07	0.15	0.14	0.42
46	52.3	127.9		0.01	0.13	0.09	0.10	0.19	0.16	0.32
47	53.5	128.8		0.00	0.12	0.09	0.06	0.15	0.17	0.41
48	54.7	64.2		0.00	0.12	0.09	0.07	0.17	0.17	0.37
49	56.0	126.9		0.00	0.12	0.09	0.07	0.16	0.18	0.39
50	56.9	178.7		0.01	0.11	0.07	0.04	0.12	0.13	0.52
63	58.2	107.0		0.01	0.18	0.13	0.06	0.12	0.14	0.38
64	59.3	136.2		0.01	0.15	0.08	0.06	0.15	0.18	0.36
65	60.3	189.0		0.00	0.19	0.11	0.08	0.14	0.18	0.30
66	61.4	139.6		0.00	0.12	0.08	0.05	0.10	0.13	0.52
67	62.5	105.4		0.00	0.10	0.04	0.03	0.05	0.07	0.71
68	63.6	125.1		0.01	0.14	0.06	0.04	0.06	0.09	0.60
69	64.9	103.0		0.01	0.17	0.13	0.07	0.10	0.10	0.43
70	66.1	110.7		0.01	0.14	0.09	0.06	0.13	0.16	0.42
71	67.2	114.7		0.01	0.10	0.05	0.04	0.07	0.10	0.64
72	68.5	117.8		0.01	0.15	0.11	0.08	0.15	0.15	0.37

73	69.7	131.8		0.01	0.13	0.06	0.05	0.12	0.16	0.46
74	71.0	87.8		0.01	0.18	0.08	0.05	0.09	0.11	0.47
75	72.1	130.3		0.01	0.12	0.08	0.04	0.10	0.14	0.51
76	72.8	182.6		0.01	0.14	0.09	0.06	0.11	0.13	0.46
78	73.7	154.5		0.00	0.13	0.09	0.05	0.10	0.12	0.51
79	74.9	128.0		0.00	0.09	0.07	0.06	0.12	0.14	0.52
80	75.9	147.4		0.01	0.11	0.10	0.05	0.09	0.11	0.52
81	77.2	144.5		0.01	0.11	0.06	0.05	0.08	0.10	0.61
82	78.2	129.3		0.00	0.14	0.06	0.06	0.10	0.12	0.52
83	79.4	110.9		0.01	0.16	0.06	0.06	0.10	0.12	0.50
84	80.7	121.8		0.00	0.11	0.09	0.06	0.11	0.12	0.52
85	82.0	107.9		0.01	0.15	0.06	0.07	0.12	0.15	0.45
86	83.3	126.6		0.01	0.14	0.09	0.07	0.10	0.13	0.47
87	85.0	103.1		0.00	0.13	0.09	0.07	0.11	0.14	0.46
88	86.3	88.6		0.01	0.13	0.08	0.07	0.12	0.14	0.47
89	87.5	95.9		0.01	0.12	0.10	0.05	0.10	0.13	0.50
90	88.9	82.2		0.01	0.13	0.09	0.06	0.10	0.13	0.48
91	90.5	68.9		0.00	0.12	0.08	0.06	0.09	0.11	0.54
92	91.2	81.4		0.00	0.14	0.09	0.07	0.10	0.13	0.46
93	92.3	54.2		0.00	0.14	0.11	0.07	0.08	0.10	0.51
94	93.7	51.1		0.00	0.18	0.09	0.11	0.19	0.20	0.23
95	94.8	84.9		0.00	0.14	0.10	0.07	0.15	0.19	0.34
96	96.3	81.5		0.01	0.14	0.05	0.06	0.14	0.17	0.43
97	97.7	80.0		0.01	0.11	0.06	0.07	0.12	0.16	0.47
98	99.2	70.6		0.01	0.12	0.07	0.06	0.12	0.15	0.47
99	100.6	63.6		0.00	0.14	0.09	0.08	0.13	0.16	0.40
100	102.1	33.3		0.04	0.25	0.07	0.08	0.10	0.12	0.34
101	103.4	55.4		0.01	0.16	0.07	0.07	0.14	0.16	0.39
102	105.6	39.8		0.00	0.10	0.05	0.06	0.12	0.18	0.50
103	107.4	47.0		0.00	0.11	0.05	0.04	0.09	0.13	0.58
104	108.8	26.3		0.00	0.04	0.05	0.05	0.10	0.14	0.63
106	110.5	171.3		0.01	0.14	0.12	0.09	0.12	0.17	0.35
107	112.1	115.3		0.00	0.12	0.13	0.09	0.13	0.17	0.37
108	113.5	105.4		0.00	0.01	0.12	0.09	0.13	0.17	0.49
109	115.4	81.9		0.01	0.11	0.11	0.09	0.13	0.17	0.38
110	117.3	65.6		0.00	0.11	0.09	0.07	0.13	0.16	0.43
111	119.0	70.8		0.00	0.18	0.14	0.10	0.14	0.16	0.28
112	120.2	133.2		0.00	0.19	0.11	0.08	0.14	0.18	0.30
113	121.5	130.1		0.01	0.16	0.11	0.07	0.14	0.17	0.33
114	122.9	105.4		0.01	0.17	0.13	0.08	0.15	0.16	0.30
115	124.6	122.0		0.00	0.14	0.11	0.07	0.16	0.19	0.32

116	126.0	128.0		0.01	0.15	0.08	0.08	0.14	0.16	0.36
118	127.5	130.5		0.00	0.17	0.12	0.06	0.10	0.13	0.40
119	128.8	130.6		0.00	0.17	0.10	0.08	0.14	0.15	0.36
120	129.9	122.3		0.00	0.19	0.10	0.08	0.14	0.16	0.33
121	131.2	129.1		0.00	0.18	0.12	0.09	0.14	0.15	0.33
122	132.6	118.7		0.00	0.16	0.12	0.11	0.17	0.17	0.28
123	134.1	122.8		0.00	0.17	0.07	0.06	0.09	0.13	0.48
124	135.7	122.8		0.00	0.17	0.11	0.08	0.12	0.15	0.36
125	137.3	125.0		0.00	0.16	0.10	0.08	0.13	0.15	0.38
126	139.2	175.7		0.00	0.15	0.12	0.07	0.14	0.16	0.36

\*Bedload composition is listed in terms of % total sample, binned in 1 phi increments. The value listed is the sieve size (mm) that caught the sample. Sediment < 0.25 mm were removed from the sample.

## Flume run 2



Run 2 contained 50% sand and 50% gravel. Feed rate =  $181 \pm 15$  g/s; Initial slope = 0.025; Final slope = 0.027;  $Q_w = 0.0095 \pm 0.001$  m<sup>3</sup>/s. Measured sand and gravel transport rates are plotted above and detailed below.

Sample	Time (min)	$Q_s$ (g/s)	% Total Bedload Composition (mm)*							
			16	8	4	2	1	0.5	0.25	
200	1.2	141.4	0.01	0.18	0.08	0.07	0.12	0.13	0.40	
201	2.5	134.1	0.01	0.16	0.11	0.08	0.13	0.14	0.36	
202	3.8	134.3	0.01	0.18	0.12	0.09	0.09	0.11	0.38	
203	5.0	146.7	0.01	0.14	0.10	0.06	0.08	0.11	0.51	
204	6.1	126.6	0.02	0.18	0.11	0.07	0.07	0.09	0.47	
205	7.1	151.2	0.01	0.18	0.12	0.07	0.09	0.11	0.44	
206	8.2	126.3	0.01	0.14	0.09	0.06	0.09	0.12	0.49	
207	9.3	121.0	0.03	0.18	0.10	0.06	0.07	0.09	0.48	
208	10.4	133.2	0.00	0.14	0.09	0.08	0.12	0.15	0.43	
209	11.8	99.8	0.01	0.14	0.10	0.07	0.11	0.13	0.44	
210	13.4	86.9	0.01	0.10	0.09	0.05	0.09	0.12	0.54	
211	14.9	91.1	0.01	0.10	0.11	0.09	0.16	0.18	0.33	
212	16.6	81.1	0.01	0.07	0.06	0.06	0.10	0.15	0.54	
213	16.9									
214	18.5	63.6	0.00	0.11	0.09	0.05	0.10	0.14	0.51	
215	20.3	60.6	0.02	0.11	0.08	0.06	0.10	0.13	0.49	
216	22.0	50.8	0.01	0.10	0.08	0.07	0.11	0.15	0.49	
217	23.7	48.1	0.01	0.12	0.07	0.06	0.09	0.13	0.52	
218	26.4	34.3	0.01	0.16	0.12	0.09	0.11	0.11	0.41	
219	28.5	32.2	0.01	0.14	0.12	0.10	0.10	0.13	0.40	
220	31.4	17.9	0.01	0.12	0.10	0.08	0.11	0.14	0.44	
221	32.9	23.2	0.01	0.11	0.09	0.08	0.11	0.15	0.46	

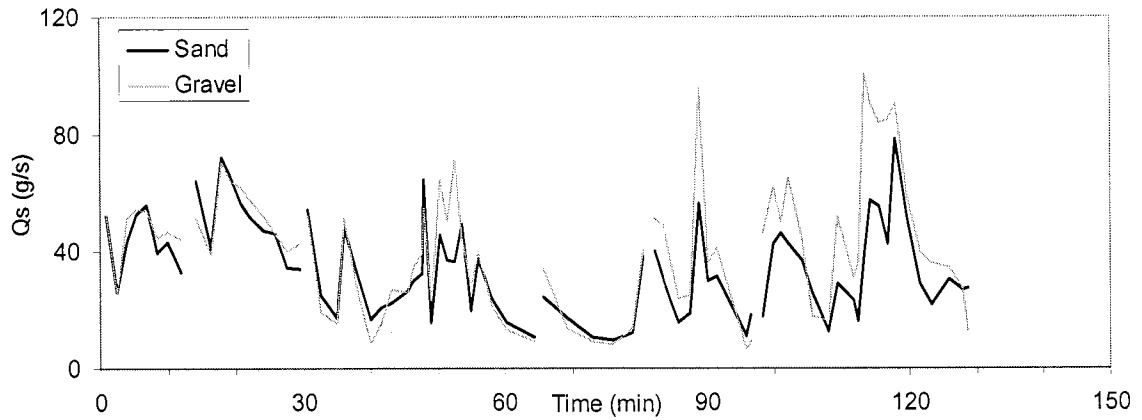
222	33.1									
223	35.6	54.5		0.01	0.21	0.14	0.08	0.08	0.11	0.38
224	38.5	11.7		0.01	0.10	0.08	0.07	0.10	0.13	0.51
225	42.4	14.6		0.01	0.11	0.07	0.05	0.09	0.13	0.54
226	45.4	36.5		0.01	0.25	0.18	0.11	0.09	0.11	0.26
227	47.2	58.0		0.00	0.17	0.15	0.10	0.10	0.12	0.36
228	50.3	37.5		0.00	0.12	0.12	0.08	0.10	0.12	0.46
229	53.6	43.0		0.00	0.13	0.12	0.09	0.13	0.15	0.38
230	54.0									
231	56.1	57.1		0.01	0.18	0.16	0.08	0.08	0.10	0.39
232	59.2	41.8		0.01	0.21	0.14	0.09	0.09	0.11	0.37
233	61.2	52.1		0.00	0.21	0.16	0.10	0.11	0.12	0.29
234	61.3									
235	63.1	60.4		0.02	0.24	0.12	0.09	0.08	0.09	0.35
236	67.6	8.4		0.00	0.17	0.09	0.06	0.09	0.12	0.47
237	72.3	29.7		0.01	0.28	0.13	0.07	0.07	0.09	0.35
238	74.5	85.5		0.01	0.28	0.12	0.09	0.08	0.10	0.32
239	76.0	105.5		0.04	0.30	0.16	0.10	0.08	0.09	0.21
240	77.6	146.4		0.03	0.26	0.12	0.09	0.09	0.11	0.28
241	79.1	105.7		0.01	0.20	0.14	0.10	0.10	0.12	0.33
242	79.8	100.2		0.01	0.20	0.13	0.10	0.12	0.14	0.30
244	80.8	140.7		0.00	0.14	0.10	0.09	0.12	0.15	0.40
245	81.9	115.5		0.01	0.11	0.08	0.08	0.11	0.14	0.47
246	83.7	65.5		0.01	0.17	0.14	0.08	0.10	0.12	0.39
247	85.1	66.1		0.01	0.25	0.14	0.09	0.10	0.11	0.30
248	86.8	69.9		0.01	0.31	0.16	0.09	0.08	0.09	0.27
249	87.9									
250	88.9	232.7		0.00	0.24	0.15	0.11	0.11	0.13	0.26
251	89.9	220.6		0.01	0.17	0.11	0.08	0.08	0.11	0.46
252	90.7	184.0		0.01	0.24	0.16	0.12	0.09	0.10	0.28
253	91.4	224.5		0.02	0.31	0.10	0.10	0.11	0.13	0.23
254	92.5	164.3		0.01	0.22	0.13	0.08	0.09	0.11	0.37
255	93.5	141.2		0.00	0.20	0.13	0.10	0.10	0.13	0.34
256	94.9	110.1		0.01	0.26	0.14	0.10	0.08	0.10	0.31
257	95.9	172.7		0.01	0.21	0.14	0.09	0.09	0.11	0.35
258	97.9	95.0		0.01	0.22	0.12	0.10	0.10	0.12	0.33
259	99.0	95.6		0.00	0.18	0.13	0.11	0.11	0.13	0.33
260	100.3	132.2		0.01	0.22	0.16	0.10	0.09	0.10	0.33
261	101.3	179.9		0.02	0.22	0.15	0.12	0.10	0.11	0.28
262	102.4	185.6		0.02	0.24	0.13	0.10	0.10	0.11	0.30
263	103.7	177.3		0.01	0.27	0.19	0.08	0.07	0.08	0.31
264	105.0	128.9		0.01	0.26	0.20	0.09	0.08	0.09	0.28
265	106.1	150.3		0.01	0.25	0.13	0.09	0.09	0.10	0.32

266	106.8									
267	107.7	159.0		0.01	0.28	0.18	0.10	0.08	0.10	0.26
268	109.0	129.0		0.02	0.24	0.12	0.08	0.09	0.10	0.35
269	110.6	86.1		0.01	0.34	0.10	0.08	0.07	0.08	0.32
270	112.1	87.8		0.01	0.31	0.22	0.10	0.08	0.08	0.20
271	113.4	137.9		0.01	0.28	0.15	0.10	0.09	0.10	0.27
272	114.5	198.8		0.00	0.26	0.12	0.12	0.12	0.13	0.25
273	115.6	152.9		0.02	0.15	0.12	0.09	0.11	0.13	0.39
274	117.1	98.4		0.01	0.21	0.11	0.09	0.10	0.11	0.37

\*Bedload composition is listed in terms of % total sample, binned in 1 phi increments. The value listed is the sieve size (mm) that caught the sample. Sediment < 0.25 mm were removed from the sample.



**Flume run 3**



Run 3 contained 40% sand and 60% gravel. Feed rate =  $181 \pm 15$  g/s; Initial slope = 0.029; Final slope = 0.040;  $Q_w = 0.0095 \pm 0.001$  m<sup>3</sup>/s. Measured sand and gravel transport rates are plotted above and detailed below.

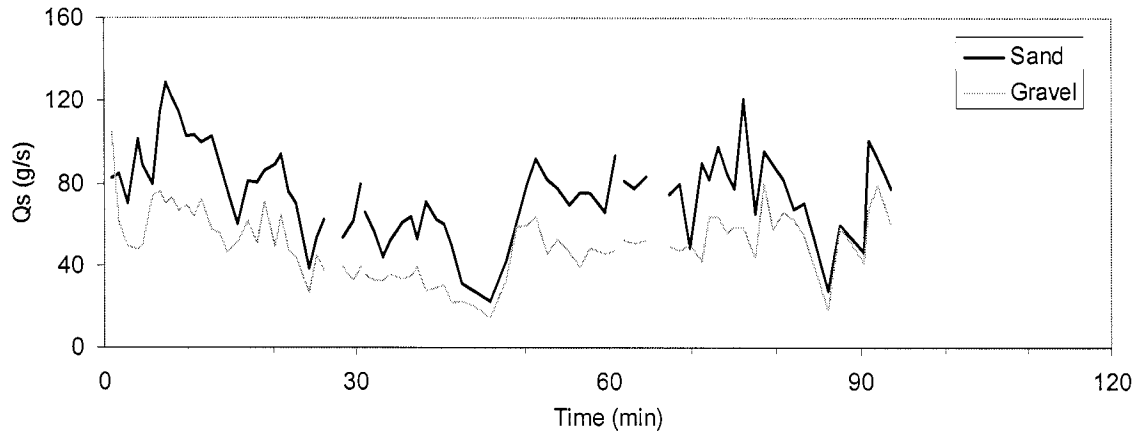
Sample	Time (min)	$Q_s$ (g/s)	% Total Bedload Composition (mm)*							
			16	8	4	2	1	0.5	0.25	
300	1.0	105.1	0.01	0.26	0.14	0.09	0.08	0.09	0.33	
301	2.4	51.2	0.01	0.27	0.12	0.10	0.09	0.11	0.30	
302	3.9	95.7	0.01	0.24	0.16	0.13	0.09	0.10	0.26	
303	5.3	107.0	0.02	0.24	0.14	0.11	0.09	0.11	0.29	
304	6.8	109.8	0.02	0.22	0.14	0.12	0.10	0.12	0.29	
305	8.3	84.6	0.02	0.26	0.15	0.10	0.10	0.11	0.27	
306	9.9	90.4	0.02	0.27	0.14	0.10	0.07	0.09	0.32	
307	11.8	77.2	0.02	0.34	0.11	0.10	0.09	0.10	0.24	
309	14.1									
310	16.3	79.7	0.01	0.27	0.11	0.10	0.09	0.10	0.33	
311	17.7	142.9	0.02	0.23	0.13	0.12	0.09	0.11	0.30	
312	19.2	129.6	0.02	0.21	0.13	0.14	0.09	0.10	0.31	
313	20.8	118.3	0.02	0.22	0.16	0.13	0.09	0.11	0.28	
314	22.0	109.5	0.01	0.24	0.14	0.14	0.09	0.10	0.28	
315	23.9	100.0	0.02	0.27	0.12	0.12	0.09	0.10	0.29	
316	25.6	92.4	0.01	0.26	0.12	0.11	0.09	0.10	0.31	
317	27.5	74.7	0.02	0.29	0.12	0.11	0.08	0.10	0.28	
318	29.4									
320	30.6	106.6	0.02	0.26	0.11	0.11	0.09	0.10	0.32	
321	32.5	44.4	0.02	0.22	0.10	0.09	0.08	0.10	0.39	
322	34.8	32.4	0.02	0.24	0.12	0.08	0.07	0.09	0.38	
323	35.9	99.8	0.01	0.26	0.12	0.12	0.09	0.10	0.30	

324	37.8	61.7		0.01	0.20	0.13	0.11	0.10	0.12	0.33
325	39.9	25.3		0.01	0.15	0.09	0.10	0.09	0.12	0.43
326	41.5	36.2		0.01	0.16	0.14	0.11	0.09	0.11	0.38
327	43.0	49.2		0.02	0.25	0.16	0.12	0.08	0.09	0.28
328	45.5	52.4		0.01	0.27	0.11	0.11	0.09	0.10	0.31
329	46.4	64.4		0.02	0.26	0.15	0.11	0.08	0.09	0.31
330	47.7	72.0		0.02	0.27	0.15	0.11	0.08	0.09	0.29
331	48.0									
332	49.1	39.0		0.02	0.29	0.16	0.12	0.07	0.08	0.25
333	50.3	110.3		0.03	0.30	0.14	0.12	0.08	0.10	0.23
334	51.5	87.3		0.02	0.29	0.14	0.13	0.08	0.09	0.25
335	52.5	107.6		0.03	0.21	0.24	0.18	0.08	0.09	0.17
336	53.5	93.5		0.02	0.22	0.13	0.11	0.10	0.11	0.32
337	54.9	48.4		0.02	0.28	0.18	0.11	0.07	0.08	0.25
338	56.0	77.3		0.01	0.19	0.16	0.16	0.11	0.12	0.26
339	58.1	45.1		0.01	0.18	0.14	0.14	0.11	0.12	0.30
340	60.2	28.9		0.01	0.21	0.13	0.10	0.10	0.11	0.34
341	64.3									
343	65.7	58.2		0.11	0.23	0.13	0.12	0.08	0.10	0.24
344	69.2	30.9		0.02	0.17	0.12	0.13	0.10	0.12	0.35
345	72.9	19.8		0.01	0.21	0.14	0.11	0.08	0.09	0.36
346	76.0	17.8		0.00	0.24	0.12	0.11	0.08	0.10	0.35
347	78.9	25.9		0.03	0.27	0.13	0.09	0.07	0.09	0.32
348	80.5	78.7		0.01	0.21	0.18	0.12	0.09	0.10	0.30
349	81.0									
350	82.2	91.5		0.03	0.31	0.12	0.10	0.07	0.08	0.30
351	83.4	78.6		0.02	0.32	0.17	0.10	0.07	0.08	0.24
352	85.7	39.7		0.03	0.37	0.12	0.08	0.05	0.06	0.29
353	87.5	43.9		0.01	0.37	0.13	0.06	0.04	0.05	0.34
354	88.7	152.3		0.02	0.34	0.15	0.12	0.07	0.08	0.22
355	90.0	65.9		0.01	0.31	0.14	0.09	0.07	0.08	0.31
356	91.5	72.6		0.01	0.28	0.16	0.11	0.07	0.09	0.28
357	95.8	18.2		0.01	0.16	0.11	0.09	0.09	0.11	0.41
358	96.5									
360	98.1	64.4		0.02	0.38	0.21	0.11	0.05	0.06	0.17
361	99.7	104.5		0.02	0.29	0.15	0.13	0.08	0.08	0.24
362	100.8	96.3		0.01	0.03	0.28	0.22	0.10	0.11	0.30
363	102.0	107.5		0.02	0.24	0.19	0.16	0.08	0.09	0.23
364	103.8	81.7		0.01	0.24	0.16	0.14	0.09	0.10	0.26
365	105.4	43.7		0.01	0.18	0.11	0.11	0.10	0.12	0.37
366	107.9	28.9		0.01	0.30	0.14	0.11	0.07	0.08	0.28
367	109.2	80.5		0.01	0.27	0.22	0.15	0.08	0.08	0.20
368	111.5	54.3		0.02	0.29	0.13	0.12	0.07	0.08	0.27

369	112.2									
370	113.1	139.9		0.01	0.37	0.20	0.14	0.07	0.07	0.15
371	114.1	148.4		0.02	0.28	0.15	0.16	0.09	0.09	0.21
372	115.3	139.8		0.01	0.28	0.18	0.13	0.07	0.08	0.24
373	116.7	127.8		0.02	0.32	0.19	0.14	0.07	0.07	0.19
374	117.8	169.0		0.02	0.24	0.16	0.13	0.08	0.09	0.29
375	119.6	110.7		0.02	0.24	0.14	0.13	0.08	0.09	0.29
376	121.4	69.3		0.02	0.28	0.16	0.13	0.07	0.08	0.27
377	123.2	57.7		0.01	0.27	0.19	0.15	0.07	0.07	0.23
378	125.8	65.1		0.01	0.23	0.17	0.12	0.07	0.08	0.31
379	127.8	54.7		0.02	0.22	0.14	0.12	0.07	0.08	0.34
380	128.6									

\*Bedload composition is listed in terms of % total sample, binned in 1 phi increments. The value listed is the sieve size (mm) that caught the sample. Sediment < 0.25 mm were removed from the sample.

**Flume run 4**



Run 4 contained 60% sand and 40% gravel. Feed rate =  $181 \pm 15$  g/s; Initial slope = 0.022; Final slope = 0.027;  $Q_w = 0.0095 \pm 0.001$  m<sup>3</sup>/s. Measured sand and gravel transport rates are plotted above and listed below.

Sample	Time (min)	$Q_s$ (g/s)	% Total Bedload Composition (mm)*							
			16	8	4	2	1	0.5	0.25	
400	0.9	187.0	0.01	0.16	0.24	0.17	0.15	0.11	0.19	
401	1.7	145.8	0.00	0.14	0.15	0.13	0.14	0.12	0.33	
402	2.8	119.3	0.00	0.08	0.18	0.15	0.20	0.16	0.23	
403	4.0	149.0	0.00	0.08	0.12	0.12	0.19	0.18	0.31	
407	4.5	138.5	0.01	0.17	0.09	0.08	0.12	0.11	0.41	
408	5.8	153.8	0.01	0.24	0.14	0.10	0.12	0.12	0.28	
409	6.6	190.5	0.00	0.17	0.13	0.10	0.14	0.14	0.32	
410	7.3	199.2	0.01	0.16	0.10	0.08	0.13	0.15	0.36	
411	8.2	194.4	0.00	0.18	0.12	0.08	0.11	0.11	0.41	
412	9.0	181.5	0.01	0.19	0.09	0.08	0.13	0.12	0.38	
413	9.8	172.4	0.00	0.21	0.11	0.09	0.13	0.13	0.34	
414	10.8	166.9	0.00	0.20	0.09	0.09	0.14	0.14	0.33	
415	11.7	172.6	0.01	0.17	0.15	0.10	0.13	0.13	0.33	
416	12.8	159.6	0.00	0.16	0.10	0.09	0.13	0.13	0.39	
417	13.7	145.6	0.01	0.16	0.11	0.10	0.14	0.13	0.35	
418	14.7	124.0	0.00	0.16	0.11	0.10	0.13	0.12	0.38	
419	15.9	111.5	0.00	0.21	0.14	0.11	0.13	0.12	0.29	
420	17.2	142.3	0.00	0.17	0.15	0.11	0.14	0.13	0.30	
421	18.2	131.3	0.00	0.17	0.11	0.10	0.12	0.12	0.37	
422	19.1	157.3	0.01	0.19	0.14	0.12	0.15	0.14	0.27	
423	20.3	138.1	0.00	0.16	0.10	0.10	0.13	0.13	0.38	
424	21.0	159.0	0.00	0.16	0.12	0.12	0.15	0.13	0.32	

425	21.9	123.6		0.00	0.17	0.12	0.10	0.13	0.13	0.35
426	22.8	115.0		0.01	0.18	0.11	0.09	0.12	0.12	0.37
427	24.2	65.6		0.01	0.17	0.14	0.09	0.11	0.10	0.37
428	25.2	98.1		0.01	0.20	0.14	0.11	0.14	0.14	0.26
429	26.1	99.6		0.01	0.16	0.11	0.10	0.14	0.13	0.35
430	27.3	76.6								
431	28.3	92.6		0.00	0.20	0.12	0.10	0.15	0.16	0.27
432	29.7	94.3		0.00	0.17	0.09	0.08	0.15	0.16	0.34
433	30.4									
435	31.0	101.1		0.01	0.16	0.10	0.08	0.12	0.13	0.40
436	32.0	88.6		0.01	0.18	0.10	0.08	0.13	0.15	0.36
437	33.2	76.3		0.01	0.19	0.12	0.10	0.15	0.14	0.29
438	34.1	87.3		0.01	0.21	0.08	0.09	0.16	0.17	0.27
439	35.5	94.1		0.00	0.16	0.09	0.10	0.15	0.18	0.31
440	36.5	99.1		0.01	0.17	0.09	0.08	0.13	0.17	0.34
441	37.3	92.4		0.01	0.19	0.12	0.10	0.14	0.17	0.26
442	38.3	98.3		0.00	0.02	0.14	0.12	0.15	0.20	0.36
443	39.4	91.4		0.01	0.14	0.09	0.08	0.11	0.15	0.43
444	40.3	91.2		0.00	0.16	0.10	0.08	0.10	0.12	0.45
445	41.3	71.4		0.00	0.13	0.09	0.08	0.11	0.13	0.47
446	42.5	53.2		0.00	0.19	0.13	0.09	0.11	0.14	0.33
447	43.8	48.0		0.00	0.17	0.14	0.11	0.15	0.17	0.25
448	45.9	36.3		0.01	0.16	0.11	0.11	0.15	0.17	0.28
449	47.7	74.6		0.00	0.02	0.25	0.16	0.15	0.17	0.24
450	49.0									
451	50.2	137.8		0.01	0.22	0.11	0.09	0.12	0.17	0.28
452	51.3	155.9		0.01	0.18	0.13	0.09	0.11	0.16	0.32
453	52.6	127.3		0.00	0.01	0.19	0.15	0.14	0.15	0.35
454	54.0	129.8		0.00	0.18	0.12	0.10	0.12	0.16	0.31
455	55.3	115.9		0.01	0.17	0.10	0.12	0.13	0.17	0.30
456	56.5	114.6		0.00	0.01	0.18	0.15	0.15	0.19	0.31
457	57.8	123.5		0.01	0.19	0.10	0.10	0.12	0.15	0.34
458	59.5	111.8		0.01	0.19	0.11	0.10	0.12	0.15	0.32
459	60.9	140.8		0.01	0.17	0.08	0.08	0.11	0.16	0.39
461	61.8	133.5		0.02	0.20	0.09	0.08	0.11	0.14	0.36
462	63.1	128.0		0.02	0.17	0.12	0.08	0.11	0.15	0.34
463	64.5	135.7		0.01	0.20	0.09	0.08	0.11	0.14	0.36
464	65.8	120.9								
465	67.3	123.9		0.01	0.16	0.12	0.10	0.12	0.15	0.33
466	68.5	127.0		0.02	0.16	0.11	0.09	0.11	0.14	0.37
467	69.9	98.2		0.01	0.25	0.14	0.11	0.10	0.12	0.27
468	71.2	132.2		0.00	0.02	0.17	0.13	0.14	0.17	0.37
469	72.1	146.1		0.02	0.23	0.10	0.09	0.10	0.12	0.34

470	73.1	161.8		0.01	0.18	0.12	0.08	0.10	0.12	0.38
471	74.2	140.4		0.02	0.17	0.11	0.10	0.12	0.14	0.34
472	75.1	136.1		0.02	0.20	0.12	0.09	0.11	0.12	0.34
473	76.1	179.3		0.00	0.02	0.19	0.12	0.12	0.13	0.42
474	77.5	108.6		0.00	0.02	0.23	0.15	0.14	0.13	0.34
475	78.5	175.1		0.01	0.22	0.12	0.10	0.13	0.14	0.27
476	79.6	146.0		0.00	0.20	0.10	0.09	0.12	0.13	0.36
477	80.8	147.6		0.01	0.22	0.12	0.09	0.10	0.12	0.33
478	82.1	129.5		0.00	0.24	0.13	0.10	0.10	0.11	0.32
479	83.4	124.8		0.01	0.21	0.13	0.09	0.09	0.10	0.37
480	86.1	45.2		0.01	0.18	0.12	0.09	0.09	0.10	0.41
481	87.6	118.0		0.01	0.23	0.15	0.10	0.10	0.11	0.29
482	90.4	87.3		0.01	0.23	0.13	0.10	0.12	0.12	0.28
483	91.0	168.0		0.00	0.02	0.22	0.16	0.13	0.14	0.33
484	91.9	171.1		0.01	0.23	0.13	0.09	0.09	0.10	0.34
485	93.5	137.5		0.01	0.21	0.13	0.09	0.10	0.11	0.35

\*Bedload composition is listed in terms of % total sample, binned in 1 phi increments. The value listed is the sieve size (mm) that caught the sample. Sediment < 0.25 mm were removed from the sample.

**VITA**

Karen Bobbitt Gran earned her Bachelor of Arts degree in geology from Carleton College in 1996. She worked as a geologist for an engineering firm in Eagan, Minnesota, before starting graduate work at the University of Minnesota in 1997. In 2000, she earned a Master of Science degree in geology. Her thesis, entitled “Riparian vegetation controls on braided river dynamics”, was advised by Chris Paola. Major results were published in *Water Resources Research* in 2001 (Gran and Paola, 2001). She taught briefly at the University of St. Thomas before starting graduate school at the University of Washington in 2000. She earned her Doctor of Philosophy degree in 2005 from the University of Washington with this study on fluvial recovery following basin-wide sediment loading at Mount Pinatubo, Philippines, advised by David Montgomery. Field results have been published in *GSA Bulletin* (Gran and Montgomery, 2005), and flume experiment results are in review at *Water Resources Research* (Gran et al., in review). The author currently resides in Duluth, Minnesota, where she is coordinating a new stream restoration certificate program at the University of Minnesota.